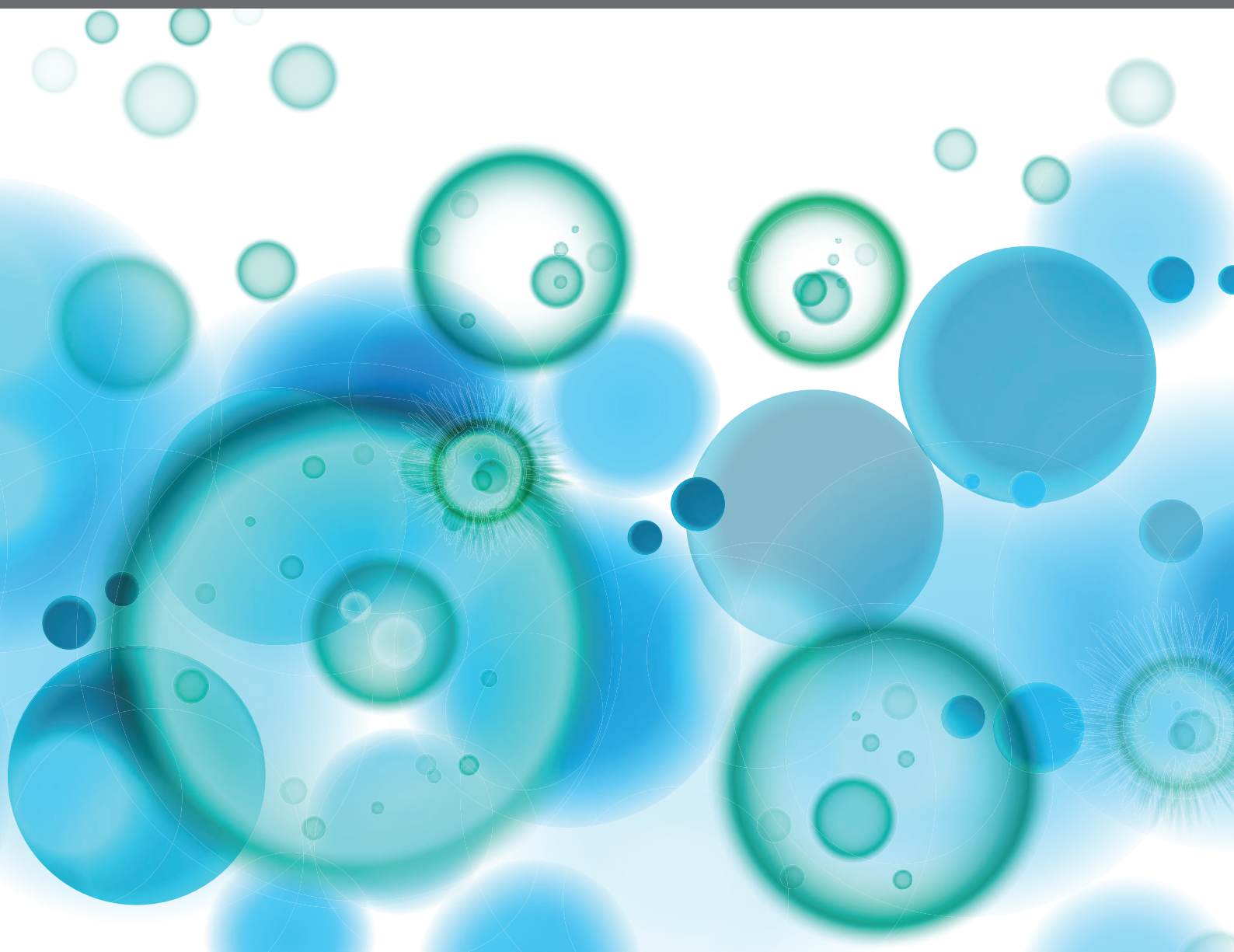


IMMUNOGLOBULIN GLYCOSYLATION ANALYSIS: STATE-OF-THE-ART METHODS AND APPLICATIONS IN IMMUNOLOGY

EDITED BY: Irena Trbojević-Akmačić, Mohamed Abdel-Mohsen,
David Falck and Erdmann Rapp
PUBLISHED IN: Frontiers in Immunology





frontiers

Frontiers eBook Copyright Statement

The copyright in the text of individual articles in this eBook is the property of their respective authors or their respective institutions or funders. The copyright in graphics and images within each article may be subject to copyright of other parties. In both cases this is subject to a license granted to Frontiers.

The compilation of articles constituting this eBook is the property of Frontiers.

Each article within this eBook, and the eBook itself, are published under the most recent version of the Creative Commons CC-BY licence.

The version current at the date of publication of this eBook is CC-BY 4.0. If the CC-BY licence is updated, the licence granted by Frontiers is automatically updated to the new version.

When exercising any right under the CC-BY licence, Frontiers must be attributed as the original publisher of the article or eBook, as applicable.

Authors have the responsibility of ensuring that any graphics or other materials which are the property of others may be included in the CC-BY licence, but this should be checked before relying on the CC-BY licence to reproduce those materials. Any copyright notices relating to those materials must be complied with.

Copyright and source acknowledgement notices may not be removed and must be displayed in any copy, derivative work or partial copy which includes the elements in question.

All copyright, and all rights therein, are protected by national and international copyright laws. The above represents a summary only. For further information please read Frontiers' Conditions for Website Use and Copyright Statement, and the applicable CC-BY licence.

ISSN 1664-8714

ISBN 978-2-88976-350-4

DOI 10.3389/978-2-88976-350-4

About Frontiers

Frontiers is more than just an open-access publisher of scholarly articles: it is a pioneering approach to the world of academia, radically improving the way scholarly research is managed. The grand vision of Frontiers is a world where all people have an equal opportunity to seek, share and generate knowledge. Frontiers provides immediate and permanent online open access to all its publications, but this alone is not enough to realize our grand goals.

Frontiers Journal Series

The Frontiers Journal Series is a multi-tier and interdisciplinary set of open-access, online journals, promising a paradigm shift from the current review, selection and dissemination processes in academic publishing. All Frontiers journals are driven by researchers for researchers; therefore, they constitute a service to the scholarly community. At the same time, the Frontiers Journal Series operates on a revolutionary invention, the tiered publishing system, initially addressing specific communities of scholars, and gradually climbing up to broader public understanding, thus serving the interests of the lay society, too.

Dedication to Quality

Each Frontiers article is a landmark of the highest quality, thanks to genuinely collaborative interactions between authors and review editors, who include some of the world's best academicians. Research must be certified by peers before entering a stream of knowledge that may eventually reach the public - and shape society; therefore, Frontiers only applies the most rigorous and unbiased reviews.

Frontiers revolutionizes research publishing by freely delivering the most outstanding research, evaluated with no bias from both the academic and social point of view. By applying the most advanced information technologies, Frontiers is catapulting scholarly publishing into a new generation.

What are Frontiers Research Topics?

Frontiers Research Topics are very popular trademarks of the Frontiers Journals Series: they are collections of at least ten articles, all centered on a particular subject. With their unique mix of varied contributions from Original Research to Review Articles, Frontiers Research Topics unify the most influential researchers, the latest key findings and historical advances in a hot research area! Find out more on how to host your own Frontiers Research Topic or contribute to one as an author by contacting the Frontiers Editorial Office: frontiersin.org/about/contact

IMMUNOGLOBULIN GLYCOSYLATION ANALYSIS: STATE-OF-THE-ART METHODS AND APPLICATIONS IN IMMUNOLOGY

Topic Editors:

Irena Trbojević-Akmačić, Genos Glycoscience Research Laboratory, Croatia

Mohamed Abdel-Mohsen, Wistar Institute, United States

David Falck, Leiden University Medical Center, Netherlands

Erdmann Rapp, Max Planck Institute for Dynamics of Complex Technical Systems,
Max Planck Society, Germany

Citation: Trbojević-Akmačić, I., Abdel-Mohsen, M., Falck, D., Rapp, E., eds. (2022).
Immunoglobulin Glycosylation Analysis: State-of-the-Art Methods and
Applications in Immunology. Lausanne: Frontiers Media SA.
doi: 10.3389/978-2-88976-350-4

Table of Contents

- 04 Editorial: Immunoglobulin Glycosylation Analysis: State-of-the-Art Methods and Applications in Immunology**
Irena Trbojević-Akmačić, Mohamed Abdel-Mohsen, David Falck and Erdmann Rapp
- 07 Effects of Estradiol on Immunoglobulin G Glycosylation: Mapping of the Downstream Signaling Mechanism**
Anika Mijakovac, Julija Jurić, Wendy M. Kohrt, Jasminka Krištić, Domagoj Kifer, Kathleen M. Gavin, Karlo Miškeć, Azra Frkatović, Frano Vučković, Marija Pezer, Aleksandar Vojta, Peter A. Nigrović, Vlatka Zoldoš and Gordan Lauc
- 20 Biophysical Evaluation of Rhesus Macaque Fc Gamma Receptors Reveals Similar IgG Fc Glycoform Preferences to Human Receptors**
Andrew R. Crowley, Nana Yaw Osei-Owusu, Gillian Dekkers, Wenda Gao, Manfred Wuhrer, Diogo M. Magnani, Keith A. Reimann, Seth H. Pincus, Gestur Vidarsson and Margaret E. Ackerman
- 29 Immunoglobulin Glycosylation – An Unexploited Potential for Immunomodulatory Strategies in Farm Animals**
Kristina Zlatina and Sebastian P. Galuska
- 42 Heritability Enrichment of Immunoglobulin G N-Glycosylation in Specific Tissues**
Xingang Li, Hao Wang, Yahong Zhu, Weijie Cao, Manshu Song, Youxin Wang, Haifeng Hou, Minglin Lang, Xiuhua Guo, Xuerui Tan, Jingdong J. Han and Wei Wang
- 61 Enhanced Immunomodulatory Effect of Intravenous Immunoglobulin by Fc Galactosylation and Nonfucosylation**
Yusuke Mimura, Yuka Mimura-Kimura, Radka Saldova, Pauline M. Rudd and Roy Jefferis
- 71 GlycoFibroTyper: A Novel Method for the Glycan Analysis of IgG and the Development of a Biomarker Signature of Liver Fibrosis**
Danielle A. Scott, Mengjun Wang, Stephane Grauzam, Sarah Pippin, Alyson Black, Peggi M. Angel, Richard R. Drake, Stephen Castellino, Yuko Kono, Don C. Rockey and Anand S. Mehta
- 81 Changes of IgG N-Glycosylation in Thyroid Autoimmunity: The Modulatory Effect of Methimazole in Graves' Disease and the Association With the Severity of Inflammation in Hashimoto's Thyroiditis**
Sara Trzos, Paweł Link-Lenczowski, Grzegorz Sokołowski and Ewa Pocheć
- 96 Distinct N-Linked Immunoglobulin G Glycosylation Patterns Are Associated With Chronic Pathology and Asymptomatic Infections in Human Lymphatic Filariasis**
Tomabu Adjobimey and Achim Hoerauf
- 108 Core Fucosylation Regulates the Function of Pre-BCR, BCR and IgG in Humoral Immunity**
Yuhan Sun, Xueying Li, Tiantong Wang and Wenzhe Li
- 120 Sialylation as an Important Regulator of Antibody Function**
Ravi Vattepu, Sunny Lyn Sneed and Robert M. Anthony



Editorial: Immunoglobulin Glycosylation Analysis: State-of-the-Art Methods and Applications in Immunology

Irena Trbojević-Akmačić^{1*}, Mohamed Abdel-Mohsen², David Falck³ and Erdmann Rapp^{4,5}

¹ Glycoscience Research Laboratory, Genos Ltd, Zagreb, Croatia, ² The Wistar Institute, Philadelphia, PA, United States,

³ Leiden University Medical Center, Center for Proteomics and Metabolomics, Leiden, Netherlands, ⁴ Max Planck Institute for Dynamics of Complex Technical Systems, Magdeburg, Germany, ⁵ glyXera GmbH, Magdeburg, Germany

Keywords: Fc receptors, glycosylation, glycomics, IgG, immunoglobulins, inflammation, infection

Editorial on the Research Topic

Immunoglobulin Glycosylation Analysis: State-of-the-Art Methods and Applications in Immunology

OPEN ACCESS

Edited and reviewed by:

Harry W. Schroeder,
University of Alabama at Birmingham,
United States

*Correspondence:

Irena Trbojević-Akmačić
iakmacic@genos.hr

Specialty section:

This article was submitted to
B Cell Biology,
a section of the journal
Frontiers in Immunology

Received: 19 April 2022

Accepted: 02 May 2022

Published: 20 May 2022

Citation:

Trbojević-Akmačić I,
Abdel-Mohsen M, Falck D and
Rapp E (2022) Editorial:
Immunoglobulin Glycosylation
Analysis: State-of-the-Art Methods
and Applications in Immunology.
Front. Immunol. 13:923393.
doi: 10.3389/fimmu.2022.923393

Immunoglobulins (Igs) are critical in the ability of our immune system to recognize and eliminate pathogenic antigens. Igs are co- and post-translationally modified by oligosaccharides (glycans) that significantly impact their structural and functional properties. All five human Ig classes (IgG, IgA, IgM, IgD, and IgE) are glycosylated; and the glycosylation of IgG, in particular, has been studied in depth. Although IgG glycosylation varies between individuals, it is stable within an individual under homeostasis. During disease, IgG glycans can dramatically change making them promising early diagnostic and prognostic biomarkers for several inflammatory, infectious, and autoimmune conditions. The goal of this Research Topic is to cover 1) advancements in analytical approaches for Ig glycosylation analysis; 2) applications of state-of-the-art methodology/technology in exploring aberrant glycosylation patterns during illness/disease; and 3) recent findings on the functional relevance of Ig glycosylation in immunity during different physiological states.

Development of new analytical approaches facilitates the expansion of our knowledge of Ig glycosylation – from its regulation and functional effects in healthy conditions to changes in glycosylation before/during disease, their connection with disease progression, and success of therapeutic interventions. Sensitivity, simplicity, and throughput are three key aims of current methodological development. The GlycoFibroTyper platform of Scott et al. exemplifies this quest for robust methods using minute amounts of sample to tackle large numbers in patients and/or longitudinal samples. The authors combine an antibody capture slide array with direct detection by matrix-assisted laser desorption/ionization (MALDI) (imaging) mass spectrometry (IMS) of PNGase F-released N-glycans – both microarrays and MALDI-MS are well established in high-throughput glycomics. The minimal sample preparation deviates from the dominant liquid chromatography (LC)-MS or LC-fluorescence approaches (1). Though much method development is still focused on IgG, the current advances in sensitivity will hopefully make the analysis of the remaining Ig isotypes more commonplace in the future (2).

IgG glycosylation depends on several demographic, genetic, and environmental factors (such as age, sex, ethnicity, and exercise). Genetic studies provide information on glycosylation regulation. We still know little due to the lack of a direct genetic template and the complexity of glycosylation. Li et al. aim at filling this gap by providing an atlas of genetic regulatory loci related to IgG N-glycosylation with their

target genes within functionally relevant tissues. This work implies that the IgG N-glycome is specific for individual tissues. Thereby, it consistently goes beyond general genome-wide association studies (GWAS) (3) in recognizing the impact of the B cell microenvironment (4). The latter also seems (indirectly) affected by estrogen. For example, Mijakovac et al. have explored estrogens impact on IgG glycosylation in the context of menopausal changes.

Glycosylation of Igs is shown to change in various pathological states and has been studied in different diseases. Nevertheless, mechanisms of these changes are still largely unexplored. The main question whether glycosylation changes are a cause or consequence (or both) of disease mostly remains unanswered. IgG glycosylation has been recently studied in the context of thyroid autoimmunity, Hashimoto's thyroiditis and Graves' disease, by Trzos et al., connecting IgG glycosylation and Hashimoto's thyroiditis severity as well as demonstrating an impact of immunosuppressive methimazole therapy on the IgG N-glycome in Graves' disease. A further study in the parasitic disease lymphatic filariasis by Adjobimey and Hoerauf demonstrates the broad relevance of the IgG N-glycome. However, this fuels the need to control for common comorbidities, for example with endemic controls. Distinct glycan profiles have been observed in endemic normal, asymptomatic individuals bearing microfilaria and patients with chronic pathology. Most notably, agalactosylated and afucosylated IgG distinguished chronic from asymptomatic patients. Linking immune competence and IgG N-glycome composition, detailed characterization on the level of individual subclasses, or antigen-specific antibodies would provide even more insight into these diseases and underlying mechanisms. The IgG subclass-specific glycosylation signatures of liver fibrosis stages obtained by Scott et al. may serve as an example. Demonstrating a greater diagnostic performance than other non-invasive liver fibrosis tests, e.g. APRI, FIB4, their comparably simple workflow highlights the potential attractiveness of IgG glycome analysis for future clinical practice.

The functional relevance of IgG glycosylation is well established and current knowledge of IgG glycosylation in different physiological states is reviewed by Zlatina and Galuska. One of the most established examples of functional effects of glycosylation is core fucosylation at Asn297 of the IgG Fc fragment that results in lower affinity toward Fcγ receptor (FcγR) IIIa, decreasing antibody-dependent cell-mediated cytotoxicity (ADCC) (Sun et al.). Various

functions and pathways of Ig sialylation, another important regulator of Ig effector functions, have been highlighted by Vattepu et al. Consequently, glycoengineering has been developed to improve the anti-inflammatory properties of intravenous immunoglobulin (IVIg) often used as a treatment for different inflammatory and autoimmune diseases (Vattepu et al.). IVIg likely has many mechanisms of action although it's often reduced to sialylated IgG glycans that diminish the affinity of IgG for activating FcγRs and promote recognition by DC-SIGN leading to the expression of inhibitory FcγRIIb. Research by Mimura et al. demonstrates that galactosylated nonfucosylated IgG, which has a high affinity for FcγRIIIa, has a 20 times higher potency to inhibit ADCC compared to native IgG. These findings indicate that IVIg anti-inflammatory activity is partially mediated by blocking FcγRs on immune cells preventing activation, for example by autoantibodies. Glycoengineered recombinant Fc proteins may be a more efficient alternative to plasma-derived IVIg in inflammatory conditions, although binding to the low-affinity FcγRs is not entirely independent of the antigen-binding fragment. Effects of antibody glycoengineering could be tested on e.g. rhesus macaques, a common non-human primate model. The work of Crowley et al. expands our knowledge on the preferences of macaque FcγRs to specific human IgG1 glycovariants and demonstrates this model species' suitability for evaluation of FcγRs affinity glycoforms. While Ig(G) glycosylation and its functionality are mostly studied in humans and mice, analogous studies in other animals are still lacking, leaving this area largely unexplored. Current knowledge on Ig glycosylation in farm animals is reviewed by Zlatina and Galuska revealing that there are notable differences in Ig glycosylation between animals.

AUTHOR CONTRIBUTIONS

IT-A wrote the initial draft which all authors critically revised and edited. All authors approved the final version.

FUNDING

DF received funding from the Dutch Research Council (NWO) in the framework of the ENW PPP Fund for the top sectors (project Proteoform-resolved pharmacokinetics of biopharmaceuticals, no. 019.012).

Stimuli. *Mol Cell Proteomics* (2011) 10:1–12. doi: 10.1074/mcp.M110.004655

Conflict of Interest: IT-A is an employee of Genos Ltd, a private research organization that specializes in high-throughput glycomic analysis. ER is co-affiliated to Max Planck Institute for Dynamics of Complex Technical Systems and glyXera. He is founder and CEO of glyXera GmbH, providing high-performance glycoanalytical products and services.

The remaining authors declare that the research was conducted in the absence of any commercial or financial relationships that could be construed as a potential conflict of interest.

Publisher's Note: All claims expressed in this article are solely those of the authors and do not necessarily represent those of their affiliated organizations, or those of the publisher, the editors and the reviewers. Any product that may be evaluated in this

REFERENCES

- de Haan N, Falck D, Wührer M. Monitoring of Immunoglobulin N- and O-Glycosylation in Health and Disease. *Glycobiology* (2020) 30:226–40. doi: 10.1093/glycob/cwz048
- Chandler KB, Mehta N, Leon DR, Suscovich TJ, Alter G, Costello CE. Multi-Isotype Glycoproteomic Characterization of Serum Antibody Heavy Chains Reveals Isotype- and Subclass-Specific N-Glycosylation Profiles. *Mol Cell Proteomics* (2019) 18:686–703. doi: 10.1074/mcp.RA118.001185
- Klarić L, Tsepilov YA, Stanton CM, Mangino M, Sikka TT, Esko T, et al. Glycosylation of Immunoglobulin G Is Regulated by a Large Network of Genes Pleiotropic With Inflammatory Diseases. *Sci Adv* (2020) 6:eaa0301. doi: 10.1126/sciadv.aax0301
- Wang J, Balog CIA, Stavenhagen K, Koeleman CAM, Scherer HU, Selman MHJ, et al. Fc-Glycosylation of IgG1 Is Modulated by B-Cell

article, or claim that may be made by its manufacturer, is not guaranteed or endorsed by the publisher.

Copyright © 2022 Trbojević-Akmačić, Abdel-Mohsen, Falck and Rapp. This is an open-access article distributed under the terms of the Creative Commons Attribution

License (CC BY). The use, distribution or reproduction in other forums is permitted, provided the original author(s) and the copyright owner(s) are credited and that the original publication in this journal is cited, in accordance with accepted academic practice. No use, distribution or reproduction is permitted which does not comply with these terms.



Effects of Estradiol on Immunoglobulin G Glycosylation: Mapping of the Downstream Signaling Mechanism

OPEN ACCESS

Edited by:

Mohamed Abdel-Mohsen,
Wistar Institute, United States

Reviewed by:

Adam Barb,
University of Georgia, United States
Amit Kumar Singh,
National Institute on Aging,
United States

*Correspondence:

Vlatka Zoldoš
vzoldos@biol.pmf.hr
Gordan Lauc
glauc@pharma.hr

[†]These authors have contributed
equally to this work

Specialty section:

This article was submitted to
B Cell Biology,
a section of the journal
Frontiers in Immunology

Received: 18 March 2021

Accepted: 06 May 2021

Published: 25 May 2021

Citation:

Mijakovac A, Jurić J, Kohrt WM,
Krištić J, Kifer D, Gavin KM, Miškec K,
Frkatović A, Vučković F, Pezer M,
Vojta A, Nigrović PA, Zoldoš V and
Lauc G (2021) Effects of
Estradiol on Immunoglobulin G
Glycosylation: Mapping of the
Downstream Signaling Mechanism.
Front. Immunol. 12:680227.
doi: 10.3389/fimmu.2021.680227

Anika Mijakovac^{1†}, Julija Jurić^{2†}, Wendy M. Kohrt^{3,4}, Jasminka Krištić², Domagoj Kifer⁵,
Kathleen M. Gavin^{3,4}, Karlo Miškec¹, Azra Frkatović², Frano Vučković², Marija Pezer²,
Aleksandar Vojta¹, Peter A. Nigrović^{6,7}, Vlatka Zoldoš^{1*} and Gordan Lauc^{2,5*}

¹ Department of Molecular Biology, University of Zagreb Faculty of Science, Zagreb, Croatia, ² Genos Glycoscience Research Laboratory, Zagreb, Croatia, ³ Division of Geriatric Medicine, School of Medicine, University of Colorado Anschutz Medical Campus, Aurora, CO, United States, ⁴ Eastern Colorado VA Geriatric Research, Education and Clinical Center, Aurora, CO, United States, ⁵ Faculty of Pharmacy and Biochemistry, University of Zagreb, Zagreb, Croatia, ⁶ Division of Rheumatology, Immunology and Allergy, Brigham and Women's Hospital, Boston, MA, United States, ⁷ Division of Immunology, Boston Children's Hospital, Boston, MA, United States

Glycans attached to immunoglobulin G (IgG) directly affect this antibody effector functions and regulate inflammation at several levels. The composition of IgG glycome changes significantly with age. In women, the most notable change coincides with the perimenopausal period. Aiming to investigate the effect of estrogen on IgG glycosylation, we analysed IgG and total serum glycomes in 36 healthy premenopausal women enrolled in a randomized controlled trial of the gonadotropin-releasing hormone analogue (GnRH_{AG}) leuprolide acetate to lower gonadal steroids to postmenopausal levels and then randomized to transdermal placebo or estradiol (E₂) patch. The suppression of gonadal hormones induced significant changes in the IgG glycome, while E₂ supplementation was sufficient to prevent changes. The observed glycan changes suggest that depletion of E₂ primarily affects B cell glycosylation, while liver glycosylation stays mostly unchanged. To determine whether previously identified IgG GWAS hits *RUNX1*, *RUNX3*, *SPINK4*, and *ELL2* are involved in downstream signaling mechanisms, linking E₂ with IgG glycosylation, we used the FreeStyle 293-F transient system expressing IgG antibodies with stably integrated CRISPR/dCas9 expression cassettes for gene up- and downregulation. *RUNX3* and *SPINK4* upregulation using dCas9-VPR resulted in a decreased IgG galactosylation and, in the case of *RUNX3*, a concomitant increase in IgG agalactosylation.

Keywords: immunoglobulin G glycosylation, estradiol, CRISPR, inflammation, Runx3

INTRODUCTION

Most proteins in human serum are glycosylated by the covalent addition of diverse glycan structures that fine-tune their function. The regulatory role of glycans has been most extensively explored on immunoglobulin G (IgG) antibodies, where different glycoforms regulate the immune response on multiple levels (1). Glycans attached to the Fc part of the IgG molecule affect interactions with different Fc receptors, which is why changes in glycosylation have direct effects on the immune system at multiple levels (2). IgG glycosylation is altered in many diseases (3), and glycan changes can even appear before the onset of disease symptoms (4–6). In some cases, changes in IgG glycans were shown to be a causative element contributing to the disease development (7–9). IgG glycans that associate with age are known functional effectors of inflammation, and changes in IgG glycosylation seem to be an important factor contributing to ageing at the molecular level (10–12) that can also be used as a biomarker to track individual trajectories of biological ageing (13).

In women, the most prominent change of glycan age coincides with the perimenopausal period (10). A recent intervention study demonstrated that estrogen regulates IgG glycosylation (14), which may explain why perimenopausal females undergo significant changes in the IgG glycome composition. Unfortunately, limitations of the glycoprofiling method used in that study, *i.e.* only IgG galactosylation was estimated from the total plasma glycome profile, prevented us from the detailed characterization of the estrogen effect on IgG glycosylation. In the present study, we aimed at a better understanding of the estrogen role in the regulation of IgG glycosylation, therefore we reanalyzed samples from the previous intervention study (14) using state-of-the-art glycoprofiling technologies (15). We first defined the components of IgG glycome affected by estradiol (E_2). We then used data from our recent large genome-wide association study (GWAS) of the IgG glycome (16) to identify candidate genes possibly involved in mediating effects of E_2 on IgG glycosylation. We selected four gene loci, *RUNX1–RUNX3*, *SPINK4*, and *ELL2*, involved in E_2 downstream signaling mechanisms, assuming that these loci represent a part of the molecular pathway linking E_2 to IgG glycosylation. *In vitro* system used in this study was based on a FreeStyle 293-F (HEK-293FS) transient expression system optimized for secreting a high quantity of native IgG antibodies (16). The system was modified by stable integration of CRISPR/dCas9 expression cassette containing either VPR (for gene upregulation) or KRAB (for gene downregulation). Using this system, we were able to demonstrate the effects of selected genes on specific IgG glycans which were previously associated with biological ageing.

METHODS

Institutional Approval

This study was conducted at the University of Colorado Anschutz Medical Campus (CU-AMC). All procedures were

performed in accordance with the ethical standards and approved by the Colorado Multiple Institutional Review Board (COMIRB) and the Scientific Advisory and Review Committee at the University of Colorado Anschutz Medical Campus (CU-AMC). The study was registered on ClinicalTrials.gov (NCT00687739) on May 28, 2008.

Participants and Screening Procedures

Participants were healthy eumenorrheic premenopausal women who volunteered to take part in the study. All volunteers underwent screening procedures, as described previously (17). The main inclusion criteria were age (25 to 49 years) and regular menstrual cycle function [no missed cycles in the previous year, cycle length 28 ± 5 days and confirmation of ovulatory status (ClearPlan Easy, Unipath Diagnostics, Waltham, MA)]. Exclusion criteria were pregnancy or lactation, hormonal contraception, oral glucocorticoids or diabetes medications, smoking, and body mass index (BMI) >39 kg/m². Following the Declaration of Helsinki, all volunteers provided written informed consent to participate, with the knowledge that the risks of the study included menopause-like effects (e.g., weight gain, bone loss, menopausal symptoms).

Experimental Design and Study Procedures

The parental trial was a randomized, double-blinded, placebo-controlled trial to determine the effects of estradiol (E_2) deficiency on body composition, bone mineral density, components of energy expenditure and physical activity in premenopausal women (17, 18). In short, all participants underwent suppression of ovarian sex hormones with gonadotropin-releasing hormone agonist therapy (GnRH_{AG}, leuprolide acetate 3.75 mg, Lupron; TAP Pharmaceutical Products, Inc; Lake Forest, IL) in the form of monthly intramuscular injections. A single injection of leuprolide acetate produces an initial stimulation (for 1 to 3 weeks) followed by a prolonged suppression of pituitary gonadotropins FSH and LH, while repeated monthly dosing suppresses ovarian hormone secretion (19). A urine pregnancy test confirmed the absence of pregnancy before each dosing. After completing the screening procedures, eligible volunteers underwent baseline testing during the early follicular phase (days 2 to 6 after the onset of menses) of the menstrual cycle. At the beginning of the following menstrual cycle, participants began 5-months of GnRH_{AG} therapy to suppress ovarian function. Participants were randomized to receive either transdermal E_2 0.075 mg/d (Bayer HealthCare Pharmaceuticals, Berkeley, CA) or placebo patches (GnRH_{AG} + E_2 , $n = 15$; GnRH_{AG} + PL, $n = 21$). The E_2 regimen kept serum E_2 concentrations in the mid-to-late follicular phase range (100 to 150 pg/ml). To reduce the risk of endometrial hyperplasia and minimize exposure to progesterone, women randomized to E_2 received medroxyprogesterone acetate (5 mg/d, as a pill) for 12 days every other month (end of months 2 and 4, and after completion of follow-up testing). During these monthly visits, participants were under supervision of the research nurse practitioner. Participants

were asked to report health and medication use changes (e.g., doctor visits, hospitalizations), as well as any study-related problems/concerns over the past 4 weeks.

Sample Collection

Blood samples were collected at three timepoints: during baseline testing (T1), during week 20 of the hormonal intervention (T2), and at the spontaneous recovery of the normal menstrual cycle function, approximately 4-months after completion of the drug intervention (T3). A single sample (~5 ml) was obtained in the morning (~8 AM), after an overnight fast (at least 10 h). Baseline samples were obtained immediately before the first GnRH_{AG} injection. Serum was separated from each collected sample upon blood withdrawal and stored at -80°C until analysis.

Sex Hormone Concentration

Collected sera were analyzed for numerous sex hormones. Estrone (E1), estradiol (E2) and progesterone (P) concentrations were determined by radioimmunoassay (RIA, Diagnostic Systems Lab, Webster, TX). Total testosterone (T) concentration was determined by chemiluminescence immunoassay (Beckman Coulter, Inc. Fullerton, CA), and sex hormone-binding globulin (SHBG) concentration was determined by immunoradiometric assay (Diagnostic Systems Laboratory).

Isolation of Immunoglobulin G, Release and Labeling of N-Glycans From IgG

The whole procedure was performed according to the already published protocol (20). In short, IgG was isolated from sera (100 µl) by affinity chromatography using a 96-well plate with protein G coupled to a monolithic stationary phase (BIA Separations, Slovenia). The isolated IgG was denatured with the addition of SDS (Invitrogen, USA) and incubation at 65°C, after which the excess of SDS was neutralized with Igepal CA-630 (Sigma-Aldrich, USA). N-glycans were released from IgG with the addition of PNGase F (Promega, USA) in a PBS buffer during the overnight incubation at 37°C. The released glycans were fluorescently labelled with 2-AB dye (Merck, Germany) in the 2 h incubation at 65°C. Free label and reducing agent were removed from the samples by hydrophilic interaction liquid chromatography solid phase extraction (HILIC-SPE). IgG N-glycans were eluted with ultrapure water and stored at -20°C.

Release and Labeling of N-Glycans From Total Serum Proteins

The whole procedure was performed as described previously (4). In short, serum proteins (10 µl) were denatured by SDS and incubated at 65°C. Excess SDS was neutralized by Igepal CA-630 (Sigma-Aldrich, USA). Serum proteins were deglycosylated by PNGase F (Promega, USA) in a PBS buffer during the overnight incubation at 37°C. Released glycans were fluorescently labelled with 2-AB dye (Merck, Germany) in the 2h incubation time at 65°C. Excess of reagents and proteins from previous steps was removed by hydrophilic interaction liquid chromatography solid phase extraction (HILIC-SPE). Serum N-glycans were eluted with ultra-pure water and stored at -20°C.

Hydrophilic Interaction Chromatography (HILIC)-UPLC Analysis of Labeled Glycans

Fluorescently labeled N-glycans were separated by ultra-performance liquid chromatography (UPLC) on a Waters Acquity UPLC H-Class Instrument consisting of a sample manager, quaternary solvent manager, and a fluorescence (FLR) detector set with excitation and emission wavelengths at 250 and 428 nm, respectively. The UPLC system was under the control of Empower 3 software, build 3471 (Waters, USA). Labeled N-glycans were separated on an amide ACQUITY UPLC[®] Glycan BEH chromatography column (Waters, USA), 100 × 2.1 mm i.d. for IgG glycans and 150 × 2.1 mm for glycans from total serum proteins, 1.7 µm BEH particles, with 100 mM ammonium formate pH 4.4 as solvent A, and 100% acetonitrile as solvent B. The separation method used a linear gradient of 75–62% acetonitrile at a flow rate of 0.40 ml/min in a 27 min analytical run for IgG glycans and a linear gradient of 70–53% acetonitrile at a flow rate of 0.561 ml/min in a 23 min analytical run for glycans from total serum proteins. Samples were kept at 10°C before injection onto the column. The separation temperature of the column was 60°C for the IgG glycans and 25°C for glycans from serum proteins. Data processing included an automatic integration method that was manually corrected to maintain the same intervals of chromatographic integration across all samples. Chromatograms were separated in the same manner into 24 peaks for IgG N-glycans and 39 peaks for N-glycans from total serum proteins. The abundance of glycans in each chromatographic peak was expressed as a percentage of the total integrated area (% area).

Plasmid Constructs

Plasmid constructs pORF-hp21 and pORF-hp27 used to enhance protein production were obtained from Invivogen, while p3SVLT was constructed by cloning a codon-optimized version of the SV40 large T antigen coding region (16) in pcDNA3 (Addgene). Unwanted BsaI restriction sites in IgG heavy and light chain (kindly provided by Gestur Vidarsson, Sanquin, Amsterdam) were removed using QuikChange Lightning Site-Directed Mutagenesis Kit (Agilent). IgG chains were then cloned into pUK21gg for the subsequent Golden Gate cloning step. Expression plasmids encoding gene-specific guide RNA (gRNA) molecules were constructed in the multi-guide system described by Josipović et al. (21). Three gRNA molecules were cloned individually in a backbone plasmid pSgMx-A or pSgMx-G (where x represents the order of gRNA molecules; 1,2,3 and A or G represents Cas9 ortholog (dSaCas9 or dSpCas9 respectively) it recognizes) (22) for each gene: *RUNX1*, *RUNX3*, *SPINK4* and *ELL2*. gRNA molecules for *RUNX1*, *RUNX3*, *ELL2* and *SPINK4* were then cloned in pSgx3 as modular “multiguide” molecules. Two non-targeting gRNA molecules and one gRNA molecule targeting *B4GALT1* for dSaCas9 and dSpCas9 were cloned in the same way described above. Together with modules for antibody heavy chain (HC) and light chain (LC), Cbh promoter and bGH terminator, single guide or multiguide RNA molecules were cloned in a backbone pBackBone-BZ by modular Golden Gate cloning method described in Josipović

et al. (21). Sequences of gRNA molecules and details of plasmids/modules used in Golden Gate cloning are given in **Supplementary Tables 6, 7**.

Cell Culture and Transfections

Stable cell lines PB-dSaCas9-VPR-1 and PB-dSpCas9-KRAB-3 were established from FreeStyle™ 293-F cells (Gibco) with piggyBac transposon system by limiting dilution method (unpublished data) and maintained in FreeStyle™ 293 Expression Medium (Gibco) in 125 ml Erlenmeyer flasks (Nalgene) and cultivated at 37°C in the atmosphere with 8% CO₂ on PSU-20i Multi-functional Orbital Shaker at 140 rpm according to the protocol from Vink et al. (16). Transfections of stable cell lines were done using 293fectin Transfection Reagent (Gibco) according to the manufacturer's protocol optimized for 2 ml per well. When cells reached ≥90 viability, they were plated in non-treated 6-well plates at a concentration of 500,000 cells/ml and were transfected with 2 µg of plasmids diluted in Opti-MEM I Reduced Serum Medium (Gibco) to reach a volume of 80 ml. For enhanced expression of immunoglobulin G, cells were transfected with a plasmid containing gRNA and IgG heavy and light chain, p3SVLT, pORF-hp21 and pORF-hp27 in the ratio: 0.69/0.01/0.05/0.25 (16). Cells were collected 5 days after transfection by centrifugation at 4,000g (5 min). The cell pellet was used for gene expression profiling, while the supernatant was used for glycan analysis.

Quantitative Real-Time PCR (qPCR)

For gene expression profiling, total RNA was extracted with RNeasy Mini Kit (Qiagen) from cell pellets collected five days after transfection. Reverse transcription was done on 50 ng of total isolated RNA using the PrimeScript RTase (TaKaRa) and random hexamer primers (Invitrogen) for TaqMan Gene Expression Assay or on 5 ng of total isolated RNA (pretreated with TURBO DNase (Invitrogen)) for SYBR Green Gene Expression Assay. Both variants of RT-qPCR were performed according to the manufacturer's protocol using the 7500 Fast Real-Time PCR System using TaqMan Gene Expression Master Mix with the following assays: Hs01021970_m1 (RUNX1), Hs00205508_m1 (SPINK4), Hs01023022_m1 (ELL2), Hs00155245_m1 (B4GALT1) and Hs02800695_m1 (HPRT1) or PowerUp SYBR Green Master Mix with primer sequences listed in **Supplementary Table 8**. The mean value of 12 replicates was normalized to the expression of the *HPRT1* gene as endogenous control and was analysed using the $\Delta\Delta C_t$ method (23). Fold change (FC) was shown relative to gene expression in cells transfected with a plasmid expressing non-targeting gRNA.

IgG Isolation From FreeStyle™ 293-F Cells, N-Glycan Release, Labeling and HILIC-UPLC Analysis

IgG was isolated from FreeStyle 293-F cell culture supernatants using Protein G Agarose fast flow beads (Merck, Germany). The beads were prewashed three times with 10× bead volume of 1× PBS. In each washing step, beads were resuspended in 1× PBS, centrifugated at 150×g for 10 s, and the supernatant was

removed. After the last wash, prewashed beads were resuspended in 1× PBS to make a 50:50 (v/v) beads slurry. Approximately 2 ml of FreeStyle 293-F cell culture supernatant were mixed with an equal volume of 1× PBS and 40 µl of prepared 50% bead slurry in a 5 ml tube. The samples were resuspended by pipetting action and incubated 1 h at room temperature with gentle shaking to allow IgG to bind to the beads. During the incubation period, the samples were resuspended twice by pipetting action. After incubation, the samples were centrifugated at 150×g for 10 s, and the supernatants were then carefully removed and discarded. The beads were washed three times with 300 µl of 1× PBS and three times with 300 µl of ultrapure water to remove non-specifically bound proteins. After washing steps, bound IgG was eluted by incubating the beads in 100 µl of 0.1 M formic acid (Merck) for 15 min at room temperature with gentle shaking. Eluted IgG was neutralised with 17 µl of 1M ammonium bicarbonate (Merck, Germany). IgG concentration in the eluate was measured using Nanodrop 8000 (Thermo Scientific, USA). Samples were subsequently dried in a vacuum concentrator.

N-glycan release, glycan labeling, clean-up of glycans and separation of glycans by HILIC-UHPLC were performed according to a previously established protocol (20) with some modifications. Briefly, dried IgG was denatured by SDS (Invitrogen, USA) and heated at 65°C. The excess of SDS was neutralised with Igepal CA-630 (Merck, Germany), and N-glycans were released by 18 h of incubation with PNGaseF (Promega, USA). The released glycans were fluorescently labeled with procainamide in a two-step reaction. In the first step, 25 µl of freshly prepared labeling solution, containing 172.8 mg/ml of procainamide hydrochloride (Thermo Fisher Scientific, USA) in a mixture of DMSO (Merck, Germany) and glacial acetic acid (Merck, Germany) (70:30, v/v), was added to each sample followed by incubation for 1 h at 65°C. Then in the next step, 25 µl of freshly prepared solution, containing 179.2 mg/ml of 2-picoline borane as a reducing agent in a mixture of DMSO and acetic acid (70:30, v/v), was added to each sample followed by incubation for 1.5 h at 65°C. Free label and reducing agent were removed from the samples using hydrophilic interaction liquid chromatography solid-phase extraction (HILIC-SPE) on a 0.2 µm GHP filter plate (Pall Corporation, USA). Glycans were eluted with ultrapure water and stored at -20°C until use. Fluorescently labeled N-glycans were separated by hydrophilic interaction chromatography on a Waters Acquity UPLC instrument (Waters, USA) consisting of a quaternary solvent manager, sample manager and FLR fluorescence detector set with excitation and emission wavelengths of 310 and 370 nm, respectively. The instrument was under the control of Empower 3 software, build 3471 (Waters, USA). Labeled N-glycans were separated on a Waters BEH Glycan chromatography column, 100 × 2.1 mm i.d., 1.7 µm BEH particles, with 100 mM ammonium formate, pH 4.4, as solvent A and ACN as solvent B. The separation method used a linear gradient of 75–62% ACN (v/v) at a flow rate of 0.4 ml/min over 31 min. Samples were maintained at 10°C before injection, and the separation temperature was 60°C. The system was calibrated using an external standard of hydrolyzed and procainamide-labeled glucose oligomers from which the retention

times for the individual glycans were converted to glucose units (GU). Data processing was performed using an automatic processing method with a traditional integration algorithm, after which each chromatogram was manually corrected to maintain the same intervals of integration for all the samples. The chromatograms were separated in the same manner as chromatograms of human plasma/serum-derived IgG glycans into 24 peaks, and the abundance of glycans in each peak was expressed as a percentage of the total integrated area. The structural assignment of the glycans present in the chromatographic peaks was done based on i) overlay with the chromatogram of human plasma IgG glycans for which structures corresponding to each peak had been previously determined (24) and ii) GU values of the glycan peaks using the GlycoStore database (www.glycostore.org).

Statistical Analysis

The area under chromatogram peaks was normalized to total chromatogram area, then each glycan peak was logit transformed, and batch corrected using ComBat method (R package 'sva') (25). Data were back transformed, and derived glycan traits were calculated as a sum or ratio of selected directly measured glycan peaks based on particular glycosylation features (i.e. sialylation or fucosylation).

Mixed models were used to estimate the effect of the intervention (R package 'lme4') (26). Hormone concentration or particular glycan level was set as dependent variable and timepoint (with levels: *baseline*, *after intervention* and *after recovery*) nested within the treatment group (*placebo* and *estradiol*) as independent variables. Also, the model was age-adjusted, and the subject's ID was included as a random intercept to account for variation between the subjects.

Change in estradiol and change in glycan abundance were calculated by subtracting values of consecutive timepoints. Mixed models were used to estimate the relationship between the change in glycans and the change in estradiol concentration.

mixed models were used. The change in glycan abundance was defined as a dependent variable, while the change in estradiol concentration was defined as a fixed effect. Group and time period nested within the group were defined as random factors. Both change in glycan abundance and change in estradiol concentration were transformed to a standard normal distribution by inverse transformation of ranks to normality.

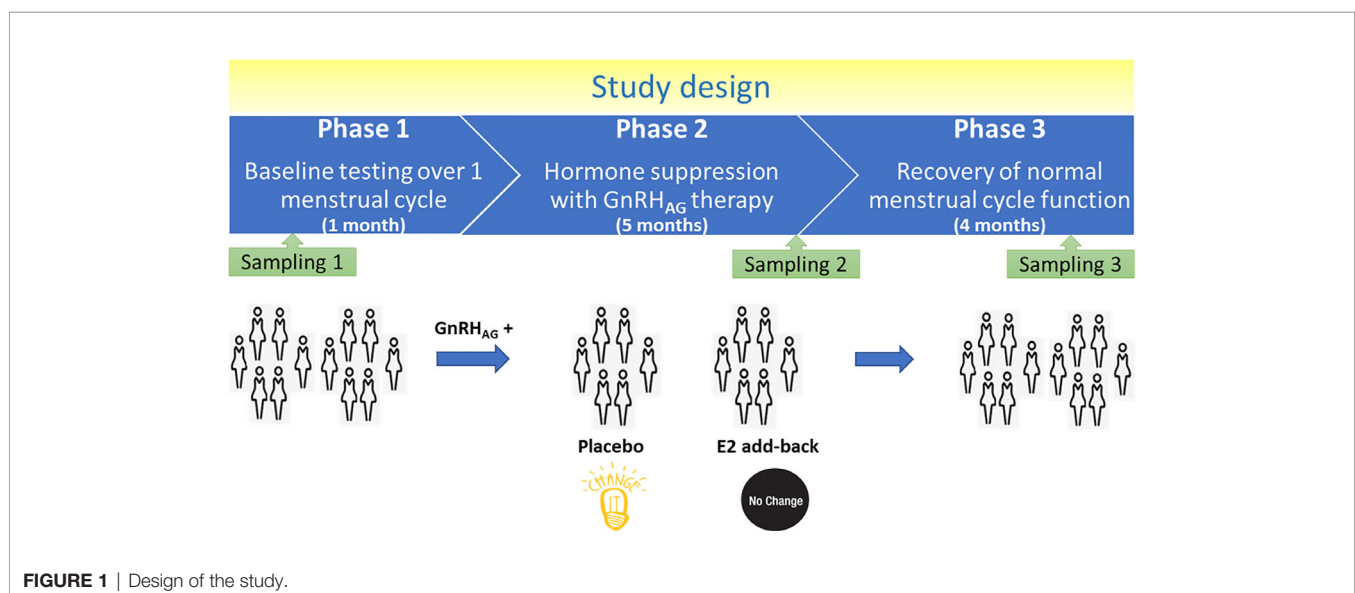
Prior modeling, glycan levels were transformed to a standard normal distribution by inverse transformation of ranks to normality (R package 'GenABEL') (27), while hormone concentrations were log transformed. Based on fitted models, changes of dependent variables after intervention or recovery (relative to baseline) were compared between the groups (placebo vs estradiol) using *post-hoc* t-test. False discovery rate was controlled using the Benjamini–Hochberg method at a significance level of 0.05.

Differences between groups for gene expression and glycan levels following CRISPR/dCas9 manipulations were tested using the non-parametric Mann–Whitney test. Results with $p < 0.05$ were considered statistically significant. All statistical analyses were performed in R programming software (version 3.6.3) (28).

RESULTS

IgG Glycome Is Affected by Estradiol

Thirty-six healthy premenopausal women were enrolled in a randomized controlled trial of the gonadotropin-releasing hormone analogue (GnRH_{AG}) leuprolide acetate to lower gonadal steroids to postmenopausal levels and then randomized to transdermal placebo (PL) or estradiol (E₂) patch (**Figure 1**) (17). In order to analyse total serum and IgG glycomes, serum samples were collected: at baseline (Sampling 1); after five months of GnRH_{AG} administration with concurrent supplementation with either E₂ or placebo (Sampling 2); and four

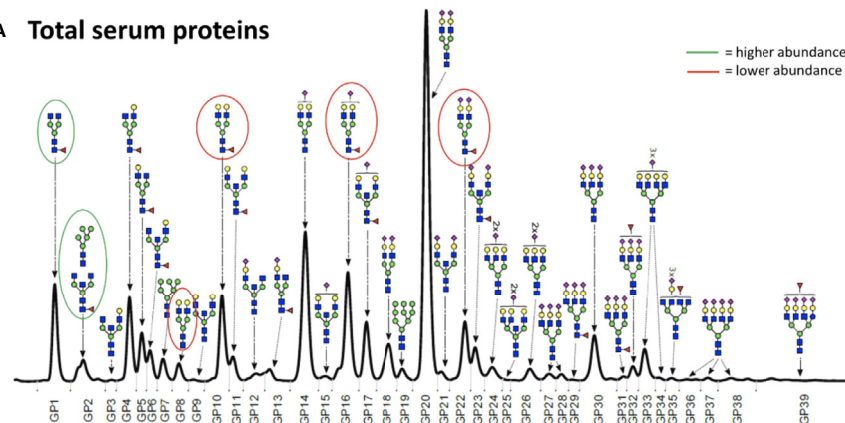


months after the end of the intervention, when natural hormonal cycling was restored (Sampling 3). **Figure 2** shows representative UHPLC chromatograms of the total serum (Figure 2A) and IgG (Figure 2B) glycomes and the direction of glycan changes after the suppression of gonadal hormones. IgG glycosylation analysis revealed significant changes in IgG glycome composition after gonadal hormone suppression (time point at the end of Phase 2), while E₂ supplementation was sufficient to prevent changes in the IgG glycome composition (Figure 3, Table 1 and Supplementary Table 1). After four months of the recovery period (Sampling 3 after the end of Phase 3), the IgG glycome composition returned to nearly pre-intervention values in the placebo group. Galactosylation was the most affected IgG glycome feature, with a significant decrease of digalactosylated glycans (G2) and an increase of monogalactosylated (G1) and agalactosylated (G0) glycans. The level of sialylated glycans (S) and the ratio of sialylation and galactosylation (S/G) of IgG significantly decreased, while the abundance of glycans with bisecting GlcNAc (B) increased. Only the abundance of core-fucosylated (F) glycans did not change by depletion of E₂. IgG glycosylation traits related to galactosylation and sialylation, which were particularly affected by the suppression

of E₂, are also the main components of the glycan age clock of the biological age. This index has initially been developed to predict chronological age (10) but was subsequently converted into the test of biological age (29). Suppression of E₂ resulted in a median increase of GlycanAge by 9.1 years, which was completely attenuated by E₂ add-back (Supplementary Figure 1). At the individual level, the extent of changes in hormone concentration (Supplementary Table 2) correlated moderately with the extent of changes in individual IgG glycans (Supplementary Table 3), suggesting that other factors (beside gonadal hormones) also strongly affect the composition of the IgG glycome.

To determine whether the effects of E₂ on glycosylation were restricted to IgG, we also analysed total serum protein N-glycome in the same samples. Changes observed in the total serum N-glycome (Figure 4) were restricted only to some neutral glycans and core-fucosylated sialylated biantennary glycans known to originate nearly exclusively from immunoglobulins (30). This suggests that depletion of E₂ affects B cell (IgG) glycosylation, while liver glycosylation does not seem to be affected, at least not in a way that would alter proportions of individual non-immunoglobulin N-glycans in the total serum glycome (Figure 2A).

A Total serum proteins



B IgG

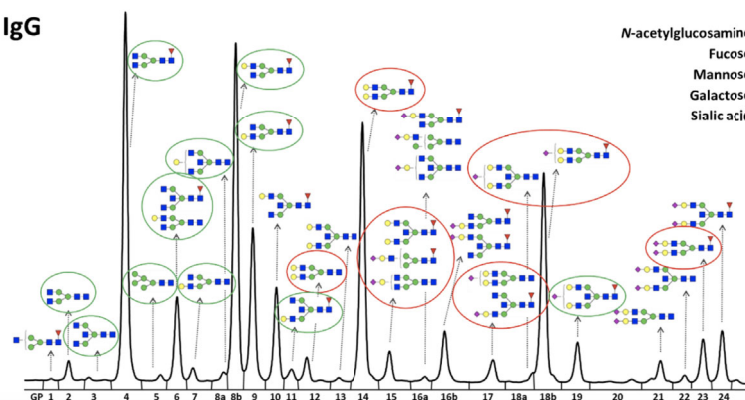


FIGURE 2 | Representative chromatograms of (A) the total serum glycome and (B) the IgG glycome. Glycans that decreased after the gonadal hormone suppression with gonadotropin-releasing hormone analogue leuprolide acetate (GnRH_{AG}) therapy are circled in red, and those that increased are circled in green.

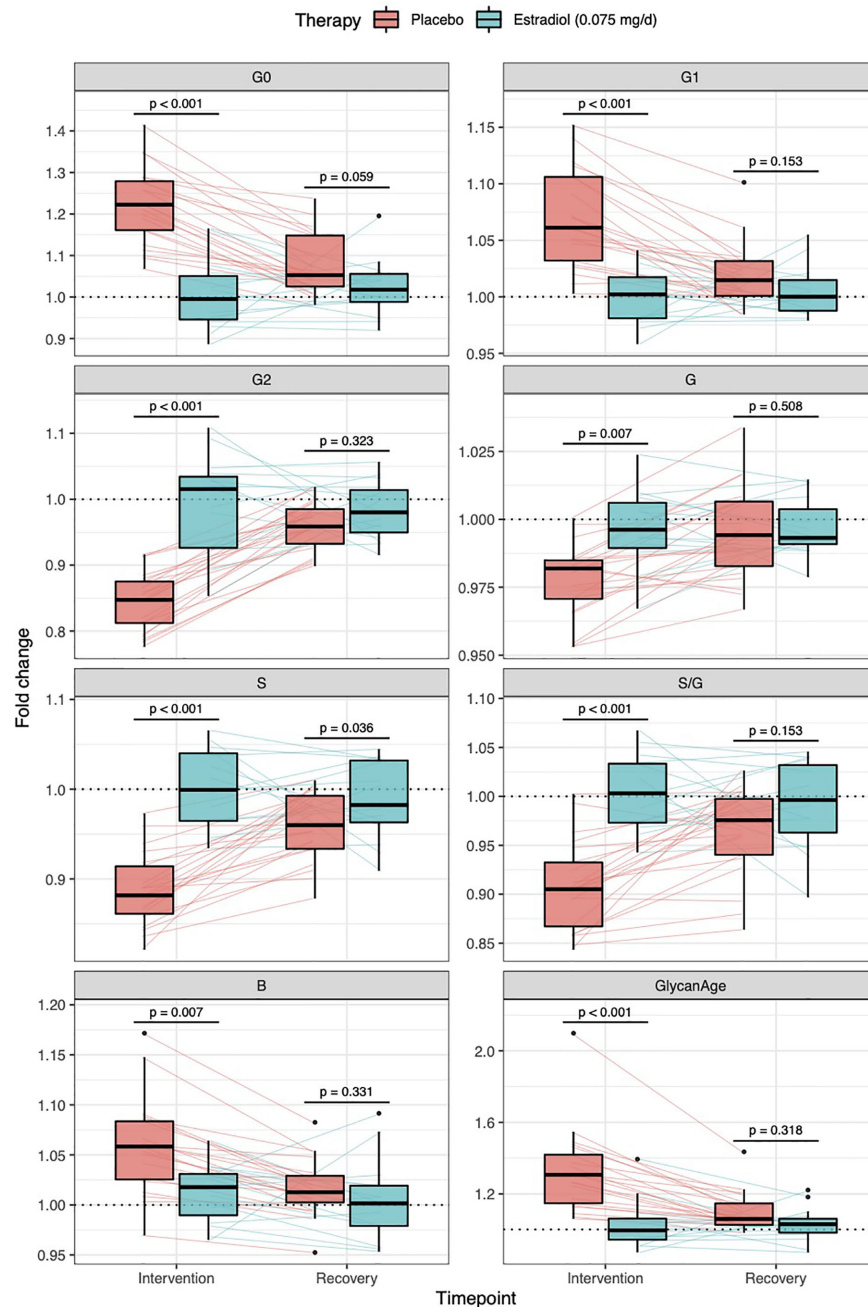


FIGURE 3 | Effects of gonadal hormone suppression on IgG glycosylation. Gonadotropin-releasing hormone analogue leuprolide acetate (GnRH_{AG}) was used to lower gonadal steroids to postmenopausal levels in healthy premenopausal women ($n = 36$) that were then randomized to transdermal placebo ($n = 21$) or estradiol patch ($n = 15$). Changes in the IgG glycome composition after five months of GnRH_{AG} (Intervention) with supplementation of E₂ (transdermal estradiol supplementation) or without supplementation of E₂ (supplementation with placebo) and four months after the end of the intervention (Recovery) are shown on the graph. G2, digalactosylated glycans; G1, monogalactosylated glycans; G0, agalactosylated glycans; S, sialylated glycans; S/G, ratio of sialylation and galactosylation; B, glycans with bisecting GlcNAc; G, all glycans with galactose.

Downstream Signaling Mechanisms Linking Estradiol With IgG Glycan Traits

Glycans are inherited as complex traits defined by multiple genes (31, 32) which play a role in the synthesis and variation of individual glycan structures. Through a series of GWAS papers in the last

decade (32–35), we mapped an extensive network of genes that potentially regulate the glycosylation of IgG. Using the Signalling Pathways Project (SPP) web knowledgebase (36), we explored the effects of E₂ on GWAS hits for IgG galactosylation and sialylation (35). Results presented in **Supplementary Figure 2** indicate that E₂

TABLE 1 | Glycan abundances (%) of directly measured IgG glycan traits at the baseline and deviations from the baseline after intervention and after recovery timepoint.

Glycan	Intervention	Glycan Abundance (%) at Baseline median (IQR)	Difference in glycan abundance (%) relative to baseline. sampling after:			
			Intervention median (IQR)	P _I	Recovery median (IQR)	P _R
GP1	Placebo	0.049 (0.040–0.051)	0.010 (0.008–0.012)	1.95×10^{-1}	0.002 (0.000–0.010)	1.48×10^{-1}
	Estradiol	0.069 (0.041–0.091)	0.009 (0.000–0.010)		–0.001 (–0.007–0.006)	
GP2	Placebo	0.269 (0.199–0.654)	0.102 (0.082–0.148)	3.53×10^{-6}	0.027 (–0.010–0.042)	1.48×10^{-1}
	Estradiol	0.361 (0.261–0.495)	–0.003 (–0.047–0.031)		0.005 (–0.026–0.028)	
GP3	Placebo	0.059 (0.059–0.070)	0.011 (0.009–0.013)	4.08×10^{-4}	0.003 (–0.001–0.011)	7.56×10^{-2}
	Estradiol	0.070 (0.061–0.096)	–0.006 (–0.010–0.004)		–0.001 (–0.008–0.003)	
GP4	Placebo	14.0 (12.4–17.6)	3.08 (2.35–3.93)	2.46×10^{-8}	0.869 (0.345–1.771)	6.58×10^{-2}
	Estradiol	17.3 (14.0–19.2)	–0.152 (–1.003–1.031)		0.187 (–0.374–0.847)	
GP5	Placebo	0.158 (0.143–0.180)	0.021 (0.011–0.028)	2.56×10^{-4}	0.009 (–0.004–0.015)	3.22×10^{-2}
	Estradiol	0.162 (0.155–0.194)	–0.004 (–0.010–0.006)		–0.004 (–0.013–0.005)	
GP6	Placebo	3.44 (2.98–4.28)	0.673 (0.567–0.824)	1.17×10^{-7}	0.200 (0.124–0.301)	1.48×10^{-1}
	Estradiol	3.71 (3.28–4.36)	0.067 (–0.114–0.253)		0.126 (–0.112–0.198)	
GP7	Placebo	0.363 (0.240–0.466)	0.039 (0.020–0.056)	3.51×10^{-3}	0.010 (–0.013–0.026)	4.56×10^{-1}
	Estradiol	0.394 (0.289–0.435)	–0.010 (–0.029–0.019)		0.000 (–0.016–0.014)	
GP8	Placebo	18.5 (17.5–19.9)	0.990 (0.604–1.246)	2.22×10^{-5}	0.139 (–0.189–0.474)	4.91×10^{-1}
	Estradiol	20.0 (18.5–21.0)	–0.030 (–0.351–0.208)		0.032 (–0.316–0.207)	
GP9	Placebo	9.66 (8.31–10.73)	0.843 (0.560–1.274)	1.14×10^{-7}	0.137 (–0.015–0.405)	3.64×10^{-1}
	Estradiol	9.69 (9.09–10.31)	–0.024 (–0.285–0.221)		0.069 (–0.050–0.313)	
GP10	Placebo	4.99 (4.69–5.38)	0.177 (0.127–0.358)	5.28×10^{-1}	0.087 (0.029–0.175)	3.50×10^{-1}
	Estradiol	4.65 (4.37–5.52)	0.125 (0.020–0.167)		–0.040 (–0.104–0.047)	
GP11	Placebo	0.636 (0.587–0.696)	0.051 (0.030–0.092)	2.46×10^{-4}	0.018 (0.000–0.031)	5.77×10^{-1}
	Estradiol	0.665 (0.555–0.715)	0.000 (–0.020–0.036)		0.015 (–0.004–0.030)	
GP12	Placebo	1.010 (0.621–1.333)	–0.178 (–0.256 to –0.129)	1.19×10^{-5}	–0.021 (–0.060–0.000)	9.52×10^{-1}
	Estradiol	0.781 (0.596–0.984)	0.000 (–0.095–0.020)		–0.020 (–0.062–0.010)	
GP13	Placebo	0.249 (0.211–0.281)	–0.010 (–0.029–0.011)	2.57×10^{-1}	–0.009 (–0.019–0.010)	4.90×10^{-1}
	Estradiol	0.230 (0.210–0.245)	0.008 (–0.020–0.019)		0.001 (–0.015–0.011)	
GP14	Placebo	20.1 (16.6–21.9)	–2.95 (–3.93 to –2.11)	4.71×10^{-7}	–0.735 (–1.383 to –0.315)	3.12×10^{-1}
	Estradiol	16.3 (14.8–18.8)	0.212 (–0.987–0.708)		–0.469 (–0.977–0.253)	
GP15	Placebo	1.98 (1.76–2.39)	–0.250 (–0.337 to –0.129)	5.39×10^{-7}	–0.031 (–0.107–0.018)	3.68×10^{-1}
	Estradiol	1.90 (1.55–2.05)	0.002 (–0.040–0.075)		–0.041 (–0.059–0.053)	

(Continued)

TABLE 1 | Continued

Glycan	Intervention	Glycan Abundance (%) at Baseline median (IQR)	Difference in glycan abundance (%) relative to baseline. sampling after:			
			Intervention median (IQR)	p_I	Recovery median (IQR)	p_R
GP16	Placebo	3.09 (2.54–3.38)	0.010 (–0.059–0.122)	4.78×10^{-1}	–0.019 (–0.088–0.039)	7.14×10^{-2}
	Estradiol	3.05 (2.89–3.26)	0.041 (–0.010–0.073)		0.026 (–0.002–0.067)	
GP17	Placebo	1.043 (0.835–1.086)	–0.100 (–0.177 to –0.060)	2.75×10^{-5}	–0.034 (–0.060 to –0.011)	1.95×10^{-1}
	Estradiol	0.895 (0.761–0.990)	–0.010 (–0.037–0.031)		0.008 (–0.048–0.016)	
GP18	Placebo	12.9 (10.3–14.1)	–2.42 (–2.99 to –1.92)	9.92×10^{-9}	–0.585 (–1.129 to –0.156)	3.23×10^{-1}
	Estradiol	11.0 (10.1–12.3)	–0.009 (–0.717–0.823)		–0.383 (–0.513–0.248)	
GP19	Placebo	1.87 (1.72–1.99)	0.062 (0.000–0.089)	9.19×10^{-3}	–0.043 (–0.064–0.039)	9.72×10^{-1}
	Estradiol	1.88 (1.61–2.18)	0.000 (–0.034–0.050)		–0.001 (–0.065–0.017)	
GP20	Placebo	0.418 (0.381–0.443)	–0.010 (–0.041–0.010)	1.75×10^{-2}	–0.014 (–0.048–0.007)	3.68×10^{-1}
	Estradiol	0.389 (0.346–0.418)	0.010 (–0.010–0.048)		0.006 (–0.014–0.019)	
GP21	Placebo	0.851 (0.762–0.974)	–0.029 (–0.051–0.022)	3.98×10^{-1}	–0.007 (–0.062–0.073)	7.58×10^{-1}
	Estradiol	0.790 (0.725–0.815)	0.010 (–0.032–0.036)		0.000 (–0.034–0.027)	
GP22	Placebo	0.12 (0.11–0.16)	0.001 (–0.020–0.010)	2.81×10^{-1}	–0.010 (–0.010–0.001)	8.83×10^{-1}
	Estradiol	0.120 (0.111–0.135)	0.001 (0.000–0.010)		0.001 (–0.010–0.010)	
GP23	Placebo	1.90 (1.70–2.09)	–0.178 (–0.218 to –0.100)	5.17×10^{-3}	–0.034 (–0.157–0.028)	1.48×10^{-1}
	Estradiol	1.91 (1.57–2.21)	–0.032 (–0.115–0.014)		0.028 (–0.112–0.061)	
GP24	Placebo	1.89 (1.65–2.10)	0.050 (–0.059–0.108)	1.53×10^{-1}	–0.060 (–0.089–0.027)	6.09×10^{-1}
	Estradiol	1.92 (1.62–2.22)	–0.008 (–0.035–0.045)		–0.020 (–0.068–0.028)	

p values describe statistical significance of difference between estradiol and placebo group after intervention (p_I) and recovery (p_R). *p* values smaller than 0.05 are bolded. IQR, limits of the interquartile range (1st–3rd quartile); GP, glycan peak.

affects the expression of B4GALT1, glycosyltransferase which adds galactose to IgG glycans, but also the genes which are not directly involved in IgG glycosylation, such as the *RUNX1–RUNX3* loci (Runt-related transcription factor 1 and RUNX family transcription factor 3, found in many promoters and enhancers, which can either activate or suppress transcription) and the *SPINK4* locus (serine peptidase inhibitor, also known as PEC-60). These genes were identified as GWAS hits for IgG galactosylation. In addition, *ELL2* (Elongation Factor for RNA Polymerase 2), another GWAS hit for IgG glycosylation, more specifically sialylation, also appears to be strongly regulated by E_2 . On the other hand, there were no conclusive results on ST6GAL1, the enzyme that adds sialic acid to IgG.

To determine the involvement of the *RUNX1–RUNX3*, *SPINK4*, and *ELL2* loci in downstream signaling mechanisms linking E_2 with IgG glycosylation, we directly manipulated their transcriptional activity in the *in vitro* IgG expression system

HEK-293FS using CRISPR/dCas9 molecular tools and subsequently analysed IgG glycan phenotype. A recently developed HEK-293FS transient system for IgG secretion with stably integrated CRISPR/dCas9 expression cassette for gene upregulation (dCas9-VPR) and downregulation (dCas9-KRAB) was used for this purpose. These cells were transfected with a plasmid containing genes for IgG heavy and light chains aiming to induce the production and secretion of IgG antibodies. Described plasmid also contains specifically designed gRNAs targeting the appropriate fusion constructs (either dCas9-VPR or dCas9-KRAB) to candidate genes *RUNX1*, *RUNX3*, *SPINK4*, and *ELL2*. As a proof of concept (*i.e.*, positive control), we targeted dCas9-KRAB to the promoter region of the *B4GALT1* gene, coding for a glycosyltransferase responsible for IgG galactosylation. We observed a significant decrease in the *B4GALT1* gene expression level and subsequent decrease in galactosylated glycans, with a concomitant increase in

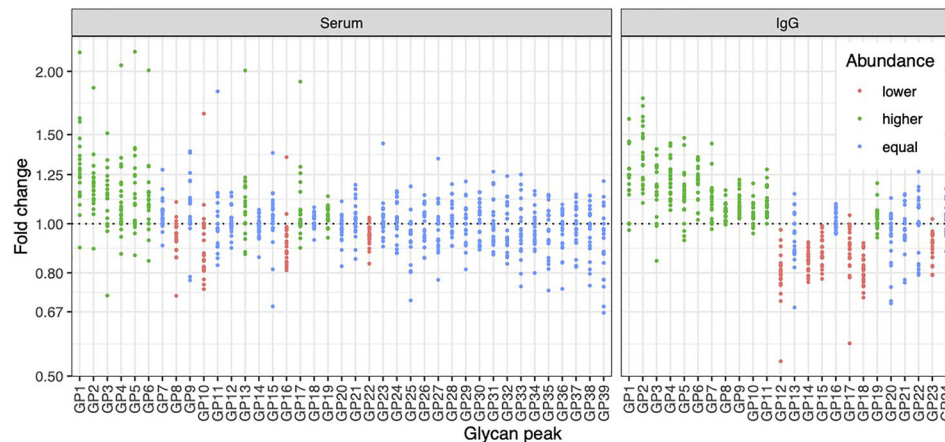


FIGURE 4 | Effects of gonadal hormone depletion on total plasma glycans and IgG glycans. Gonadotropin-releasing hormone analogue leuprolide acetate (GnRH_{AG}) was used to lower gonadal steroids to postmenopausal levels in healthy premenopausal women ($n = 36$) that were then randomized to transdermal placebo ($n = 21$) or estradiol patch ($n = 15$). Changes in the total plasma glycome and IgG glycome composition after five months of GnRH_{AG} without supplementation of E₂ (supplementation with placebo) are shown. Each dot is a change in a single individual. Changes that are statistically significant after correction for multiple testing are shown in red (statistically significant decrease) or in green (statistically significant increase).

agalactosylated glycans, as expected (Figure 5A). Subsequently, we upregulated *RUNX1*, *RUNX3*, and *SPINK4* genes using dCas9-VPR and downregulated *RUNX1*, *RUNX3* and *ELL2* genes using dCas9-KRAB. Using specific gRNA for our targets, we found significant changes in the expression of *RUNX1/VPR*, *RUNX3/VPR*, *RUNX3/KRAB*, and *SPINK4/VPR*. The changes in gene expression were replicated in two independent sets of experiments (Supplementary Table 4). However, only the changes in *RUNX3/VPR* and *SPINK4/VPR* were accompanied by significant change in IgG glycosylation profile, in both cases related to the level of IgG galactosylation (Figure 5B). We found a decrease in galactosylated glycans upon upregulation of *RUNX3* and *SPINK4* and a concomitant increase in agalactosylated glycans in the case of *RUNX3* (Figure 5B). The dataset for all glycan traits is available in Supplementary Table 5.

DISCUSSION

The composition of IgG glycome is an essential aspect in the regulation of the immune system (1). However, molecular mechanisms contributing to changes of the IgG glycome composition are only vaguely understood. Here we show that estradiol is an important factor in regulating IgG glycosylation in women and that its effects on N-glycosylation are limited explicitly to B cells, as depletion of E₂ did not cause N-glycosylation changes of other serum proteins. Previous analysis of the same cohort of patients demonstrated that depletion of E₂ decreases galactosylation of IgG (14), and here we expand this finding to the decrease of sialylation and an increase of bisecting GlcNAc. Particularly interesting is the change in the ratio of sialylation and galactosylation (S/G,

Figure 3, Supplementary Table 1), suggesting that the depletion of gonadal hormones directly affects sialylation and that the decrease in sialylation is not just a reflection of decreased galactose levels (needed for subsequent sialylation). It was previously reported that estrogen affects the expression of the *ST6GAL1* gene in both mice and humans (37). Unfortunately, we were not able to prove this using ours *in vitro* transient expression system. Therefore mechanistic aspects of this association remain to be demonstrated.

When mechanisms regulating protein glycosylation are investigated, the focus is always on the expression of glycosyltransferases, the enzymes that synthesize glycans (38). Nevertheless, in general, there is a slight correlation between glycosyltransferase expression levels and levels of glycans it synthesizes (39), which indicates that regulatory mechanisms may be more complex than a simple change in the expression of glycosyltransferases. Indeed, in a series of GWAS studies performed in the last decade, we identified a network of at least 30 genes associated with and potentially involved in regulating IgG glycosylation (32–35).

One of the potential mechanisms by which E₂ could increase IgG galactosylation is through direct activation of the *B4GALT1* galactosyltransferase, which adds galactose to IgG. *In vitro* studies showed that both overexpression of estrogen receptor (40) and treatment of cells with E₂ leads to increased expression of the *B4GALT1* gene (41, 42). Our study decreased *B4GALT1* expression using CRISPR/dCas9-KRAB fusion in a unique IgG-secreting model cell system resulting in the expected change of the IgG glycome composition. It confirmed the importance of this critical biosynthetic enzyme for IgG galactosylation and proved the efficacy of our FreeStyle 293-F cell system, containing stably integrated dCas9-VPR and -KRAB and secreting IgG, for functional validation of GWAS hits for IgG glycosylation.

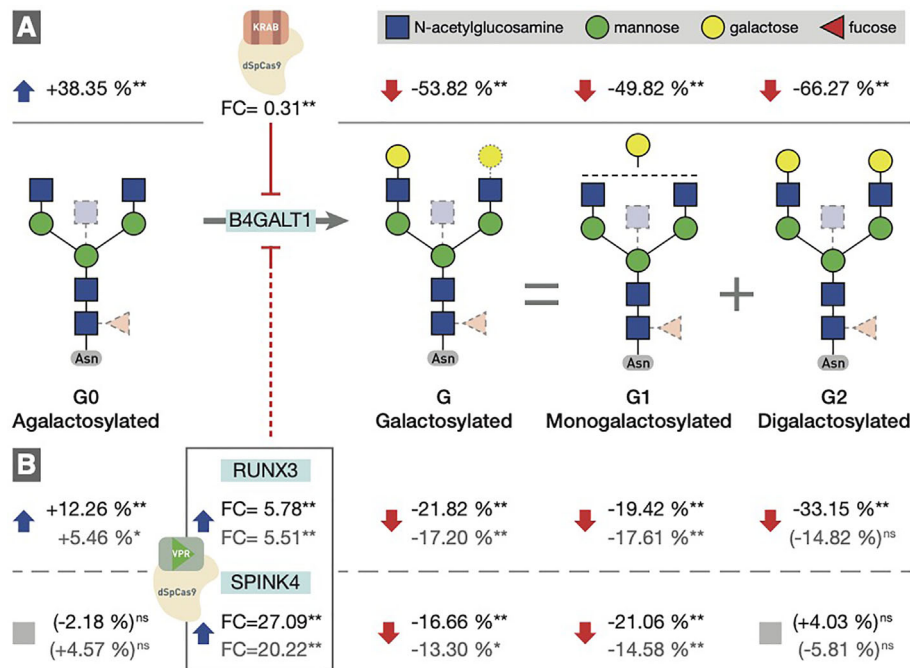


FIGURE 5 | (A) Downregulation of the *B4GALT1* gene by dCas9-KRAB induced changes in IgG galactosylation. Fold change (FC) between cells in which *B4GALT1* was directly downregulated by dCas9/KRAB and control cells (containing non-targeting gRNA) was 0.31, and subsequent change was recorded in IgG glycan phenotype: an increase of agalactosylated glycan structures appeared with a concomitant decrease in mono- and digalactosylated glycans (G1, G2). Corresponding changes in glycan structures are given as a relative change with non-targeting gRNA glycan levels as a baseline. Agalactosylated glycan structures (G0) are converted to galactosylated structures (G) by the enzymatic activity of *B4GALT1*. **(B)** Changes in IgG glycosylation resulting from upregulation of *RUNX3* and *SPINK4* by dCas9/VP. FC values between cells in which *RUNX3* and *SPINK4* were directly upregulated by dCas9/VP and control cells (containing non-targeting gRNA) are given for the first experiment (indicated in black) and the replicate (indicated in gray). The resulting putative inhibition of *B4GALT1* was confirmed indirectly by the effect on the glycosylation profile. The indirect and speculative nature of *RUNX3*/*SPINK4* effect on galactosylation is indicated by the dashed red line. Statistical significance: * <0.05 ; ** <0.01 ; ns, not significant.

By analysing the Signalling Pathways Project (SPP) web knowledgebase (36), we found that several other GWAS hits for the IgG glycosylation, which are not glycosyltransferases but genes with other functions, such as transcription factors *RUNX1* and *RUNX3*, as well as *SPINK4* and *ELL2*, also seem to be regulated by estradiol. However, the fact that these genes were both involved in the regulation of IgG glycosylation and affected by E_2 is not strong enough to prove their direct involvement in B cell IgG glycosylation because their effects could also be through an indirect mechanism. Using CRISPR/dCas9 molecular tools, we were able to increase the expression of *RUNX3*, which resulted in lower levels of IgG galactosylation (Figure 5).

With this experiment, we confirmed that *RUNX3* is involved in regulating IgG glycosylation in our *in vitro* model system of B cells (16). The first experimental validation of this GWAS hit positions *RUNX3* as a potential target for pharmacological interventions. *RUNX3* gene downregulation may improve IgG galactosylation and sialylation and may have potential anti-inflammatory effects. Activation of *SPINK4* had similar effects on the IgG glycome composition as activation of *RUNX3*. However, because the basal expression of *SPINK4* in HEK-293FS cells was low, we could not confirm if its suppression

would have the opposite effect. Furthermore, *SPINK4* is located in relative proximity to *B4GALT1* (i.e., 50 kb distance). Therefore, although we did not observe a statistically significant change in transcript levels at the time of analysis, we cannot exclude the possibility that the binding of the dCas9-VP fusion construct, used for the activation of *SPINK4* in the region between *SPINK4* and *B4GALT1*, negatively affected *B4GALT1* expression. One putative mechanism could be spurious upregulation of *B4GALT1* antisense RNA 1 (*B4GALT1*-AS1), which is also located in this region, although we have not verified this hypothesis experimentally. We did not observe any statistically significant effects of *ELL2* on IgG glycosylation. This was not surprising because *ELL2* is a GWAS hit for sialylation and our *in vitro* expression system produces IgG antibodies with very low levels of sialic acid which presents a difficulty for evaluation of effects on sialylation. Therefore, the role of *ELL2* in the regulation of IgG glycosylation by estrogen still needs further exploration.

For the first time, the molecular mechanism through which E_2 could regulate IgG glycosylation has been identified and functionally validated in the present study. Considering multiple functional roles of IgG glycans in balancing the immune system, this pathway may be a target for the future

development of a new class of anti-inflammatory drugs acting downstream of E₂ and having only a subset of the molecular consequences of hormone therapy.

DATA AVAILABILITY STATEMENT

The raw data supporting the conclusions of this article will be made available by the authors, without undue reservation.

ETHICS STATEMENT

The studies involving human participants were reviewed and approved by the Scientific Advisory and Review Committee at the University of Colorado Anschutz Medical Campus. The patients/participants provided their written informed consent to participate in this study.

AUTHOR CONTRIBUTIONS

GL, VZ, and PN designed the study. JJ, JK, and MP performed glycosylation analysis and interpreted glycan data. AM and KM performed CRISPR/dCas9 gene manipulations in HEK-293FS cells, collected IgG antibodies, and interpreted the data. WK and KG performed the intervention study. DK, AF, FV and AV analysed the data. GL wrote the initial draft of the manuscript. All authors contributed to the article and approved the submitted version.

REFERENCES

- Seeling M, Brückner C, Nimmerjahn F. Differential Antibody Glycosylation in Autoimmunity: Sweet Biomarker or Modulator of Disease Activity? *Nat Rev Rheumatol* (2017) 13:621–30. doi: 10.1038/nrrheum.2017.146
- Nimmerjahn F, Ravetch JV. Fcγ Receptors as Regulators of Immune Responses. *Nat Rev Immunol* (2008) 8:34–47. doi: 10.1038/nri2206
- Gudelj I, Lauc G, Pezer M. Immunoglobulin G Glycosylation in Aging and Diseases. *Cell Immunol* (2018) 333:65–79. doi: 10.1016/j.cellimm.2018.07.009
- Wittenbecher C, Štambuk T, Kuxhaus O, Rudman N, Vučković F, Štambuk J, et al. Plasma N-Glycans as Emerging Biomarkers of Cardiometabolic Risk: A Prospective Investigation in the EPIC-Potsdam Cohort Study. *Diabetes Care* (2020) 43:661–8. doi: 10.2337/dc19-1507
- Gudelj I, Salo PP, Trbojević-Akmačić I, Albers M, Primorac D, Perola M, et al. Low Galactosylation of IgG Associates With Higher Risk for Future Diagnosis of Rheumatoid Arthritis During 10 Years of Follow-Up. *Biochim Biophys Acta - Mol Basis Dis* (2018) 1864:2034–39. doi: 10.1016/j.bbdis.2018.03.018
- Ercan A, Cui J, Chatterton DE, Deane KD, Hazen MM, Brintnell W, et al. Aberrant IgG Galactosylation Precedes Disease Onset, Correlates With Disease Activity, and Is Prevalent in Autoantibodies in Rheumatoid Arthritis. *Arthritis Rheum* (2010) 62:2239–48. doi: 10.1002/art.27533
- Tanigaki K, Sacharidou A, Peng J, Chambliss KL, Yuhanna IS, Ghosh D, et al. Hypoalylated IgG Activates Endothelial IgG Receptor FcγRIIb to Promote Obesity-Induced Insulin Resistance. *J Clin Invest* (2017) 128:309–22. doi: 10.1172/JCI89333
- Peng J, Vongpatanasin W, Sacharidou A, Kifer D, Yuhanna IS, Banerjee S, et al. Supplementation With the Sialic Acid Precursor N-Acetyl-D-Mannosamine Breaks the Link Between Obesity and Hypertension. *Circulation* (2019) 140:2005–18. doi: 10.1161/CIRCULATIONAHA.119.043490
- Hafkenschied L, Moel E, Smolik I, Tanner S, Meng X, Jansen BC, et al. N-Linked Glycans in the Variable Domain of IgG Anti-Citrullinated Protein Antibodies

FUNDING

Glycosylation analysis was performed in Genos Glycoscience Research Laboratory and partly supported by the European Union's Horizon 2020 grant IMForFuture (grant #721815), European Structural and Investment Funds grants "Centre of Competence in Molecular Diagnostics grant" (#KK.01.2.2.03.0006), and "Croatian National Centre of Research Excellence in Personalized Healthcare" (#KK.01.1.1.01.0010) and European Regional Development Fund, under grant agreement No. KK.01.1.1.04.0085, project "Genomic engineering and gene regulation in cell lines and model organisms by CRISPR/Cas9 technology—CasMouse".

ACKNOWLEDGMENTS

We acknowledge the members of our research groups who carried out the day-to-day activities for the project. Finally, we want to thank the women who volunteered to participate in the study for their time and efforts.

SUPPLEMENTARY MATERIAL

The Supplementary Material for this article can be found online at: <https://www.frontiersin.org/articles/10.3389/fimmu.2021.680227/full#supplementary-material>

- Predict the Development of Rheumatoid Arthritis. *Arthritis Rheumatol* (2019) 71:1626–33. doi: 10.1002/art.40920
- Krištić J, Vučković F, Menni C, Klarić L, Keser T, Beceheli I, et al. Glycans are a Novel Biomarker of Chronological and Biological Ages. *J Gerontol - Ser A Biol Sci Med Sci* (2014) 69:779–89. doi: 10.1093/gerona/glt190
- De Haan N, Reidling KR, Driessen G, Van Der Burg M, Wührer M. Changes in Healthy Human IgG Fc-Glycosylation After Birth and During Early Childhood. *J Proteome Res* (2016) 15:1853–61. doi: 10.1021/acs.jproteome.6b00038
- Cheng HD, Tirosh I, de Haan N, Stöckmann H, Adamczyk B, McManus CA, et al. IgG Fc Glycosylation as an Axis of Humoral Immunity in Childhood. *J Allergy Clin Immunol* (2020) 145:710–3.e9. doi: 10.1016/j.jaci.2019.10.012
- Dall'Olio F, Vanhooren V, Chen CC, Slagboom PE, Wührer M, Franceschi C. N-Glycomic Biomarkers of Biological Aging and Longevity: A Link With Inflammaging. *Ageing Res Rev* (2013) 12:685–98. doi: 10.1016/j.arr.2012.02.002
- Ercan A, Kohrt WM, Cui J, Deane KD, Pezer M, Yu EW, et al. Estrogens Regulate Glycosylation of IgG in Women and Men. *JCI Insight* (2017) 2:e89703. doi: 10.1172/jci.insight.89703
- Hanić M, Lauc G, Trbojević-Akmačić I. N-Glycan Analysis by Ultra-Performance Liquid Chromatography and Capillary Gel Electrophoresis With Fluorescent Labeling. *Curr Protoc Protein Sci* (2019) 97:1–21. doi: 10.1002/cpps.95
- Vink T, Oudshoorn-Dickmann M, Roza M, Reitsma JJ, de Jong RN. A Simple, Robust and Highly Efficient Transient Expression System for Producing Antibodies. *Methods* (2014) 65:5–10. doi: 10.1016/j.jymeth.2013.07.018
- Shea KL, Gavin KM, Melanson EL, Gibbons E, Stavros A, Wolfe P, et al. Body Composition and Bone Mineral Density After Ovarian Hormone Suppression With or Without Estradiol Treatment. *Menopause* (2015) 22:1045–52. doi: 10.1097/GME.0000000000000430
- Melanson EL, Lyden K, Gibbons E, Gavin KM, Wolfe P, Wierman ME, et al. Influence of Estradiol Status on Physical Activity in Premenopausal Women. *Med Sci Sports Exerc* (2018) 50:1704–9. doi: 10.1249/MSS.0000000000001598

19. Belchetz PE, Plant TM, Nakai Y, Keogh EJ, Knobil E. Hypophysial Responses to Continuous and Intermittent Delivery of Hypothalamic Gonadotropin-Releasing Hormone. *Sci (80-)* (1978) 202:631–3. doi: 10.1126/science.100883
20. Trbojević-Akmačić I, Ugrina I, Lauc G. Comparative Analysis and Validation of Different Steps in Glycomics Studies. *Methods Enzymol* (2017) 586:37–55. doi: 10.1016/bs.mie.2016.09.027
21. Josipović G, Tadić V, Klasić M, Zanki V, Bečeheli I, Chung F, et al. Antagonistic and Synergistic Epigenetic Modulation Using Orthologous CRISPR/dCas9-based Modular System. *Nucleic Acids Res* (2019) 47:9637–57. doi: 10.1093/nar/gkz709
22. Josipović G, Zoldoš V, Vojta A. Active Fusions of Cas9 Orthologs. *J Biotechnol* (2019) 301:18–23. doi: 10.1016/j.jbiotec.2019.05.306
23. Livak KJ, Schmittgen TD. Analysis of Relative Gene Expression Data Using Real-Time Quantitative PCR and the 2^{(-Delta Delta C(T))} Method. *Methods* (2001) 25:402–8. doi: 10.1006/meth.2001.1262S1046-2023(01)91262-9[pai]
24. Keser T, Pavic T, Lauc G, Gornik O. Comparison of 2-Aminobenzamide, Procainamide and RapiFluor-MS as Derivatizing Agents for High-Throughput HILIC-UPLC-FLR-MS N-Glycan Analysis. *Front Chem* (2018) 6:324. doi: 10.3389/fchem.2018.00324
25. Leek JT, Johnson WE, Parker HS, Jaffe AE, Storey JD. The Sva Package for Removing Batch Effects and Other Unwanted Variation in High-Throughput Experiments. *Bioinformatics* (2012) 28:882–3. doi: 10.1093/bioinformatics/bts034
26. Bates D, Mächler M, Bolker B, Walker S. Fitting Linear Mixed-Effects Models Using Lme4. *J Stat Softw* (2015) 67:1–48. doi: 10.18637/jss.v067.i01
27. Karssen LC, van Duijn CM, Aulchenko YS. The GenABEL Project for statistical genomics. *F1000Res* (2016) 5:914. doi: 10.12688/f1000research.8733.1
28. Team RDC. *R: A Language and Environment for Statistical Computing*. Vienna, Austria: The R Foundation (2009). Available at: <http://www.r-project.org>.
29. Vilaj M, Gudelj I, Trbojević-Akmačić I, Lauc G, Pezer M. IgG Glycans as a Biomarker of Biological Age. In: A Moskalev, editor. *Biomarkers of Human Aging. Healthy Ageing and Longevity*. Cham: Springer (2019). p. 81–99. doi: 10.1007/978-3-030-24970-0_7
30. Clerc F, Reidinger KR, Jansen BC, Kammeijer GSM, Bondt A, Wuhner M. Human Plasma Protein N-Glycosylation. *Glycoconj J* (2016) 33:309–43. doi: 10.1007/s10719-015-9626-2
31. Pučić M, Knežević A, Vidić J, Adamczyk B, Novokmet M, Polašek O, et al. High Throughput Isolation and Glycosylation Analysis of IgG-variability and Heritability of the IgG Glycome in Three Isolated Human Populations. *Mol Cell Proteomics* (2011) 10:M111.010090. doi: 10.1074/mcp.M111.010090
32. Krištić J, Zaytseva OO, Ram R, Nguyen Q, Novokmet M, Vučković F, et al. Profiling and Genetic Control of the Murine Immunoglobulin G Glycome. *Nat Chem Biol* (2018) 14:516–24. doi: 10.1038/s41589-018-0034-3
33. Lauc G, Huffman JE, Pučić M, Zgaga L, Adamczyk B, Mužinić A, et al. Loci Associated With N-Glycosylation of Human Immunoglobulin G Show Pleiotropy With Autoimmune Diseases and Haematological Cancers. *PLoS Genet* (2013) 9:e1003225. doi: 10.1371/journal.pgen.1003225
34. Shen X, Klarić L, Sharapov S, Mangino M, Ning Z, Wu D, et al. Multivariate Discovery and Replication of Five Novel Loci Associated With Immunoglobulin G N-Glycosylation. *Nat Commun* (2017) 8:447. doi: 10.1038/s41467-017-00453-3
35. Klarić L, Tsepilov YA, Stanton CM, Mangino M, Sikka TT, Esko T, et al. Glycosylation of Immunoglobulin G Is Regulated by a Large Network of Genes Pleiotropic With Inflammatory Diseases. *Sci Adv* (2020) 6:eax0301. doi: 10.1126/sciadv.aax0301
36. Ochsner SA, Abraham D, Martin K, Ding W, McOwiti A, Kankanamge W, et al. The Signaling Pathways Project, an Integrated 'Omics Knowledgebase for Mammalian Cellular Signaling Pathways. *Sci Data* (2019) 6:252. doi: 10.1038/s41597-019-0193-4
37. Engdahl C, Bondt A, Harre U, Raufer J, Pfeifle R, Camponeschi A, et al. Estrogen Induces St6gal1 Expression and Increases IgG Sialylation in Mice and Patients With Rheumatoid Arthritis: A Potential Explanation for the Increased Risk of Rheumatoid Arthritis in Postmenopausal Women. *Arthritis Res Ther* (2018) 20(1):84. doi: 10.1186/s13075-018-1586-z
38. Moremen KW, Tiemeyer M, Nairn AV. Vertebrate Protein Glycosylation: Diversity, Synthesis and Function. *Nat Rev Mol Cell Biol* (2012) 13:448–62. doi: 10.1038/nrm3383
39. Nairn AV, Aoki K, dela Rosa M, Porterfield M, Lim JM, Kulik M, et al. Regulation of Glycan Structures in Murine Embryonic Stem Cells: Combined Transcript Profiling of Glycan-Related Genes and Glycan Structural Analysis. *J Biol Chem* (2012) 287:37835–56. doi: 10.1074/jbc.M112.405233
40. Nott SL, Huang Y, Li X, Fluharty BR, Qiu X, Welshons WV, et al. Genomic Responses From the Estrogen-Responsive Element-Dependent Signaling Pathway Mediated by Estrogen Receptor α Are Required to Elicit Cellular Alterations. *J Biol Chem* (2009) 284:15277–88. doi: 10.1074/jbc.M900365200
41. Hah N, Danko CG, Core L, Waterfall JJ, Siepel A, Lis JT, et al. A Rapid, Extensive, and Transient Transcriptional Response to Estrogen Signaling in Breast Cancer Cells. *Cell* (2011) 145:622–34. doi: 10.1016/j.cell.2011.03.042
42. Coser KR, Chesnes J, Hur J, Ray S, Isselbacher KJ, Shioda T. Global Analysis of Ligand Sensitivity of Estrogen Inducible and Suppressible Genes in MCF7/ BUS Breast Cancer Cells by DNA Microarray. *Proc Natl Acad Sci USA* (2003) 100:13994–9. doi: 10.1073/pnas.2235866100

Conflict of Interest: GL is the founder and owner of Genos Ltd, a private research organization that specializes in high-throughput glycomic analyses and has several patents in this field. JJ, JK, AF, FV and MP are employees of Genos Ltd.

The remaining authors declare that the research was conducted in the absence of any commercial or financial relationships that could be construed as a potential conflict of interest.

The handling editor declared a past co-authorship with one of the authors GL.

Copyright © 2021 Mijakovac, Jurić, Kohrt, Krištić, Kifer, Gavin, Miškec, Frkatović, Vučković, Pezer, Vojta, Nigrović, Zoldoš and Lauc. This is an open-access article distributed under the terms of the Creative Commons Attribution License (CC BY). The use, distribution or reproduction in other forums is permitted, provided the original author(s) and the copyright owner(s) are credited and that the original publication in this journal is cited, in accordance with accepted academic practice. No use, distribution or reproduction is permitted which does not comply with these terms.



Biophysical Evaluation of Rhesus Macaque Fc Gamma Receptors Reveals Similar IgG Fc Glycoform Preferences to Human Receptors

Andrew R. Crowley¹, Nana Yaw Osei-Owusu¹, Gillian Dekkers², Wenda Gao³, Manfred Wuhrer⁴, Diogo M. Magnani⁵, Keith A. Reimann⁵, Seth H. Pincus^{6,7}, Gestur Vidarsson² and Margaret E. Ackerman^{1,8*}

¹ Department of Microbiology and Immunology, Geisel School of Medicine at Dartmouth, Dartmouth College, Hanover, NH, United States, ² Sanquin Research and Landsteiner Laboratory, Academic Medical Centre, Department of Experimental Immunohematology, University of Amsterdam, Amsterdam, Netherlands, ³ Antigen Pharmaceuticals Inc., Boston, MA, United States, ⁴ Center for Proteomics and Metabolomics, Leiden University Medical Center, Leiden, Netherlands, ⁵ Nonhuman Primate Reagent Resource, MassBiologics of the University of Massachusetts Medical School, Boston, MA, United States, ⁶ Department of Microbiology, Immunology and Parasitology, Louisiana State University Health Sciences Center, New Orleans, LA, United States, ⁷ Department of Chemistry and Biochemistry, Montana State University, Bozeman, MT, United States, ⁸ Thayer School of Engineering, Dartmouth College, Hanover, NH, United States

OPEN ACCESS

Edited by:

Mohamed Abdel-Mohsen,
Wistar Institute, United States

Reviewed by:

Naeem Khan,
Western Michigan University,
United States
Isaak Quast,
Monash University, Australia

*Correspondence:

Margaret E. Ackerman
margaret.e.ackerman@dartmouth.edu

Specialty section:

This article was submitted to
B Cell Biology,
a section of the journal
Frontiers in Immunology

Received: 06 August 2021

Accepted: 27 September 2021

Published: 12 October 2021

Citation:

Crowley AR, Osei-Owusu NY,
Dekkers G, Gao W, Wuhrer M,
Magnani DM, Reimann KA, Pincus SH,
Vidarsson G and Ackerman ME (2021)
Biophysical Evaluation of Rhesus
Macaque Fc Gamma Receptors
Reveals Similar IgG Fc Glycoform
Preferences to Human Receptors.
Front. Immunol. 12:754710.
doi: 10.3389/fimmu.2021.754710

Rhesus macaques are a common non-human primate model used in the evaluation of human monoclonal antibodies, molecules whose effector functions depend on a conserved N-linked glycan in the Fc region. This carbohydrate is a target of glycoengineering efforts aimed at altering antibody effector function by modulating the affinity of Fcγ receptors. For example, a reduction in the overall core fucose content is one such strategy that can increase antibody-mediated cellular cytotoxicity by increasing Fc-FcγRIIIa affinity. While the position of the Fc glycan is conserved in macaques, differences in the frequency of glycoforms and the use of an alternate monosaccharide in sialylated glycan species add a degree of uncertainty to the testing of glycoengineered human antibodies in rhesus macaques. Using a panel of 16 human IgG1 glycovariants, we measured the affinities of macaque FcγRs for differing glycoforms via surface plasmon resonance. Our results suggest that macaques are a tractable species in which to test the effects of antibody glycoengineering.

Keywords: nonhuman primate, IgG, Fc gamma receptor, N glycan, rhesus macaque, ADCC - antibody dependent cellular cytotoxicity, phagocytosis, complement dependent cytotoxicity

INTRODUCTION

Like many proteins destined for secretion, human immunoglobulin G (IgG) is subject to a variety of post-translational modifications as it migrates through the secretory pathway of plasma cells. A prominent modification is the attachment of an N-linked glycan to both heavy chains in the crystallizable fragment (Fc) portion (1). While the amino acid sequon is conserved, the precise identity of the specific N-linked glycoform incorporated is not genetically encoded.

Among glycosylated IgG Fc domains, there exist a variety of observed glycoforms – 36 in total for humans (2), eight of which account for 90% of all IgG in normal sera (3). The frequency of IgG Fc glycoforms within the distribution of the total glycan repertoire tends to be predictable in healthy individuals (4), with some variation due to factors such as age, sex, and pregnancy (5–11). In general, this profile consists of high levels of fucosylation (95%), low levels of bisecting GlcNAc (15%), intermediate levels of galactose (45%), and low sialylation (10%) (3). This balance can be perturbed by a heightened immune response however (12, 13), and distinct antigen-specific antibody fractions may differ from each other and from the average serum IgG Fc glycan profile within a given individual (14–16).

Occupancy of this conserved glycosylation site is critical to the ability of an IgG molecule to interact with human Fcγ receptors (FcγR), as the absence or removal of the N-glycan produces an antibody with dramatically diminished or outright eliminated affinity for FcγR and no detectable effector function (17, 18). Slight changes in the composition of the Fc glycan can impart changes to the Fc-FcγR dynamic that may resonate all the way to the severity of clinical presentation (19–27). More specifically, an increase in galactose content has been associated with increased propensity of the Fc domain to hexamerize (28), as well as with a slight (≤ 2 fold) increase in affinity for most of the low affinity (i.e., not FcγRI) FcγRs (29, 30), while the absence of a fucose molecule branching from the asparagine-proximal N-acetylglucosamine (GlcNAc) has been credited with up to an astounding 50-fold increase in affinity for FcγRIIIa/b (31–33). This increase in affinity translates to improvement in antibody-dependent cellular cytotoxicity by FcγRIIIa-bearing natural killer (NK) cells (34, 35), which has made it an attractive tool for enhancing the efficacy of therapeutic monoclonal antibodies (mAbs) (36, 37).

Pre-clinical animal models serve as an important bridge for such glycoengineered mAbs migrating from the lab to the clinic. Like that of humans, macaque IgG features a conserved N-linked glycan motif, which is necessary for binding to macaque FcγR (38, 39). Despite having a degree of homology to humans that makes them a tractable and popular animal model for biomedical research, like all models, macaques can be sufficiently immunologically distinct that care should be exercised when attempting to extrapolate observations in non-human primates to humans (40). Whereas the macaque IgG subclasses are more functionally monolithic than those in humans (39), genetic diversity among FcγR is significantly greater among macaques than in humans, particularly for FcγRII (41). Additionally, macaques do not express an equivalent of the GPI-linked human FcγRIIIb, and the clinically-relevant functional differences in high and low FcγRIIIa binding affinity allotypes observed in humans are not reflected among frequent alleles in macaques (42). These characteristics help to set expectations and guide design and interpretation of experiments conducted in these models. Yet, other aspects of antibody immunobiology have yet to be fully investigated; the impact of antibody glycosylation on receptor binding is one such area of concern. Macaque IgG is more likely to feature a bisecting GlcNAc residue

and shows greater variability in galactose content than human IgG Fc (43, 44). Furthermore, human IgG Fc sialylation is carried out with N-acetylneuraminic acid (NANA) whereas macaques use N-glycolylneuraminic acid (NGNA) (43). The most striking effect of glycovariation in human IgG is very clearly the “fucose effect” for FcγRIII, which has been proposed to be mediated by disruption of glycan-glycan contacts (45, 46) or *via* altered conformational sampling (47). Regardless of mechanism, this effect is readily observed from mice to humans (48), and the receptor glycosylation site associated with it is conserved in rhesus macaques (38). The available data suggest that the effect of afucosylation on macaque FcγRIIIa affinity is also conserved (49), although perhaps with more modest fold-change increases in affinity than what has been observed in humans.

Using a panel of glycoengineered human IgG1 antibodies, we report the affinities of the low affinity rhesus macaque (RM) Fcγ receptors for each of 16 glycoforms, and further validate our observations by analysis of relationships between rhesus serum IgG Fc glycan profiles and FcγR binding levels. This work provides a more complete picture of the glycopreferences of macaque FcγRs, allowing for more confident design of experiments and interpretation of data when engineered human antibodies are tested in non-human primate models.

RESULTS AND DISCUSSION

A panel of 16 previously described IgG Fc glycovariants generated *via* a series of chemical and genetic methods that alter the dominant species of glycan within production runs of an anti-trinitrophenol (TNP) human IgG1 monoclonal antibody (mAb) (50, 51) was used to investigate the glycopreferences of rhesus macaque FcγR recognition (**Supplemental Table 1**). Briefly, these tools selectively achieved a greater than nine-fold reduction in the amount of core fucose (from 95% to 10%), a ten-fold or greater increase in the frequency of bisected species (from 5% to >50%), and terminal sialylation (3% to >40%), as previously reported in greater detail (51). Variation in galactose content ranged from 10% to 80%. Collectively, this panel of variants represents well the diversity of glycan changes that exist within human serum and in recombinant expressed and glycoengineering monoclonal antibodies.

The affinity of the low affinity macaque FcγRs for these variable glycoforms was measured using a multiplexed surface plasmon resonance (SPR) approach in which the glycovariants were covalently linked to a sensor chip and the FcγRs were the analyte in solution. Some of the differences imparted by modulating the Fc glycan were readily apparent from raw sensorgrams (**Figure 1**). While all the interactions exhibit a fast-on association dynamic, the off-rate was noticeably slower in the case of the higher affinity FcγRIIIa. This observation was particularly striking for interactions with afucosylated IgG wherein dissociation was not always complete by the end of the 5-minute step.

Equilibrium dissociation constants (K_D) were fitted to the responses at steady state to define binding affinities for each

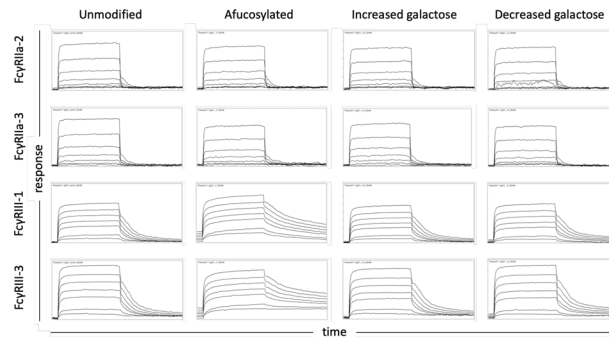


FIGURE 1 | Exemplary sensor data of FcγR-IgG interactions. Sensorgrams depicting the association and dissociation of FcγR from IgG over time for prevalent FcγRII (2 and 3) and FcγRIII (1 and 3) allotypes (rows) and differentially glycosylated IgG (columns). The equilibrium dissociation constants reported in this work were calculated using the response measured at the end of the association phase when interactions had achieved steady state. Each receptor was evaluated over a three order of magnitude concentration range.

receptor and IgG Fc glycoform variant in two separate experiments that compared the set of glycovariants with each modification to the set without (**Figure 2**). Among glycan modifications, reduction in core fucose of human IgG1 resulted in the most dramatic change in receptor binding affinity — improving the affinity of rhesus macaque FcγRIII as compared to Fc glycoforms without intentionally reduced fucose content (**Figure 2A**). While there was some variability in the magnitude and statistical confidence in the effect of reduced fucose between experimental runs and across the major FcγR allotypes (**Figure 3**), these results were generally consistent with a prior report of the sensitivity of RM FcγRIIIa to IgG Fc fucosylation (49).

In contrast, the presence or absence of bisecting GlcNAc did not have a statistically significant effect on the binding affinity of any RM FcγR tested (**Figures 2B, 3**). While a prior study suggested that the presence of bisecting GlcNAc resulted in improved effector function in the context of human FcγR (52), other work has suggested that these observations were instead driven by variable fucosylation (51, 53). The observation that bisected glycans cannot subsequently become fucosylated appears to have resulted in some confounding of cause and effect with respect to the role of bisection (54).

Nor was there an impact associated with variable terminal sialic acid content (**Figures 2C, 3**). Again, while some studies have suggested that sialic acid influences receptor binding affinity

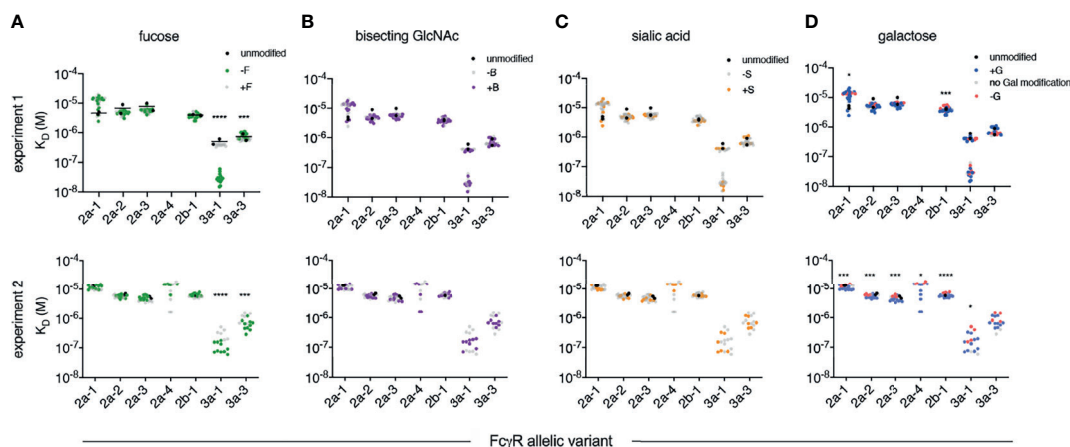


FIGURE 2 | Affinity of rhesus macaque FcγRs for a panel of human IgG1 glycovariants. Equilibrium dissociation constants (K_D) of rhesus macaque alleles having unique extracellular domains observed in two independent experiments (rows). Within each experiment, glycovariants were printed in replicate and each replicate is plotted. Results are presented such that each panel emphasizes a different category of glycomodification, including variable fucosylation (F) (**A**), bisecting N-Acetylglucosamine (B) (**B**), sialylation (S) (**C**), and galactosylation (G) (**D**). A natively glycosylated preparation (black) is plotted along with variants with (+) or lacking (-) the glycan emphasized in that panel. Statistically significant differences were tested using an unpaired t test comparing glycovariants with (+) and without (-) the modification (* $p < 0.05$, *** $p < 0.0005$, **** $p < 0.0001$).

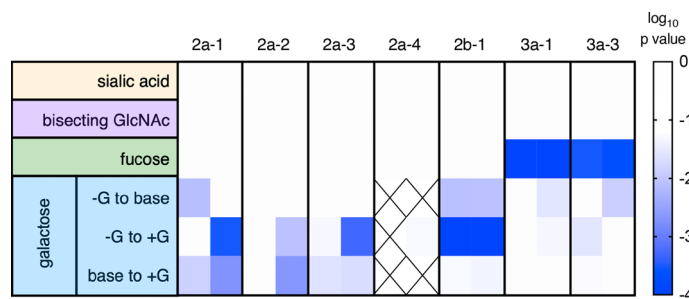


FIGURE 3 | Summary of receptor affinity differences. Statistical significance of differences in affinity associated with variable glycosylation. Glycan modifications are tabulated by row and receptors by column, for each of the two independent experimental runs. Confidence in differences is indicated in color. Crosshatches indicate missing data. The effect of varying (+ versus -) sialic acid, bisecting GlcNAc, and fucose were evaluated by unpaired t test, and for galactose [+G, unmodified (base), and -G] with an ordinary one-way ANOVA corrected for multiple comparisons.

(55, 56), others have reported contradictory results (30, 57). Using this same well-characterized panel of glycovariants, variation in sialic acid content between 12–64% appeared to have essentially no general effect on binding affinity across diverse human FcγR (51).

Further mirroring their human counterparts, rhesus macaque FcγRs had marginally, but often statistically significantly, heightened affinities for IgG with increased levels of galactosylation (Figures 2D, 3). To address these differences with improved resolution, analysis of the effect of variable galactosylation when fucose, sialic acid, and bisecting GlcNAc were held constant were analyzed in paired comparisons (Figure 4). As in the global data analysis, both experimental data sets showed a small but reproducible improvement to FcγRII binding affinity with increasing galactose content when other glycan attributes such as extent of fucosylation or bisection were held constant. These results are consistent with the phenotype observed in humans, where increasing galactose content improved affinity in a small but consistent manner among the low affinity FcγRs (30, 51). Similar

paired analysis of fucose, bisecting GlcNAc, and sialic acid showed a small but statistically significant enhancement of binding affinity to FcγRII among otherwise matched but variably bisected variants when data from all FcγRII receptors and both experiments were considered (Supplemental Figure 1). However, this relationship was not observed to hold in both individual experimental replicates.

Because the effect of variable fucose content is of clinical relevance in both natural immune responses (19–24) and in optimization of antibody therapy (31, 53), we further probed this aspect of RM receptor binding profiles with additional antibody specificities. Rhesusized antibody to CD20 engineered to lack fucose (Supplemental Figure 2) showed improved binding affinity to RM FcγRIII, as did a Dual Variable Domain (DVD) format bispecific (Figure 5) that was similarly modified to reduce fucose content (Supplemental Figure 3). These experiments show that fucose effect is consistent across both rhesus and human IgG1 Fc domains in the context of distinct antibody specificities and even formats. Indeed, the slowed dissociation rate of afucosylated IgG Fc forms was apparent across data collected in this study, including the experiment for which that effect was obscured by concomitant changes to the association rate for FcγRIIIa-3 that appeared to affect the equilibrium affinities reported here. Importantly, the functional consequences of improved FcγRIII binding afforded by afucosylation are well established in mice and humans, where improvements in ADCC activity are readily observed to result [summarized in (58)]. While it appears that similar observations have yet to be reported in assays conducted with macaque effector cells, whose receptor expression profiles are poorly defined and genetic diversity in receptors is extensive, the same glycosylation site associated with this phenotype is conserved in rhesus FcγRIII allotypes. The lack of this glycosylation site in other FcγR (e.g., FcγRI and FcγRII) explains the receptor-specific nature of the “fucose effect”.

Lastly, to begin to further generalize these observations about glycan binding preferences beyond the human IgG1 backbone, we analyzed serum IgG glycoprevalences among a small set of healthy RM, and investigated relationships between galactose and fucose content and binding to RM FcγR. Though confidence in correlative relationships between glycan profiles and receptor binding signals are limited by small sample size and the potential effect of differing

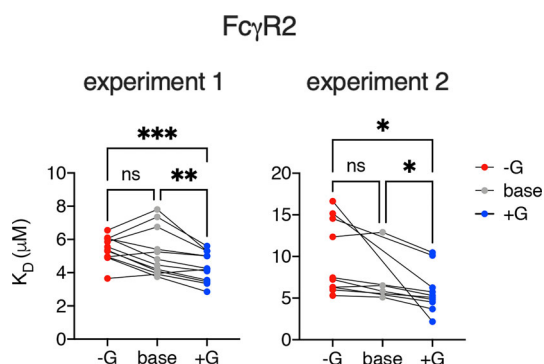


FIGURE 4 | Increased galactosylation is associated with improved affinity for FcγRII. The effect of increased and decreased galactose content on binding to FcγRII variants among IgG Fc glycotypes for which other glycan characteristics (e.g., fucosylation, sialylation, bisection) were held constant. Statistically significant differences were tested using a mixed effect model with Tukey's test of multiple comparisons (* $p < 0.05$, ** $p < 0.01$, *** $p < 0.001$). ns, not significant.

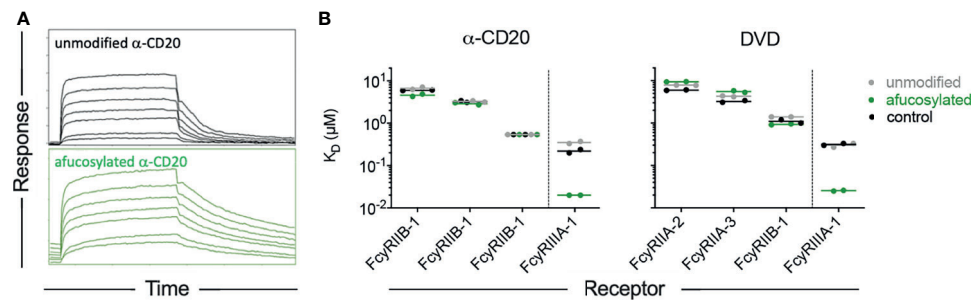


FIGURE 5 | The fucose effect is generalizable across antibodies but not receptors. **(A)** Representative sensorgrams showing association and dissociation profiles of RM FcγRIIIa-3 from unmodified and afucosylated forms of a rhesusized version of rituximab. **(B)** Equilibrium binding affinities of CDR grafted CD20-specific antibodies with rhesus IgG1 Fc domains (left), and a dual variable domain (DVD) bispecific antibody (right) in unmodified and afucosylated forms, and in comparison to an unmodified rhesus IgG1 antibody of a differing specificity (control).

levels of serum IgG between animals, increased binding of serum samples with greater levels of Fc galactosylation was observed across diverse FcγRII and FcγRIII allotypes, as was the effect of reduced fucosylation for FcγRIII (**Figure 6**). Collectively, these observations support further generalization of the effects these glycoprofiles have on FcγR binding to polyclonal pools of mixed specificity, light chain usage, and subclasses of rhesus macaque IgG.

CONCLUSIONS

This work establishes that the low affinity Fcγ receptors of RM demonstrate preferences for glycoforms of human IgG1 that largely mirror that of their human equivalents. Rhesus macaques therefore likely serve as an appropriate model for the evaluation of glycoengineered human antibodies. While the panel of glycovariants focused on human IgG1, this subclass is overwhelmingly represented among therapeutic monoclonal antibodies, and where evaluated, the glycan preferences appear to hold across human IgG subclasses (32, 59). We show here that the effect of fucose on RM FcγRIII recognition is generalizable across both human and rhesus monoclonal antibodies with distinct variable domains, a dual variable domain bispecific construct, and to polyclonal rhesus serum IgG. These results have important implications for the use of RM to study recombinant glycoengineered antibodies in preclinical and mechanistic studies of antibody therapies, as well as in attempting to relate antibody glycotypes raised in response to vaccination (60–62) or *via* vectored antibody delivery (63), to *in vitro* effector activities or *in vivo* outcomes.

METHODS

Protein Expression and Purification

The engineering and characterization of the variably glycosylated panel of anti-TNP human IgG1s (50, 51) and rhesus macaque FcγRs (38) have been described previously. These modifications include

manipulation of fucose (F), bisecting GlcNAc (B), sialic acid (S), and galactose (G) content (**Supplemental Table 1**). Unmodified anti-CD20 [anti-CD20 (2B8R1), Nonhuman Primate Reagent Resource Cat# PR-2287, RRID: AB_2716323] and afucosylated anti-CD20 [anti-CD20 (2B8R1F8), Nonhuman Primate Reagent Resource Cat# PR-8288, RRID: AB_2819341] were derived from rituximab and grafted into rhesus variable regions. Representative mass spectrometry-based glycoprofiles of these reagents are shown in **Supplemental Figure 2**. Unmodified and afucosylated forms of an HIV-specific double variable domain bispecific Ab that binds to both gp120 and gp41 of the envelope protein through fusion of CD4 (d2) with gp41-specific 7B2 monoclonal antibody linked through the H4 linker CD4 (d2)-H4-7B2 (64, 65) were constitutively expressed in either wild type or fucosyl-transferase Fut8^{-/-} CHO cells. Unmodified and afucosylated DVDs showed equivalent binding to antigen by ELISA, but differential interaction with biotinylated fucose-specific *Lens culinaris* lectin, and the human CD16-expressing KHYG-1 Natural Killer cells (66) (kindly provided by Dr. David Evans, Wisconsin National Primate Research Center) (**Supplemental Figure 3**).

Surface Plasmon Resonance

Antibodies were covalently coupled to a carboxymethyl-dextran-functionalized sensor (CMD200M, Xantec Bioanalytics) using carbodiimide chemistry. A Continuous Flow Microspotter (CFM) (Carterra) allowed the complete panel, with replicates, to be printed on a single sensor chip. The sensor surface was activated by a mixture of 10.4 mM EDC (ThermoFisher, 77149) and 2.8 mM sulfo-N-hydroxysuccinimide (ThermoFisher, A39269) formulated in 10 mM MES (pH 5.0). Antibodies formulated in 10 mM sodium acetate (pH 5.0) at 50 and 100 nM were applied to the activated regions for 10 minutes. The regions were then washed with sodium acetate for 5 minutes. Unreacted substrate was capped using 1 M ethanolamine (Sigma-Aldrich, 15014-100ML) applied by the flow cell of the imaging-based surface plasmon resonance instrument (SPRi) (MX96, IBIS Technologies). Remaining ligand was removed and the overall capacity of the sensor tested using successive injections (5 rounds in total) of 25 μg/mL anti-human Fc and 10 mM glycine (pH 3.0).

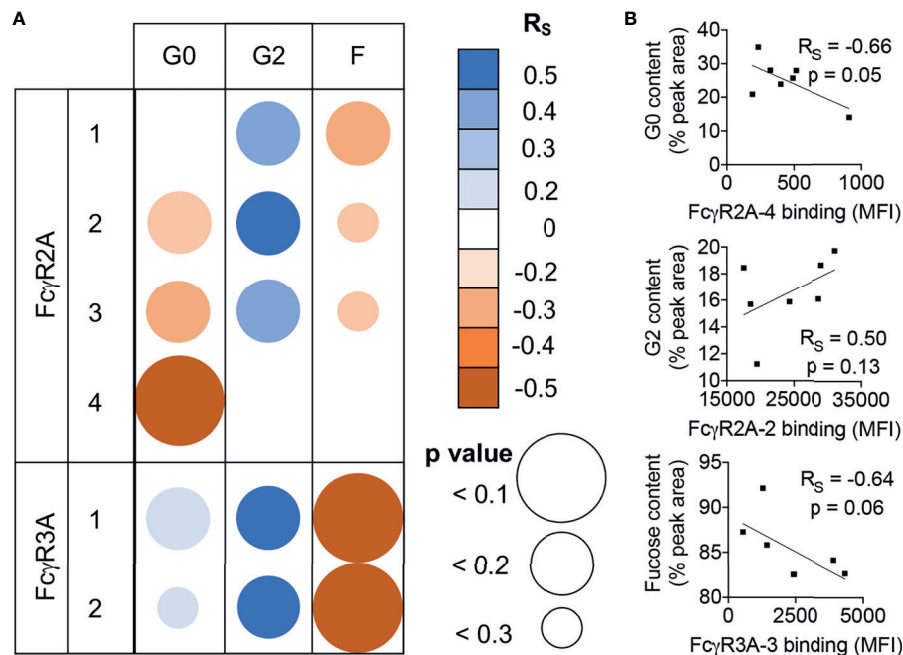


FIGURE 6 | Similar FcγR binding glycopreferences are observed for RM serum IgG. **(A)** Correlations of receptor binding signal in multiplex assay and glycan species prevalence in rhesus macaque serum IgG for each allotypic variant of RM FcγR1a and FcγR1a. Unadjusted Spearman correlation coefficient (R_s) strength and direction are indicated in color, and confidence (p value) in size. **(B)** Exemplary scatter plots of relatively stronger correlative relationships between relative galactose and fucose content (% peak area) in relation to FcγR binding median fluorescent intensity (MFI). Correlation coefficients and exact p values are indicated in inset.

The Fc receptor analytes were formulated at 20 μ M in a running buffer consisting of 1x phosphate buffered saline containing 0.05% Tween 20. Each receptor was tested over an 8-point series of 1:3 dilutions, running from the lowest concentration to the highest. Association was measured over a 5-minute period before switching the flow cell to running buffer to capture 5 minutes of dissociation. Two blank injections of the running buffer following each receptor series were sufficient to completely dissociate these low-affinity analytes and prepare the sensor for the next receptor.

Raw data was processed using SprintX (IBIS Technologies). The background signal of the nearest unconjugated interspot was subtracted from the adjacent regions of interest to account for bulk shift and non-specific binding. The blank injection immediately preceding each series of receptor was also subtracted from each concentration of receptor. Equilibrium affinity values (K_D) for each receptor-glycovariant pair were calculated in Scrubber 2 (BioLogic Software) using the average signal during a ten-second window at the end of the association phase when the system had reached equilibrium. The maximum response (R_{max}) predicted for a saturated system was calculated for each region of interest. Regions with an R_{max} of less than 25 were discarded for insufficient signal.

Rhesus Serum IgG Receptor Binding and Glycan Analysis

Serum samples from seven healthy rhesus macaques were profiled for binding to rhesus FcγR-conjugated fluorescent beads in a multiplexed

assay (67). Briefly, recombinant rhesus FcγR were covalently coupled to uniquely fluorescently coded magnetic microspheres, incubated in dilute serum, and bound antibody was detected with a phycoerythrin-conjugated anti-IgG detection antibody prior to data acquisition on a Luminex FlexMap. Median fluorescent intensities were reported for each sample for each FcγR.

For glycan analysis, rhesus macaque IgG was purified from serum *via* Melon Gel (manufacturer), followed by digestion with both SpeB and IdeA enzymes (Genovis), and purification of cleaved Fc domains by Protein A affinity chromatography (GE Life Sciences), each according to the manufacturer's recommendations. IgG glycan analysis was performed as described previously (68). Briefly, purified Fc was treated with PNGase F (New England Biolabs). Subsequently, protein was precipitated with ethanol and released glycans were evaporatively concentrated prior to fluorescent labeling with 2-aminobenzamide. After washing and removal of excess dye, glycans were analyzed using HILIC HPLC on a 150 3 2-mm TSKgel Amide-80 column (Tosoh Bioscience) with 3-mm packing material on a 1200 series HPLC (Agilent Technologies). Peak identities were confirmed *via* use of a glycan standard (Ludger). Quantification by area-under-the-curve analysis was performed with ChemStation software (Agilent Technologies).

Statistical Analysis

Statistical analysis was performed in Graphpad Prism version 9. Global comparisons (**Figure 2**) of glycovariants with (+) and

without (-) fucose, bisecting GlcNAc, and sialic acid modifications were evaluated for each individual receptor allotype by t test. Galactose content, which was alternatively increased, unmodified, or decreased, was evaluated by one-way ANOVA adjusted for multiple comparisons according to the procedure of Benjamini, Krieger, and Yekutieli. Paired comparisons (**Figure 4** and **Supplemental Figure 1**) of glycovariants with and without fucose, bisecting GlcNAc, and sialic acid modifications but for which other glycan modifications were held constant (i.e.: for fucose content, +G was paired with -F+G, and +G+S was paired with -F+G+S) were evaluated by paired t test across of FcγRII types and allotypes and FcγRIII allotypes. Paired comparisons evaluating the effect of variable galactosylation were evaluated using a mixed effect model with Tukey's test of multiple comparisons, comparing the effect of each galactose characteristic (+G, unmodified G, and -G) when other modifications (F, B, and S)) were held constant. Strength and direction of relationships between Fc glycoform prevalences in rhesus serum IgG and FcγR binding signals were evaluated by Spearman's rank correlation coefficient and statistic.

DATA AVAILABILITY STATEMENT

The raw data supporting the conclusions of this article will be made available by the authors, without undue reservation.

REFERENCES

- Schroeder HW Jr., Cavacini L. Structure and Function of Immunoglobulins. *J Allergy Clin Immunol* (2010) 125(2 Suppl 2):S41–52. doi: 10.1016/j.jaci.2009.09.046
- Jennewein MF, Alter G. The Immunoregulatory Roles of Antibody Glycosylation. *Trends Immunol* (2017) 38(5):358–72. doi: 10.1016/j.it.2017.02.004
- Bakovic MP, Selman MH, Hoffmann M, Rudan I, Campbell H, Deelder AM, et al. High-Throughput IgG Fc N-Glycosylation Profiling by Mass Spectrometry of Glycopeptides. *J Proteome Res* (2013) 12(2):821–31. doi: 10.1021/pr300887z
- Dwek RA. Biological Importance of Glycosylation. *Dev Biol Stand* (1998) 96:43–7. doi: 10.1007/978-94-011-5288-4_1
- Chen G, Wang Y, Qiu L, Qin X, Liu H, Wang X, et al. Human IgG Fc-Glycosylation Profiling Reveals Associations With Age, Sex, Female Sex Hormones and Thyroid Cancer. *J Proteomics* (2012) 75(10):2824–34. doi: 10.1016/j.jprot.2012.02.001
- Keusch J, Levy Y, Shoenfeld Y, Youinou P. Analysis of Different Glycosylation States in IgG Subclasses. *Clin Chim Acta* (1996) 252(2):147–58. doi: 10.1016/0009-8981(96)06326-7
- Parekh R, Roitt I, Isenberg D, Dwek R, Rademacher T. Age-Related Galactosylation of the N-Linked Oligosaccharides of Human Serum IgG. *J Exp Med* (1988) 167(5):1731–6. doi: 10.1084/jem.167.5.1731
- Rook GA, Steele J, Brealey R, Whyte A, Isenberg D, Sumar N, et al. Changes in IgG Glycoform Levels Are Associated With Remission of Arthritis During Pregnancy. *J Autoimmun* (1991) 4(5):779–94. doi: 10.1016/0896-8411(91)90173-A
- Shikata K, Yasuda T, Takeuchi F, Konishi T, Nakata M, Mizuuchi T. Structural Changes in the Oligosaccharide Moiety of Human IgG With Aging. *Glycoconj J* (1998) 15(7):683–9. doi: 10.1023/A:1006936431276
- van de Geijn FE, Wuhrer M, Selman MH, Willemsen SP, de Man YA, Deelder AM, et al. Immunoglobulin G Galactosylation and Sialylation Are Associated With Pregnancy-Induced Improvement of Rheumatoid Arthritis and the

AUTHOR CONTRIBUTIONS

Conceptualization, AC and MA. Investigation, AC, GD, SP, WG, and NO-O. Writing – original draft, AC and MA. Writing – review and editing, all authors. Data analysis and curation, AC, NO-O, and MA. Funding acquisition, GV and MA. All authors contributed to the article and approved the submitted version.

FUNDING

This work was supported in part by the NIGMS and the NIAID R01 AI131975, NIAID P01 AI120756, AI136758, and NIH NCI supplement to 2P30 CA 023108-41, the BioMT Molecular Tools Core supported by NIGMS COBRE award P20-GM113132. Reagents provided by the NIH Nonhuman Primate Reagent Resource were supported by the awards P40 OD028116 (ORIP) and U24 AI126683 (NIAID).

SUPPLEMENTARY MATERIAL

The Supplementary Material for this article can be found online at: <https://www.frontiersin.org/articles/10.3389/fimmu.2021.754710/full#supplementary-material>

- Postpartum Flare: Results From a Large Prospective Cohort Study. *Arthritis Res Ther* (2009) 11(6):R193. doi: 10.1186/ar2892
- Yamada E, Tsukamoto Y, Sasaki R, Yagyu K, Takahashi N. Structural Changes of Immunoglobulin G Oligosaccharides With Age in Healthy Human Serum. *Glycoconj J* (1997) 14(3):401–5. doi: 10.1023/A:1018582930906
- Lau C, Huffman JE, Pucic M, Zgaga L, Adamczyk B, Muzinic A, et al. Loci Associated With N-Glycosylation of Human Immunoglobulin G Show Pleiotropy With Autoimmune Diseases and Haematological Cancers. *PLoS Genet* (2013) 9(1):e1003225. doi: 10.1371/journal.pgen.1003225
- Novokmet M, Lukic E, Vuckovic F, Ethuric Z, Keser T, Rajsl K, et al. Changes in IgG and Total Plasma Protein Glycomes in Acute Systemic Inflammation. *Sci Rep* (2014) 4:4347. doi: 10.1038/srep04347
- Selman MH, de Jong SE, Soonawala D, Kroon FP, Adegnik AA, Deelder AM, et al. Changes in Antigen-Specific IgG1 Fc N-Glycosylation Upon Influenza and Tetanus Vaccination. *Mol Cell Proteomics* (2012) 11(4):M111 014563. doi: 10.1074/mcp.M111.014563
- Kao D, Lux A, Schaffert A, Lang R, Altmann F, Nimmerjahn F. IgG Subclass and Vaccination Stimulus Determine Changes in Antigen Specific Antibody Glycosylation in Mice. *Eur J Immunol* (2017) 47(12):2070–9. doi: 10.1002/eji.201747208
- Mahan AE, Jennewein MF, Suscovich T, Dionne K, Tedesco J, Chung AW, et al. Antigen-Specific Antibody Glycosylation Is Regulated via Vaccination. *PLoS Pathog* (2016) 12(3):e1005456. doi: 10.1371/journal.ppat.1005456
- Nose M, Wiggzell H. Biological Significance of Carbohydrate Chains on Monoclonal Antibodies. *Proc Natl Acad Sci U S A* (1983) 80(21):6632–6. doi: 10.1073/pnas.80.21.6632
- Mimura Y, Sondermann P, Ghirlando R, Lund J, Young SP, Goodall M, et al. Role of Oligosaccharide Residues of IgG1-Fc in Fc Gamma RIIB Binding. *J Biol Chem* (2001) 276(49):45539–47. doi: 10.1074/jbc.M107478200
- Ackerman ME, Crispin M, Yu X, Baruah K, Boesch AW, Harvey DJ, et al. Natural Variation in Fc Glycosylation of HIV-Specific Antibodies Impacts Antiviral Activity. *J Clin Invest* (2013) 123(5):2183–92. doi: 10.1172/JCI65708
- Larsen MD, de Graaf EL, Sonneveld ME, Plomp HR, Nouta J, Hoepel W, et al. Afucosylated IgG Characterizes Enveloped Viral Responses and Correlates With COVID-19 Severity. *Science* (2021) 371(6532). doi: 10.1126/science.abc8378

21. Thulin NK, Brewer RC, Sherwood R, Bournazos S, Edwards KG, Ramadoss NS, et al. Maternal Anti-Dengue IgG Fucosylation Predicts Susceptibility to Dengue Disease in Infants. *Cell Rep* (2020) 31(6):107642. doi: 10.1016/j.celrep.2020.107642
22. Wang TT, Sewatanon J, Memoli MJ, Wrammert J, Bournazos S, Bhaumik SK, et al. IgG Antibodies to Dengue Enhanced for FcγRIIIa Binding Determine Disease Severity. *Science* (2017) 355(6323):395–8. doi: 10.1126/science.aai8128
23. Kapur R, Kustiawan I, Vestreheim A, Koeleman CA, Visser R, Einarsdottir HK, et al. A Prominent Lack of IgG1-Fc Fucosylation of Platelet Alloantibodies in Pregnancy. *Blood* (2014) 123(4):471–80. doi: 10.1182/blood-2013-09-527978
24. Kapur R, Valle LD, Sonneveld M, Ederveen AH, Visser R, Ligthart P, et al. Low Anti-RhD IgG-Fc-Fucosylation in Pregnancy: A New Variable Predicting Severity in Haemolytic Disease of the Fetus and Newborn. *Br J Haematol* (2014) 166(6):936–45. doi: 10.1111/bjh.12965
25. Chakraborty S, Gonzalez J, Edwards K, Mallajosyula V, Buzzanco AS, Sherwood R, et al. Proinflammatory IgG Fc Structures in Patients With Severe COVID-19. *Nat Immunol* (2021) 22(1):67–73. doi: 10.1038/s41590-020-00828-7
26. Lu LL, Chung AW, Rosebrock TR, Ghebremichael M, Yu WH, Grace PS, et al. A Functional Role for Antibodies in Tuberculosis. *Cell* (2016) 167(2):433–43 e14. doi: 10.1016/j.cell.2016.08.072
27. Ho CH, Chien RN, Cheng PN, Liu JH, Liu CK, Su CS, et al. Aberrant Serum Immunoglobulin G Glycosylation in Chronic Hepatitis B Is Associated With Histological Liver Damage and Reversible by Antiviral Therapy. *J Infect Dis* (2015) 211(1):115–24. doi: 10.1093/infdis/jiu388
28. van Osch TLJ, Nouta J, Derksen NIL, van Mierlo G, van der Schoot E, Wührer M, et al. Fc Galactosylation Promotes Hexamerization of Higg1 Leading to Enhanced Classic Complement Activation. *J Immunol* (2021). doi: 10.4049/jimmunol.2100399
29. Yamaguchi Y, Nishimura M, Nagano M, Yagi H, Sasakawa H, Uchida K, et al. Glycoform-Dependent Conformational Alteration of the Fc Region of Human Immunoglobulin G1 as Revealed by NMR Spectroscopy. *Biochim Biophys Acta* (2006) 1760(4):693–700. doi: 10.1016/j.bbagen.2005.10.002
30. Subedi GP, Barb AW. The Immunoglobulin G1 N-Glycan Composition Affects Binding to Each Low Affinity Fc Gamma Receptor. *MAbs* (2016) 8(8):1512–24. doi: 10.1080/19420862.2016.1218586
31. Shields RL, Lai J, Keck R, O'Connell LY, Hong K, Meng YG, et al. Lack of Fucose on Human IgG1 N-Linked Oligosaccharide Improves Binding to Human FcγRIII and Antibody-Dependent Cellular Toxicity. *J Biol Chem* (2002) 277(30):26733–40. doi: 10.1074/jbc.M202069200
32. Niwa R, Natsume A, Uehara A, Wakitani M, Iida S, Uchida K, et al. IgG Subclass-Independent Improvement of Antibody-Dependent Cellular Cytotoxicity by Fucose Removal From Asn297-Linked Oligosaccharides. *J Immunol Methods* (2005) 306(1-2):151–60. doi: 10.1016/j.jim.2005.08.009
33. Bruhns P, Iannascoli B, England P, Mancardi DA, Fernandez N, Jorieu S, et al. Specificity and Affinity of Human FcγRIII Receptors and Their Polymorphic Variants for Human IgG Subclasses. *Blood* (2009) 113(16):3716–25. doi: 10.1182/blood-2008-09-179754
34. Brady LJ, Velayudhan J, Visone DB, Daugherty KC, Bartron JL, Coon M, et al. The Criticality of High-Resolution N-Linked Carbohydrate Assays and Detailed Characterization of Antibody Effector Function in the Context of Biosimilar Development. *MAbs* (2015) 7(3):562–70. doi: 10.1080/19420862.2015.1016692
35. Shinkawa T, Nakamura K, Yamane N, Shoji-Hosaka E, Kanda Y, Sakurada M, et al. The Absence of Fucose But Not the Presence of Galactose or Bisecting N-Acetylglucosamine of Human IgG1 Complex-Type Oligosaccharides Shows the Critical Role of Enhancing Antibody-Dependent Cellular Cytotoxicity. *J Biol Chem* (2003) 278(5):3466–73. doi: 10.1074/jbc.M210665200
36. Junttila TT, Parsons K, Olsson C, Lu Y, Xin Y, Theriault J, et al. Superior *In Vivo* Efficacy of Afucosylated Trastuzumab in the Treatment of HER2-Amplified Breast Cancer. *Cancer Res* (2010) 70(11):4481–9. doi: 10.1158/0008-5472.CAN-09-3704
37. Cameron F, McCormack PL. Obinituzumab: First Global Approval. *Drugs* (2014) 74(1):147–54. doi: 10.1007/s40265-013-0167-3
38. Chan YN, Boesch AW, Osei-Owusu NY, Emileh A, Crowley AR, Cocklin SL, et al. IgG Binding Characteristics of Rhesus Macaque FcγRIIIa. *J Immunol* (2016) 197(7):2936–47. doi: 10.4049/jimmunol.1502252
39. Boesch AW, Osei-Owusu NY, Crowley AR, Chu TH, Chan YN, Weiner JA, et al. Biophysical and Functional Characterization of Rhesus Macaque IgG Subclasses. *Front Immunol* (2016) 7:589. doi: 10.3389/fimmu.2016.00589
40. Crowley AR, Ackerman ME. Mind the Gap: How Interspecies Variability in IgG and Its Receptors May Complicate Comparisons of Human and Non-Human Primate Effector Function. *Front Immunol* (2019) 10:697. doi: 10.3389/fimmu.2019.00697
41. Haj AK, Arbanas JM, Yamniuk AP, Karl JA, Bussan HE, Drinkwater KY, et al. Characterization of Mauritian Cynomolgus Macaque FcγRIIIa Alleles Using Long-Read Sequencing. *J Immunol* (2019) 202(1):151–9. doi: 10.4049/jimmunol.1800843
42. Grunst MW, Grandea AG3rd, Janaka SK, Hammad I, Grimes P, Karl JA, et al. Functional Interactions of Common Allotypes of Rhesus Macaque FcγRIIIa and FcγRIIIb With Human and Macaque IgG Subclasses. *J Immunol* (2020) 205(12):3319–32. doi: 10.4049/jimmunol.2000501
43. Raju TS, Briggs JB, Borge SM, Jones AJ. Species-Specific Variation in Glycosylation of IgG: Evidence for the Species-Specific Sialylation and Branch-Specific Galactosylation and Importance for Engineering Recombinant Glycoprotein Therapeutics. *Glycobiology* (2000) 10(5):477–86. doi: 10.1093/glycob/10.5.477
44. Mahan AE, Tedesco J, Dionne K, Baruah K, Cheng HD, De Jager PL, et al. A Method for High-Throughput, Sensitive Analysis of IgG Fc and Fab Glycosylation by Capillary Electrophoresis. *J Immunol Methods* (2015) 417:34–44. doi: 10.1016/j.jim.2014.12.004
45. Ferrara C, Grau S, Jager C, Sondermann P, Brunker P, Waldhauer I, et al. Unique Carbohydrate-Carbohydrate Interactions Are Required for High Affinity Binding Between FcγRIII and Antibodies Lacking Core Fucose. *Proc Natl Acad Sci U S A* (2011) 108(31):12669–74. doi: 10.1073/pnas.1108455108
46. Mizushima T, Yagi H, Takemoto E, Shibata-Koyama M, Isoda Y, Iida S, et al. Structural Basis for Improved Efficacy of Therapeutic Antibodies on Defucosylation of Their Fc Glycans. *Genes Cells* (2011) 16(11):1071–80. doi: 10.1111/j.1365-2443.2011.01552.x
47. Falconer DJ, Subedi GP, Marcella AM, Barb AW. Antibody Fucosylation Lowers the FcγRIIIa/CD16a Affinity by Limiting the Conformations Sampled by the N162-Glycan. *ACS Chem Biol* (2018) 13(8):2179–89. doi: 10.1021/acscchembio.8b00342
48. Dekkers G, Bentlage AEH, Plomp R, Visser R, Koeleman CAM, Beentjes A, et al. Conserved FcγRIIIa Glycan Discriminates Between Fucosylated and Afucosylated IgG in Humans and Mice. *Mol Immunol* (2018) 94:54–60. doi: 10.1016/j.molimm.2017.12.006
49. Moldt B, Shibata-Koyama M, Rakasz EG, Schultz N, Kanda Y, Dunlop DC, et al. A Nonfucosylated Variant of the Anti-HIV-1 Monoclonal Antibody B12 has Enhanced FcγRIIIa-Mediated Antiviral Activity *In Vitro* But Does Not Improve Protection Against Mucosal SHIV Challenge in Macaques. *J Virol* (2012) 86(11):6189–96. doi: 10.1128/JVI.00491-12
50. Dekkers G, Plomp R, Koeleman CA, Visser R, von Horst HH, Sandig V, et al. Multi-Level Glyco-Engineering Techniques to Generate IgG With Defined Fc-Glycans. *Sci Rep* (2016) 6:36964. doi: 10.1038/srep36964
51. Dekkers G, Treffers L, Plomp R, Bentlage AEH, de Boer M, Koeleman CAM, et al. Decoding the Human Immunoglobulin G-Glycan Repertoire Reveals a Spectrum of Fc-Receptor- and Complement-Mediated-Effector Activities. *Front Immunol* (2017) 8:877. doi: 10.3389/fimmu.2017.00877
52. Hodoniczky J, Zheng YZ, James DC. Control of Recombinant Monoclonal Antibody Effector Functions by Fc N-Glycan Remodeling *In Vitro*. *Biotechnol Prog* (2005) 21(6):1644–52. doi: 10.1021/bp050228w
53. Shinkawa T, Nakamura K, Yamane N, Shoji-Hosaka E, Kanda Y, Sakurada M, et al. The Absence of Fucose But Not the Presence of Galactose or Bisecting N-Acetylglucosamine of Human IgG1 Complex-Type Oligosaccharides Shows the Critical Role of Enhancing Antibody-Dependent Cellular Cytotoxicity. *J Biol Chem* (2002) 278(5):3466–73. doi: 10.1074/jbc.RA118.005294
54. Ferrara C, Brunker P, Suter T, Moser S, Puntener U, Umana P. Modulation of Therapeutic Antibody Effector Functions by Glycosylation Engineering: Influence of Golgi Enzyme Localization Domain and Co-Expression of Heterologous Beta1, 4-N-Acetylglucosaminyltransferase III and Golgi Alpha-Mannosidase II. *Biotechnol Bioeng* (2006) 93(5):851–61. doi: 10.1002/bit.20777

55. Anthony RM, Nimmerjahn F, Ashline DJ, Reinhold VN, Paulson JC, Ravetch JV. Recapitulation of IVIG Anti-Inflammatory Activity With a Recombinant IgG Fc. *Science* (2008) 320(5874):373–6. doi: 10.1126/science.1154315
56. Kaneko Y, Nimmerjahn F, Ravetch JV. Anti-Inflammatory Activity of Immunoglobulin G Resulting From Fc Sialylation. *Science* (2006) 313(5787):670–3. doi: 10.1126/science.1129594
57. Yu X, Baruah K, Harvey DJ, Vasiljevic S, Alonzi DS, Song BD, et al. Engineering Hydrophobic Protein-Carbohydrate Interactions to Fine-Tune Monoclonal Antibodies. *J Am Chem Soc* (2013) 135(26):9723–32. doi: 10.1021/ja4014375
58. Pereira NA, Chan KF, Lin PC, Song Z. The "Less-is-More" in Therapeutic Antibodies: Afucosylated Anti-Cancer Antibodies With Enhanced Antibody-Dependent Cellular Cytotoxicity. *MAbs* (2018) 10(5):693–711. doi: 10.1080/19420862.2018.1466767
59. Bruggeman CW, Dekkers G, Bentlage AEH, Treffers LW, Nagelkerke SQ, Lissenberg-Thunnissen S, et al. Enhanced Effector Functions Due to Antibody Defucosylation Depend on the Effector Cell Fcγ Receptor Profile. *J Immunol* (2017) 199(1):204–11. doi: 10.4049/jimmunol.1700116
60. Barouch DH, Alter G, Broge T, Linde C, Ackerman ME, Brown EP, et al. Protective Efficacy of Adenovirus/Protein Vaccines Against SIV Challenges in Rhesus Monkeys. *Science* (2015) 349(6245):320–4. doi: 10.1126/science.aab3886
61. Miller-Novak LK, Das J, Musich TA, Demberg T, Weiner JA, Venzon DJ, et al. Analysis of Complement-Mediated Lysis of Simian Immunodeficiency Virus (SIV) and SIV-Infected Cells Reveals Sex Differences in Vaccine-Induced Immune Responses in Rhesus Macaques. *J Virol* (2018) 92(19). doi: 10.1128/JVI.00721-18
62. Vaccari M, Gordon SN, Fourati S, Schifanella L, Liyanage NP, Cameron M, et al. Adjuvant-Dependent Innate and Adaptive Immune Signatures of Risk of SIVmac251 Acquisition. *Nat Med* (2016) 22(7):762–70. doi: 10.1038/nm.4105
63. Welles HC, Jennewein MF, Mason RD, Narpala S, Wang L, Cheng C, et al. Vectored Delivery of Anti-SIV Envelope Targeting mAb via AAV8 Protects Rhesus Macaques From Repeated Limiting Dose Intrarectal SIVsmE660 Challenge. *PLoS Pathog* (2018) 14(12):e1007395. doi: 10.1371/journal.ppat.1007395
64. Craig RB, Summa CM, Corti M, Pincus SH. Anti-HIV Double Variable Domain Immunoglobulins Binding Both Gp41 and Gp120 for Targeted Delivery of Immunoconjugates. *PLoS One* (2012) 7(10):e46778. doi: 10.1371/journal.pone.0046778
65. Pincus SH, Craig RB, Weachter L, LaBranche CC, Nabi R, Watt C, et al. Bispecific Anti-HIV Immunoadhesins That Bind Gp120 and Gp41 Have Broad and Potent HIV-Neutralizing Activity. *Vaccines* (2021) 9(774). doi: 10.3390/vaccines9070774
66. Alpert MD, Harvey JD, Lauer WA, Reeves RK, Piatak MJr., Carville A, et al. ADCC Develops Over Time During Persistent Infection With Live-Attenuated SIV and Is Associated With Complete Protection Against SIV (mac)251 Challenge. *PLoS Pathog* (2012) 8(8):e1002890. doi: 10.1371/journal.ppat.1002890
67. Boesch AW, Brown EP, Cheng HD, Ofori MO, Normandin E, Nigrovic PA, et al. Highly Parallel Characterization of IgG Fc Binding Interactions. *MAbs* (2014) 6(4):915–27. doi: 10.4161/mabs.28808
68. Storcksdieck genannt Bonsmann M, Niezold T, Temchura V, Pissani F, Ehrhardt K, Brown EP, et al. Enhancing the Quality of Antibodies to HIV-1 Envelope by GagPol-Specific Th Cells. *J Immunol* (2015) 195(10):4861–72. doi: 10.4049/jimmunol.1501377

Conflict of Interest: WG was employed by Antigen Pharmaceuticals Inc.

The remaining authors declare that the research was conducted in the absence of any commercial or financial relationships that could be construed as a potential conflict of interest.

Publisher's Note: All claims expressed in this article are solely those of the authors and do not necessarily represent those of their affiliated organizations, or those of the publisher, the editors and the reviewers. Any product that may be evaluated in this article, or claim that may be made by its manufacturer, is not guaranteed or endorsed by the publisher.

Copyright © 2021 Crowley, Osei-Owusu, Dekkers, Gao, Wuhrer, Magnani, Reimann, Pincus, Vidarsson and Ackerman. This is an open-access article distributed under the terms of the Creative Commons Attribution License (CC BY). The use, distribution or reproduction in other forums is permitted, provided the original author(s) and the copyright owner(s) are credited and that the original publication in this journal is cited, in accordance with accepted academic practice. No use, distribution or reproduction is permitted which does not comply with these terms.



Immunoglobulin Glycosylation – An Unexploited Potential for Immunomodulatory Strategies in Farm Animals

Kristina Zlatina* and Sebastian P. Galuska

Institute of Reproductive Biology, Research Institute for Farm Animal Biology (FBN), Dummerstorf, Germany

OPEN ACCESS

Edited by:

David Falck,
Leiden University Medical Center,
Netherlands

Reviewed by:

Jianying Yang,
INSERM Immuno Rhumatologie
Moléculaire (IRM), France
Rita Carsetti,
Bambino Gesù Children Hospital
(IRCCS), Italy

*Correspondence:

Kristina Zlatina
zlatina@fhn-dummerstorf.de

Specialty section:

This article was submitted to
B Cell Biology,
a section of the journal
Frontiers in Immunology

Received: 04 August 2021

Accepted: 23 September 2021

Published: 18 October 2021

Citation:

Zlatina K and Galuska SP (2021)
Immunoglobulin Glycosylation –
An Unexploited Potential
for Immunomodulatory
Strategies in Farm Animals.
Front. Immunol. 12:753294.
doi: 10.3389/fimmu.2021.753294

The function of antibodies, namely the identification and neutralization of pathogens, is mediated by their antigen binding site (Fab). In contrast, the subsequent signal transduction for activation of the immune system is mediated by the fragment crystallizable (Fc) region, which interacts with receptors or other components of the immune system, such as the complement system. This aspect of binding and interaction is more precise, readjusted by covalently attached glycan structures close to the hinge region of immunoglobulins (Ig). This fine-tuning of Ig and its actual state of knowledge is the topic of this review. It describes the function of glycosylation at Ig in general and the associated changes due to corresponding glycan structures. We discuss the functionality of IgG glycosylation during different physiological statuses, like aging, lactation and pathophysiological processes. Further, we point out what is known to date about Ig glycosylation in farm animals and how new achievements in vaccination may contribute to improved animal welfare.

Keywords: immunoglobulin, antibody, glycosylation, Fc receptor, pregnancy, lactation, vaccination

INTRODUCTION

Immunoglobulins (Ig) are essential players in the immune system. They recognize foreign molecules *via* their antigen binding sites, which are located in the variable domain of the antigen binding fragment (Fab) (**Figure 1A**). The recognition and binding of foreign molecules can induce several different defense strategies. For instance, soluble molecules such as toxins can be agglutinated and/or neutralized (**Figure 1B**). Furthermore, opsonization by Ig is an important process to counteract the invasion of pathogens. The recognition of antigens on the surface of pathogens subsequently initiate antibody-dependent cellular cytotoxicity (ADCC), antibody-dependent cellular phagocytosis (ADCP), or a complement-dependent cytotoxicity (CDC) (**Figure 1B**). Each of these three mechanisms is driven by an interaction of the fragment crystallizable (Fc) region with receptors of an effector cell or members of the complement system.

Remarkably, such interactions with the Fc region are influenced by its glycosylation status. For this reason, the detailed analysis of the glycosylation patterns of Igs during physiological and pathophysiological processes and the knowledge of the glycan-dependent functionality of Igs in mice and humans are increasingly being explored. However, very little is known about the

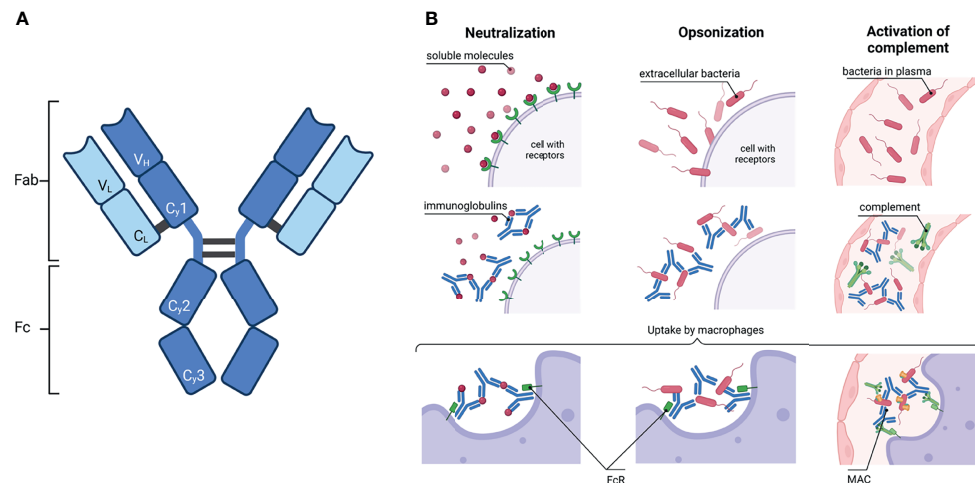


FIGURE 1 | Immunoglobulin: schematic structure and how they activate the immune system. **(A)** A common IgG structure consisting of two heavy chain (dark blue) with three constant (C γ 1-3) and one variable domain (V γ) and two light chain (light blue) with one constant (C λ) and one variable domain (V λ). The heavy and light chains are covalently connected by disulfide bonds. The IgG is further subdivided in the antigen binding fragment (Fab) and fragment crystallisable (Fc). **(B)** Activation of the immune system by antibodies. Left column: Ig can neutralize soluble molecules, e.g. bacteria toxins, to protect endogenous cells. Middle column: The binding of Ig to virus or bacteria antigens is called opsonisation. Right column: Ig bound to pathogens can activate the complement. Complement factors C1q recognize Ig and induce the complement cascade; a membrane attack complex (MAC) is formed in the end. In the end, macrophages or neutrophils phagocytose the complex of Ig with either soluble molecules or bacteria or, additionally, with the components of the complement. Created with BioRender.com.

glycosylation patterns of Igs in other mammals, such as farm animals. This is surprising given that an optimal functioning adaptive immune system is essential to ensure the health and welfare of animals.

This review gives a general overview of Ig glycosylation and its effect on the mechanisms of the adaptive immune system with the aim to demonstrate how Ig glycosylation has the potential to support the health and welfare of farm animals.

GLYCOSYLATION OF IG

In eukaryotes, the majority of extracellular proteins is glycosylated (1). This post-translational modification of proteins is important to initiate cellular processes, such as recognition, communication, differentiating and binding events. Remarkably, the glycosylation status of proteins depends on several aspects. Firstly, within the animal kingdom, significant differences in the glycosylation machinery exist; for example, enzymes that are necessary for the synthesis and utilization of monosaccharides are species dependent, so that one and the same protein can be decorated with various glycan structures. Furthermore, the cell type, its differentiation state, and its metabolism status have an impact on the glycosylation patterns. Therefore, different physiological and pathological conditions frequently come with an altered glycosylation status. The most prominent forms of protein-glycosylations are the N- and the O-glycosylation.

In the case of N-glycosylation, a precursor structure is co-translational transferred to an asparagine (Asn) residue of the nascent protein in the endoplasmic reticulum. The Asn must be

part of the amino acid sequon Asn-X-Ser/Thr, whereby X can be any amino acid with the exception of proline. Thereafter, N-glycan processing starts, which includes numerous possible trimming and elongation events in the endoplasmic reticulum and Golgi apparatus (see **Supplemental Figure S1** for more information). Approximately 70% of all proteins carry one or more potential N-glycosylation sites (1). Further, Igs have several N-glycosylation sites (2). The number and positions differ between the individual Ig-classes and subtypes (**Figure 2**). For example, all IgG molecules are generally N-glycosylated in the Fc region at the conserved Asn₂₉₇ (**Figure 2A**). Approximately 15–25% are additional N-glycosylated at the Fab region. However, no conserved N-glycosylation site exists in the Fab region (3). Altogether, N-glycans approximately account for 2–3% of their molecular weight. In contrast to IgG, the Ig-classes IgM, IgD and IgE contain significantly more conserved N-glycosylation sites and are much more N-glycosylated (~12–14% of the molecular weight) (2).

Besides N-glycans, Igs can also contain O-glycans (**Figure 2**). O-glycans are attached to the oxygen atom of serine (Ser) or threonine (Thr) residues. In contrast to N-glycosylation sites, no specific sequon exists and, thus, O-glycosylation sites are difficult to predict. To date, little is known about the impact of O-glycans on the functionality of Igs. For this reason, the review is focused on the structure and mode of action of N-glycans on Igs.

Commonly, Igs are primarily decorated with complex N-glycans, but oligomannose and hybrid N-glycans can also be present (**Figure 3A**). In **Figure 3B**, for example, common N-glycans at Asn₂₉₇ of human IgG are displayed, which frequently contain core fucose, bisecting N-acetylglucosamine (GlcNAc), galactose (Gal), and N-acetylneuraminic acid (Neu5Ac) residues.

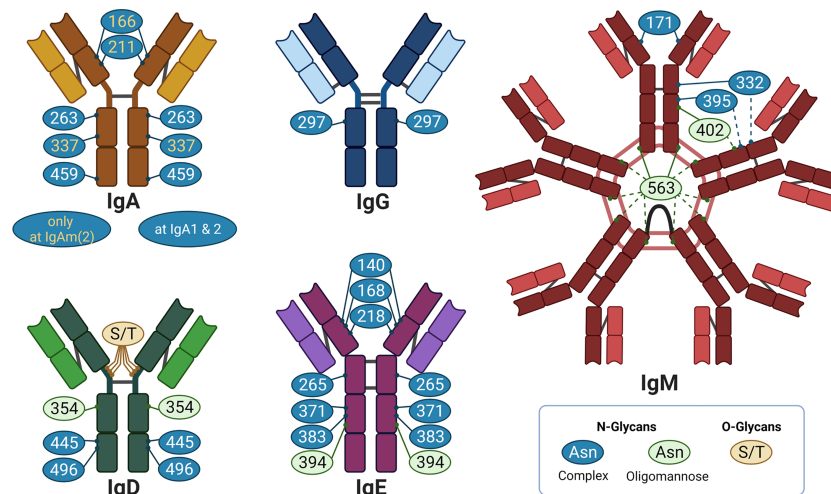


FIGURE 2 | Overview of glycosylation sites of different Ig: IgA, IgG, IgM, IgD, and IgE in individual colors. The bright color illustrates the light chain, the dark color the heavy chain. The grey lines indicate disulphide bridges. Created with BioRender.com.

Oligomannose structures are mainly located in the Fab region of IgG (5). Overall, it appears that the heterogeneity of the glycan structures is higher in the Fab region (5).

Glycans not only contribute to an altered molecular weight but also change the structural conformation (**Figure 4**). The presence of glycans at Asn₂₉₇ within C_{H2} of Fc entails an “open” conformation (**Figure 4A** top), while enzymatic deglycosylation leads to a “closed” structure instead (6). Further, it is being explored whether distinct sugars, like sialic acid, induce additional conformational changes of the C_{H2} of Fc (7–9). Sonderrmann et al. described that the addition of sialic acid leads to a more “closed” Fc structure as compared to the

presence of other glycan species or desialylated glycans (bottom in **Figure 4A**). Similar results were obtained by Ahmed et al. (8). In this review, the PDB structures used by Sonderrmann et al. and those generated by Ahmed et al. were aligned in order to compare the structural conformation. Five Fc regions are overlaid in **Figure 4B**, and their structures are related depending on the conformation between “open” and “closed”. Their glycans, which were present and obtained during the structural characterization, are given below the corresponding PDB entry. This comparison shows that the presence of sugar residues, like sialic acid and fucose, lead to closer Fc conformation. However, it has to be mentioned that, in fluids,

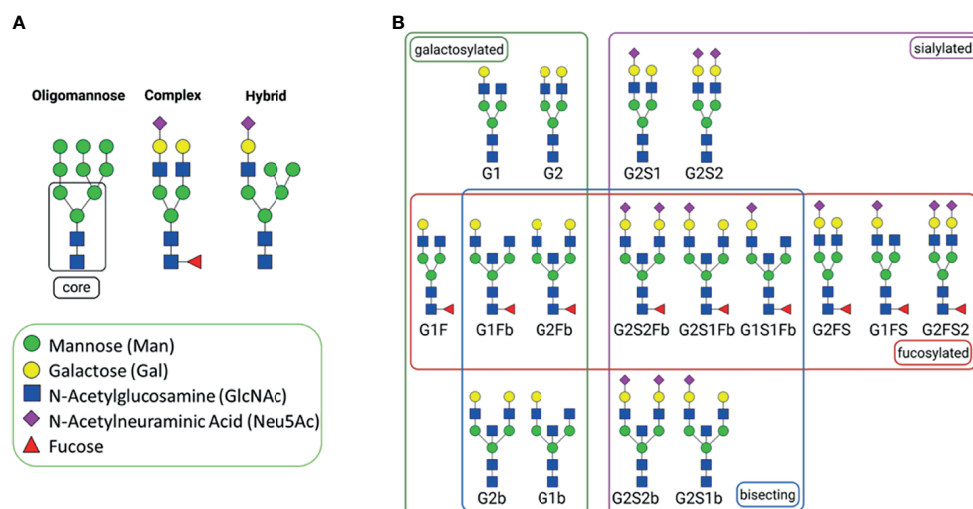


FIGURE 3 | N-Glycans. **(A)** general types of N-glycans; all of them have a common core structure, highlighted with a square (1). **(B)** Commonly abundant glycans of human IgG, grouped by glycan affiliation. The N-glycans were created using GlycoWorkbench 2.1 (4) and arranged with BioRender.com.

molecules are flexible and glycans significantly increase structural variations, which cannot be completely reproduced when the crystal structures are obtained. Therefore, molecular dynamic tools have to be applied. Frank et al. analyzed Fc structures using such a strategy and observed high flexibility of both the glycans and the C_H2 of Fc (10). Nevertheless, whether and to what extent different glycan patterns contribute not only to structural changes but also to the functionality of IgGs is under discussion.

The Impact of Glycosylation on the Functionality of Igs

Among other mechanisms of the immune system, Igs mediate an immune response through the complement system. The classical pathway of the complement system is activated when the C1-complex molecule C1q binds to IgGs or IgM, which recognize an antigen on the cell membrane. The Ig/C1q complex induces a cascade of enzymatic reactions, leading to the formation of the membrane attack complex (MAC) and, thus, perforation of cellular membranes. Remarkably, the interaction with C1q is modulated by N-glycans of IgG₁ at Asn₂₉₇ (11). For instance, terminal galactose increases the binding to C1q (examples for different N-glycans are shown in **Figure 3A**). The observed effects might be the result of a changed 3D structure of the Fc region, as displayed in **Figure 4**. Thus, N-glycans seem to influence one of the key mechanisms of the classical complement pathway.

Moreover, the lectin complement pathway can be induced if agalactosylated N-glycans are present on IgG. Typically, this pathway is initiated by the binding of mannan-binding protein

(MBP) to oligomannose on the cell surface of pathogens. Via the MBP associated serine protease (MASP) an activation of the complement system is initiated. Malhotra et al. observed that agalactosyl N-glycans on IgG are also recognized by MBP, leading to an activation of the lectin complement pathway (12) (**Figure 5A**). Interestingly, these same glycan structures (mannose or GlcNAc residues) are also recognized by the mannose binding receptor (CD 206). This receptor is expressed in macrophages and dendritic cells (13). The binding of CD 206 to agalactosylated IgGs results in their uptake.

Further immunomodulatory interaction partners of Igs are their related Fc receptors (FcR). The major classes of Fc receptors are Fc-gamma receptors (FcγR), FcαR, FcεR, and FcμR, which bind IgG, IgA, IgE, and IgM, respectively. FcμR recognize IgA molecules in addition to IgM, although with a lower affinity. Besides the extracellular Ig binding domain, Fc receptors may intracellularly have an activating or inhibitory motif, namely the immunoreceptor tyrosine-based activation motif (ITAM) (e.g. FcγRI, FcγRIIa, FcγRIIc, FcγRIIIa) or the immunoreceptor tyrosine-based inhibitory motif (ITIM) (e.g. FcγRIIb). Interestingly, the removal of N-glycans from the Fc region of IgG significantly reduces their binding to FcγR and, thus, their effector functions (14–16) (**Figure 5B**). However, further structural changes alter the IgG/FcγR interplay. For instance, removal of core fucose enhance the monocyte, macrophages, granulocyte, and natural killer cells mediated ADCC (17–19). Moreover, defucosylated IgGs have a higher affinity to FcγRIIIa, resulting in improved effector functions (18, 20, 21) (**Figure 5A**). FcγRIIIa and FcγRIIIb are also glycoproteins, and their N-

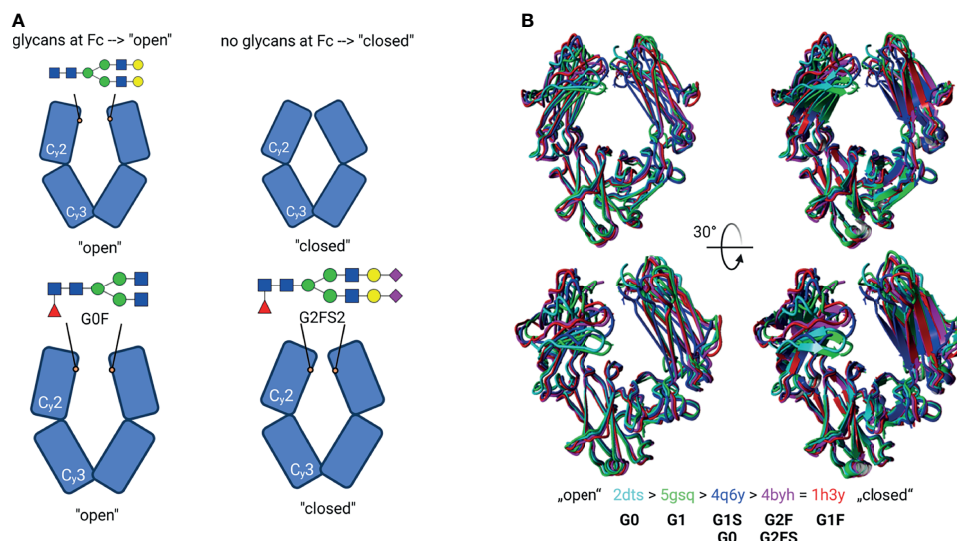


FIGURE 4 | Glycosylation-induced conformational changes. **(A)** Schematic model of the IgG Fc structure with or without glycans. Top: Glycan structures by self-induce conformational changes, resulting in an “open” structure. The de-glycosylated Fc have a “closed” structure instead. Bottom: Suggested model for individual glycan-induced conformational changes. Different glycan structures are discussed to influence the distance between the C_γ2 domains. E.g., sialylated (G2FS2) glycans lead to a sterically closer conformation of C_γ2 to each other. Created with BioRender.com **(B)** Superpose of different Fc structures. The PDB entries correspond to the colour code in the cartoon- and tube-styled structures; additionally, their glycan structures are given. The structures were classified as “open” and “closed” conformation. The structures were superimposed using YASARA. The N-glycans were created using GlycoWorkbench 2.1 (4).

glycans at Asn₁₆₂ are involved in binding with IgG *via* an direct interaction with N-glycans of the IgG at the Fc Asn₂₉₇ (22). It seems that a core fucose at the Fc Asn₂₉₇ inhibit this glycan-glycan interaction and reduces the affinity toward FcγRIIIa (23).

Also, sialic acid plays a key role in FcR mediated signaling. Terminal α2,6-linked Neu5Ac has an anti-inflammatory function (24). The presence of Neu5Ac reduces the binding to activating FcγR, and this interaction subsequently leads to increased expression of inhibitory FcγRIIb (25, 26) (**Figure 5C**). It is under debate whether the interaction of FcγR is reduced to sialylated IgG and the binding of CD23/DC-SIGN to IgG is increased instead (27, 28). A recent study investigated the binding of human sialylated IgG to cells expressing CD23 or DC-SIGN (29). It could not verify the binding of Fc- or Fab-sialylated IgG to one of the proteins. Crispin et al. could also not verify the binding of IgG Fc to DC-SIGN (9, 30). The impact of sialylation was also investigated in the case of IgM. For instance, sialic acid residues on glycans of IgM induce its internalization in T cells and a subsequent suppression of T-cell responses (31). This effect could be counteracted by desialylation and might be the result of a reduced binding affinity of FcμR for asialylated IgM (**Figure 5D**). Furthermore, the activity of IgE is influenced by its sialylation status (32). This type of Ig plays a crucial role in type 1 hypersensitivity. After exposure to allergens, cross-linked IgE activate basophil and/or mast cells, leading to their activation and the release of inflammatory mediators, such as histamine

(33). Interestingly, the amount of IgE present seems to be less important than the grade of IgE-sialylation to the extent of reaction (32). There are hints that the activation of FcεRI is less efficient when asialylated IgE is bound. However, the exact mechanism is still not fully understood (**Figure 5E**).

These examples demonstrate that the N-glycan structures of Igs significantly influence their immunomodulatory capacities, which explains the rapidly growing interest in glycan-mediated mechanisms in different areas of life sciences and medicine during the last decade.

Aging

One of these scientific fields is aging, since the adaptive immune systems undergoes several changes during aging. Newborn mammals receive their first Igs from their mother. In humans and other mammals with a hemochorial placenta, such as rodents and primates, IgG can pass through the placenta barrier. As a consequence, offsprings are already equipped with IgG during pregnancy. Since, during pregnancy, IgG Fc N-glycans become significantly more galactosylated, sialylated, and less bisected (34), comparable glycosylation patterns can be observed in newborns (**Figure 6**). This glycosylation status of IgGs relates to the anti-inflammatory character of IgG (24). The increase of anti-inflammatory Igs might be necessary to suppress possible immune reactions between the unborn baby and the mother during pregnancy (35). When children begin to produce

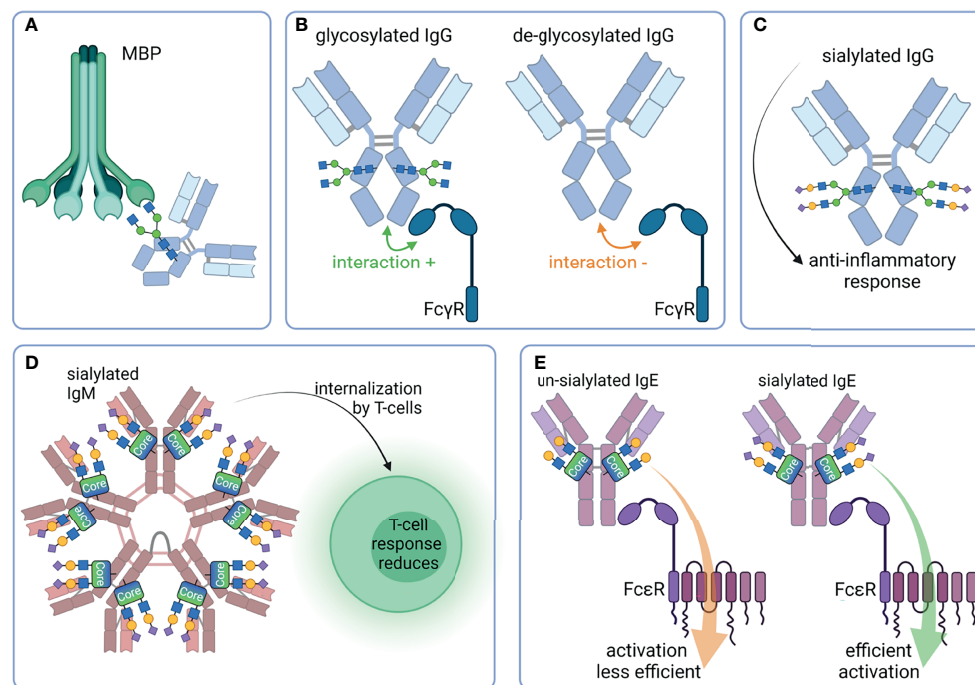


FIGURE 5 | Overview of selected properties of Ig that are affected by glycosylation. **(A)** Mannan-binding protein (MBP) binds G0 glycan structures of IgG and induces the lectin complement pathway. **(B)** FcγR bind better to glycosylated Fc as compared to de-glycosylated Fc. **(C)** Sialylated IgG has an anti-inflammatory effect. **(D)** Sialylated IgM are internalized by T-cells, leading to a reduced T-cell response. **(E)** Un-sialylated IgE activates FcεR less efficient than sialylated IgE. Created with BioRender.com.

endogenous IgG, an altered glycosylation can be observed (**Figure 6**). Digalactosylated N-glycans decrease, but the level of monogalactosylated structures remains stable (35). Thus, in sum, the ratio of N-glycans with at least one galactose residue stays constant. In contrast, the status fucosylation and sialylation decreases and that of bisecting N-glycans increase (35). However, from the age of 40, the level of IgG galactosylation decreases (36, 39).

Moreover, the glycosylation of the Fab region was investigated in this context. Interestingly, during pregnancy, the glycosylation status of the IgG Fab region changes as well (5). These alterations were much more heterogeneous and different as compared to Fc glycosylation. For example, the percentage of monosialylated structures at Fc increases slightly during pregnancy and decreases after delivery. The opposite was observed at the Fab. Here, the monosialylated structures stay nearly at the same level during pregnancy and their amount increases after delivery. This fine-tuning of the glycosylation seems to regulate the effectiveness of IgGs during different physiological conditions, such as pregnancy or childhood.

Ig Glycosylation Status During Lactation

As mentioned above, in species with a hemochorial placenta, such as rodents, primates, and humans, IgG can pass through the placenta barrier to equip offspring with Ig, whereas species with an epitheliochorial placenta, like ruminants, horses and pigs, are not able to transfer Ig *via* the umbilical cord. In these animals, the source of the first Igs is the colostrum. For instance, the gut of calves and piglets allows an unselective transition of proteins into blood circulation, approximately within the first 12–36 h postpartum. Calves and piglets that do not receive colostrum within the first 12 h have, for instance, reduced weight and increased mortality rates (40), and the administration of colostrum to calves within the first weeks of life reduces diarrheic disease (41). Thus, colostrum represents an essential

source for Igs in farm animals, such as pigs and cows. However, Igs in matured milk also are important biomolecules to prevent pathogen invasion and to support the health of calves and piglets during their suckling period. This is also the case in species with a hemochorial placenta, such as humans. The major classes of Ig in milk are IgG, the secretory IgA (sIgA), and IgM. Their concentration varies during the lactation period (see **Table 1**) and is species and probably also breed-specific.

There are several examples showing the importance of Ig glycans for the prevention of pathological bacteria in human. The members of the family Enterobacteriaceae, for instance, have Type 1 fimbriae on their surface with an adhesin that possesses mannose-specific lectin-like properties. This allows the bacteria to adhere to nasopharynx or colonic epithelial cells. After adhesion, they subsequently spread in the blood stream. The incubation of these bacteria with isolated secretory IgA (sIgA) from human milk leads to their agglutination, thus, their ability to bind to epithelial cells is inhibited (44). This is possible because glycans at the sIgA-Fc contain glycan structures with terminal mannose residues, which can bind using their fimbriae. **Figure 7** displays a schematic illustration of sIgA. Its specific joining chain (~16 kDa) connects the IgA dimers, and sIgA is associated with the secretory component (~75 kDa) that is additionally involved in the transport of IgA across epithelial cells. This transport is important to allow a transfer from the blood into milk. Usually, the secretory component shields these truncated glycan structures. However, acidic conditions in the digestive tract can disrupt the interaction between the secretory component and sIgA and enable the presentation of these sIgA glycans to bacteria (45) (**Figure 7**).

Furthermore, the S-fimbriated *E. coli* adhere to terminal Neu5Ac(α 2,3)Gal at buccal epithelial cells and can induce neonate meningitis and sepsis. This interaction can be competitively inhibited by soluble glycans or glycoproteins, including sIgA from the human colostrum, which reduces the

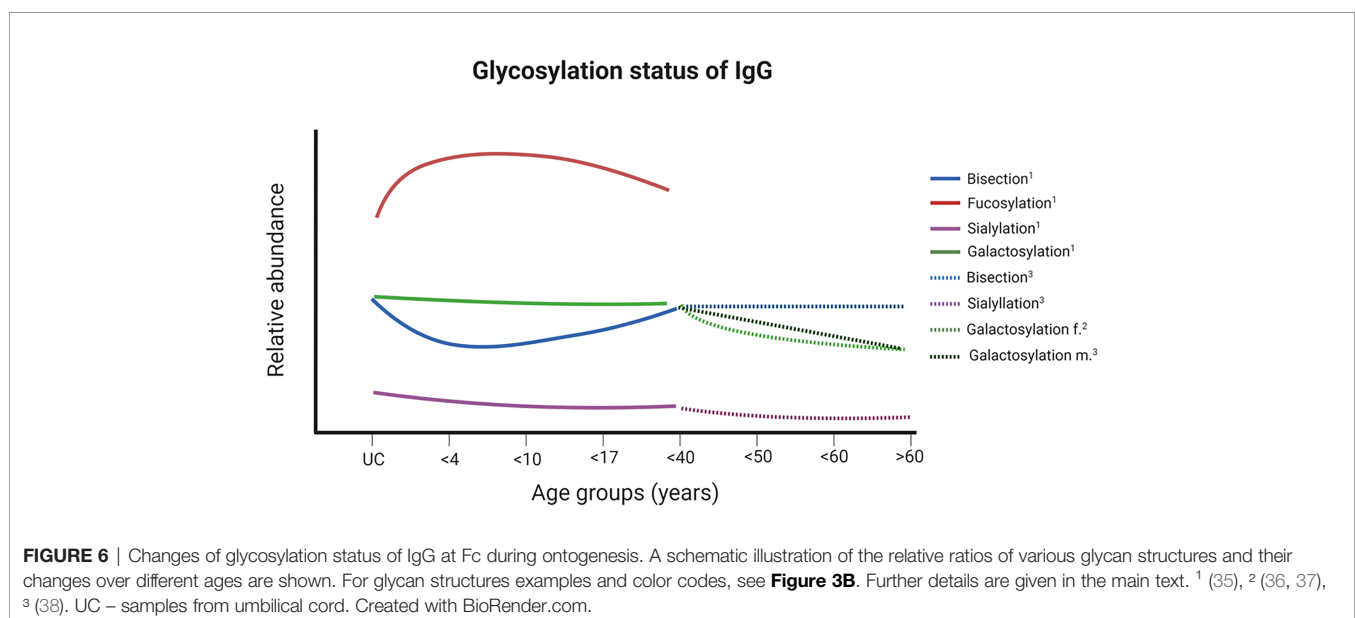


TABLE 1 | Species dependent Ig amounts in colostrum and milk.

Species	Ig	Colostrum [mg/ml]	Mature milk [mg/ml]	Reference
<i>H. sapiens</i> (human)	IgG	0.4	0.04	(42)
	IgM	0.3	0.03	(42)
	IgA	6-40	0.26-1.8	(42)
<i>B. taurus</i> (cattle)	IgG	15-180	0.5	(42)
	IgM	3-5	0.04	(42)
	IgA	1-6	0.05 -0.1	(42)
<i>O. aries</i> (sheep)	IgG	94-162	1	(43)
	IgM	1.3-21.2	0.2	(43)
	IgA	3.5	0.2	(43)
<i>E. ferus</i> (horse)	IgG1/IgG2 (IgGa)	82	0.2	(43)
	IgG4/IgG5 (IgGb)	183	0.3	(43)
	IgG3/IgG5 [IgG(T)]	44	0.1	(43)
	IgM	2.3	0.07	(43)
	IgA	9	0.7	(43)
<i>S. scrofa d.</i> (pig)	IgG	618	1.6	(43)
	IgM	3.8	1.5	(43)
	IgA	11.3	4.3	(43)

binding of *E. coli* to the host cells (47). The motif Neu5Ac(α 2,3)Gal is also a common terminal structure of N-glycan on IgG. Thus, these antibodies might also act as competitors against bacterial adherence *via* their glycans. Moreover, Hanisch et al. demonstrated a strong interaction of S-fimbriae with N-glycolylneuraminic acid (Neu5Gc) (48). This sialic acid is usually not found in humans but in farm animals, like donkeys, cows, and pigs, and might prevent bacterial adherence and, thereby, an infection in their offspring.

Interestingly, a recent study detected Neu5Gc on glycans of sIgA in donkey milk (46). The milk sample was from an animal in the mid-lactating stage. They detected 5 N-glycosylation sites at the secretory component (N₈₃LT, N₁₃₅GT, N₂₉₁QT, N₄₂₃GT, and N₅₃₀LT), two sites at the heavy chain of IgA (N₁₃₉AS, N₃₃₈VS [according to UniProt: N₁₃₄AS, N₃₃₃VS]), and one at the joining chain (N₇₂IS). Furthermore, several O-glycans were present at the hinge region. The detected N-glycans were very heterogenic and included several fucosylated and sialylated structures with Neu5Ac as well as Neu5Gc. In addition, oligomannose N-glycans were present at the Fc region on Asn₂₉₁ (46). It would be interesting if comparable inhibitory results can be achieved in relation to the adhesion of bacteria, as

shown for sIgA from human milk. With the remarkable exception of Neu5Gc containing N-glycans, several of the glycan structures are comparable.

In bovine milk, primarily, the glycosylation status of IgG was analyzed, representing the main Ig class in bovine milk (Table 1) (42, 43, 49, 50). In two studies, the composition of glycans from bovine milk at different time points of lactation period were examined. Feeney et al. investigated the IgG specific glycans by lectin-array assays at day 1, 2, 3, and 10 after birth (50). Takimori et al. determined the amount of IgG and its glycosylation status at the 1st day and 1st, 2nd, 3rd as well as 4th week postpartum using MALDI-TOF MS (49). In this way, the short and longer term changes can be characterized. The biggest difference was observed in the sialylation of glycans (Figure 8) (50). The highest amount of sialylated glycans was detected in the colostrum, which rapidly decreases within the first three days (50). After 10 days, Neu5Ac is no longer detectable and only minor amounts of Neu5Gc are present. These results are in line with those of Takimori et al., who found that 50% of all IgG-glycans in the colostrum were sialylated. After 7 days, these sialylated structures were almost absent (49). Interestingly, the sialylated structures were only located at the Fc but not at the Fab

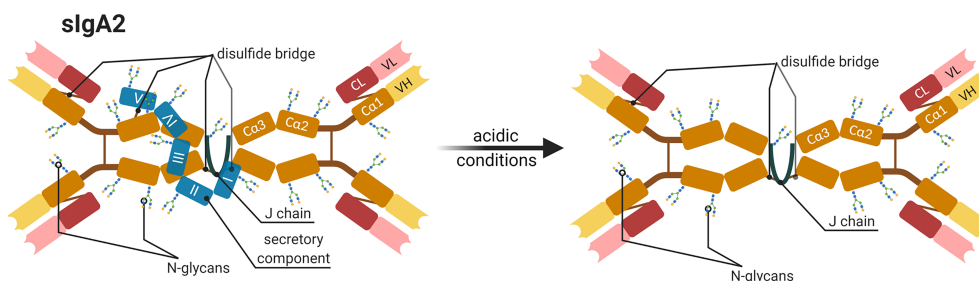


FIGURE 7 | Schematic representation of a human secretory IgA subtype 2 (sIgA2). All components and possible glycosylation sites of sIgA2 as well as the changes occurring under acidic conditions are shown. The IgA dimer compose of four heavy chains (orange and yellow C α 1-3 and VH), four light chains (red and pastel-red), and a joining chain (J chain in dark blue) that connects dimers and a secretory component (blue I-V) by disulfide bridges (brown line) (45, 46). Created with BioRender.com.

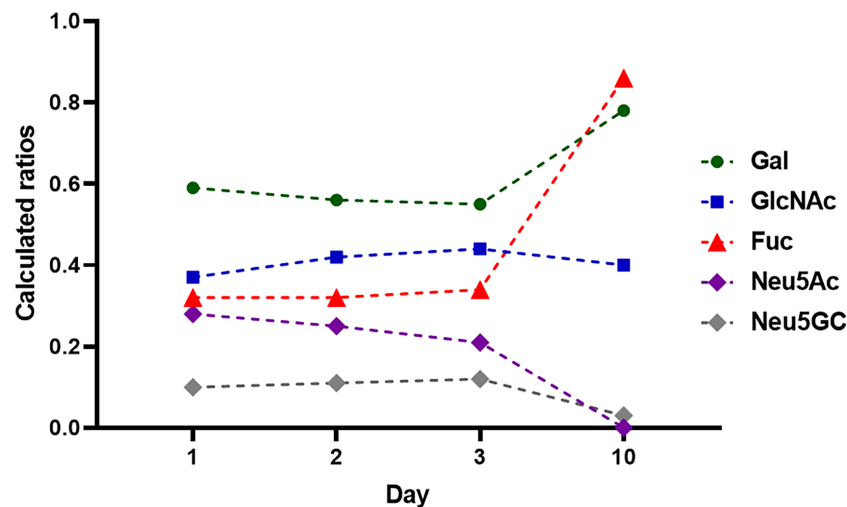


FIGURE 8 | Monosaccharide composition during lactation from day 1–10. 1 mg IgG were analyzed at each time point. The monosaccharides ratios were calculated to 1 mol Man. Values are from (50).

fragment. Further, they investigated the glycosidic linkage between Neu5Ac and Gal using MALDI-TOF MS, which was in most cases α 2,6-linkages. Feeney et al. used lectins to determine the linkage. The lectin MAA (from *Maackia amurensis*) detects mainly α 2,3-linked Neu5Ac, whereas SNA (from *Sambucus nigra*) preferentially binds α 2,6-linked Neu5Ac residues. The signal intensity using SNA indicated a higher abundance of α 2,6-linked Neu5Ac residues, which is also in line with the results of Takimori et al. (49, 50) and suggest that, during first days of lactation, higher amounts of anti-inflammatory IgGs are present in bovine milk (24, 51, 52). In contrast to the sialylation status, the amounts of fucose and galactose residues at IgG stay constant within the first three days of lactation and slightly increase at day 10 (Figure 8) (50). GlcNAc and Man are stable throughout the first 10 days. The roles of individual glycan structures on IgG in milk are unknown. In Takimori et al.'s study, the glycosylation status does not influence the binding to FcRn (49).

The results of Feeney et al. were obtained using the milk of Holstein Frisian cows representing high-performance dairy cows (50). The breed used by Takimori et al. was unfortunately not named. Breeds with lower level of milk production might have another glycosylation status during lactation. The few existing studies on buffalo milk could provide a first clue here. Two studies analyzed the glycan patterns of IgG in buffalo (*Bubalus bubalis*) milk at one single time point during lactation. The work of Bhanu et al. investigated a colostrum sample, and the work of Jineshet analyzed milk 14 days after parturition (53, 54). Bhanu et al. identified 54 different N-glycans, including oligomannose, neutral complex, and hybrid N-glycans, in addition to sialylated N-glycans (Neu5Ac and Neu5Gc). More than 20 of these glycans were fucosylated and the oligomannose N-glycans represented only a marginal ratio. However, the amount of sialylated N-glycans outweighed that of neutral structures. The high amount

of sialylated and low amounts of fucosylated N-glycans are comparable to the results of Feeney et al. using bovine colostrum (50). The analysis of buffalo IgG glycans in mature milk (from day 10 of lactation) revealed the following distribution: 14% sialylated, 19% bisecting and 34% fucosylated glycans (54). However, in contrast to mature bovine milk, in which Neu5Ac was not detectable and only minor amounts of Neu5Gc were present, in buffalo milk, significant amounts of Neu5Ac and Neu5Gc were also detectable on day 14 of lactation (54). Thus, the dramatic loss of sialylated N-glycans does not take place in buffalo milk. Whether this glycosylation allows a broader panel of immunomodulatory mechanism is unknown so far. Nevertheless, the studies demonstrate that striking differences between various animal species exist.

RELATION BETWEEN IGG GLYCOSYLATION AND PATHOPHYSIOLOGY

Notably, the glycosylation patterns of Igs change also during pathophysiological processes. Previous studies indicate that glycosylation patterns alter during inflammatory processes like alloimmune thrombocytopenia (55) and active infections with pathogens such as HIV (56) or tuberculosis (57). On the other hand, changed glycosylation patterns can be detected in patients with chronic diseases like inflammatory bowel disease (58); autoimmune diseases like rheumatoid arthritis (RA) (59) and systemic lupus erythematosus (60); and neurological disorders such as multiple sclerosis (61, 62), Alzheimer's disease (63), or Myasthenia gravis (64). In chronic diseases, it is mostly unknown where these changes come from and what their cause is. It is important to investigate whether pathological effects lead to an altered glycosylation or an altered glycosylation leads to

pathological effects. In the latter case, it would be necessary to examine the cause for a changed glycosylation. This knowledge would be helpful to treat the diseases properly.

However, in some cases, such as RA, first insights have been described. About 0.5–1% percent of adults are affected by RA (65). Women are affected three times as often as men (66). Increased incidences of agalactosylated antibodies were earlier associated with higher disease activity (67). In 75–90% of patients, the disease activity reduces during pregnancy and increases again after delivery (68). As described above, pregnancy comes with changes in the glycosylation of antibodies. One study determining the glycosylation status during pregnancy revealed altered galactosylation and sialylation at the Fc of IgG (69). Furthermore, significant changes in bisecting N-glycans and fucosylation were observed for several IgG subclasses (69). Other studies have investigated the N-glycans of proteins from the whole serum and observed, for instance, decreased bisection N-glycans but an increase of galactosylation (70, 71). Reduced levels of pro-inflammatory bisection N-glycans, for instance, suggest an association with the reduced disease activity of RA patients during pregnancy.

In sum, a number of examples demonstrate that, in humans, sialylated N-glycans on IgG lead to immunosuppressive effects, whereas high levels of IgG without terminal sialic acid, galactose, and fucose residues but carrying bisecting N-glycans enhance inflammatory disorders and their severity. Thus, it is surprising that, with farm animals, studies investigating potential alteration in the glycosylation status of Ig during various physiological and pathophysiological processes are rare or completely missing so far. Knowledge about such glycan-dependent mechanisms might help develop novel strategies to increase welfare of farm animals.

Vaccination Induced Immunization and Its Impact on Glycosylation of Ig

Since lack of terminal sialic acid, galactose, and fucose residues on N-glycans of the Fc region and higher amounts bisecting N-glycans increases the inflammatory capacity of IgGs, such glycosylation patterns are preferred after vaccination against pathogens (72). Bartsch et al. (73) recently examined how adjuvants influence the glycosylation of IgG with a special focus on sialic acid and galactose residues. In this study, mice were immunized for the first time with 100 µg ovalbumin (Ova) with different adjuvants and boosted second time with an Ova-PBS solution. The applied adjuvants included, among others, incomplete Freund adjuvant (IFA), complete Freund adjuvant (CFA), and alum. Interestingly, remarkable differences were found concerning the glycosylation of IgG. The application of eCFA (enriched CFA), IFA, and Montanide led to a significant reduction of galactosylation and sialylation. This effect was noticeably weaker when the adjuvants Alum, Adju-Phos, AddaVax, LPS, MPLA, R848, Poly (I:C) were applied. It should be noted that the stronger effectors - eCFA, IFA and Montanide - are “water in oil adjuvants”. The highest impact of all tested adjuvants were observed when eCFA was used. CFA was enriched with heat-killed *Mycobacterium tuberculosis* (Mtb). The effects might be mediated by the cord factor (glycolipid trehalose dimycolate) in Mtb extracts (57, 74). Whether

comparable effects can be also achieved in farm animals is unknown.

Glycoengineered Monoclonal Antibodies

Monoclonal antibodies (mAb) are an important and growing group of biotherapeutics for the treatment of cancer and chronic diseases. The Food and Drug Administration (FDA) approved more than 60 different mAbs and fusion molecules in the last few decades, which target in the most cases cancer cells (75). An optimized glycosylation has also already moved into the focus for therapeutic treatments with mAb. As mentioned above, the glycosylation status depends on many physiological conditions within an organism. Consequently, the glycosylation status is significantly influenced by the incubation and growing conditions of the IgG-producing cells and their genotype. To get a defined glycosylation pattern, the glycosylation-machinery of a cell lines can be manipulated using knock-out or knock-in strategies. For example, to obtain mAbs with nonfucosylated glycan structures, it is possible to knock out the α -1,6-fucosyltransferase (FUT8) (76) or overexpress β 1,4-N-acetylglucosaminyltransferase III (GnTIII) (77). GnTIII catalyzes the addition of bisecting GlcNAc, which subsequently inhibits core-fucosylation. In both cases, the unfucosylated mAbs would enhance the ADCC, for example (17–19). Another option is to treat the mAbs *in vitro* using glycosidases. For instance, sialidases and galactosidases can be used to release sialic acid and galactose residues to obtain proinflammatory sets of antibodies (78). Consequently, the glycoengineering of therapeutic Abs is a powerful strategy to significantly improve their targeted application, such as with passive immunization.

Avian Egg Yolk Antibodies (IgY)

A further interesting type of antibody is the avian IgY. These Igs are of importance in various scientific fields. The number of publications listed on PubMed under the keyword “immunoglobulin y” increased steadily in the last years (see **Figure 9A**). Among others, it is gaining great interest for its application as a potential tool in diagnostic, therapeutic and biotechnology, since IgYs formed in poultry are very specific against mammalian proteins and have a high binding affinity. This is based on the phylogenetic distance between birds and mammals, thus, immunization works very well (79–82). The production of IgY is a further advantage. IgY can be easily isolated from the egg yolks of one and the same chicken. This is a non-invasive method and no blood has to be taken from the animals.

Compared to the mammalian IgG the avian IgY has one more constant domain in the heavy chain (CH3) and no hinge region. Further, there are two potential N-glycosylation sites. One at the CH2 and one at CH3 domain (83) (see **Figure 9B**). The analysis of the glycosylation status of IgY revealed mainly two types of N-glycans: oligomannose and complex type (see **Figure 3A**) with 37.2% and 62.8% respectively (83). Other studies detected also few hybrid glycans types at IgY (84, 85). The main structures, which were detected, in addition to their distribution are listed in **Table 2**. The CH3 domains contain only oligomannose structures, and the CH2 domain only complex-type structures (83).

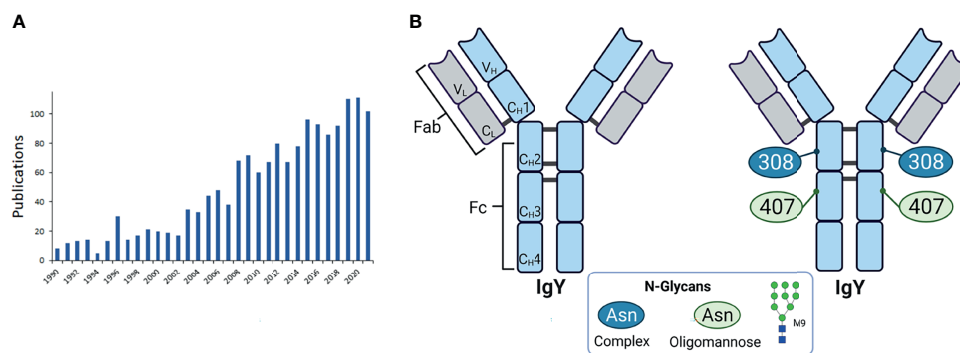


FIGURE 9 | Avian egg yolk antibodies. **(A)** Entries of publications in PubMed with the keyword “immunoglobulin y” since 1990. **(B)** Structure of IgY. Shown are the domains of IgY with the two heavy chains (light blue) containing four constant domains (C_{H1-4}) and one variable domain (V_H), and two light chains (light grey) with one constant (C_L) and one variable domain (V_L). The heavy and light chains are covalently connected by disulfide bonds. The IgY is further subdivided in the antigen binding fragment (Fab) and fragment crystallisable (Fc). On the right the glycosylation sites are indicated with the detected glycan types. M9 is depicted as a representative of oligomannose type. Representative glycans for complex types are listed in **Table 2** and depicted in **Figure 3B**. Created with BioRender.com.

Further studies confirmed these results (85). For instance, Gilgunn et al. find on IgY originating from serum mainly complex, bi-, tri- and tetra-antennary glycans, which were partially bisected, fucosylated and sialylated. Besides these complex and high mannose structures, also hybrid structures were detected. Surprisingly, the impact of the glycosylation status on the activation of the host immune system and regulatory as well as signalling pathways have not been investigated so far and might represent a novel immunomodulatory tool improve animal welfare in poultry farming.

CONCLUSION AND OUTLOOK

The outlined importance of N-glycans for the structure of Igs and the resulting immunomodulatory capacities explain the rapidly growing interest in glycan-mediated mechanisms during the last decade and the application of highly defined glycoengineered Ig in human medicine (75–77). Thus, it is even more surprising that, in veterinary medicine, such studies are still limited or completely missed.

It would be interesting to determine, whether feeding, social environment and vaccination have an impact on the Ig glycosylation status, since these factors influence the general metabolism of the animals. In addition, the knowledge of the relationship and influence of different adjuvants on vaccination success might increase the protection of farm animals against pathogens. Moreover, in the case of maternal vaccination, the offspring would be better protected during lactation, when milk

IgGs contain optimized glycosylation patterns. The offspring of species with a hemochorial placenta, like humans, primates and rodents benefit during the pregnancy by a passive immunization, because here IgG can pass the blood-placenta barrier and protect the offspring. Species with an epitheliochorial placenta, like ruminants, including cattle, pigs, goat and sheep, but also horses, whales, and lower primates are not able to immunize their offspring passively through the placenta. Newborns of these species especially depends on a passive immunization from milk. Therefore, it would be interesting to examine if the glycosylation pattern of Ig changes during its transport from dams blood into the milk, and further through the stomach and gut of the offspring, until it reaches the blood system (**Figure 10**). This aspect is under present investigation in our lab. The knowledge about this could promote the development of vaccines and adjuvants to shift glycan structures to increase the efficiency of the immunisation. It would also promote the development and application of Ig with specific glycan patterns. In conventional farming it is common that calves are not suckled by their mothers. The colostrum given is usually from a colostrum pool, frozen colostrum or commercially available colostrum powder. At this point, glycoengineered antibodies could be additionally supplemented.

In sum, farm animals would benefit from a more detailed knowledge about all these aspects. Furthermore, animals in zoological gardens or species whose population sizes are small could have better chances of survival for their offspring. Thus, we propose that the glycosylation of Abs might represent a powerful target or tool to develop novel strategies to support the health and welfare of animals.

TABLE 2 | Distribution of glycan types, calculated due to the molar basis of total N-glycans (83).

Oligomannose type	Monoglucosylated 26.8%	Others 10.5%	
Complex type	Neutral 29.9%	Monosialylated, 29.3%	Disialylated 3.7%
Structures corresponding Figure 3B	G1F; G1b; G1Fb; G2Fb	G1S1Fb, G2S1Fb, G2FS	G2S2Fb

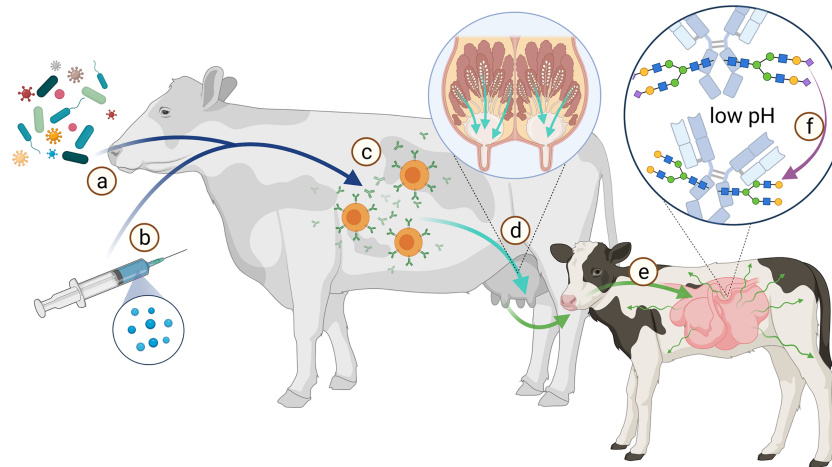


FIGURE 10 | Scheme of the route from antigen to immunization of offspring. The immune system of the dam is stimulated by various pathogens (A) or vaccination (B) to produce antibodies (C). These Abs are transported from the bloodstream into the milk (D). During the first hours after birth, the calf's intestine is permeable to proteins such as Abs (E). This allows the calf to absorb Abs from the colostrum. Especially sialic acid residues (magenta diamond) are acid-sensitive and are cleaved from the glycans at low pH (F). Created with BioRender.com.

AUTHOR CONTRIBUTIONS

KZ and SG wrote the manuscript and gave the approval to the final version of the manuscript. All authors contributed to the article and approved the submitted version.

FUNDING

The publication of this article was funded by the Open Access Fund of the Research Institute for Farm Animal Biology (FBN).

ACKNOWLEDGMENTS

We gratefully thank Andreas Vernunft for many helpful discussions.

SUPPLEMENTARY MATERIAL

The Supplementary Material for this article can be found online at: <https://www.frontiersin.org/articles/10.3389/fimmu.2021.753294/full#supplementary-material>

REFERENCES

- Stanley P, Taniguchi N, Aebi M. *Essentials of Glycobiology*. Cold Spring Harbor (NY: N-Glycans (2015).
- Arnold JN, Wormald MR, Sim RB, Rudd PM, Dwek RA. The Impact of Glycosylation on the Biological Function and Structure of Human Immunoglobulins. *Annu Rev Immunol* (2007) 25:21–50. doi: 10.1146/annurev.immunol.25.022106.141702
- van de Bovenkamp FS, Hafkenscheid L, Rispens T, Rombouts Y. The Emerging Importance of IgG Fab Glycosylation in Immunity. *J Immunol* (2016) 196:1435–41. doi: 10.4049/jimmunol.1502136
- Ceroni A, Maass K, Geyer H, Geyer R, Dell A, Haslam SM. GlycoWorkbench: A Tool for the Computer-Assisted Annotation of Mass Spectra of Glycans. *J Proteome Res* (2008) 7:1650–9. doi: 10.1021/pr7008252
- Bondt A, Rombouts Y, Selman MH, Hensbergen PJ, Reiding KR, Hazes JM, et al. Immunoglobulin G (IgG) Fab Glycosylation Analysis Using a New Mass Spectrometric High-Throughput Profiling Method Reveals Pregnancy-Associated Changes. *Mol Cell Proteomics* (2014) 13:3029–39. doi: 10.1074/mcp.M114.039537
- Krapp S, Mimura Y, Jefferis R, Huber R, Sonderrmann P. Structural Analysis of Human IgG-Fc Glycoforms Reveals a Correlation Between Glycosylation and Structural Integrity. *J Mol Biol* (2003) 325:979–89. doi: 10.1016/S0022-2836(02)01250-0
- Sonderrmann P, Pincetic A, Maamary J, Lammens K, Ravetch JV. General Mechanism for Modulating Immunoglobulin Effector Function. *Proc Natl Acad Sci USA* (2013) 110:9868–72. doi: 10.1073/pnas.1307864110
- Ahmed AA, Giddens J, Pincetic A, Lomino JV, Ravetch JV, Wang L-X, et al. Structural Characterization of Anti-Inflammatory Immunoglobulin G Fc Proteins. *J Mol Biol* (2014) 426:3166–79. doi: 10.1016/j.jmb.2014.07.006
- Crispin M, Yu X, Bowden TA. Crystal Structure of Sialylated IgG Fc: Implications for the Mechanism of Intravenous Immunoglobulin Therapy. *Proc Natl Acad Sci USA* (2013) 110:E3544–6. doi: 10.1073/pnas.1310657110
- Frank M, Walker RC, Lanzilotta WN, Prestegard JH, Barb AW. Immunoglobulin G1 Fc Domain Motions: Implications for Fc Engineering. *J Mol Biol* (2014) 426:1799–811. doi: 10.1016/j.jmb.2014.01.011
- Wada R, Matsui M, Kawasaki N. Influence of N-Glycosylation on Effector Functions and Thermal Stability of Glycoengineered IgG1 Monoclonal Antibody With Homogeneous Glycoforms. *MAbs* (2019) 11:350–72. doi: 10.1080/19420862.2018.1551044
- Malhotra R, Wormald MR, Rudd PM, Fischer PB, Dwek RA, Sim RB. Glycosylation Changes of IgG Associated With Rheumatoid Arthritis can Activate Complement via the Mannose-Binding Protein. *Nat Med* (1995) 1:237–43. doi: 10.1038/nm0395-237
- Martinez-Pomares L. The Mannose Receptor. *J Leukoc Biol* (2012) 92:1177–86. doi: 10.1189/jlb.0512231
- Mimura Y, Church S, Ghirlando R, Ashton PR, Dong S, Goodall M, et al. The Influence of Glycosylation on the Thermal Stability and Effector Function Expression of Human IgG1-Fc: Properties of a Series of Truncated Glycoforms. *Mol Immunol* (2000) 37(12–13):697–706. doi: 10.1016/S0161-5890(00)00105-x

15. Allhorn M, Olsson AI, Nimmerjahn F, Collin M. Human IgG/Fc Gamma R Interactions are Modulated by Streptococcal IgG Glycan Hydrolysis. *PLoS One* (2008) 3:e1413. doi: 10.1371/journal.pone.0001413
16. Dekkers G, Treffers L, Plomp R, Bentlage AE, Boer M, Koeleman CA, et al. Decoding the Human Immunoglobulin G-Glycan Repertoire Reveals a Spectrum of Fc-Receptor- and Complement-Mediated-Effector Activities. *Front Immunol* (2017) 8:877. doi: 10.3389/fimmu.2017.00877
17. Niwa R, Natsume A, Uehara A, Wakitani M, Iida S, Uchida K, et al. IgG Subclass-Independent Improvement of Antibody-Dependent Cellular Cytotoxicity by Fucose Removal From Asn297-Linked Oligosaccharides. *J Immunol Methods* (2005) 306:151–60. doi: 10.1016/j.jim.2005.08.009
18. Matsumiya S, Yamaguchi Y, Saito J-i, Nagano M, Sasakawa H, Otaki S, et al. Structural Comparison of Fucosylated and Nonfucosylated Fc Fragments of Human Immunoglobulin G1. *J Mol Biol* (2007) 368:767–79. doi: 10.1016/j.jmb.2007.02.034
19. Chung S, Quarmby V, Gao X, Ying Y, Lin L, Reed C, et al. Quantitative Evaluation of Fucose Reducing Effects in a Humanized Antibody on Fcγ Receptor Binding and Antibody-Dependent Cell-Mediated Cytotoxicity Activities. *MAbs* (2012) 4:326–40. doi: 10.4161/mabs.19941
20. Shields RL, Lai J, Keck R, O'Connell LY, Hong K, Meng YG, et al. Lack of Fucose on Human IgG1 N-Linked Oligosaccharide Improves Binding to Human Fcγ3a Receptor and Antibody-Dependent Cellular Toxicity. *J Biol Chem* (2002) 277:26733–40. doi: 10.1074/jbc.M202069200
21. Shinkawa T, Nakamura K, Yamane N, Shoji-Hosaka E, Kanda Y, Sakurada M, et al. The Absence of Fucose But Not the Presence of Galactose or Bisecting N-Acetylglucosamine of Human IgG1 Complex-Type Oligosaccharides Shows the Critical Role of Enhancing Antibody-Dependent Cellular Cytotoxicity. *J Biol Chem* (2003) 278:3466–73. doi: 10.1074/jbc.M210665200
22. Ferrara C, Stuart F, Sondermann P, Brünker P, Umaña P. The Carbohydrate at Fcγ3a Asn-162. An Element Required for High Affinity Binding to non-Fucosylated IgG Glycoforms. *J Biol Chem* (2006) 281:5032–6. doi: 10.1074/jbc.M510171200
23. Ferrara C, Grau S, Jäger C, Sondermann P, Brünker P, Waldhauer I, et al. Unique Carbohydrate-Carbohydrate Interactions Are Required for High Affinity Binding Between Fcγ3a and Antibodies Lacking Core Fucose. *Proc Natl Acad Sci USA* (2011) 108(31):12669–74. doi: 10.1073/pnas.1108455108
24. Kaneko Y, Nimmerjahn F, Ravetch JV. Anti-Inflammatory Activity of Immunoglobulin G Resulting From Fc Sialylation. *Science* (2006) 313:670–3. doi: 10.1126/science.1129594
25. Anthony RM, Nimmerjahn F, Ashline DJ, Reinhold VN, Paulson JC, Ravetch JV. Recapitulation of IVIG Anti-Inflammatory Activity With a Recombinant IgG Fc. *Science* (2008) 320:373–6. doi: 10.1126/science.1154315
26. Anthony RM, Kobayashi T, Wermeling F, Ravetch JV. Intravenous Gamaglobulin Suppresses Inflammation Through a Novel T(H)2 Pathway. *Nature* (2011) 475:110–3. doi: 10.1038/nature10134
27. Anthony RM, Wermeling F, Karlsson MC, Ravetch JV. Identification of a Receptor Required for the Anti-Inflammatory Activity of IVIG. *Proc Natl Acad Sci U.S.A.* (2008) 105:19571–8. doi: 10.1073/pnas.0810163105
28. Sondermann P, Huber R, Oosthuizen V, Jacob U. The 3.2-Å Crystal Structure of the Human IgG1 Fc Fragment-Fc γ3a Complex. *Nature* (2000) 406:267–73. doi: 10.1038/35018508
29. Temting AR, Dekkers G, van de Bovenkamp FS, Plomp HR, Bentlage AE, Zitting Z, et al. Human DC-SIGN and CD23 do Not Interact With Human IgG. *Sci Rep* (2019) 9:9995. doi: 10.1038/s41598-019-46484-2
30. Yu X, Vasiljevic S, Mitchell DA, Crispin M, Scanlan CN. Dissecting the Molecular Mechanism of IVIG Therapy: The Interaction Between Serum IgG and DC-SIGN is Independent of Antibody Glycoform or Fc Domain. *J Mol Biol* (2013) 425:1253–8. doi: 10.1016/j.jmb.2013.02.006
31. Colucci M, Stöckmann H, Butera A, Masotti A, Baldassarre A, Giorda E, et al. Sialylation of N-Linked Glycans Influences the Immunomodulatory Effects of IgM on T Cells. *J Immunol* (2015) 194:151–7. doi: 10.4049/jimmunol.1402025
32. Shade K-TC, Conroy ME, Washburn N, Kitaoka M, Huynh DJ, Laprise E, et al. Sialylation of Immunoglobulin E is a Determinant of Allergic Pathogenicity. *Nature* (2020) 582:265–70. doi: 10.1038/s41586-020-2311-z
33. Stanworth DR. The Discovery of IgE. *Allergy* (1993) 48:67–71. doi: 10.1111/j.1398-9995.1993.tb00687.x
34. Einarisdottir HK, Selman MH, Kapur R, Scherjon S, Koeleman CA, Deelder AM, et al. Comparison of the Fc Glycosylation of Fetal and Maternal Immunoglobulin G. *Glycoconj J* (2013) 30:147–57. doi: 10.1007/s10719-012-9381-6
35. Haan N, Reiding KR, Driessen G, van der Burg M, Wuhrer M. Changes in Healthy Human IgG Fc-Glycosylation After Birth and During Early Childhood. *J Proteome Res* (2016) 15:1853–61. doi: 10.1021/acs.jproteome.6b00038
36. Parekh R, Roitt I, Isenberg D, Dwek R, Rademacher T. Age-Related Galactosylation of the N-Linked Oligosaccharides of Human Serum IgG. *J Exp Med* (1988) 167:1731–6. doi: 10.1084/jem.167.5.1731
37. Kristić J, Vučković F, Menni C, Klarić L, Keser T, Beccheli I, et al. Glycans Are a Novel Biomarker of Chronological and Biological Ages. *J Gerontol A Biol Sci Med Sci* (2014) 69:779–89. doi: 10.1093/gerona/glt190
38. Baković MP, Selman MH, Hoffmann M, Rudan I, Campbell H, Deelder AM, et al. High-Throughput IgG Fc N-Glycosylation Profiling by Mass Spectrometry of Glycopeptides. *J Proteome Res* (2013) 12:821–31. doi: 10.1021/pr300887z
39. Ruhaak LR, Uh H-W, Beekman M, Koeleman CA, Hokke CH, Westendorp RG, et al. Decreased Levels of Bisecting GlcNAc Glycoforms of IgG are Associated With Human Longevity. *PLoS One* (2010) 5:e12566. doi: 10.1371/journal.pone.0012566
40. Lilius EM, Marnila P. The Role of Colostral Antibodies in Prevention of Microbial Infections. *Curr Opin Infect Dis* (2001) 14:295–300. doi: 10.1097/00001432-200106000-00008
41. Berge AC, Besser TE, Moore DA, Sischo WM. Evaluation of the Effects of Oral Colostrum Supplementation During the First Fourteen Days on the Health and Performance of Preweaned Calves. *J Dairy Sci* (2009) 92:286–95. doi: 10.3168/jds.2008-1433
42. Jensen RG. *Handbook of Milk Composition*. San Diego: Academic Press (1995). p. 919.
43. Butler JE, Kehrl ME. Immunoglobulins and Immunocytes in the Mammary Gland and Its Secretions. In: J Mestecky, editor. *Mucosal Immunology*. Amsterdam, Boston: Elsevier Academic Press (2005). p. 1763–93.
44. Wold AE, Mestecky J, Tomana M, Kobata A, Ohbayashi H, Endo T, et al. Secretory Immunoglobulin A Carries Oligosaccharide Receptors for Escherichia Coli Type 1 Fimbrial Lectin. *Infect Immun* (1990) 58:3073–7. doi: 10.1128/IAI.58.9.3073-3077.1990
45. Royle L, Roos A, Harvey DJ, Wormald MR, van Gijlswijk-Janssen D, Redwan E-RM, et al. Secretory IgA N- and O-Glycans Provide a Link Between the Innate and Adaptive Immune Systems. *J Biol Chem* (2003) 278:20140–53. doi: 10.1074/jbc.M301436200
46. Gnanesh Kumar BS, Rawal A. Sequence Characterization and N-Glycoproteomics of Secretory Immunoglobulin A From Donkey Milk. *Int J Biol Macromolecules* (2020) 155:605–13. doi: 10.1016/j.ijbiomac.2020.03.253
47. Schroten H, Stapper C, Plogmann R, Köhler H, Hacker J, Hanisch FG. Fab-Independent Antiadhesion Effects of Secretory Immunoglobulin A on S-Fimbriated Escherichia Coli are Mediated by Sialyloligosaccharides. *Infect Immun* (1998) 66:3971–3. doi: 10.1128/IAI.66.8.3971-3973.1998
48. Hanisch FG, Hacker J, Schroten H. Specificity of S Fimbriae on Recombinant Escherichia Coli: Preferential Binding to Gangliosides Expressing NeuGc Alpha (2-3)Gal and NeuAc Alpha (2-8)NeuAc. *Infect Immun* (1993) 61:2108–15. doi: 10.1128/IAI.61.5.2108-2115.1993
49. Takimori S, Shimaoka H, Furukawa J-I, Yamashita T, Amano M, Fujitani N, et al. Alteration of the N-Glycome of Bovine Milk Glycoproteins During Early Lactation. *FEBS J* (2011) 278:3769–81. doi: 10.1111/j.1742-4658.2011.08299.x
50. Feeney S, Gerlach JQ, Slattery H, Kilcoyne M, Hickey RM, Joshi L. Lectin Microarray Profiling and Monosaccharide Analysis of Bovine Milk Immunoglobulin G Oligosaccharides During the First 10 Days of Lactation. *Food Sci Nutr* (2019) 7:1564–72. doi: 10.1002/fsn.3.950
51. Alter G, Ottenhoff TH, Joosten SA. Antibody Glycosylation in Inflammation, Disease and Vaccination. *Semin Immunol* (2018) 39:102–10. doi: 10.1016/j.simm.2018.05.003
52. Kronimus Y, Dodel R, Galuska SP, Neumann S. IgG Fc N-Glycosylation: Alterations in Neurologic Diseases and Potential Therapeutic Target? *J Autoimmun* (2019) 96:14–23. doi: 10.1016/j.jaut.2018.10.006
53. Bhanu LS, Amano M, Nishimura S-I, Aparna HS. Glycome Characterization of Immunoglobulin G From Buffalo (Bubalus Bubalis) Colostrum. *Glycoconj J* (2015) 32:625–34

54. Jinesh P, Lijina P, Gnanesh Kumar BS. Sequence and N-Glycan Diversity Analysis of Immunoglobulin G From Buffalo Milk Using RP-UHPLC MS/MS. *Amino Acids* (2021) 53(4):533–9. doi: 10.1007/s00726-021-02945-5
55. Sonneveld ME, Natunen S, Sainio S, Koeleman CA, Holst S, Dekkers G, et al. Glycosylation Pattern of Anti-Platelet IgG Is Stable During Pregnancy and Predicts Clinical Outcome in Alloimmune Thrombocytopenia. *Br J Haematol* (2016) 174:310–20. doi: 10.1111/bjh.14053
56. Ackerman ME, Crispin M, Yu X, Baruah K, Boesch AW, Harvey DJ, et al. Natural Variation in Fc Glycosylation of HIV-Specific Antibodies Impacts Antiviral Activity. *J Clin Invest* (2013) 123:2183–92. doi: 10.1172/JCI65708
57. Lu LL, Chung AW, Rosebrock TR, Ghebremichael M, Yu WH, Grace PS, et al. A Functional Role for Antibodies in Tuberculosis. *Cell* (2016) 167:433–443.e14. doi: 10.1016/j.cell.2016.08.072
58. Miyoshi E, Shinzaki S, Fujii H, Iijima H, Kamada Y, Takehara T. Role of Aberrant IgG Glycosylation in the Pathogenesis of Inflammatory Bowel Disease. *Proteomics Clin Appl* (2016) 10:384–90. doi: 10.1002/prca.201500089
59. Parekh RB, Dwek RA, Sutton BJ, Fernandes DL, Leung A, Stanworth D, et al. Association of Rheumatoid Arthritis and Primary Osteoarthritis With Changes in the Glycosylation Pattern of Total Serum IgG. *Nature* (1985) 316:452–7. doi: 10.1038/316452a0
60. Vučković F, Kristić J, Gudelj I, Teruel M, Keser T, Pezer M, et al. Association of Systemic Lupus Erythematosus With Decreased Immunosuppressive Potential of the IgG Glycome. *Arthritis Rheumatol* (2015) 67:2978–89. doi: 10.1002/art.39273
61. Decker Y, Schomburg R, Németh E, Vitkin A, Fousse M, Liu Y, et al. Abnormal Galactosylation of Immunoglobulin G in Cerebrospinal Fluid of Multiple Sclerosis Patients. *Mult Scler* (2016) 22:1794–803. doi: 10.1177/1352458516631036
62. Wührer M, Selman MH, McDonnell LA, Kümpfel T, Derfuss T, Khademi M, et al. Pro-Inflammatory Pattern of IgG1 Fc Glycosylation in Multiple Sclerosis Cerebrospinal Fluid. *J Neuroinflamm* (2015) 12:235. doi: 10.1186/s12974-015-0450-1
63. Lundström SL, Yang H, Lyutvinskiy Y, Rutishauser D, Herukka S-K, Soininen H, et al. Blood Plasma IgG Fc Glycans Are Significantly Altered in Alzheimer's Disease and Progressive Mild Cognitive Impairment. *J Alzheimers Dis* (2014) 38:567–79. doi: 10.3233/JAD-131088
64. Selman MH, Niks EH, Titulaer MJ, Verschuuren JJ, Wührer M, Deelder AM. IgG Fc N-Glycosylation Changes in Lambert-Eaton Myasthenic Syndrome and Myasthenia Gravis. *J Proteome Res* (2011) 10:143–52. doi: 10.1021/pr1004373
65. Scott DL, Wolfe F, Huizinga TW. Rheumatoid Arthritis. *Lancet* (2010) 376:1094–108. doi: 10.1016/S0140-6736(10)60826-4
66. Elsouiri K, Arboleda V, Heiser S, Kesselman MM, Demory Beckler M. Microbiome in Rheumatoid Arthritis and Celiac Disease: A Friend or Foe. *Cureus* (2021) 13:e15543. doi: 10.7759/cureus.15543
67. Ercan A, Cui J, Chatterton DE, Deane KD, Hazen MM, Brintnell W, et al. Aberrant IgG Galactosylation Precedes Disease Onset, Correlates With Disease Activity, and Is Prevalent in Autoantibodies in Rheumatoid Arthritis. *Arthritis Rheum* (2010) 62:2239–48. doi: 10.1002/art.27533
68. Man YA de, Dolhain RJ, van de Geijn FE, Willemsen SP, Hazes JM. Disease Activity of Rheumatoid Arthritis During Pregnancy: Results From a Nationwide Prospective Study. *Arthritis Rheum* (2008) 59:1241–8. doi: 10.1002/art.24003
69. Bondt A, Selman MH, Deelder AM, Hazes JM, Willemsen SP, Wührer M, et al. Association Between Galactosylation of Immunoglobulin G and Improvement of Rheumatoid Arthritis During Pregnancy is Independent of Sialylation. *J Proteome Res* (2013) 12:4522–31. doi: 10.1021/pr400589m
70. Reiding KR, Vreeker GC, Bondt A, Bladergroen MR, Hazes JM, van der Burgt YE, et al. Serum Protein N-Glycosylation Changes With Rheumatoid Arthritis Disease Activity During and After Pregnancy. *Front Med (Lausanne)* (2017) 4:241. doi: 10.3389/fmed.2017.00241
71. Reiding KR, Bondt A, Hennig R, Gardner RA, O'Flaherty R, Trbojević-Akmačić I, et al. High-Throughput Serum N-Glycomics: Method Comparison and Application to Study Rheumatoid Arthritis and Pregnancy-Associated Changes. *Mol Cell Proteomics* (2019) 18:3–15. doi: 10.1074/mcp.RA117.000454
72. Vaccari M, Gordon SN, Fourati S, Schifanella L, Liyanage NP, Cameron M, et al. Adjuvant-Dependent Innate and Adaptive Immune Signatures of Risk of SIVmac251 Acquisition. *Nat Med* (2016) 22:762–70. doi: 10.1038/nm.4105
73. Bartsch YC, Eschweiler S, Leliavski A, Lunding HB, Wagt S, Petry J, et al. IgG Fc Sialylation Is Regulated During the Germinal Center Reaction Following Immunization With Different Adjuvants. *J Allergy Clin Immunol* (2020) 146:652–666.e11. doi: 10.1016/j.jaci.2020.04.059
74. Hunter RL, Olsen MR, Jagannath C, Actor JK. Multiple Roles of Cord Factor in the Pathogenesis of Primary, Secondary, and Cavitary Tuberculosis, Including a Revised Description of the Pathology of Secondary Disease. *Ann Clin Lab Sci* (2006) 36:371–86.
75. Shepard HM, Phillips GL D, Thanos C, Feldmann M. Developments in Therapy With Monoclonal Antibodies and Related Proteins. *Clin Med (Lond)* (2017) 17:220–32. doi: 10.7861/clinmedicine.17-3-220
76. Beck A, Reichert JM. Marketing Approval of Mogamulizumab: A Triumph for Glyco-Engineering. *MAbs* (2012) 4:419–25. doi: 10.4161/mabs.20996
77. Cameron F, McCormack PL. Obinutuzumab: First Global Approval. *Drugs* (2014) 74:147–54. doi: 10.1007/s40265-013-0167-3
78. Thomann M, Schlothauer T, Dashivets T, Malik S, Avenal C, Bulau P, et al. In Vitro Glycoengineering of IgG1 and Its Effect on Fc Receptor Binding and ADCC Activity. *PloS One* (2015) 10:e0134949. doi: 10.1371/journal.pone.0134949
79. Larsson A, Bälöw RM, Lindahl TL, Forsberg PO. Chicken Antibodies: Taking Advantage of Evolution—a Review. *Poult Sci* (1993) 72:1807–12. doi: 10.3382/ps.0721807
80. Ching KH, Collarini EJ, Abdiche YN, Bedinger D, Pedersen D, Izquierdo S, et al. Chickens With Humanized Immunoglobulin Genes Generate Antibodies With High Affinity and Broad Epitope Coverage to Conserved Targets. *MAbs* (2018) 10:71–80. doi: 10.1080/19420862.2017.1386825
81. Pereira EP, van Tilburg MF, Florean EO, Guedes MI. Egg Yolk Antibodies (IgY) and Their Applications in Human and Veterinary Health: A Review. *Int Immunopharmacol* (2019) 73:293–303. doi: 10.1016/j.intimp.2019.05.015
82. Leiva CL, Gallardo MJ, Casanova N, Terzolo H, Chacana P. IgY-Technology (Egg Yolk Antibodies) in Human Medicine: A Review of Patents and Clinical Trials. *Int Immunopharmacol* (2020) 81:106269. doi: 10.1016/j.intimp.2020.106269
83. Suzuki N, Lee YC. Site-Specific N-Glycosylation of Chicken Serum IgG. *Glycobiology* (2004) 14:275–92. doi: 10.1093/glycob/cwh031
84. Gilgunn S, Millán Martín S, Wormald MR, Zapatero-Rodríguez J, Conroy PJ, O'Kennedy RJ, et al. Comprehensive N-Glycan Profiling of Avian Immunoglobulin Y. *PloS One* (2016) 11:e0159859. doi: 10.1371/journal.pone.0159859
85. Sheng L, He Z, Liu Y, Ma M, Cai Z. Mass Spectrometry Characterization for N-Glycosylation of Immunoglobulin Y From Hen Egg Yolk. *Int J Biol Macromolecules* (2018) 108:277–83. doi: 10.1016/j.ijbiomac.2017.12.012

Conflict of Interest: The authors declare that the research was conducted in the absence of any commercial or financial relationships that could be construed as a potential conflict of interest.

Publisher's Note: All claims expressed in this article are solely those of the authors and do not necessarily represent those of their affiliated organizations, or those of the publisher, the editors and the reviewers. Any product that may be evaluated in this article, or claim that may be made by its manufacturer, is not guaranteed or endorsed by the publisher.

Copyright © 2021 Zlatina and Galuska. This is an open-access article distributed under the terms of the Creative Commons Attribution License (CC BY). The use, distribution or reproduction in other forums is permitted, provided the original author(s) and the copyright owner(s) are credited and that the original publication in this journal is cited, in accordance with accepted academic practice. No use, distribution or reproduction is permitted which does not comply with these terms.



Heritability Enrichment of Immunoglobulin G N-Glycosylation in Specific Tissues

Xingang Li^{1,2}, Hao Wang^{2,3}, Yahong Zhu⁴, Weijie Cao^{2,3}, Manshu Song^{2,3}, Youxin Wang³, Haifeng Hou⁵, Minglin Lang⁶, Xiuhua Guo³, Xuerui Tan⁷, Jingdong J. Han⁸ and Wei Wang^{1,2,3,5,7*}

¹ Centre for Precision Health, Edith Cowan University, Joondalup, WA, Australia, ² School of Medical and Health Sciences, Edith Cowan University, Joondalup, WA, Australia, ³ Beijing Key Laboratory of Clinical Epidemiology, School of Public Health, Capital Medical University, Beijing, China, ⁴ Beijing Lucidus Bioinformation Technology Co., Ltd., Beijing, China, ⁵ School of Public Health, Shandong First Medical University & Shandong Academy of Medical Sciences, Tai'an, China, ⁶ Chinese Academy of Sciences (CAS) Center for Excellence in Biotic Interactions, College of Life Science, University of Chinese Academy of Sciences, Beijing, China, ⁷ The First Affiliated Hospital, Shantou University Medical College, Shantou, China, ⁸ Peking-Tsinghua Center for Life Sciences, Academy for Advanced Interdisciplinary Studies, Center for Quantitative Biology (CQB), Peking University, Beijing, China

OPEN ACCESS

Edited by:

Mohamed Abdel-Mohsen,
Wistar Institute, United States

Reviewed by:

Hong Zan,
The University of Texas Health Science
Center at San Antonio, United States
Megan Patricia Leask,
University of Otago, New Zealand

*Correspondence:

Wei Wang
wei.wang@ecu.edu.au

Specialty section:

This article was submitted to
B Cell Biology,
a section of the journal
Frontiers in Immunology

Received: 15 July 2021

Accepted: 12 October 2021

Published: 03 November 2021

Citation:

Li X, Wang H, Zhu Y, Cao W, Song M, Wang Y, Hou H, Lang M, Guo X, Tan X, Han JJ and Wang W (2021) Heritability Enrichment of Immunoglobulin G N-Glycosylation in Specific Tissues. *Front. Immunol.* 12:741705. doi: 10.3389/fimmu.2021.741705

Genome-wide association studies (GWAS) have identified over 60 genetic loci associated with immunoglobulin G (IgG) N-glycosylation; however, the causal genes and their abundance in relevant tissues are uncertain. Leveraging data from GWAS summary statistics for 8,090 Europeans, and large-scale expression quantitative trait loci (eQTL) data from the genotype-tissue expression of 53 types of tissues (GTEx v7), we derived a linkage disequilibrium score for the specific expression of genes (LDSC-SEG) and conducted a transcriptome-wide association study (TWAS). We identified 55 gene associations whose predicted levels of expression were significantly associated with IgG N-glycosylation in 14 tissues. Three working scenarios, i.e., tissue-specific, pleiotropic, and coassociated, were observed for candidate genetic predisposition affecting IgG N-glycosylation traits. Furthermore, pathway enrichment showed several IgG N-glycosylation-related pathways, such as asparagine N-linked glycosylation, N-glycan biosynthesis and transport to the Golgi and subsequent modification. Through phenome-wide association studies (PheWAS), most genetic variants underlying TWAS hits were found to be correlated with health measures (height, waist-hip ratio, systolic blood pressure) and diseases, such as systemic lupus erythematosus, inflammatory bowel disease, and Parkinson's disease, which are related to IgG N-glycosylation. Our study provides an atlas of genetic regulatory loci and their target genes within functionally relevant tissues, for further studies on the mechanisms of IgG N-glycosylation and its related diseases.

Keywords: genome-wide association study, immunoglobulin G, N-glycosylation, single nucleotide polymorphism, transcriptome-wide association study

INTRODUCTION

Glycosylation is one of the most ubiquitous and essential posttranslational modifications (PTM) for extracellular proteins in eukaryotes, with the addition of linear or branched oligosaccharide sidechains called glycans to the backbones of proteins (1). According to the glycans covalently attached to asparagine, threonine, or serine side chains, they are named either “N-linked” or “O-linked” (2). Based on the well-known asparagine (Asn)-X-Serine (Ser)/threonine (Thr) sequon, a given eukaryotic glycoprotein may have one or more N-linked glycosylation (N-glycosylation) sites (3). In terms of the relatively clear functional domains and the highly conserved glycosylation site at the equivalent position of Asn-297 of each heavy chain across mammalian species, immunoglobulin G (IgG) has been regarded as an ideal N-glycoprotein model for researching N-glycosylation (4, 5).

N-Glycan is initially synthesized from a lipid-linked, oligosaccharide moiety (Glc3Man9GlcNAc2-P-P-dol) on the lumen side of the endoplasmic reticulum (ER) and transferred to the nascent polypeptide chains in the ER. N-glycan is then conservatively trimmed to a core moiety (Man5GlcNAc2-Asn) by a series of exoglycosidases in the ER before transfer to the Golgi apparatus for the following optional glycan assembly (6). Assembly of the glycan-extended tree is controlled by multiple exoglycosidases and the Golgi-localized glycosyltransferases, resulting in a wide variety of oligosaccharide structures showing high species specificity (7). At present, almost 200 glycosylation-related genes have been identified in the human genome (summarized in GlycoGene Database (GGDB, <https://acgg.asia/ggdb2/>) (8), representing approximately 1% of all human genes. However, glycan branching in the Golgi is highly dependent on microenvironment, such as tissue-specific regulation of the expression of glycoenzymes along the Golgi assembly line. Due to the lack of N-glycan profiling data for particular tissues, even to the best-known glycoprotein, human IgG, it remains unclear whether its N-glycosylation is regulated differentially across multiple tissues and how tissue-specific regulation contributes to its diverse N-glycosylation.

GWAS have identified over 60 susceptibility loci associated with the alternative N-glycan peaks (N-GPs) of IgG, which is the qualification and quantification of enzymatically released N-glycans by ultra-performance liquid chromatography (UPLC) after the IgG is isolated from plasma (9–12). Four of the 200 glycoenzymes (8) are located in these identified GWAS loci, including *FUT6*, *FUT8*, *B4GALT1*, and *MGAT3*, implying their contribution to the alternative IgG N-glycosylation. However, over 90% of identified GWAS hits are difficult to characterize biologically due to the pitfalls of GWAS approach, e.g., very small effect size, within the noncoding region, pleiotropic, and/or noncausative (13). Thus, a large number of functionally relevant genes underpinning these GWAS associations of IgG N-glycosylation remain unidentified.

Furthermore, immune cells, e.g., plasma cells which synthesize and secrete IgG, are highly motile between blood and lymphatic circulation, traveling around the lymphoid nodes and mucosa-associated lymphoid tissues (MALTs), a diffuse lymphoid tissue system found in submucosal parts of the body

(e.g., gastrointestinal tract, nasopharynx, thyroid, breast, lung, salivary glands, and skin), throughout the body to reach a site of inflammation (14). On amount of the existence of tissue-specific gene expression (15) and the limitation that only plasma IgG has been investigated in population-based studies for the genetic effect of IgG N-glycosylation, it is still unclear whether or not the N-glycosylation of IgG is regulated differentially among multiple MALTs. Likewise, how the genetic susceptibility of quantitative trait loci (QTL) identified by GWAS affects IgG N-glycosylation through the tissue-specific regulation of gene expression remains unknown. Recent genomic/transcriptomic-based statistical approaches (16, 17) may help to shed light on the complicated mechanisms of IgG N-glycan biosynthesis, especially concerning tissue-specific regulation.

In the present study, to identify genetically regulated genes associated with IgG N-glycosylation traits across the multitude of tissues, we leveraged the data of GWAS on IgG N-glycosylation from 8,090 participants of European ancestry (11) and the data from a large-scale expression QTL (eQTL) study, i.e., Genotype-Tissue Expression of 53 types of tissue (GTEx v7) (18). We first conducted a linkage disequilibrium scores for the specific expression of genes (LDSC-SEG) (16) to filtrate which tissues are most likely to be enriched with each specific IgG N-GPs having significant GWAS results (20 out of 23 GPs have significant GWAS hits). To avoid the tissue bias in following transcriptome-wide association study (TWAS), we selected corresponding tissue types in expression panels of functional summary-based imputation (FUSION), matched with the LDSC-SEG screening tissues and the LDSC-SEG significant IgG N-GPs for TWAS analyses (17). To investigate whether the significance of TWAS hits resulted from the regulation of gene expression or a genetically associated effect, we conducted joint and conditional analyses on each TWAS hit. We next explored the biological pathways of candidate genes from TWAS and accessed the network of corresponding gene sets by protein-protein interaction (PPI) analysis within IgG N-glycosylation-related tissues. At last, we retrieved the single nucleotide polymorphisms (SNPs) underlying the TWAS hits in phenome databases to discover the complex traits and diseases sharing genetic susceptibility with IgG N-glycosylation. A schematic analysis plan of our study can be found in **Figure 1**.

The study aimed to characterize the genetic predispositions of IgG N-glycosylation in their enriched tissues, thus extending our understanding of the genetic regulation of IgG N-glycosylation-related gene expression in the corresponding tissues and to determine their association with susceptibility genes for IgG N-glycosylation-related traits and diseases.

MATERIALS AND METHODS

GWAS Dataset of IgG N-Glycosylation

The IgG N-glycosylation GWAS summary statistics used in LDSC-SEG and TWAS were acquired from the NHGRI-EBI GWAS Catalog (19) for study GCST009860, the most recent large-scale GWAS meta-analysis (8,090 participants of European ancestry) (11). The GWAS summary statistics were downloaded

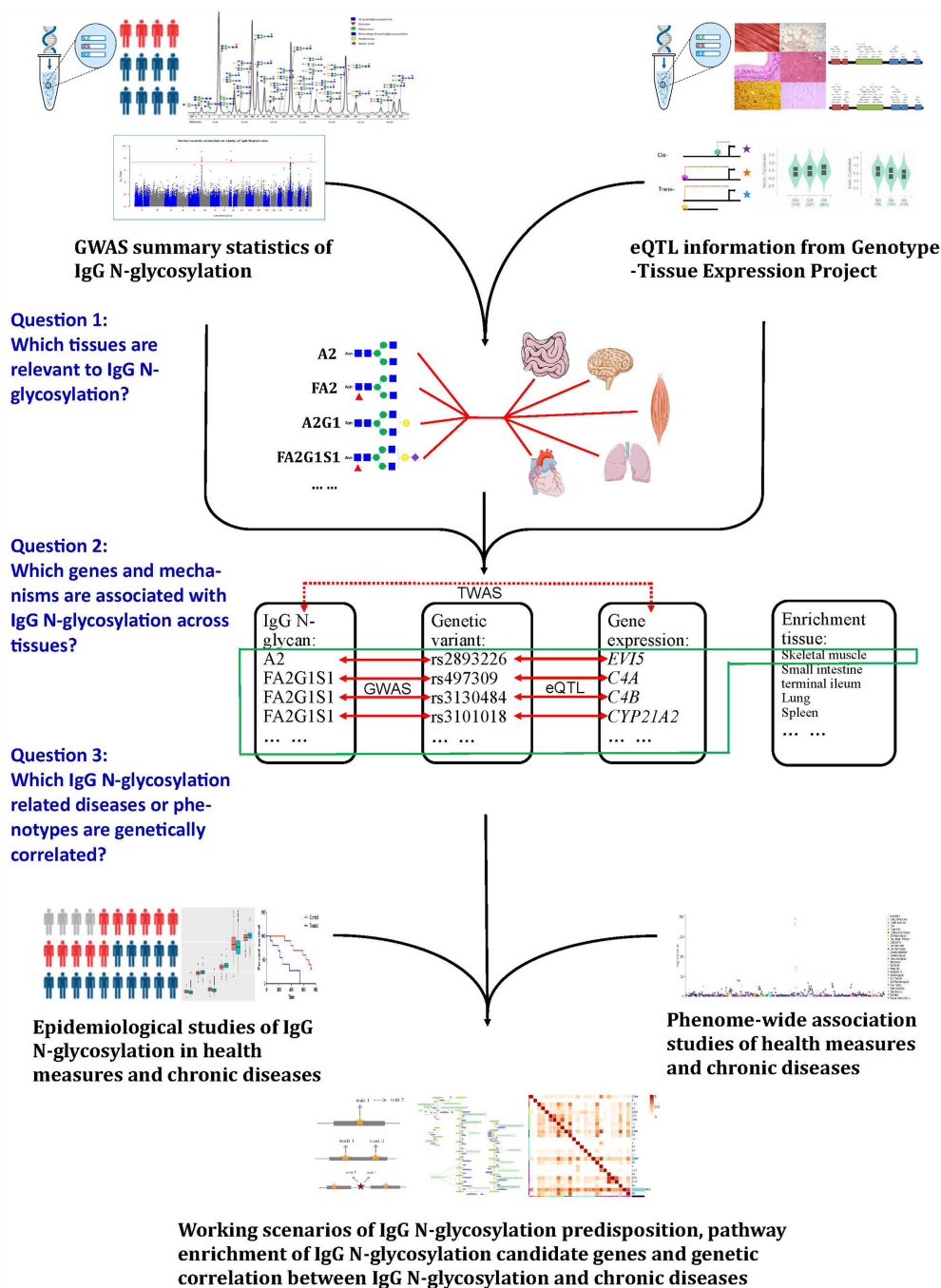


FIGURE 1 | A schematic analysis plan in the study. Leveraging IgG N-glycosylation genome-wide association studies (GWAS), summary statistics, and gene expression datasets: (1) to filtrate the tissues enriched in IgG N-glycosylation signal, (2) to identify the genes most significantly associated with IgG N-glycosylation features, and (3) to investigate the diseases or phenotypes involved with IgG N-glycosylation.

from <https://datashare.is.ed.ac.uk/handle/10283/3238/> on May 27, 2020. Information about IgG N-glycosylation peaks (IGPs) is given in **Supplementary Table 1** by both Edinburgh code and Zagreb code. Additional details on the quantification of IGPs and genotyping can be found in previous studies (9, 10).

To be consistent with our previous studies, we used the Zagreb code (GP1–GP24) for naming each GP profiled by UPLC in the IgG N-glycome. Detailed naming and compositional information of GPs were given in a previous report (9, 20) and are listed in **Supplementary Table 2**. Meanwhile, being consistent with public

data from GTEx, we used the same tissue names as those in GTEx. Of the total 24 GPs, significant GWAS summary statistics of 20 GPs were investigated by LDSC-SEG. Whereas the remaining four GPs (GP1, GP3, GP5, and GP21) were excluded due to a lack of GWAS statistical significance.

Transcriptomic Dataset for Linkage Disequilibrium Score Regression of Specifically Expressed Genes in LDSC-SEG

Integrating GWAS with large-scale functional genomic data has been proposed as an effective approach to characterize the functional effects of associated genetic variants, especially for cross-tissue study (21). LDSC-SEG provides a solid bioinformatics tool for discerning which tissues or cell types are most relevant to a particular disease or health phenotype (16). Therefore, LDSC-SEG is able to perform the tissue enrichment analyses for a specific phenotype by integrating stratified linkage disequilibrium score regression from GWAS summary statistics with tissue-specifically expressed gene sets in a huge volume of gene expression data (22).

Data for LDSD-SEG analysis were prepared as described in a previous study (<https://alkesgroup.broadinstitute.org/LDSCORE/>) (16). A total of 53 multitissue samples from GTEx v7 were included in this LDSC-SEG analysis (<https://github.com/bulik/ldsc>) (18).

Transcriptomic Panels for TWAS in FUSION

TWAS (23) combine genetically predicted gene expression levels with GWAS results on a specific phenotype, to discover genes whose *cis*-regulated expressions are associated with that phenotype (17, 24–27). The above approach has been successfully performed on pathogenesis studies of neurodegenerative disorder (Parkinson's disease) (28), psychiatric disorders (schizophrenia, attention deficit hyperactivity, autism spectrum, and bipolar disorder) (29–31), and also cancer studies (pancreatic, breast, prostate, and ovarian cancers) (32–36).

Through TWAS analysis, the relationships between SNPs and gene expression levels were first obtained to build-up reference panels composed of predictive models. These models were then used to predict trait-associated gene expressions, *via* the statistically significant SNPs from the GWAS summary statistics of an interesting trait based on a large independent cohort (17, 25).

The FUSION method was performed to estimate heritability, build predictive models, and identify transcriptome-wide associations. By FUSION, the associations between the IgG N-GPs and the expression levels of candidate genes in corresponding tissues were identified *via* the coassociated genetic variants (as SNPs) which are identified as statistically significant in GWAS (as QTLs) and also in GTEx (as eQTLs).

Transcriptomic imputation (TI) in FUSION method was conducted using eQTL reference panels which were derived from tissue-specific gene expression coupled with genotypic data. In the current study, 27 tissues were identified as relevant

with IgG N-glycosylation by LDSC-SEG, while three tissues were unavailable in FUSION. Hence, 24 tissue panels were used as TI reference panels, while the 1,000 Genomes v3 LD panel (<http://ftp.1000genomes.ebi.ac.uk/vol1/ftp/release/20130502/>) was hired as an LD reference. A Bonferroni-corrected study-wise threshold was calculated by $p = 0.05/\text{number of genes in each panel}$ (Supplementary Table 2). As previous GWAS on IgG N-GPs reported that immune tissues are relevant to IgG N-glycosylation (10, 11), we employed three immune tissues, i.e., spleen, whole blood, and Epstein-Barr virus (EBV)-transformed lymphocytes as a complementary strategy of expression panel selection in FUSION, along with 20 GWAS-significant IgG N-GPs to conduct a parallel TWAS analysis.

Identification of IgG N-Glycosylation Relevant Tissues by LDSC-SEG

The linkage disequilibrium score for the specific expression of genes (LDSC-SEG) is a computational approach to identify phenotype-relevant tissues using stratified LD score regression (<https://alkesgroup.broadinstitute.org/LDSCORE/>) (16). In a given tissue, if there is an enrichment of the highest specific expression in the regions surrounding the heritability of a disease/phenotype, it will support the likely correlation between this disease/phenotype and this tissue (16). By this approach, we investigated 53 tissues from the GTEx project (<http://gtexportal.org/>) (18), to designate the tissues relevant to IgG N-glycosylation features. All procedures follow the tutorial in Github (<https://github.com/bulik/ldsc>).

Performing TWAS on IgG N-Glycosylation GWAS Dataset

TWAS has been proposed as a robust tool to integrate GWAS summary statistics, *cis*-SNP-expression effect sizes, and LD reference panels to evaluate the association between the *cis*-genetic element of expression and disease/phenotype (28, 30, 31). Thus, using the colocalized SNPs between GWAS statistics and eQTL data as linkers, TWAS is able to identify the candidate genes for the potential mechanism underlying the variant-disease/phenotype associations, which are challenging for GWAS approach.

In the present study, we conducted FUSION tool (<http://gusevlab.org/projects/fusion/>) (17) for each transcriptome reference panel designated by an LDSC-SEG approach. Briefly, to estimate the heritability of each gene expression, we first conducted a robust version of Genome-wide Complex Trait Analysis-Genome-based restricted maximum likelihood (GCTA-GREML). This step generated the heritability estimates of expression for each gene with the p of the likelihood ratio test.

FUSION has created five different models to calculate the predictive weights of expression or intron usage: best linear unbiased prediction (blup), Bayesian sparse linear mixed model (bslmm), LASSO regression (lasso), Elastic Net (enet), and top SNPs (topl). After weighting, the cross-validation for each of the desired models was performed. The model gaining the best cross-validation prediction accuracy was chosen and the corresponding predictive expression or intron usage was

correlated to IgG N-glycosylation GWAS summary statistics to conduct TWAS and filtrate significant associations. The significance for heritability estimates of the genes or intron usage at a Bonferroni-corrected $p < 0.05$ were reported as TWAS hits. Accounting for more suggestive information on gene coexpression, we also applied an FDR of 5% within each expression reference panel to obtain a bigger risk gene set for pathway analysis.

Joint and Conditional Testing GWAS Signal Analysis

Using the postprocess module in FUSION (<http://gusevlab.org/projects/fusion/>), joint and conditional testing methods were performed to determine the contribution of gene expression association in each significant TWAS hit. After the weight of gene expression was removed, the residual TWAS signal was recalculated and evaluated with genome-wide Bonferroni correction. The testing region was defined by the transcribed region of the genes. In each testing, every association of GWAS was conditioned upon the joint gene model by one SNP.

Colocalization Analyses and Functional Annotation

Using *coloc* approach (37), the colocalization analyses were conducted to strengthen the detection of candidate genes at IgG N-glycosylation GWAS loci by hunting the evidence of shared causal variants between functional eQTL traits and GWAS traits. The colocalization test converts correlation statistics to effect size based on the sample size of the study for a given function, i.e., gene expression. Then, under the assumption that the standard error approximation is inversely proportional to the square root of the sample size, the approximate colocalization effect size is calculated. The statistics of posterior probability (PP) were presented for the five hypotheses (PP.H0: unrelated; PP.H1: only functionally relevant; PP.H2: only GWAS relevant; PP.H3: independent function/GWAS related; and PP.H4: colocalized function/GWAS related). The current study mainly concerned the PP.H4, which represents the posterior probability that GWAS significant signal and eQTL locus are the same locus, ranging from 0 to 1, where 0 means 0% probability and 1 means 100% probability. Colocalization is declared if the posterior PP.H4 for the model with a shared causal variant exceeded 0.750.

The online tool, *HaploReg* v4.1 (<https://pubs.broadinstitute.org/mammals/haploreg/haploreg.php>) (38) was used to annotate the potential functions of the best eQTLs which were identified by FUSION and *coloc*, for dbSNP function, promoter and enhancer activity regions, DNase, protein-binding regions, and transcription factor-binding motifs.

Gene-Set Analyses

Agnostic analyses were performed in STRING portal (<http://string-db.org/>) (39), according to Gene Ontology (GO), Kyoto Encyclopedia of Genes and Genomes (KEGG), and Reactome databases to identify pathways relevant to IgG N-glycosylation. Gene clustering was conducted using the GeneNetwork v2.0 (<https://genenetwork.nl>) (40), which was based on RNA sequencing database ($n = 31,499$).

Phenome-Wide Association Studies and Genetic Correlation Investigation

To identify more diseases/phenotypes associated with the most significant eQTL of each TWAS gene, we performed a phenome-wide association study (pheWAS) on each leading SNP, by leveraging the public data in the GWASAtlas (<https://atlas.ctglab.nl>) (41). Based on p -values, the top 5 phenotypes (excluding IgG N-glycosylation and repeated phenotypes) were presented. The genetic correlation between the diseases/phenotypes identified by pheWAS was determined by LDSC, using available data in the GWASAtlas. We utilized the most recent GWAS data (i.e., until 2020) for analysis. A Bonferroni correction was utilized to adjust the significance threshold with the number of tested traits.

RESULTS

Identification of IgG N-Glycosylation-Relevant Tissues by Heritability Enrichment of Expressed Genes

To better comprehend how peripheral tissues affect IgG N-GPs and to avoid tissue bias in following TWAS, we conducted a tissue enrichment analysis using the LDSC-SEG method to leverage the newest IgG N-glycosylation GWAS summary statistics (11) and eQTL data from the GTEx consortium (v7) (15, 18). The study comprised 48 tissue types ($n = 80$ to 491, **Supplementary Table 1**) with a 5% false discovery rate (FDR) threshold.

Seventeen GPs were enriched in 27 of the 53 types of tissue in the gene expression panels of GTEx v7 at a 5% FDR threshold ($-\log_{10} p > 1.32$) (**Supplementary Table 3, Figure 2; Supplementary Figure 1**). These 17 GPs and 27 relevant tissues were therefore chosen as the primary strategy for gene expression panel selection in the following TWAS analysis.

For the three immune tissues selected as the complementary strategy, only three GPs including FA2[6]G1 glycan (GP8), FA2[6]BG1 glycan (GP10), and FA2G2S1 glycan (GP18) were enriched in spleen and whole blood, but no enrichment was found in EBV-transformed lymphocytes (**Supplementary Table 3**). These results indicated that genetic effects of IgG N-GPs on the regulation of gene expression are tissue selective, and more likely to be enriched not only in the tissues of immune organs but also broadly in multiple MALTs across peripheral organs, such as skin, lung, breast mammary tissue, small intestine, esophagus muscularis, testis, and uterus.

Constructing a List of Tissue-Dependent Associations Between Genes and IgG N-Glycan Traits

To identify the *cis*-regulated genes associated with IgG N-GPs within their functionally relevant tissues, we conducted a TWAS analysis using the FUSION method (see URLs in the *Data Availability Statement*), in terms of the same IgG N-glycosylation GWAS summary statistics (11) and the reference transcriptome panels derived from GTEx v7 (15, 18). In total, 116,076 features of tissue-specific gene expression were tested (see details in **Supplementary Table 1**). Based on the primary strategy of expression panel selection by LDSC-SEG (24 tissue



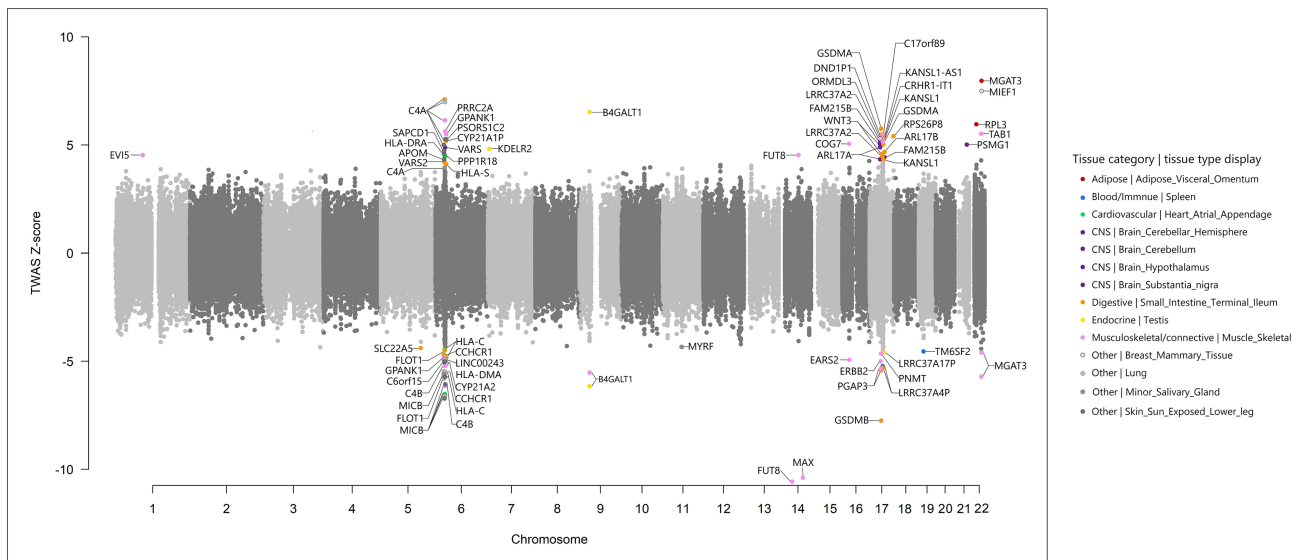


FIGURE 3 | Miami plot of the transcriptome-wide association study for IgG N-glycosylation ($n = 8,090$) using gene expression models in 24 tissues. Each point refers to a single gene tested, with the physical position plotted on the x-axis, and a Z-score of association between gene expression and IgG N-glycan peaks plotted on the y-axis. Bonferroni-adjusted significant genes within corresponding transcriptome panels are labeled in multiple colors according to different tissue categories and tissue types.

were observed (**Table 1** SNPs with asterisks). (2) A single SNP is within or associated with a single gene or multiple genes and simultaneously associated with a single or multiple GPs within multiple corresponding tissues. This suggests pleiotropic effects of the genetic variants for different GPs or genes among multiple tissues (accounting for 44 observed associations, **Table 1** SNPs with daggers). (3) A single SNP is associated or located in a single gene but associated with multiple GPs within only one tissue, indicating that the genetic variant is coassociated with these two GPs while they were highly correlated with each other *via* coassociation with the same gene (accounting for six observed associations, **Table 1** SNPs with section symbols). For example, rs761830 is correlated with A2 glycan (GP2) ($Z = -11.70$, $p = 1.34E-31$) and FA2G2 glycan (GP14) ($Z = 4.52$, $p = 6.22E-06$), linked with *FUT8* gene in skeletal muscle in two reverse directions. In such a case, the corresponding SNP is likely to regulate its target genes in two opposite directions to influence these two GPs (**Table 1**).

IgG N-Glycosylation TWAS Hits Are Driven by Genetic Regulation on Gene Expression

As multiple TWAS hits overlapped with the significant results of previous IgG N-glycosylation GWAS, we conducted joint and conditional analyses to address how much GWAS signal remains after the association of the functional annotation is removed. The postprocess module in FUSION was performed to report the statistics for the jointly significant genes.

Our results demonstrated that all known IgG N-glycosylation GWAS susceptibility loci could be explained entirely or mostly by the

expression of corresponding genes identified in TWAS, supporting the concept that these TWAS hits were mainly driven by the genetic regulation of gene expression in these loci (**Supplementary Table 4** and **Supplementary Figure 2**). For instance, association analysis conditioning on the expression of *FUT8*, which depended on the associations between expression SNPs (eSNPs) and A2 glycan (GP2) in skeletal muscle, showed expression-driven signals in a previously implicated GWAS locus and explained 59.1% of the variance (rs761830 lead SNP_{GWAS} $p = 1.32E-54$, conditional lead SNP_{GWAS} $p = 2.49E-23$) (**Figure 5A**). By the associations of eSNPs with FA2G2 glycan (GP14) in skeletal muscle, the expression level of *FUT8* explained 94.7% of the variances at this locus (rs761830 lead SNP_{GWAS} $p = 6.83E-06$, conditional lead SNP_{GWAS} $p = 3.00E-01$) was observed (**Figure 5B**). The joint and conditional analyses for *WNT3* completely explained the variance of the locus by 100% on chromosome 17 through the associations of eSNPs with FA2[6]BG1 glycan (GP10) in the small intestine terminal ileum (rs199438 lead SNP_{GWAS} $p = 1.3E-07$, conditional lead SNP_{GWAS} $p = 1$) (**Figure 5C**).

Similarly, we performed joint and conditional analyses on the remaining 43 novel IgG N-glycosylation TWAS hits with the expression of corresponding genes. The result showed that the majority of these TWAS hits were also mostly driven by the regulatory effect of genetic variants on the expression levels of targeted genes (**Supplementary Figure 3** and **Supplementary Table 5**). For example, association analysis conditioning on the expression of *EVI5* which depended on the associations between eQTLs and A2 glycan (GP2) in the skeletal muscle panel, demonstrated that expression-driven signals in this novel IgG N-glycosylation locus explained 49.9% of the variance (rs169201 lead SNP_{GWAS} $p = 5.17E-10$, conditional lead SNP_{GWAS} $p = 1.09E10-05$) (**Figure 5D**).

TABLE 1 | Significant TWAS genes for IgG N-glycosylation original.

Tissue types in GTEx	Cytogenetic band	TWAS identified gene	IgG N-glycosylation feature	Lead QTL	Best eQTL	TWAS Z-score	TWAS p-value	COLOC PP.H4
Muscle_Skeletal	1p22.1	<i>EVI5</i>	GP2	rs11800409	rs2893226*	4.53	5.93E-06	0.193
	6p21.33 ^a	<i>C4A</i>	GP16	rs3130923	rs497309 [†]	5.61	2.05E-08	0.075
	6p21.33 ^a	<i>C4B</i>	GP16	rs1800629	rs3130484 [†]	-5.21	1.90E-07	0.936
	6p21.33 ^a	<i>CYP21A2</i>	GP16	rs1800629	rs3101018 [†]	-5.15	2.59E-07	0.946
	6p21.33 ^a	<i>GPANK1</i>	GP16	rs3130923	rs3130484 [†]	5.50	3.87E-08	0.682
	6p21.33 ^a	<i>GPANK1</i>	GP19	rs2523591	rs3130484 [†]	-5.03	4.81E-07	0.645
	6p21.33 ^a	<i>HLA-C^b</i>	GP16	rs2516408	rs2523578 [†]	-5.18	2.26E-07	0.000
	6p21.33 ^a	<i>MICB</i>	GP16	rs3130923	rs2516408 [†]	-6.13	9.04E-10	0.993
	6p21.33 ^a	<i>PRRC2A</i>	GP16	rs3130923	rs2515919*	5.53	3.23E-08	0.230
	9p21.1 ^a	<i>B4GALT1^b</i>	GP18	rs10813951	rs1411609*	-5.53	3.23E-08	0.000
	14q23.3 ^a	<i>FUT8^b</i>	GP2	rs11847263	rs761830 [§]	-11.70	1.34E-31	0.098
	14q23.3 ^a	<i>FUT8^b</i>	GP14	rs11158593	rs761830 [§]	4.52	6.22E-06	0.908
	14q23.3 ^a	<i>MAX</i>	GP2	rs11847263	rs1953230*	-11.34	8.37E-30	0.532
	16p12.2 ^a	<i>COG7^b</i>	GP18	rs250555	rs250583*	5.05	4.46E-07	0.721
	16p12.2	<i>EARS2</i>	GP18	rs250555	rs4967958*	-4.93	8.11E-07	0.447
	17q12	<i>ERBB2</i>	GP2	rs907091	rs2102928*	-5.00	5.76E-07	0.103
	17q12	<i>PGAP3</i>	GP2	rs907091	rs907089*	-5.36	8.14E-08	0.000
	17q12	<i>PNMT</i>	GP2	rs907091	rs2271308*	-4.62	3.90E-06	0.009
	17q21.1	<i>GSDMA</i>	GP2	rs907091	rs8065126*	5.76	8.62E-09	0.000
	17q21.31	<i>KANSL1</i>	GP14	rs169201	rs169201 [†]	5.02	5.22E-07	0.987
	17q25.3 ^a	<i>C17orf89^b</i>	GP18	rs2659007	rs883884*	5.40	6.52E-08	0.050
	22q13.1 ^a	<i>MGAT3^b</i>	GP19	rs5757678	rs1005522 [§]	-5.71	1.12E-08	0.988
	22q13.1 ^a	<i>MGAT3^b</i>	GP24	rs5750830	rs1005522 [§]	-4.58	4.55E-06	0.981
	22q13.1 ^a	<i>TAB1^b</i>	GP19	rs738289	rs5757650*	4.95	7.35E-07	0.543
Small_Intestine_Terminal_Ileum	5q31.1	<i>SLC22A5</i>	GP2	rs11746555	rs2073643*	-4.41	1.03E-05	0.042
	6p21.33 ^a	<i>C4A</i>	GP16	rs3130923	rs3101018 [†]	7.01	2.46E-12	0.655
	6p21.33 ^a	<i>CCHCR1</i>	GP16	rs3130923	rs1265087 [†]	-4.91	9.04E-07	0.000
	6p21.33 ^a	<i>CYP21A1P</i>	GP16	rs1800629	rs3101018 [†]	5.19	2.08E-07	0.950
	6p21.33 ^a	<i>FLOT1</i>	GP16	rs3130557	rs3094220*	-4.46	8.08E-06	0.731
	6p21.33 ^a	<i>HLA-C^b</i>	GP16	rs2516408	rs1265098*	-5.62	1.88E-08	0.120
	6p21.33 ^a	<i>HLA-S</i>	GP16	rs3130923	rs2844623 [†]	4.60	4.22E-06	0.068
	6p21.33 ^a	<i>VAR52</i>	GP16	rs3130557	rs3130557 [†]	4.49	7.21E-06	0.954
	17q12	<i>PGAP3</i>	GP2	rs907091	rs903502*	-5.41	6.38E-08	0.122
	17q21.1	<i>GSDMA</i>	GP2	rs907091	rs3859192*	4.89	9.88E-07	0.065
	17q21.1	<i>GSDMB^b</i>	GP2	rs907091	rs9303281*	-7.76	8.21E-15	0.967
	17q21.31	<i>ARL17B</i>	GP2	rs415430	rs17698176*	4.59	4.53E-06	0.021
	17q21.31	<i>DND1P1</i>	GP10	rs17689471	rs17689471 [†]	5.33	1.00E-07	0.990
	17q21.31	<i>KANSL1</i>	GP10	rs17689471	rs169201 [†]	5.19	2.07E-07	0.922
	17q21.31	<i>KANSL1-AS1</i>	GP10	rs17689471	rs17689471 [†]	5.29	1.21E-07	0.990
	17q21.31	<i>LRRC37A2</i>	GP10	rs7224296	rs169201 [†]	5.05	4.48E-07	0.972
	17q21.31	<i>LRRC37A4P</i>	GP10	rs17689471	rs17689471 [†]	-5.29	1.19E-07	0.972
	17q21.31	<i>RPS26P8</i>	GP10	rs17689471	rs17689471 [†]	5.32	1.07E-07	0.822
	17q21.31-q21.32 ^a	<i>WNT3^b</i>	GP10	rs7224296	rs199438*	4.68	2.88E-06	0.373
Skin_Sun_Exposed_Lower_Leg	6p21.33 ^a	<i>APOM</i>	GP16	rs3130923	rs1150755*	4.65	3.28E-06	0.021
	6p21.33 ^a	<i>C4A</i>	GP16	rs3130923	rs1150753 [†]	4.99	5.99E-07	0.090
	6p21.33 ^a	<i>C4B</i>	GP16	rs1800629	rs3101018 [†]	-6.11	1.02E-09	0.940
	6p21.33 ^a	<i>C6orf15</i>	GP16	rs3130923	rs1265093*	-5.11	3.25E-07	0.001
	6p21.33 ^a	<i>CYP21A2</i>	GP16	rs1800629	rs1150753 [†]	-5.01	5.33E-07	0.931
	6p21.33 ^a	<i>HLA-C^b</i>	GP16	rs2516408	rs2523578 [†]	-5.73	9.93E-09	0.000
	6p21.32 ^a	<i>HLA-DRA^b</i>	GP16	rs1150752	rs2858867*	4.71	2.48E-06	0.146
	6p21.33 ^a	<i>MICB</i>	GP16	rs3130923	rs2516408 [†]	-6.69	2.17E-11	0.993
	6p21.33 ^a	<i>PSORS1C2</i>	GP16	rs3130923	rs1265099*	5.24	1.65E-07	0.027
	6p21.33 ^a	<i>SAPCD1</i>	GP16	rs3130923	rs1144709*	4.75	2.05E-06	0.791
	17q21.31	<i>CRHR1-IT1</i>	GP10	rs17689471	rs17689471 [†]	5.20	2.04E-07	0.990
Spleen	17q21.31	<i>DND1P1</i>	GP10	rs17689471	rs17689918 [†]	5.29	1.20E-07	0.989
	17q21.31	<i>KANSL1-AS1</i>	GP10	rs17689471	rs17689918 [†]	5.31	1.11E-07	0.988
	17q21.31	<i>LRRC37A4P</i>	GP10	rs17689471	rs17689918 [†]	-5.25	1.55E-07	0.989
	17q21.31-q21.32 ^a	<i>WNT3^b</i>	GP10	rs7224296	rs199520*	4.58	4.74E-06	0.858
	19p13.11	<i>TM6SF2</i>	GP10	rs7257072	rs2916074*	-4.55	5.37E-06	0.056
Heart_Atrial_Appendage	6p21.32	<i>HLA-DMA</i>	GP16	rs209473	rs2854275*	-4.86	1.19E-06	0.214

(Continued)

TABLE 1 | Continued

Tissue types in GTEx	Cytogenetic band	TWAS identified gene	IgG N-glycosylation feature	Lead QTL	Best eQTL	TWAS Z-score	TWAS p-value	COLOC PP.H4
Lung	6p21.33 ^a	<i>C4A</i>	GP16	rs3130923	rs497309 [†]	5.26	1.42E-07	0.174
	6p21.33 ^a	<i>CCHCR1</i>	GP16	rs3130923	rs1265087 [†]	-4.75	2.08E-06	0.000
	6p21.33 ^a	<i>HLA-C^b</i>	GP16	rs2516408	rs1265087 [†]	-4.45	8.54E-06	0.098
	6p21.33 ^a	<i>MICB</i>	GP16	rs3130923	rs2516412 [†]	-6.52	7.05E-11	0.992
	6p21.33 ^a	<i>PPP1R18</i>	GP16	rs3130557	rs3094663 [*]	4.67	3.04E-06	0.740
	6p21.33 ^a	<i>C4A</i>	GP16	rs3130923	rs1150753 [†]	6.13	8.59E-10	0.122
	6p21.33 ^a	<i>CCHCR1</i>	GP16	rs3130923	rs1265087 [†]	-5.54	2.95E-08	0.000
	6p21.33 ^a	<i>FLOT1</i>	GP16	rs3130557	rs3130557 [†]	-5.80	6.74E-09	1.000
	6p21.33 ^a	<i>HLA-C^b</i>	GP16	rs2516408	rs2844623 [†]	-4.76	1.89E-06	0.000
	6p21.33 ^a	<i>LINC00243</i>	GP16	rs3130557	rs3130557 [†]	-5.04	4.57E-07	0.922
Testis	6p21.33 ^a	<i>MICB</i>	GP16	rs3130923	rs2516412 [†]	-5.63	1.83E-08	0.992
	7p22.1	<i>KDELR2</i>	GP4	rs17198191	rs17198191 [*]	4.82	1.41E-06	0.999
	9p21.1 ^a	<i>B4GALT1^b</i>	GP4	rs10813951	rs17247766 [§]	6.51	7.69E-11	0.006
	9p21.1 ^a	<i>B4GALT1^b</i>	GP14	rs10813951	rs17247766 [§]	-6.16	7.48E-10	0.000
Minor_Salivary_Gland	17q21.32	<i>LRRC37A17P</i>	GP14	rs415430	rs169201 [†]	-4.58	4.73E-06	0.980
	6p21.33 ^a	<i>C4A</i>	GP9	rs2516408	rs3101018 [†]	4.37	1.26E-05	0.231
	6p21.33 ^a	<i>MICB</i>	GP9	rs2516408	rs2516412 [†]	-6.59	4.46E-11	0.939
Brain_Cerebellar_Hemisphere	11q12.2	<i>MYRF</i>	GP9	rs174576	rs449397 [*]	-4.35	1.35E-05	0.097
	17q21.31	<i>ARL17A</i>	GP14	rs415430	rs169201 [†]	4.44	8.87E-06	0.982
	17q21.32	<i>FAM215B</i>	GP14	rs415430	rs199439 [*]	4.49	7.17E-06	0.974
Brain_Cerebellum	17q21.31	<i>KANSL1</i>	GP14	rs169201	rs17692129 [*]	4.48	7.59E-06	0.731
	17q21.31	<i>ARL17A</i>	GP14	rs415430	rs199443 [*]	4.66	3.09E-06	0.977
	17q21.32	<i>FAM215B</i>	GP14	rs415430	rs169201 [†]	4.78	1.74E-06	0.981
Breast_Mammary_Tissue	17q21.31	<i>LRRC37A2</i>	GP14	rs415430	rs169201 [†]	4.49	7.14E-06	0.982
	17q21.1	<i>ORMDL3^b</i>	GP7	rs4795400	rs25645 [*]	5.12	3.02E-07	0.028
Adipose_Visceral_Omentum	22q13.1 ^a	<i>MIEF1</i>	GP23	rs909674	rs738288 [*]	7.50	6.37E-14	0.501
	22q13.1 ^a	<i>MGAT3^b</i>	GP23	rs909674	rs5750830 [*]	7.96	1.74E-15	0.729
	22q13.1 ^a	<i>RPL3</i>	GP23	rs1005522	rs139393 [*]	5.52	3.43E-08	0.098
Brain_Hypothalamus	21q22.2	<i>PSMG1</i>	GP19	rs7282582	rs2297256 [*]	5.02	5.12E-07	0.799
Brain_Substantia_nigra	6p21.33 ^a	<i>VARS</i>	GP19	rs2523591	rs2523500 [*]	4.86	1.17E-06	0.097

Detailed naming and compositional information of GPs was given in previous reports and in **Supplementary Table 1**.

GP, IgG N-glycan peak; GP1-24, Zagreb code for the names of GPs in the qualification and quantification of enzymatically released IgG N-glycans by ultra-performance liquid chromatography (UPLC); Lead QTL, SNP with the strongest association in the locus in GWAS analysis; Best eQTL, SNP with the strongest association in the locus in TWAS analysis; COLOC PP.H4, the posterior probability of hypothesis 4 in COLOC approach.

^aRegions have been implicated in previous IgG N-glycosylation GWAS.

^bGenes have been implicated in previous IgG N-glycosylation GWAS.

^{*}The tissue-specific SNP.

[†]The coassociated SNPs.

[§]The tissue-sharing SNPs.

Association analysis conditioning on the expression of *SLC22A5* which depended on the associations between eQTLs and A2 glycan (GP2) in the small intestine terminal ileum panel, showed expression-driven signals in this novel locus that explained 55.7% of the variance (rs738288 lead SNP_{GWAS} $p = 2.16E-22$, conditional lead SNP_{GWAS} $p = 9.19-11$) (**Figure 5E**). For a novel locus of IgG N-glycosylation identified by TWAS in 21q22.2, conditioning on PSMG1 explained 95.1% of the variance (rs8065126 lead SNP_{GWAS} $p = 1.63E-05$, conditional lead SNP_{GWAS} $p = 3.42E-01$) (**Figure 5F**).

Colocalization of TWAS Signals Provides Evidence of Causality

To strengthen the detection of candidate genes as potential causal genes, the colocalization analyses were conducted between total 90 TWAS hits and all corresponding GTEx v7 eQTLs (15), using “*coloc*” package (37).

The colocalization results for this current study, the posterior probability for the fifth hypothesis (colocalized function/GWAS

related), are given in the last column of **Table 1**. Using 0.750 as the cutoff value here, 38 out of a total 90 TWAS hits obtained significant possibilities for the colocalization shared between GWAS association and eQTL association (**Table 1**). It is particularly important for the TWAS hits in the extended patterns of LD regions, such as HLA region on chromosome 6. Only 14 out of 40 TWAS hit in HLA region had the significant possibilities for colocalization, hinting that the extended patterns of LD regions are still challenging for TWAS approaches. Half of TWAS hits in nonextended patterns of LD regions were declared as shared causal variants with supportive posterior possibilities.

Functional Annotation

We used *HaploReg* v4.1 to perform the functional analysis of a total of 18 lead eQTLs showing the best colocalized associations with IGP in both TWAS and GWAS results. Among them, rs2297256 was in the 3'-UTR, while rs2516412, rs2534680, rs3101018, rs761830, and rs1005522 were located in the upstream transcript regions, and the remaining 12 lay in the intronic regions (**Supplementary Table 6**).

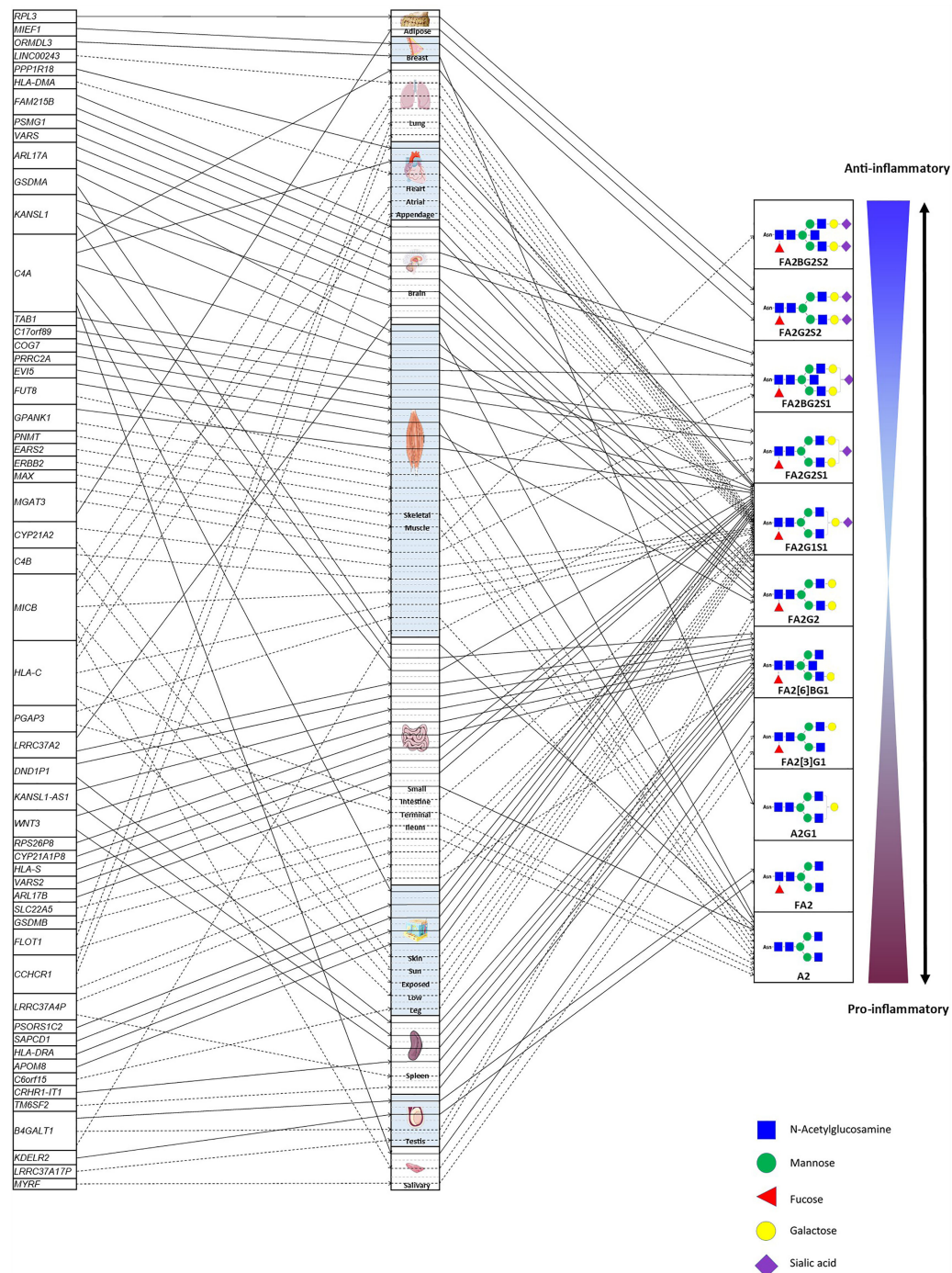
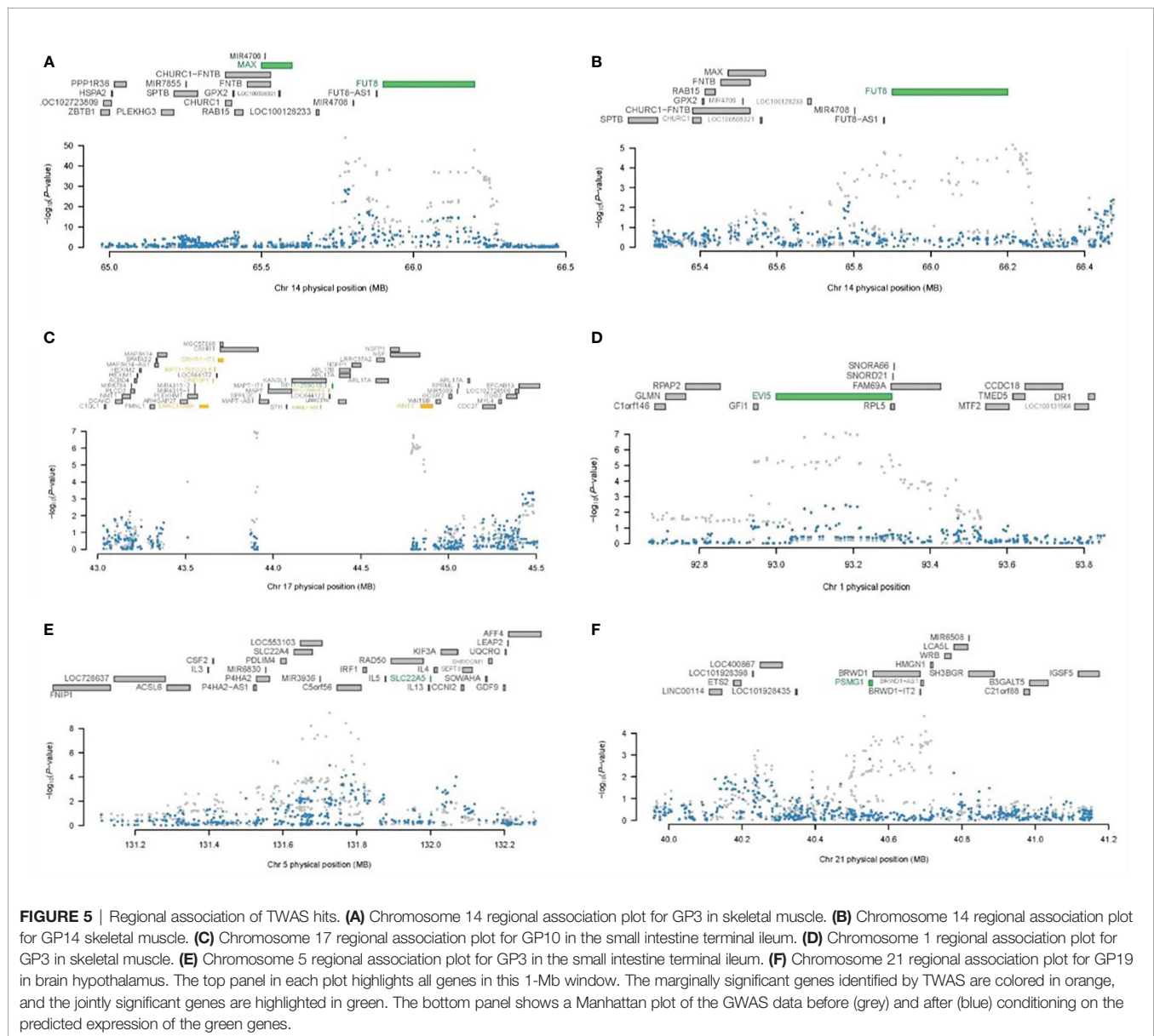


FIGURE 4 | The atlas of TWAS statistically significant genes regulating IgG N-glycosylation within specific tissues. The left column lists the candidate genes of IgG N-glycosylation. The middle column comprises the tissues enriched to the candidate genes of IgG N-glycosylation. The various types of brain tissue from the GETx consortium (v7) were allocated to the “brain” tissue group to reduce FDR. The right column indicates the IgG N-glycosylation traits associated with candidate genes within relevant tissues. F, core (if the first letter) or antennary fucose; A2, biantennary; B, bisecting N-acetylglucosamine; Gx, galactose; Sx, sialic acid; x, number of galactoses or sialic acids in a glycan structure. Detailed naming and compositional information of GPs was given in previous reports (9, 20) and is listed in **Supplementary Table 1**. The solid lines with arrows show the positive effects of the expression of candidate genes on the specific IgG N-glycosylation trait, whereas the dotted lines with arrows show negative effects.



According to the data from the Encyclopedia of ENA Elements (ENCODE) project (43), 16 out of the total 18 lead eQTLs (except rs169201 and rs199520) were identified in strong promoter or/and enhancer activity regions; 15 of the total 18 (except rs1144709, rs169201, and rs199520) in DNase hypersensitivity site regions; rs2516421, rs2534680, rs3101018, and rs17198191 in transcription factor-binding regions; 14 of the total 18 (except rs3130484, rs761830, rs9303281, and rs17689471) in the regulatory motifs (Supplementary Table 6).

Gene Set Enrichment and PPI Network Analysis

To investigate how many biological pathways may be potentially relevant with the genes identified by TWAS, enrichment analyses for GO, KEGG pathways, and Reactome were performed using

the STRING database (see URLs in the *Data Availability Statement*). A total of 55 candidate genes identified by TWAS were significantly enriched in 42 gene sets focusing on three functional processes: glycosylation (10 gene sets), immune response (23 gene sets), and protein translation (9 gene sets) (Table 2).

The ten significantly enriched glycosylation-relevant gene sets were mainly involved in the pathways of N-glycan biosynthesis, e.g., N-glycan biosynthesis, complex type (Mann-Whitney U test, $p = 4.59\text{E-}06$), transport to the Golgi and subsequent modification ($p = 4.00\text{E-}05$), N-glycan antennae elongation in the medial/trans-Golgi ($p = 2.10\text{E-}05$), and asparagine N-linked glycosylation ($p = 4.07\text{E-}04$). Twenty-one out of the 24 immune response-related gene sets were mainly enriched with infections, such as *Staphylococcus aureus* infection ($p = 1.40\text{E-}05$), allograft

rejection ($p = 5.60\text{E-}04$), graft-versus-host disease ($p = 5.60\text{E-}04$), and several specific immunological diseases, e.g., systemic lupus erythematosus (SLE) ($p = 1.66\text{E-}04$), autoimmune thyroid disease (AHD) ($p = 1.82\text{E-}04$), viral myocarditis ($p = 2.50\text{E-}04$), and leishmaniasis ($p = 5.50\text{E-}04$). At last, nine gene sets were related to protein translation, e.g., tRNA aminoacylation ($p = 9.05\text{E-}05$), amino acid activation ($p = 1.44\text{E-}04$), and tRNA metabolic process ($p = 7.47\text{E-}03$) (**Table 2**).

GO enrichment on TWAS hits strengthened several pathways which are biologically relevant to IgG N-glycosylation. The known glycosyltransferase genes (8) in our TWAS hits, including *FUT8*, *B4GALT1*, *MGAT3*, *KDEL2*, and *COG7* were enriched in the processes of asparagine N-linked glycan biosynthesis, transport to the Golgi and subsequent modification, and N-glycan antennae elongation in the medial/trans-Golgi glycosylation. These processes have been implicated in the physioregulation of IgG N-glycosylation (44, 45). By KEGG pathway analysis, six genes, i.e., *C4A*, *C4B*, *FCGR2A*, *HLA-DMA*, *HLA-DRA*, and *HLA-DRB1*, were enriched as the top 2 significant results in the pathways of *Staphylococcus aureus* infection (KEGG term hsa05322, FDR = $1.42\text{E-}05$) and systemic lupus erythematosus (KEGG term hsa05150, FDR = $2.00\text{E-}04$). Three of these genes (*HLA-DMA*, *HLA-DRA*, and *HLA-DRB1*) were enriched in the pathways of several autoimmune and inflammatory diseases, i.e., autoimmune thyroid disease, IBD, RA, and asthma (KEGG terms in **Table 2**), demonstrating their core functions in the pathways.

Through these core genes, these pathways are highly associated with cytokine-cytokine receptor interaction (hsa04060), antigen processing and presentation (hsa04612), T-cell receptor signaling pathway (hsa04660), B-cell receptor signaling pathway (hsa04662), and leukocyte trans-endothelial migration (hsa04670). These pathways play crucial roles in the appropriate functioning of all immunoglobulins, especially for the most abundant type in plasma, i.e., IgG. From Reactome (see URLs in the *Data Availability Statement*) enrichment, three gene sets are enriched into three N-glycosylation pathways, i.e., asparagine N-linked glycosylation (HSA-446203), transport to the Golgi and subsequent modification (HSA-948021), and N-glycan antennae elongation in the medial/trans-Golgi (HSA-975576).

To validate whether these TWAS-identified candidate genes associated with IgG N-glycosylation were inclined to be coexpressed within corresponding tissues, we measured the protein-protein interaction (PPI) network for the connectivity of the genes by GeneNetwork v2.0 (see URLs in the *Data Availability Statement*). The genes were clustered based on their coexpression of public RNA-seq data ($n = 31,499$). Most genes identified by TWAS within each specific tissue reference panel demonstrated coexpression (**Supplementary Figure S4**). For example, skeletal muscle contributed the most numerous significant TWAS hits across all tissues by 24 candidate genes, while 20 genes were clustered into one network with *ERBB2*, *PGAP3*, and *PNMT* demonstrating strong coexpression (**Supplementary Figure 4**). In small intestine terminal ileum, all 18 genes identified by TWAS show coexpression, in which *PGAP3*, *GSDMB*, *HLA-S*, *CCHCR1*, *VARS2*, and *KANSL1* are intensively coexpressed (**Supplementary Figure 4**). Therefore,

the coexpressed gene sets within corresponding tissues could support the result of IgG N-glycosylation TWAS analyses based on tissue enrichment by LDSC-SEG.

Phenome-Wide Association Study and Genetic Correlation Analysis

To identify other phenotypes which are likely to be associated or comorbid with IgG N-glycosylation, we conducted a pheWAS for each IgG N-glycosylation eQTL in the GWAS database based on a European population (41). Since all eQTLs are associated with IgG N-glycosylation, we chose to exclude and remove the duplicated phenotypes related to the same eQTL from the result list, in order to emphasize the remaining top 5 phenotypes ranked by p for each eQTL. In total, nearly 100 phenotypes were identified as significantly associated with these eQTLs, including anthropometric health measurements (weight, height, blood pressure, and blood cell count), immune and metabolic diseases (SLE, inflammatory bowel disease (IBD), rheumatoid arthritis (RA), primary sclerosing cholangitis (PSC), and type 2 diabetes (T2D)), and neurological and psychiatric disorders (Parkinson's disease (PD), schizophrenia, and bipolar disorder) (**Supplementary Table 7**).

To reconfirm the pheWAS results, we investigated the genetic correlations between these phenotypes using the most recent GWAS data from the UK Biobanks by Multi-marker Analysis of GenoMic Annotation (MAGMA), and SNP heritability, and genetic correlation with LDSC (41). Most of these disease-related phenotypes were implicated in previous GWAS studies (46–51). By analyzing the genes assigned to each significant SNP within a 1-kb window from both sides with default parameters (SNP-wise mean model) (52) and the gene set defined by MSigDB v.6.1 (53), the MAGMA results showed strong correlations between height, waist-hip ratio (WHR), systolic blood pressure (SBP), PD, and IBD with IgG N-glycosylation ($p < 2.5\text{E-}06$) (**Figure 6A**). Through the calculation of the SNP heritability and pairwise genetic correlations by LDSC (22), genetic correlations were calculated between the GWAS of disease-related phenotypes. The results showed strong positive correlations between IgG N-glycosylation, SBP, triglyceride cholesterol (TC), T2D, IBD, PSC, Crohn's disease (CD), and ulcerative colitis (UC), consistent with the above pheWAS results (**Figure 6B**).

DISCUSSION

In this study, we conducted a systematic transcriptome-wide association study, combining the analysis of LDSC-SEG and TWAS to gain insight into the tissue specificity and tissue-dependent genetic effect of IgG N-glycosylation, based on summary statistics of the most recent IgG N-glycosylation GWAS on 8,090 individuals of European ancestry. In so doing, we addressed fundamental questions regarding the heritable tissue enrichment of IgG N-glycosylation and constructed an atlas of tissue-dependent associations between genes and IgG N-glycan traits.

TABLE 2 | Significant pathways of TWAS genes identified through gene network analysis.

GO	Category	Description	p-value	Hits
hsa_M00075	KEGG pathway	N-Glycan biosynthesis, complex type	4.59E-06	FUT8 B4GALT1 MGAT3
R-HSA-975576	Reactome gene sets	N-Glycan antennae elongation in the medial/trans-Golgi	2.10E-05	FUT8 B4GALT1 MGAT3
R-HSA-948021	Reactome gene sets	Transport to the Golgi and subsequent modification	4.00E-05	FUT8 B4GALT1 MGAT3 KDEL2 COG7
hsa00510	KEGG pathway	N-Glycan biosynthesis	1.44E-04	FUT8 B4GALT1 MGAT3
R-HSA-446203	Reactome gene sets	Asparagine N-linked glycosylation	4.07E-04	FUT8 B4GALT1 MGAT3 KDEL2 COG7
GO:0006487	GO biological processes	Protein N-linked glycosylation	5.69E-04	FUT8 B4GALT1 MGAT3
GO:0043413	GO biological processes	Macromolecule glycosylation	2.08E-03	FUT8 B4GALT1 MGAT3 COG7
GO:0006486	GO biological processes	Protein glycosylation	2.08E-03	FUT8 B4GALT1 MGAT3 COG7
GO:0070085	GO biological processes	Glycosylation	2.41E-03	FUT8 B4GALT1 MGAT3 COG7
GO:0009101	GO biological processes	Glycoprotein biosynthetic process	5.97E-03	FUT8 B4GALT1 MGAT3 COG7
hsa05150	KEGG pathway	<i>Staphylococcus aureus</i> infection	5.51E-06	C4A C4B HLA-DMA HLA-DRA
hsa05330	KEGG pathway	Allograft rejection	6.69E-05	HLA-C HLA-DMA HLA-DRA
hsa05332	KEGG pathway	Graft-versus-host disease	8.42E-05	HLA-C HLA-DMA HLA-DRA
hsa04940	KEGG pathway	Type I diabetes mellitus	9.72E-05	HLA-C HLA-DMA HLA-DRA
hsa05322	KEGG pathway	Systemic lupus erythematosus	1.66E-04	C4A C4B HLA-DMA HLA-DRA
hsa05320	KEGG pathway	Autoimmune thyroid disease	1.82E-04	HLA-C HLA-DMA HLA-DRA
hsa05416	KEGG pathway	Viral myocarditis	2.50E-04	HLA-C HLA-DMA HLA-DRA
hsa05140	KEGG pathway	Leishmaniasis	4.69E-04	HLA-DMA HLA-DRA TAB1
hsa04612	KEGG pathway	Antigen processing and presentation	5.48E-04	HLA-C HLA-DMA HLA-DRA
hsa05168	KEGG pathway	Herpes simplex infection	5.83E-04	HLA-C HLA-DMA HLA-DRA TAB1
hsa05145	KEGG pathway	Toxoplasmosis	1.66E-03	HLA-DMA HLA-DRA TAB1
hsa05166	KEGG pathway	HTLV-I infection	1.94E-03	HLA-C HLA-DMA HLA-DRA WNT3
GO:0002250	GO biological processes	Adaptive immune response	2.68E-03	C4A C4B HLA-C HLA-DMA HLA-DRA MICB
hsa04514	KEGG pathway	Cell adhesion molecules (CAMs)	3.31E-03	HLA-C HLA-DMA HLA-DRA
GO:0002253	GO biological processes	Activation of immune response	3.75E-03	C4A C4B HLA-DRA MICB FLOT1 TAB1
hsa04145	KEGG pathway	Phagosome	4.00E-03	HLA-C HLA-DMA HLA-DRA
GO:0045807	GO biological processes	Positive regulation of endocytosis	4.00E-03	C4A C4B FLOT1
GO:0002478	GO biological processes	Antigen processing and presentation of exogenous peptide antigen	5.71E-03	HLA-C HLA-DMA HLA-DRA
GO:0002449	GO biological processes	Lymphocyte-mediated immunity	6.08E-03	C4A C4B HLA-C MICB
GO:0019884	GO biological processes	Antigen processing and presentation of exogenous antigen	6.36E-03	HLA-C HLA-DMA HLA-DRA
GO:0002460	GO biological processes	Adaptive immune response based on somatic recombination of immune receptors built from immunoglobulin	6.71E-03	C4A C4B HLA-C MICB
GO:0048002	GO biological processes	Antigen processing and presentation of peptide antigen	7.16E-03	HLA-C HLA-DMA HLA-DRA
hsa05169	KEGG pathway	Epstein-Barr virus infection	8.35E-03	HLA-C HLA-DRA TAB1
R-HSA-379724	Reactome gene sets	tRNA aminoacylation	9.05E-05	VARS VARS2 EARS2
GO:0006418	GO biological processes	tRNA aminoacylation for protein translation	1.11E-04	VARS VARS2 EARS2
GO:0043039	GO biological processes	tRNA aminoacylation	1.35E-04	VARS VARS2 EARS2
GO:0043038	GO biological processes	amino acid activation	1.44E-04	VARS VARS2 EARS2
hsa00970	KEGG pathway	Aminoacyl-tRNA biosynthesis	3.48E-04	VARS VARS2 EARS2
R-HSA-72766	Reactome gene sets	Translation	3.07E-03	RPL3 VARS VARS2 EARS2

(Continued)

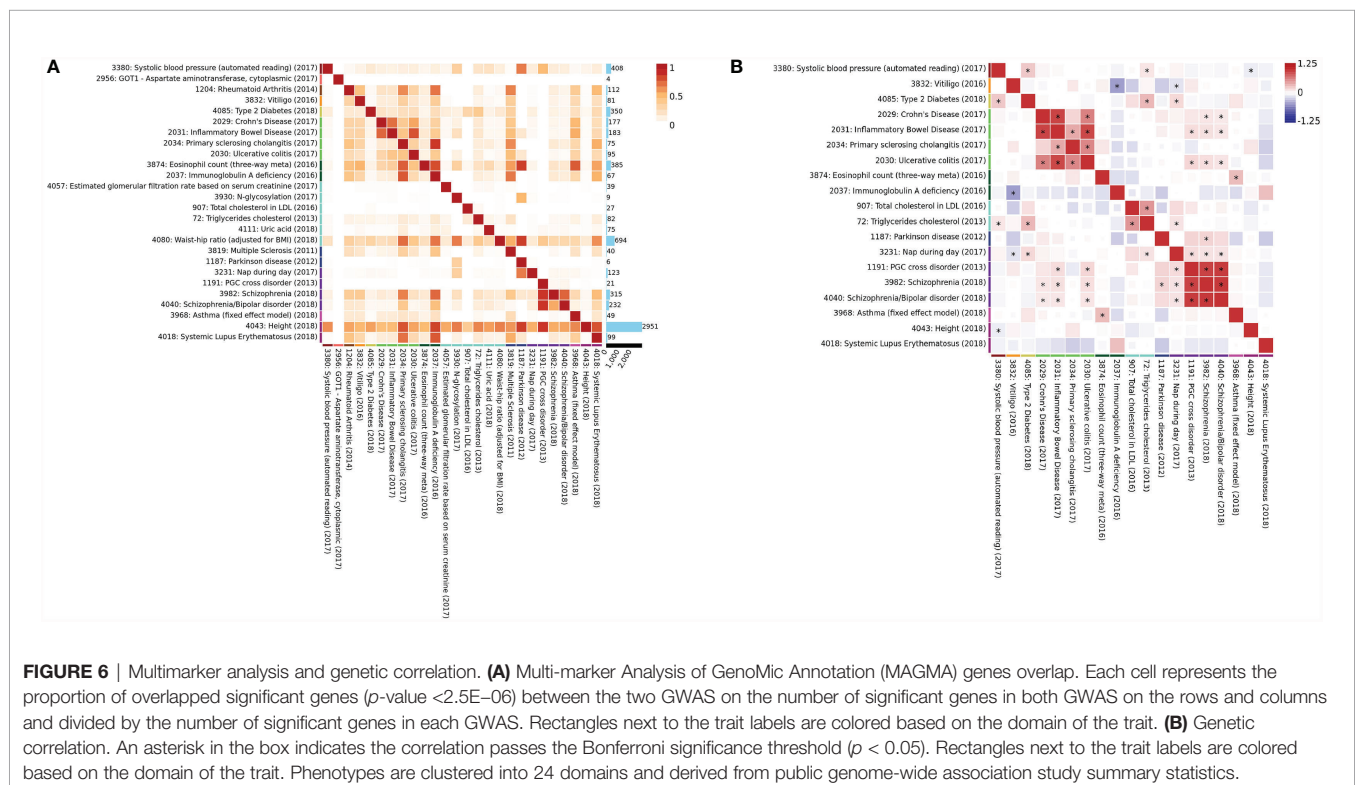
TABLE 2 | Continued

GO	Category	Description	p-value	Hits
GO:0006399	GO biological processes	tRNA metabolic process	7.47E-03	VARS VARS2 EARS2
GO:0055088	GO biological processes	Lipid homeostasis	3.79E-03	TM6SF2 APOM ORMDL3
GO:0006612	GO biological processes	Protein targeting to membrane	8.46E-03	ERBB2 RPL3 MIEF1

By the enrichment of 17 IgG N-GPs in 27 biologically relevant tissues in our study, we have obtained strong genetic evidence that most MALTs, e.g., skin, lung, breast mammary tissue, small intestine, esophagus muscularis, testis, and uterus, are enriched to specific IgG N-glycan traits (**Figure 2**). It has been established that the IgG secreting cells (i.e., plasma cells) mature from B lymphocytes and are translocated from primary lymphoid tissue (bone marrow) to secondary lymphoid tissue which consists of the lymph nodes, spleen and MALT for secreting IgG and initiating adaptive immune responses (14). However, previous studies measured the N-glycosylation of IgG in humans mainly isolated from plasma, obtaining the average profile of whole IgG N-glycome, and therefore a lack of information about the functionally relevant tissues. A wet experiment on laboratory animals provided evidence to support the assumption that IgG against commensal gut bacteria can be synthesized and deposited locally within MALTs in organ-cultured pig small intestinal mucosal explants (54).

Using IgG as a model glycoprotein, our study demonstrates the evidence of genetically regulated gene expression for the

tissue selectivity of protein N-glycosylation in eukaryotes. Eukaryotic N-glycosylation in the ER and Golgi apparatus is highly complicated, due to a variety of exoglycosidase and glycosyltransferase reactions. The tissue-selective manifestation of protein N-glycosylation has been observed in recent studies, e.g., between paired tumorigenic and adjacent nontumorigenic colon tissues in humans (55), and between sites within the same proteins from liver and brain tissues in the mouse (56). As a simple glycoprotein, IgG usually contains only one N-glycosylation site in the constant heavy chain region and the N-glycan moieties of IgG have no more than two antennae. But, in fact, hundreds of forms of glycans have been observed at this single N-glycosylation site. Due to the limitation of sampling from diverse human health tissues for N-glycosylation profiling, there is still a lack of evidence from the N-glycome level for the tissue specificity of IgG N-glycosylation. The results of tissue enrichment in our study have bridged the gap and exhibited tissue-selective manifestation for IgG N-glycosylation, leading to the next hypothesis that certain N-glycans of IgG may specifically be modified within some tissues and be affected by



tissue-specific environments. Consequently, the current study advances the knowledge of tissue specificity on human IgG N-glycosylation and in turn increases the statistical power for the following TWAS analysis of candidate gene prioritization (21).

In this current study, we demonstrated that the TWAS approach is able to discover more IgG N-glycosylation-related genes without any prior information. We identified 12 candidate genes in eight regions are in known susceptibility loci reported by previous IgG N-glycosylation GWAS (9–11). Furthermore, we discovered 43 genes at 10 novel regions and six known regions for the first time to be associated with IgG N-glycosylation. For the known genome loci, TWAS discovered more candidate genes whose expressions in specific tissue are likely related to IgG N-glycosylation by integrating GWAS signals with eQTL knowledge, for example, *C4A*, *C4B*, *CYP21A2*, and *GPANK1* in 6p21.33 for FA2G1S1 glycan (GP16) in skeletal muscle. In addition, TWAS explored candidate genes in novel genomic loci, e.g., *EVI5* in 1p22.1 and *PGAP3*, *ERBB2*, *PNMT*, and *GSDMA* in 17q12 for A2 glycan (GP2) in skeletal muscle. These results provided more genomic context, including candidate genes, regulatory variants, and relevant tissues for future functional studies of IgG N-glycosylation.

A gene expressed specifically in a tissue type or cell type usually reflects the biological processes in which the gene is involved and its biological functions (57). In the current study, we demonstrate that associations along IgG N-GP/SNP/gene expression in a tissue-specific SNP scenario appear to be dependent on using expression data derived from N-GP-enriched tissue. For instance, FA2G1S1 glycan (GP16) is positively associated with the expression of *PSORS1C2* in sun-exposed lower leg skin *via* a single eSNP rs1265099 ($Z = 5.24$, $p = 1.65E-07$) but is not associated with any other genes or tissues. *PSORS1C2* encodes a keratinocyte cornification-associated protein, which is specifically expressed in two skin tissue types evaluated by GTEx v7 (**Supplementary Figure 5**). The protein product of this gene plays a primary role in the terminal differentiation of keratinocytes (58). Recent studies have shown that *PSORS1C2* is strongly upregulated in peeling skin disease (59) and is also associated with autoimmune skin diseases including vitiligo (60) and psoriasis (61) by GWAS analyses. Also, aberrant IgG FA2G1S1 glycan (GP16) has been observed to be associated with SLE (62) and colorectal cancer (63). Our finding that this IgG FA2G1S1 glycan (GP16) genetic predisposition (rs1265099) may have tissue-specific effects on the expression of *PSORS1C2* within skin tissue thus supports the hypothesis that skin tissue can contribute to the regulation of IgG FA2G1S1 glycan biosynthesis and/or have the potential to serve as a proxy for several skin-related autoimmune diseases. In total, four genes (*PSORS1C2*, *HLA-DRA*, *APOM*, and *SAPCD1*) were significant in sun-exposed lower leg skin TWAS models. Broadly, half of the significant genes show tissue specificity on IgG N-glycosylation in other TWAS tissue models. These tissue-specific candidate gene sets are a promising source for further investigations into genetic effects underlying the interactions between highly diverse IgG N-GPs and tissue-specific genetic expression within corresponding tissues.

In contrast, genetic variants that affect gene expression levels in multiple tissues are more likely to affect multiple complex traits

(64). The pleiotropic gene findings in this study can confirm that IgG N-glycosylation TWAS genes expressed in multiple tissues are more likely to have a wide range of downstream phenotypic consequences (i.e., diverse N-glycosylation modification). As an example in the present study, 19 genes are identified as IgG N-glycosylation candidate genes in the small intestine terminal ileum with 10 pleiotropic and 9 tissue-specific genes. Within the ten pleiotropic genes, *C4A*, *FLOT1*, *HLA-C*, and *WNT3* perform important roles in N-glycosylation-related biological processes, while the remaining nine tissue-specific genes are associated with intestine-related functions, e.g., *FLOT1* is responsible for encoding flotillin 1 and is ubiquitously expressed across all tissue types evaluated by GTEx v7 (**Supplementary Figure 6**). Flotillin 1 localizes to the caveolae and plays a role in several super pathways, e.g., the angiopoietin-like protein 8 regulatory pathway, cytoskeletal signaling, regulation of lipid metabolism and beta-adrenergic signaling. As a tissue-specific gene, *GSDMB* was reported to be expressed exclusively in the epithelium of the gastrointestinal tract in a highly tissue-specific manner (65). *SLC22A5* was reported as being responsible for carnitine transport across apical membranes of intestinal epithelial cells (66). Pleiotropic genes and eSNPs account for almost half of the other significant TWAS hits. Most of these hits have previously been reported in the three core N-glycosylation-related biological processes, including N-glycosylation, immune response, and protein translation, while tissue-specific genes are mainly annotated as being involved in the physiological activities of corresponding tissues. This result partially explains why plasma IgG N-glycosylation demonstrates a relatively stable holistic pattern on each monosaccharide glycan although based on such complicated branching patterns. The pleiotropic candidate genes maintain the primary patterns of N-glycosylation in most related tissues for a house-keeping N-glycosylated level, whereas the tissue-dependent candidate genes regulate tissue-specific IgG N-glycan patterns to adopt local inflammation, maintaining homeostasis during physiology and pathophysiology processes.

By the evidence of the coassociations among eSNP and IgG N-GPs, our results shed considerable light on the regulatory mechanism of the equilibrium between some pairs of IgG N-glycosylation. For example, in terms of Z -score in TWAS results, rs761830 simultaneously correlated with A2 glycan (GP2) ($Z = -11.70$, $p = 1.34E-31$) and FA2G2 glycan (GP14) ($Z = 4.52$, $p = 6.22E-06$) and linked them with *FUT8* gene in skeletal muscle in two reverse directions (**Supplementary Table 2** and **Figure 2**). This linked association provides two layers of meaning. Firstly, in IgG N-glycosylation GWAS statistics, the effect allele (rs761830-A) at the *FUT8* locus is associated with a decreased level of GP2 (rs761830, $p = 4.08E-38$) but an increased level of GP14 (rs761830, $p = 6.83E-06$). The finding indicates that these two GPs share identical heritability, being associated antagonistically in the IgG N-glycome. Conversely, increasing A2 glycan (GP2) and decreasing FA2G2 glycan (GP14) are consistent with the changing of certain IgG N-GPs which have been observed in association studies on chronic diseases (**Supplementary Table 8**), such as dyslipidemia (DL) (67), SLE (62), RA (68), and chronic kidney disease (CKD) (69). Secondly, eQTL statistics of GTEx v7

shows the effect allele rs761830-A is responsible for increased changes in gene expression of *FUT8* in skeletal muscle (rs761830, $p = 2.60 \times 10^{-6}$). Hence, the genetic predisposition tagged by SNP rs761830 whose allelic regulation on the expression of *FUT8* gene in skeletal muscle may contribute to the equilibrium of IgG N-GP regulations, such as the above-mentioned two types of N-GPs.

By GO pathway enrichment and pheWAS investigation, our study provides additional evidence for the involvement of IgG N-glycosylation in several IgG N-GP-related diseases. Since the establishment of UPLC-based high-throughput IgG N-glycomic profiling (70), certain specific IgG N-GPs differed significantly from the average patterns and were indicative of clinical conditions, such as the level of monosialylated glycans which was most strongly correlated with MetS-related risk factors, especially with systolic blood pressure (SBP) (71). Further research in other independent cohorts confirmed the existence of a similar relationship between selective IgG N-glycan patterns and signs of autoimmunity, e.g., IBD (49, 72), SLE (62), and RA (73), neurological disorders, e.g., Parkinson's disease (4) and dementia (74), and vascular diseases, e.g., ischemic stroke (75) and cancers (63), as previously mentioned (**Supplementary Table S7**). The consistency of candidate genes, combined with the coexpression of IgG N-glycosylation-related genes within multiple tissues, GO enrichment gene sets, and the pheWAS investigation on TWAS eSNPs implies that IgG N-glycosylation may be the mediated phenotype sharing genetic correlations with its related diseases. The allelic regulatory genetic variants of IgG N-glycosylation within certain tissues may be involved in the pathophysiological processes of its related diseases *via* regulation of their target genes in tissue-specific modes.

Efforts to generate ever-larger sets of tissue-specific genetic effects data will facilitate data mining opportunities for investigating the regulatory mechanisms underlying trait and gene associations (76). Although the current study has been restricted to the use of eQTL data and GWAS data generated from independent subpopulations of European ancestry with limited sample sizes, future functional genomic endeavors of tissue-specific regulation on IgG N-glycosylation will benefit from a larger replication cohort simultaneously having IgG N-glycosylation features, genotype data, and gene expression profiles from different tissues. A recent study showed that targeted sialic glycan degradation reinforces the anticancer immune response in an animal experiment as evidenced by the sialylation effect on the surface of cancer cells (77). The construction of *in vitro* and *in vivo* models for IgG N-glycosylation are therefore urgently needed for providing more solid experiment-based evidence to confirm the hypothesis generated from the current study. We also note that our study utilized eQTLs as genetic predictors of gene expression. Nevertheless, pleiotropic effects on both gene expression and phenotype could not be ruled out without further analyses. Probabilistic fine-mapping approaches and transcription factor enrichment analyses (78–80) can positively exclude spurious results. Furthermore, a gene may have regulatory characteristics other than *cis*-regulation, e.g., *trans*-regulation, or that does not pass through eQTLs, but still could have downstream effects on expression (81). In theory, beyond the current knowledge of

regulatory models, there could be other novel regulatory elements and underlining mechanisms. However, based on allelic *cis*-regulation, we have been able to successfully prioritize a potential causal gene set of 55 genes for IgG N-glycosylation and its related complex traits and diseases.

In summary, we have performed the first comprehensive analysis so far to identify the most relevant tissues for IgG N-glycosylation and to detect a large number of genetic variants which may regulate their target genes and further contribute to IgG N-glycosylation within corresponding tissues. This knowledge provides a starting point for further mechanistic work on IgG N-glycosylation, which would advance our understanding of IgG N-glycosylation biology and guide the design of future functional studies to explore the specific variants and the heritable regulation of IgG N-glycosylation. More importantly, our approach of combining LDSC-SEG and TWAS is widely applicable to complex traits for which GWAS summary statistics are available and helps our understanding of the molecular basis of the trait at multiple omics levels.

DATA AVAILABILITY STATEMENT

IgG N-glycosylation GWAS summary statistics are available at: <https://datashare.is.ed.ac.uk/handle/10283/3238/>. Hapmap3 SNPs from 1000 Genomes data are available at: <ftp://ftp.1000genomes.ebi.ac.uk/vol1/ftp/release/20130502/>. LDSC-SEG software and reference are available at: <https://alkesgroup.broadinstitute.org/LDSCORE/>. FUSION software and reference LD are available at: <http://gusevlab.org/projects/fusion/>. For LDSC-SEG, see <https://github.com/bulik/ldsc>. For FUSION, see <http://gusevlab.org/projects/fusion/>. For GTEx portal, see <http://gtexportal.org/>. For coloc, see <https://cran.r-project.org/web/packages/coloc/index.html>. For HaploReg v4.1, see <https://pubs.broadinstitute.org/mammals/haploreg/haploreg.php>. For STRING, see <http://string-db.org/>. For GeneNetwork v2.0 see <https://genenetwork.nl/>. For GWASAtlas, see <https://atlas.ctglab.nl/>.

AUTHOR CONTRIBUTIONS

WW conceived the design of this study. XL, HW, and YZ performed the statistical and computational analyses. WC, HH, and MS assisted with data management. WW and XL wrote the manuscript. YW, ML, XG, XT, and JH supervised the project and oversaw the manuscript. All authors contributed to the article and approved the submitted version.

FUNDING

This work was supported by an Australia-China International Collaborative grant (NHMRC APP1112767-NSFC 81561128020), National Natural Science Foundation of China grant (NSFC 81773527 & 81573215), China Scholarship Council grant (CSC-

201708110200), and Bioyong Industry Engagement Scholarship (G1002655) and School of Medical and Health Sciences Seed Grant Scheme 2021 (27223) from Edith Cowan University.

ACKNOWLEDGMENTS

The authors appreciate the GTEx and GWAS consortia for making their summary statistics publicly available for the

benefit of this study. We thank Prof. Alan Bittles AM, PhD and FRSM, for comments on the manuscript.

SUPPLEMENTARY MATERIAL

The Supplementary Material for this article can be found online at: <https://www.frontiersin.org/articles/10.3389/fimmu.2021.741705/full#supplementary-material>

REFERENCES

- Ohtsubo K, Marth JD. Glycosylation in Cellular Mechanisms of Health and Disease. *Cell* (2006) 126(5):855–67. doi: 10.1016/j.cell.2006.08.019
- Wang Y, Adua E, Russell A, Roberts P, Ge S, Zeng Q, et al. Glycomics and its Application Potential in Precision Medicine. *Science/AAAS Wahington DC* (2016) 354(6319):36–9. doi: 10.1126/science.354.6319.1601-b
- Helenius A, Aebi M. Intracellular Functions of N-Linked Glycans. *Science* (2001) 291(5512):2364–9. doi: 10.1126/science.291.5512.2364
- Russell AC, Šimurina M, Garcia M, Novokmet M, Wang Y, Rudan I, et al. The N-Glycosylation of Immunoglobulin G as a Novel Biomarker of Parkinson's Disease. *Glycobiology* (2017) 27(5):501–10. doi: 10.1093/glycob/cwx022
- Seeling M, Bruckner C, Nimmerjahn F. Differential Antibody Glycosylation in Autoimmunity: Sweet Biomarker or Modulator of Disease Activity? *Nat Rev Rheumatol* (2017) 13(10):621–30. doi: 10.1038/nrrheum.2017.146
- Gochee CF, Monica T. Environmental Effects on Protein Glycosylation. *Biotechnology* (1990) 8(5):421–7. doi: 10.1038/nbt0590-421
- Schachter H. The 'Yellow Brick Road' to Branched Complex N-Glycans. *Glycobiology* (1991) 1(5):453–61. doi: 10.1093/glycob/1.5.453
- Narimatsu H. Construction of a Human Glycogene Library and Comprehensive Functional Analysis. *Glycoconj J* (2004) 21(1-2):17–24. doi: 10.1023/b:Glyc.0000043742.99482.01
- Lau G, Huffman JE, Pučić M, Zgaga L, Adamczyk B, Mužinić A, et al. Loci Associated With N-Glycosylation of Human Immunoglobulin G Show Pleiotropy With Autoimmune Diseases and Haematological Cancers. *PLoS Genet* (2013) 9(1):e1003225. doi: 10.1371/journal.pgen.1003225
- Shen X, Klarić L, Sharapov S, Mangino M, Ning Z, Wu D, et al. Multivariate Discovery and Replication of Five Novel Loci Associated With Immunoglobulin G N-Glycosylation. *Nat Commun* (2017) 8(1):447. doi: 10.1038/s41467-017-00453-3
- Klarić L, Tsepilov YA, Stanton CM, Mangino M, Sikka TT, Esko T, et al. Glycosylation of Immunoglobulin G is Regulated by a Large Network of Genes Pleiotropic With Inflammatory Diseases. *Sci Adv* (2020) 6(8):eaax0301. doi: 10.1126/sciadv.aax0301
- Wahl A, van den Akker E, Klaric L, Štambuk J, Benedetti E, Plomp R, et al. Genome-Wide Association Study on Immunoglobulin G Glycosylation Patterns. *Front Immunol* (2018) 9:277(277). doi: 10.3389/fimmu.2018.00277
- Tam V, Patel N, Turcotte M, Bossé Y, Paré G, Meyre D. Benefits and Limitations of Genome-Wide Association Studies. *Nat Rev Genet* (2019) 20(8):467–84. doi: 10.1038/s41576-019-0127-1
- Delves PJ, Martin SJ, Burton DR, Roitt IM. *Roitt's Essential Immunology*. Chichester, West Sussex: John Wiley & Sons (2017).
- The GTEx Consortium. Genetic Effects on Gene Expression Across Human Tissues. *Nature* (2017) 550(7675):204–13. doi: 10.1038/nature24277
- Finucane HK, Reshef YA, Anttila V, Slowikowski K, Gusev A, Byrnes A, et al. Heritability Enrichment of Specifically Expressed Genes Identifies Disease-Relevant Tissues and Cell Types. *Nat Genet* (2018) 50(4):621–9. doi: 10.1038/s41588-018-0081-4
- Gusev A, Ko A, Shi H, Bhatia G, Chung W, Penninx BWJH, et al. Integrative Approaches for Large-Scale Transcriptome-Wide Association Studies. *Nat Genet* (2016) 48(3):245–52. doi: 10.1038/ng.3506
- The GTEx Consortium. The Genotype-Tissue Expression (GTEx) Pilot Analysis: Multitissue Gene Regulation in Humans. *Science* (2015) 348(6235):648–60. doi: 10.1126/science.1262110
- Buniello A, MacArthur JAL, Cerezo M, Harris LW, Hayhurst J, Malangone C, et al. The NHGRI-EBI GWAS Catalog of Published Genome-Wide Association Studies, Targeted Arrays and Summary Statistics 2019. *Nucleic Acids Res* (2019) 47(D1):D1005–12. doi: 10.1093/nar/gky1120
- Royle L, Campbell MP, Radcliffe CM, White DM, Harvey DJ, Abrahams JL, et al. HPLC-Based Analysis of Serum N-Glycans on a 96-Well Plate Platform With Dedicated Database Software. *Anal Biochem* (2008) 376(1):1–12. doi: 10.1016/j.ab.2007.12.012
- Wainberg M, Sinnott-Armstrong N, Mancuso N, Barbeira AN, Knowles DA, Golan D, et al. Opportunities and Challenges for Transcriptome-Wide Association Studies. *Nat Genet* (2019) 51(4):592–9. doi: 10.1038/s41588-019-0385-z
- Bulik-Sullivan BK, Loh P-R, Finucane HK, Ripke S, Yang J, Schizophrenia Working Group of the Psychiatric Genomics C, et al. LD Score Regression Distinguishes Confounding From Polygenicity in Genome-Wide Association Studies. *Nat Genet* (2015) 47(3):291–5. doi: 10.1038/ng.3211
- Schaid DJ, Chen W, Larson NB. From Genome-Wide Associations to Candidate Causal Variants by Statistical Fine-Mapping. *Nat Rev Genet* (2018) 19(8):491–504. doi: 10.1038/s41576-018-0016-z
- Barbeira AN, Dickinson SP, Bonazzola R, Zheng J, Wheeler HE, Torres JM, et al. Exploring the Phenotypic Consequences of Tissue Specific Gene Expression Variation Inferred From GWAS Summary Statistics. *Nat Commun* (2018) 9(1):1825. doi: 10.1038/s41467-018-03621-1
- Gamazon ER, Wheeler HE, Shah KP, Mozaffari SV, Aquino-Michaels K, Carroll RJ, et al. A Gene-Based Association Method for Mapping Traits Using Reference Transcriptome Data. *Nat Genet* (2015) 47(9):1091–8. doi: 10.1038/ng.3367
- Hormozdiari F, van de Bunt M, Segrè Ayellet V, Li X, Joo Jong Wha J, Bilow M, et al. Colocalization of GWAS and eQTL Signals Detects Target Genes. *Am J Hum Genet* (2016) 99(6):1245–60. doi: 10.1016/j.ajhg.2016.10.003
- Zhu Z, Zhang F, Hu H, Bakshi A, Robinson MR, Powell JE, et al. Integration of Summary Data From GWAS and eQTL Studies Predicts Complex Trait Gene Targets. *Nat Genet* (2016) 48(5):481–7. doi: 10.1038/ng.3538
- Li YI, Wong G, Humphrey J, Raj T. Prioritizing Parkinson's Disease Genes Using Population-Scale Transcriptomic Data. *Nat Commun* (2019) 10(1):994. doi: 10.1038/s41467-019-08912-9
- Gusev A, Mancuso N, Won H, Kousi M, Finucane HK, Reshef Y, et al. Transcriptome-Wide Association Study of Schizophrenia and Chromatin Activity Yields Mechanistic Disease Insights. *Nat Genet* (2018) 50(4):538–48. doi: 10.1038/s41588-018-0092-1
- Gandal MJ, Zhang P, Hadjimechael E, Walker RL, Chen C, Liu S, et al. Transcriptome-Wide Isoform-Level Dysregulation in ASD, Schizophrenia, and Bipolar Disorder. *Science* (2018) 362(6420):eaat8127. doi: 10.1126/science.aat8127
- Liao C, Laporte AD, Spiegelman D, Akcimen F, Joobor R, Dion PA, et al. Transcriptome-Wide Association Study of Attention Deficit Hyperactivity Disorder Identifies Associated Genes and Phenotypes. *Nat Commun* (2019) 10(1):4450. doi: 10.1038/s41467-019-12450-9
- Gusev A, Lawrenson K, Lin X, Lyra PC, Kar S, Vavra KC, et al. A Transcriptome-Wide Association Study of High-Grade Serous Epithelial Ovarian Cancer Identifies New Susceptibility Genes and Splice Variants. *Nat Genet* (2019) 51(5):815–23. doi: 10.1038/s41588-019-0395-x
- Zhong J, Jermusyk A, Wu L, Hoskins JW, Collins I, Mocci E, et al. A Transcriptome-Wide Association Study (TWAS) Identifies Novel Candidate

- Susceptibility Genes for Pancreatic Cancer. *J Natl Cancer Inst* (2020) 112 (10):1003–12. doi: 10.1093/jnci/djz246
34. Wu L, Wang J, Cai Q, Cavazos TB, Emami NC, Long J, et al. Identification of Novel Susceptibility Loci and Genes for Prostate Cancer Risk: A Transcriptome-Wide Association Study in Over 140,000 European Descendants. *Cancer Res* (2019) 79(13):3192–204. doi: 10.1158/0008-5472.Can-18-3536
 35. Wu L, Shi W, Long J, Guo X, Michailidou K, Beesley J, et al. A Transcriptome-Wide Association Study of 229,000 Women Identifies New Candidate Susceptibility Genes for Breast Cancer. *Nat Genet* (2018) 50(7):968–78. doi: 10.1038/s41588-018-0132-x
 36. Mancuso N, Gayther S, Gusev A, Zheng W, Penney KL, Kote-Jarai Z, et al. Large-Scale Transcriptome-Wide Association Study Identifies New Prostate Cancer Risk Regions. *Nat Commun* (2018) 9(1):4079. doi: 10.1038/s41467-018-06302-1
 37. Giambartolomei C, Vukcevic D, Schadt EE, Franke L, Hingorani AD, Wallace C, et al. Bayesian Test for Colocalisation Between Pairs of Genetic Association Studies Using Summary Statistics. *PLoS Genet* (2014) 10(5):e1004383. doi: 10.1371/journal.pgen.1004383
 38. Ward LD, Kellis M. HaploReg: A Resource for Exploring Chromatin States, Conservation, and Regulatory Motif Alterations Within Sets of Genetically Linked Variants. *Nucleic Acids Res* (2012) 40(Database issue):D930–4. doi: 10.1093/nar/gkr917
 39. Szklarczyk D, Gable AL, Lyon D, Junge A, Wyder S, Huerta-Cepas J, et al. STRING V11: Protein–Protein Association Networks With Increased Coverage, Supporting Functional Discovery in Genome-Wide Experimental Datasets. *Nucleic Acids Res* (2018) 47(D1):D607–13. doi: 10.1093/nar/gky1131
 40. Deelen P, van Dam S, Herkert JC, Karjalainen JM, Brugge H, Abbott KM, et al. Improving the Diagnostic Yield of Exome Sequencing by Predicting Gene-Phenotype Associations Using Large-Scale Gene Expression Analysis. *Nat Commun* (2019) 10(1):2837. doi: 10.1038/s41467-019-10649-4
 41. Watanabe K, Stringer S, Frei O, Umičević Mirkov M, de Leeuw C, Polderman TJC, et al. A Global Overview of Pleiotropy and Genetic Architecture in Complex Traits. *Nat Genet* (2019) 51(9):1339–48. doi: 10.1038/s41588-019-0481-0
 42. Zhou Y, Zhou B, Pache L, Chang M, Khodabakhshi AH, Tanaseichuk O, et al. Metascape Provides a Biologist-Oriented Resource for the Analysis of Systems-Level Datasets. *Nat Commun* (2019) 10(1):1523. doi: 10.1038/s41467-019-09234-6
 43. The ENCODE Project Consortium. An Integrated Encyclopedia of DNA Elements in the Human Genome. *Nature* (2012) 489(7414):57–74. doi: 10.1038/nature11247
 44. Schwarz F, Aebl M. Mechanisms and Principles of N-Linked Protein Glycosylation. *Curr Opin Struct Biol* (2011) 21(5):576–82. doi: 10.1016/j.sbi.2011.08.005
 45. Aebl M, Bernasconi R, Clerc S, Molinari M. N-Glycan Structures: Recognition and Processing in the ER. *Trends Biochem Sci* (2010) 35(2):74–82. doi: 10.1016/j.tibs.2009.10.001
 46. Warren HR, Evangelou E, Cabrera CP, Gao H, Ren M, Mifsud B, et al. Genome-Wide Association Analysis Identifies Novel Blood Pressure Loci and Offers Biological Insights Into Cardiovascular Risk. *Nat Genet* (2017) 49 (3):403–15. doi: 10.1038/ng.3768
 47. Keller MF, Saad M, Bras J, Bettella F, Nicolaou N, Simon-Sanchez J, et al. Using Genome-Wide Complex Trait Analysis to Quantify 'Missing Heritability' in Parkinson's Disease. *Hum Mol Genet* (2012) 21(22):4996–5009. doi: 10.1093/hmg/dd335
 48. Pulit SL, Stoneman C, Morris AP, Wood AR, Glastonbury CA, Tyrrell J, et al. Meta-Analysis of Genome-Wide Association Studies for Body Fat Distribution in 694 649 Individuals of European Ancestry. *Hum Mol Genet* (2019) 28(1):166–74. doi: 10.1093/hmg/ddy327
 49. de Lange KM, Moutsianas L, Lee JC, Lamb CA, Luo Y, Kennedy NA, et al. Genome-Wide Association Study Implicates Immune Activation of Multiple Integrin Genes in Inflammatory Bowel Disease. *Nat Genet* (2017) 49(2):256–61. doi: 10.1038/ng.3760
 50. Julia A, Lopez-Longo FJ, Perez Venegas JJ, Bonas-Guarch S, Olive A, Andreu JL, et al. Genome-Wide Association Study Meta-Analysis Identifies Five New Loci for Systemic Lupus Erythematosus. *Arthritis Res Ther* (2018) 20(1):100. doi: 10.1186/s13075-018-1604-1
 51. Mahajan A, Taliun D, Thurner M, Robertson NR, Torres JM, Rayner NW, et al. Fine-Mapping Type 2 Diabetes Loci to Single-Variant Resolution Using High-Density Imputation and Islet-Specific Epigenome Maps. *Nat Genet* (2018) 50(11):1505–13. doi: 10.1038/s41588-018-0241-6
 52. de Leeuw CA, Mooij JM, Heskes T, Posthuma D. MAGMA: Generalized Gene-Set Analysis of GWAS Data. *PLoS Comp Biol* (2015) 11(4):e1004219. doi: 10.1371/journal.pcbi.1004219
 53. Liberzon A, Subramanian A, Pinchback R, Thorvaldsdóttir H, Tamayo P, Mesirov JP. Molecular Signatures Database (MSigDB) 3.0. *Bioinformatics* (2011) 27(12):1739–40. doi: 10.1093/bioinformatics/btr260
 54. Hansen GH, Niels-Christiansen L-L, Immerdal L, Danielsen EM. Antibodies in the Small Intestine: Mucosal Synthesis and Deposition of Anti-Glycosyl IgA, IgM, and IgG in the Enterocyte Brush Border. *Am J Physiol Gastrointest Liver Physiol* (2006) 291(1):G82–90. doi: 10.1152/ajpgi.00021.2006
 55. Sethi MK, Kim H, Park CK, Baker MS, Paik YK, Packer NH, et al. In-Depth N-Glycome Profiling of Paired Colorectal Cancer and non-Tumorigenic Tissues Reveals Cancer-, Stage- and EGFR-Specific Protein N-Glycosylation. *Glycobiology* (2015) 25(10):1064–78. doi: 10.1093/glycob/cwv042
 56. Medzihradsky KF, Kaasik K, Chalkley RJ. Tissue-Specific Glycosylation at the Glycopeptide Level. *Mol Cell Proteomics* (2015) 14(8):2103–10. doi: 10.1074/mcp.M115.050393
 57. Liu X, Yu X, Zack DJ, Zhu H, Qian J. TiGER: A Database for Tissue-Specific Gene Expression and Regulation. *BMC Bioinformatics* (2008) 9(1):271. doi: 10.1186/1471-2105-9-271
 58. Abbas Zadeh S, Mlitz V, Lachner J, Golabi B, Mildner M, Pammer J, et al. Phylogenetic Profiling and Gene Expression Studies Implicate a Primary Role of PSORS1C2 in Terminal Differentiation of Keratinocytes. *Exp Dermatol* (2017) 26(4):352–8. doi: 10.1111/exd.13272
 59. Wada T, Matsuda Y, Muraoka M, Toma T, Takehara K, Fujimoto M, et al. Alu-Mediated Large Deletion of the CDSN Gene as a Cause of Peeling Skin Disease. *Clin Genet* (2014) 86(4):383–6. doi: 10.1111/cge.12294
 60. Jin Y, Andersen G, Yorgov D, Ferrara TM, Ben S, Brownson KM, et al. Genome-Wide Association Studies of Autoimmune Vitiligo Identify 23 New Risk Loci and Highlight Key Pathways and Regulatory Variants. *Nat Genet* (2016) 48(11):1418–24. doi: 10.1038/ng.3680
 61. Aterido A, Julià A, Ferrándiz C, Puig L, Fonseca E, Fernández-López E, et al. Genome-Wide Pathway Analysis Identifies Genetic Pathways Associated With Psoriasis. *J Invest Dermatol* (2016) 136(3):593–602. doi: 10.1016/j.jid.2015.11.026
 62. Vuckovic F, Kristic J, Gudelj I, Teruel M, Keser T, Pezer M, et al. Association of Systemic Lupus Erythematosus With Decreased Immunosuppressive Potential of the IgG Glycome. *Arthritis Rheumatol* (2015) 67(11):2978–89. doi: 10.1002/art.39273
 63. Vuckovic F, Theodoratou E, Thaci K, Timofeeva M, Vojta A, Stambuk J, et al. IgG Glycome in Colorectal Cancer. *Clin Cancer Res* (2016) 22(12):3078–86. doi: 10.1158/1078-0432.Ccr-15-1867
 64. Richardson TG, Hemani G, Gaunt TR, Relton CL, Davey Smith G. A Transcriptome-Wide Mendelian Randomization Study to Uncover Tissue-Dependent Regulatory Mechanisms Across the Human Phenome. *Nat Commun* (2020) 11(1):185. doi: 10.1038/s41467-019-13921-9
 65. Tamura M, Tanaka S, Fujii T, Aoki A, Komiyama H, Ezawa K, et al. Members of a Novel Gene Family, Gsdm, are Expressed Exclusively in the Epithelium of the Skin and Gastrointestinal Tract in a Highly Tissue-Specific Manner. *Genomics* (2007) 89(5):618–29. doi: 10.1016/j.ygeno.2007.01.003
 66. Kato Y, Sugiura M, Sugiura T, Wakayama T, Kubo Y, Kobayashi D, et al. Organic Cation/Carnitine Transporter OCTN2 (Slc22a5) is Responsible for Carnitine Transport Across Apical Membranes of Small Intestinal Epithelial Cells in Mouse. *Mol Pharmacol* (2006) 70(3):829–37. doi: 10.1124/mol.106.024158
 67. Liu D, Chu X, Wang H, Dong J, Ge S-Q, Zhao Z-Y, et al. The Changes of Immunoglobulin G N-Glycosylation in Blood Lipids and Dyslipidaemia. *J Transl Med* (2018) 16(1):235. doi: 10.1186/s12967-018-1616-2
 68. Sebastian A, Alzain MA, Asweto CO, Song H, Cui L, Yu X, et al. Glycan Biomarkers for Rheumatoid Arthritis and its Remission Status in Han Chinese Patients. *OMICS* (2016) 20(6):343–51. doi: 10.1089/omi.2016.0050
 69. Barrios C, Zierer J, Gudelj I, Štambuk J, Ugrina I, Rodríguez E, et al. Glycosylation Profile of IgG in Moderate Kidney Dysfunction. *J Am Soc Nephrol* (2016) 27(3):933–41. doi: 10.1681/ASN.2015010109
 70. Pučić M, Knežević N, Vidić J, Adamczyk B, Novokmet M, Polašek O, et al. High Throughput Isolation and Glycosylation Analysis of IgG-variability and

- Heritability of the IgG Glycome in Three Isolated Human Populations. *Mol Cell Proteomics* (2011) 10(10):M111. 010090. doi: 10.1074/mcp.M111.010090
71. Wang Y, Klaric L, Yu X, Thaqi K, Dong J, Novokmet M, et al. The Association Between Glycosylation of Immunoglobulin G and Hypertension: A Multiple Ethnic Cross-Sectional Study. *Medicine (Baltimore)* (2016) 95(17):e3379. doi: 10.1097/md.00000000000003379
 72. Trbojević Akmačić I, Ventham NT, Theodoratou E, Vučković F, Kennedy NA, Krištić J, et al. Inflammatory Bowel Disease Associates With Proinflammatory Potential of the Immunoglobulin G Glycome. *Inflamm Bowel Dis* (2015) 21(6):1237–47. doi: 10.1097/MIB.0000000000000372
 73. Gudelić I, Lauc G, Pezer M. Immunoglobulin G Glycosylation in Aging and Diseases. *Cell Immunol* (2018) 333:65–79. doi: 10.1016/j.cellimm.2018.07.009
 74. Zhang X, Yuan H, Lyu J, Meng X, Tian Q, Li Y, et al. Association of Dementia With Immunoglobulin G N-Glycans in a Chinese Han Population. *NPJ Aging Mech Dis* (2021) 7(1):3. doi: 10.1038/s41514-021-00055-w
 75. Liu D, Zhao Z, Wang A, Ge S, Wang H, Zhang X, et al. Ischemic Stroke is Associated With the Pro-Inflammatory Potential of N-Glycosylated Immunoglobulin G. *J Neuroinflamm* (2018) 15(1):123. doi: 10.1186/s12974-018-1161-1
 76. The GTEx Consortium. The GTEx Consortium Atlas of Genetic Regulatory Effects Across Human Tissues. *Science* (2020) 369(6509):1318–30. doi: 10.1126/science.aaz1776
 77. Gray MA, Stanczak MA, Mantuano NR, Xiao H, Pijnenborg JFA, Malaker SA, et al. Targeted Glycan Degradation Potentiates the Anticancer Immune Response *In Vivo*. *Nat Chem Biol* (2020) 16(12):1376–84. doi: 10.1038/s41589-020-0622-x
 78. van de Bunt M, Cortes A, Consortium I, Brown MA, Morris AP, McCarthy MI. Evaluating the Performance of Fine-Mapping Strategies at Common Variant GWAS Loci. *PLoS Genet* (2015) 11(9):e1005535. doi: 10.1371/journal.pgen.1005535
 79. Benner C, Spencer CC, Havulinna AS, Salomaa V, Ripatti S, Pirinen M. FINEMAP: Efficient Variable Selection Using Summary Data From Genome-Wide Association Studies. *Bioinformatics* (2016) 32(10):1493–501. doi: 10.1093/bioinformatics/btw018
 80. Mancuso N, Freund MK, Johnson R, Shi H, Kichaev G, Gusev A, et al. Probabilistic Fine-Mapping of Transcriptome-Wide Association Studies. *Nat Genet* (2019) 51(4):675–82. doi: 10.1038/s41588-019-0367-1
 81. Vösa U, Claringbould A, Westra HJ, Bonder MJ, Deelen P, Zeng B, et al. Large-Scale Cis- and trans-eQTL Analyses Identify Thousands of Genetic Loci and Polygenic Scores That Regulate Blood Gene Expression. *Nat Genet* (2021) 53(9):1300–10. doi: 10.1038/s41588-021-00913-z

Conflict of Interest: YZ was employed by the company Beijing Lucidus Bioinformation Technology Co., Ltd.

The remaining authors declare that the research was conducted in the absence of any commercial or financial relationships that could be construed as a potential conflict of interest.

Publisher's Note: All claims expressed in this article are solely those of the authors and do not necessarily represent those of their affiliated organizations, or those of the publisher, the editors and the reviewers. Any product that may be evaluated in this article, or claim that may be made by its manufacturer, is not guaranteed or endorsed by the publisher.

Copyright © 2021 Li, Wang, Zhu, Cao, Song, Wang, Hou, Lang, Guo, Tan, Han and Wang. This is an open-access article distributed under the terms of the Creative Commons Attribution License (CC BY). The use, distribution or reproduction in other forums is permitted, provided the original author(s) and the copyright owner(s) are credited and that the original publication in this journal is cited, in accordance with accepted academic practice. No use, distribution or reproduction is permitted which does not comply with these terms.



Enhanced Immunomodulatory Effect of Intravenous Immunoglobulin by Fc Galactosylation and Nonfucosylation

Yusuke Mimura^{1*}, Yuka Mimura-Kimura¹, Radka Saldova^{2,3}, Pauline M. Rudd^{2,4} and Roy Jefferis⁵

¹ Department of Clinical Research, National Hospital Organization Yamaguchi Ube Medical Center, Ube, Japan,

² NIBRT GlycoScience Group, National Institute for Bioprocessing Research and Training, Dublin, Ireland, ³ UCD School of Medicine, College of Health and Agricultural Science, University College Dublin, Dublin, Ireland, ⁴ Bioprocessing Technology Institute, Agency for Science, Technology and Research, Centros, Singapore, ⁵ Institute of Immunology and Immunotherapy, College of Medical and Dental Sciences, University of Birmingham, Birmingham, United Kingdom

OPEN ACCESS

Edited by:

Irena Trbojević-Akmačić,
Genos Glycoscience Research
Laboratory, Croatia

Reviewed by:

Adrian Walter Zuercher,
CSL Behring AG, Switzerland
Fabian Käsemann,
CSL Behring AG, Switzerland

*Correspondence:

Yusuke Mimura
mimura.yusuke.qy@mail.hosp.go.jp

Specialty section:

This article was submitted to
B Cell Biology,
a section of the journal
Frontiers in Immunology

Received: 19 November 2021

Accepted: 10 January 2022

Published: 28 January 2022

Citation:

Mimura Y, Mimura-Kimura Y,
Saldova R, Rudd PM
and Jefferis R (2022) Enhanced
Immunomodulatory Effect of
Intravenous Immunoglobulin by Fc
Galactosylation and Nonfucosylation.
Front. Immunol. 13:818382.
doi: 10.3389/fimmu.2022.818382

Intravenous immunoglobulin (IVIG) is used as an immunomodulatory agent in the treatment of various autoimmune/inflammatory diseases although its mechanism of action remains elusive. Recently, nonfucosylated IgG has been shown to be preferentially bound to Fcγ receptor IIIa (FcγRIIIa) on circulating natural killer cells; therefore, we hypothesized that nonfucosylated IVIG may modulate immune responses through FcγRIIIa blockade. Here, homogeneous fucosylated or nonfucosylated glycoforms of normal polyclonal IgG bearing sialylated, galactosylated or nongalactosylated Fc oligosaccharides were generated by chemoenzymatic glycoengineering to investigate whether the IgG glycoforms can inhibit antibody-dependent cellular cytotoxicity (ADCC). Among the six IgG glycoforms, galactosylated, nonfucosylated IgG [(G2)₂] had the highest affinity to FcγRIIIa and 20 times higher potency to inhibit ADCC than native IgG. A pilot study of IVIG treatment in mice with collagen antibody-induced arthritis highlighted the low-dose (G2)₂ glycoform of IVIG (0.1 g/kg) as an effective immunomodulatory agent as the 10-fold higher dose of native IVIG. These preliminary results suggest that the anti-inflammatory activity of IVIG is in part mediated via activating FcγR blockade by galactosylated, nonfucosylated IgG and that such nonfucosylated IgG glycoforms bound to FcγRs on immune cells play immunomodulatory roles in health and disease. This study provides insights into improved therapeutic strategies for autoimmune/inflammatory diseases using glycoengineered IVIG and recombinant Fc.

Keywords: glycoengineering, antibody-dependent cellular cytotoxicity, intravenous immunoglobulin, autoimmune disease, natural killer cell, Fcγ receptor, oligosaccharide

INTRODUCTION

IVIG is a therapeutic preparation of normal polyclonal IgG derived from pooled plasma of thousands of healthy donors and is administered at a high dose for the treatment of autoimmune/inflammatory disorders, including immune thrombocytopenia (ITP), Kawasaki Disease and Guillain-Barré syndrome (1–4). The anti-inflammatory activity of IVIG is shown to reside in the Fc portion of IgG from a clinical study on the treatment of ITP with the Fc fragments (5). Although various mechanisms of action of IVIG have been proposed, including blockade of activating FcγRs (6–8), expansion of regulatory T cells (9–11), and upregulation of inhibitory FcγRIIb via sialylated IgG binding to type II lectin receptors (12, 13), the precise mechanism of action of IVIG in autoimmune diseases remains inconclusive (2, 3, 14).

A possible differential role has been proposed for Fc oligosaccharides of IgG to influence the immunomodulatory effect of IVIG (3, 15, 16). The oligosaccharide attached at Asn297 residue of each C_H2 domain of IgG-Fc is essential for optimal expression of biological activities mediated through FcγRs (FcγRI, FcγRIIa/b/c, FcγRIIIa/b) and the C1q component of complement (17–20). The Fc oligosaccharides of serum-derived IgG are highly heterogeneous due to variable addition and processing of outer-arm sugar residues [sialic acid, galactose and bisecting N-acetylglucosamine (GlcNAc)] and fucose onto the core diantennary heptasaccharide (GlcNAc₂Mannose₃GlcNAc₂, designated G0) (**Supplementary Figure 1** and **Supplementary Table 1**) (21). The differentially glycosylated species (glycoforms) of IgG-Fc express unique biological activities, modulating antibody effector functions including ADCC and complement-dependent cytotoxicity (17, 18, 20, 22). In particular, nonfucosylation of IgG-Fc increases FcγRIIIa binding and ADCC ~50-fold (23, 24), which has been exploited for the development of therapeutic recombinant monoclonal antibodies for treatment of cancers, inflammatory and infectious diseases (25–28). On the other hand, biological significance of naturally occurring nonfucosylated glycoforms present at 5–10% of serum IgG (or IVIG) remains unclear. Recently, the majority of IgG antibodies bound to FcγRIIIa on circulating natural killer cells have been shown to be nonfucosylated, in contrast to those in the sera of the same subjects which are mostly fucosylated (29). Here, we hypothesized that nonfucosylated IgG in serum can saturate FcγRIIIa on immune cells due to its high affinity and modulate immune responses. We demonstrate that nonfucosylated glycoforms of normal polyclonal IgG can markedly inhibit ADCC compared with the fucosylated glycoforms. Notably, the galactosylated, nonfucosylated (G2)₂ glycoform exhibits a significant therapeutic efficacy *in vivo* at a low dose and is comparable to the 10-fold higher dose of native IVIG. These results provide improved therapeutic strategies for autoimmune diseases using IVIG. The anti-inflammatory activity of the (G2)₂

glycoform sheds light on the association between glycosylation changes of total serum IgG and the pathophysiology of certain autoimmune diseases.

METHODS

Expression of EndoS, EndoS D233Q and α-L-Fucosidase AlfC

Expression vectors pET-30a(+)-ndoS D233Q and pET28a(+)-α-L-fucosidase encoding EndoS D233Q from *Streptococcus pyogenes* and α-L-fucosidase AlfC from *Lactobacillus casei*, respectively, were generously provided by Dr. Wei Huang (30, 31). Expression vector encoding EndoS wildtype was prepared by site-directed mutagenesis using pET-30a(+)-ndoS D233Q, Quickchange Lightning site-directed mutagenesis kit (Agilent), forward primer 5'-GGCCTGGACGTTGACGTGGAACACGATAGCATTCCGAAAGTG-3', and reverse primer 5'-TTCCACGTCAACGTCCAGGCCATCCAGGTTGTACTTGTACAC-3'. The vectors were transformed into BL21(DE3) competent cells (Novagen), and the enzymes were expressed and purified as previously described (30, 31).

Preparation of Glycan Oxazolines

The glycan donors sialoglycan oxazoline (S2G2-Ox), galactosylated glycan oxazoline (G2-Ox), and nongalactosylated glycan oxazoline (G0-Ox) were prepared from sialylglycopeptide (SGP) (Tokyo Chemical Industry Co. Ltd.) in a modified version of the previously described method (32). Briefly, SGP (20 mg) dissolved in 100 μl of 50 mM phosphate (pH 6.0) was digested at 37°C for 8 h with EndoS-coupled Sepharose-4 that had been prepared by coupling EndoS to CNBr-activated Sepharose-4 (GE Healthcare) to release sialoglycan, according to the manufacturer's instruction. For G2-Ox and G0-Ox preparation, SGP (40 mg) was digested with EndoS-coupled Sepharose-4 and neuraminidase (2 U, Roche) overnight and the supernatant containing the desialylated glycan was divided into two aliquots, with one for preparation of G2-Ox and the other for G0-Ox. For the latter, the galactosylated glycan was digested with β (1-3,4)-galactosidase (Agilent) at 37°C for 48 h. The glycan in each aliquot (~100 μl) was converted to glycan oxazoline by the addition of 2-chloro-1,3-dimethylimidazolium chloride (23.4 mg) and triethylamine (47.2 μl) on ice for 1 h. The reaction was diluted with 4 ml of butanol:ethanol:water (4:1:1, v/v/v) and purified on cellulose column (2 ml in a Poly-Prep Chromatography Column, Bio-Rad) equilibrated with the same solution (33). After washing the column with 12 ml of the solution and 2 ml of absolute ethanol, glycan oxazoline was eluted with distilled water. The glycan-containing fractions were detected with anthrone/sulfuric acid and dried under vacuum.

Preparation of Homogeneous Glycoforms of Normal IgG

A series of fully sialylated and the truncated glycoforms of normal IgG were prepared by chemoenzymatic glycoengineering, according to the previously described method (30). Briefly, commercial IVIG (Gammagard, Shire Japan) dissolved at ~40

Abbreviations: 2-AB, 2-aminobenzamide; ADCC, antibody-dependent cellular cytotoxicity; CAIA, collagen antibody-induced arthritis; CRP, C-reactive protein; ENGase, endoglycosidase; FcγR, receptor for Fc portion of IgG; GlcNAc, N-acetylglucosamine; HILIC, hydrophilic interaction liquid chromatography; ITP, immune thrombocytopenia; IVIG, intravenous immunoglobulin; SGP, sialylglycopeptide; UPLC, ultra-performance liquid chromatography.

mg/ml in 50 mM acetate, 5 mM CaCl₂ (pH 5.5) was deglycosylated with EndoS-coupled Sepharose-4 at 37°C for 8 h to prepare IgG bearing Fuc-GlcNAc at Asn297 (Fuc-GlcNAc-IgG), then dialyzed against 50 mM Tris-HCl (pH 7.4). To prepare IgG bearing GlcNAc (GlcNAc-IgG) it was further digested with α -L-fucosidase AlfC at 37°C for 48 h. For transglycosylation, either GlcNAc-IgG or Fuc-GlcNAc-IgG at ~25 mg/ml was incubated with 0.6 mg/ml EndoS D233Q in the presence of 3 mM glycan oxazoline at 30°C for 4 h. The completion of transglycosylation was confirmed by SDS-PAGE and the remodeled IgG glycoforms were purified on protein G-Sepharose 4 Fast flow column (GE Healthcare).

Glycan Analysis of Homogeneous IgG Glycoforms

IgG (1 mg) was digested with papain (20 μ g) in 0.1 M phosphate, 0.15 M NaCl, 2 mM EDTA (pH 7.0) at 37°C overnight, then treated with 50 μ M iodoacetamide for 30 min on ice, and dialyzed against 10 mM phosphate buffer (pH 8.0). The Fab and Fc were separated by diethylaminoethyl-cellulose anion exchange chromatography (DE52; Whatman Biosystems, Chalfont St Giles, UK) equilibrated with the same buffer. The dialyzed papain digest was applied to the column, and the Fab was obtained in the fall-through fractions. After washing the column with five column volumes of 10 mM phosphate (pH 8.0), 10 mM phosphate-buffered saline (pH 7.4) (PBS) was added to elute the Fc (21). The oligosaccharides were released with peptide-N-glycosidase F from the Fc of an individual IgG glycoform in the SDS-PAGE gel bands and labeled with 2-aminobenzamide (2-AB) by using Signal 2-AB plus labeling kit (Agilent) as previously described (34). The fluorescently labeled oligosaccharides were separated by using a Waters ACQUITY H-class Bio ultraperformance liquid chromatography (UPLC) system on a sub-2 μ m hydrophilic interaction based stationary phase with a Waters ACQUITY UPLC Glycan BEH Amide column (2.1 \times 150 mm i.d., 1.7 μ m BEH particles) as previously described (35). The oligosaccharide peaks were assigned in accordance with the previous study (36).

Fc γ Receptor (Fc γ R) Binding Assays

The binding of the IgG glycoforms to Fc γ Rs was analyzed as previously described (37). Briefly, recombinant human Fc γ R proteins (Fc γ RIIIa V158/F158 and Fc γ RIIIa R131/H131) (R&D Systems) at 2.5 – 5 μ g/ml in PBS were coated on high-binding microtiter plates (Corning 3690 High Binding Half Area) overnight at 4°C. The Fc γ R-coated plates were washed with PBS containing 0.05% Tween 20 (PBS-T) three times and blocked with PBS containing 1% bovine serum albumin for 1 h at room temperature. Serially diluted IgG glycoforms were added to the Fc γ RIIIa-coated plates and allowed to bind for 2 h at 37°C. After washing with PBS-T three times, the bound IgG was detected with goat F(ab')₂ anti-human IgG F(ab')₂-peroxidase conjugate (Abcam). After incubation for 2 h at 37°C, the plates were washed five times with PBS-T and developed with 50 μ l of 3,3',5,5'-tetramethylbenzidine substrate per well, which was stopped by the addition of 12.5 μ l of 12.5% H₂SO₄ per well. Absorbance was measured at 450 nm on a MultiskanTM microplate reader (Thermo

Fisher Scientific). The concentration of IgG corresponding to half-maximal binding on the ELISA binding curve was considered as an apparent affinity to the respective Fc γ R and was compared between the IgG glycoforms.

ADCC Reporter Bioassay

ADCC reporter bioassay mediated by Fc γ RIIIa V158 or F158 was performed, according to the manufacturer's instruction (Promega). Briefly, CD20-expressing Raji cells grown in RPMI1640 cell culture medium supplemented with 10% heat-inactivated fetal bovine serum (Gibco), 2 mM glutamine, 100 μ g/ml penicillin and 100 U/ml streptomycin (10% RPMI) were plated after washing once with PBS and resuspended in RPMI1640 medium containing 4% fetal bovine serum, ultra-low IgG (Life Technologies) at 12,500 cells/25 μ l/well in white opaque tissue culture plates (BD Falcon 353296), followed by the addition of 25 μ l of rituximab (anti-CD20 IgG) that was 4-fold serially diluted from the starting concentration of 10 μ g/ml with the same medium. An individual normal IgG glycoform dissolved in PBS was added to each well (7.5 μ l/well). Jurkat cells stably expressing human Fc γ RIIIa V158 (or F158) and NFAT-luciferase reporter in 10% RPMI were added at 75,000 cells/17.5 μ l/well to rituximab-opsonized Raji cells at 37°C, 5% humidified CO₂ for 6 h. BioGlo luciferase assay reagent was added (75 μ l/well), and chemiluminescence was measured with a luminometer (Fluoroskan Ascent FL, Thermo Fisher Scientific). Inhibition of ADCC was examined with increasing concentrations of native IgG (0 – 10 mg/ml), with various fucosylation levels of sialylated IgG or galactosylated IgG (0%, 25%, 50%, and 100%) at 0.2 mg/ml, and with the six individual IgG glycoforms at 0.1 mg/ml. Additionally, titration of the IgG glycoforms (0 – 2 mg/ml) was performed to compare the ADCC inhibitory capability at 0.1 μ g/ml rituximab.

Statistical Analysis

The ELISA data for the IgG glycoforms–Fc γ R interactions and the ADCC reporter bioassay data were fitted to sigmoidal dose-response curves (GraphPad Prism v6). The differences in the concentration of rituximab that gave 50% of the maximal response (EC₅₀) in the presence or absence of the glycoforms of IgG were tested by the extra sum of squares *F*-test (GraphPad Prism v6). Likewise, the differences in 50% inhibitory concentration (IC₅₀) of the IgG glycoforms for inhibition of the ADCC reporter activity were tested. *p* < 0.05 was considered statistically significant.

RESULTS

Remodeling of IgG Glycosylation by Chemoenzymatic Glycoengineering

A glycoform of normal polyclonal IgG bearing homogeneous oligosaccharide chains (S2G2)₂, (S2G2F)₂, (G2)₂, (G2F)₂, (G0)₂, or (G0F)₂ was prepared by transfer of the glycan donor S2G2-Ox, G2-Ox or G0-Ox to fucosylated or nonfucosylated GlcNAc residues of IgG with EndoS D233Q. Complete transfer of the respective glycans was confirmed by SDS-PAGE (**Figure 1A**) and the structures of the glycans released with peptide-N-glycosidase F from the Fc fragments were analyzed by HILIC-UPLC,

exhibiting a single peak of each glycoform, in contrast to heterogeneous peaks of native IgG (**Figure 1B**, **Supplementary Figure 1**, and **Supplementary Table 1**).

Binding of IgG Glycoforms to Human FcγRs

Binding to FcγRIIa (H131 or R131) or FcγRIIIa (V158 or F158) was compared between the six IgG glycoforms and native IgG by ELISA (**Figure 2**). All the IgG glycoforms exhibited comparable FcγRIIa binding profiles to native IgG, which confirms no adverse effect of the glycoengineering processes on the FcγR binding capability of the remodeled IgG glycoforms (**Figure 2A**). Galactosylation had positive influence on FcγRIIa binding (**Figure 2A**) while the nongalactosylated glycoforms [(G0)₂ and (G0F)₂] had generally lower affinity, with the differences in the apparent affinity between the (G2)₂ and the (G0F)₂ being ~2-fold for both FcγRIIa H131 and R131 variants. On the other hand, nonfucosylation had profound influence on FcγRIIIa binding, with the differences in the apparent affinity between the nonfucosylated glycoforms and the fucosylated counterparts being 30–70-fold for the V158 variant and 4–30-fold for the F158 variant (**Figure 2B**). Notably, the (G2)₂ glycoform had the highest affinity to both FcγRIIIa V158 and F158 variants while the sialylated, fucosylated (S2G2F)₂ glycoform had the lowest affinity to FcγRIIIa (**Figure 2B**).

The (G2)₂ Glycoform of Normal IgG Potently Inhibits ADCC

The influence of normal polyclonal IgG on ADCC was examined with increasing concentrations of normal IgG in rituximab (anti-CD20 antibody)-mediated, FcγRIIIa-based ADCC reporter bioassay. Inhibition of ADCC was observed in a dose-

dependent manner for both FcγRIIIa V158 and F158 variants where the EC₅₀ values progressively increased in a range of 0.1–1 mg/ml of normal IgG (**Figure 3**).

The influence of fucosylation of normal IgG on ADCC inhibition was examined by titration of the fucosylation levels of sialylated or galactosylated IgG at 0.2 mg/ml (**Figure 4A**). Decrease in the fucosylation levels resulted in progressive increases in the inhibitory activity for both sialylated and galactosylated IgG. This result clearly indicates that the glycoform of normal IgG is important for modulation of ADCC.

Inhibition of ADCC was further examined using the six IgG glycoforms at 0.1 mg/ml (**Figure 4B**). ADCC was markedly inhibited with non-fucosylated IgG [(S2G2)₂, (G2)₂ and (G0)₂] as compared with the fucosylated IgG counterparts [(S2G2F)₂, (G2F)₂ and (G0F)₂]. Additionally, titration of these IgG glycoforms was performed to compare the IC₅₀ for ADCC inhibition between the IgG glycoforms (**Figure 4C**). The IC₅₀ values obtained for (G2)₂, (S2G2)₂, (G0)₂, and native IgG were 0.1, 0.16, 0.28 and 2.0 mg/ml, respectively. This indicates that the inhibitory capacities of the (G2)₂, (S2G2)₂, and (G0)₂ glycoforms are 20, 12.5, and 7-fold higher than that of native IgG, respectively. Notably, galactosylation and nonfucosylation of normal IgG resulted in the most potent inhibition of ADCC (**Figures 4B, C**), which is explained by its enhanced affinity for FcγRIIIa (**Figure 2B**). In contrast, sialylation or nongalactosylation of IgG had a subtle but negative impact on the inhibition of ADCC (**Figures 4B, C**), which corresponds to the decreased affinities to FcγRIIIa (**Figure 2B**).

On the other hand, FcγRIIa-mediated antibody-dependent cellular phagocytosis (ADCP) was inhibited by normal IgG at >1 mg/ml (**Supplementary Figure 2A**); however, ADCP was not modulated by IgG glycoforms (**Supplementary Figure 2B**).

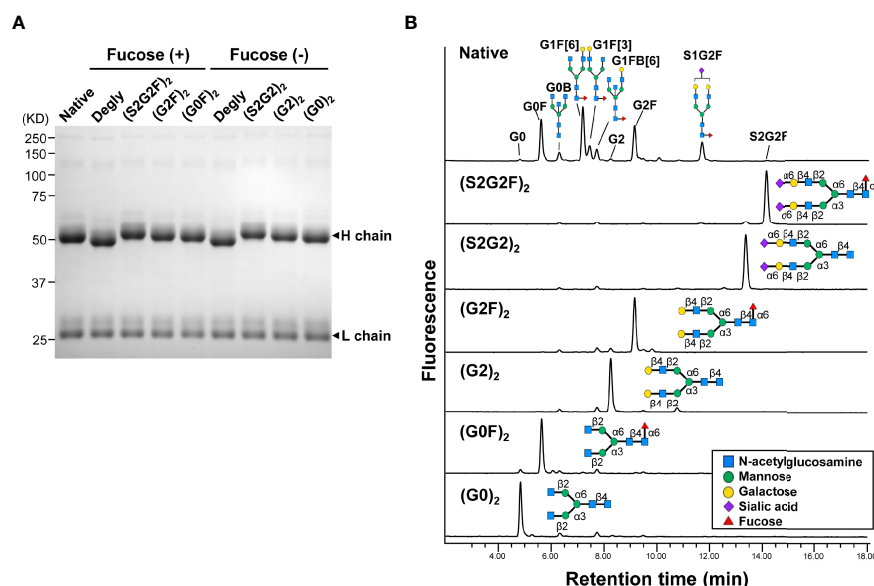


FIGURE 1 | Homogeneous glycoforms of normal polyclonal IgG prepared by chemoenzymatic glycoengineering. **(A)** SDS-PAGE of the glycoforms of IgG. All the IgG glycoforms including the native protein used in this study were purified by protein G affinity chromatography. **(B)** HILIC-UPLC analysis of glycans released from the Fc fragments of IgG glycoforms. The peaks of the oligosaccharides of native IgG are listed in **Supplementary Table 1**.

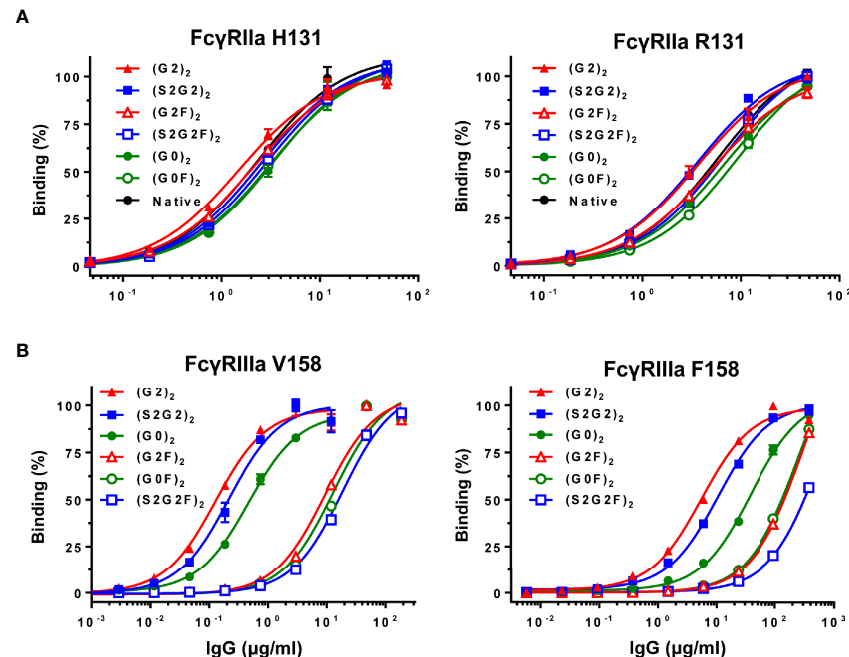


FIGURE 2 | Binding of IgG glycoforms to FcγRs. **(A)** FcγRIIa H131 and R131 variants. **(B)** FcγRIIIa V158 and F158 variants. All data points represent the calculated mean of two independent measurements from a total of at least two experiments. The data were fitted to a sigmoidal dose-response curve (GraphPad Prism).

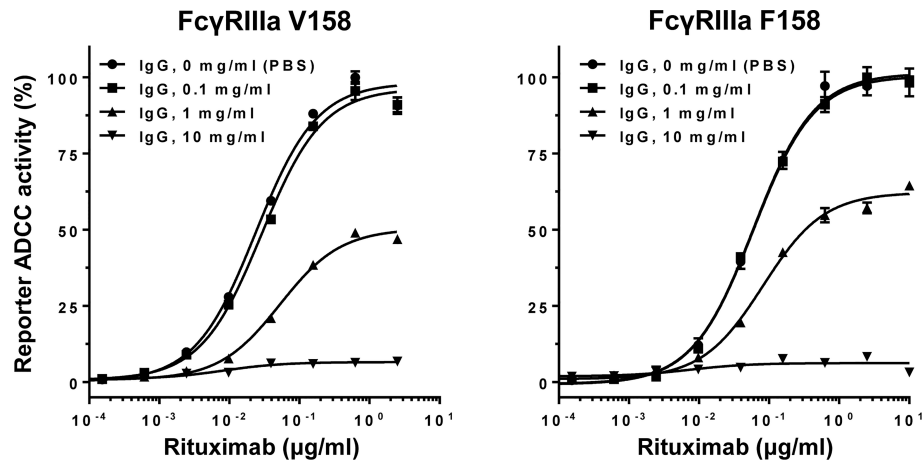


FIGURE 3 | Normal polyclonal IgG inhibits ADCC in a dose-dependent manner. Note that activation of FcγRIIIa V158 or F158 variant was inhibited by normal IgG at >0.1 mg/ml. Error bars, mean \pm S.E. ($n = 3$).

(G2)₂ IVIG Attenuates Collagen Antibody-Induced Arthritis in Mice

Whether the IgG glycoforms exert anti-inflammatory effects was examined in mice with collagen antibody-induced arthritis (CAIA) (**Supplementary Figure 3**). Low-dose (0.1 g/kg) IgG glycoforms [(G2)₂, (S2G2)₂, (S2G2F)₂, native] and high-dose (1 g/kg) native IgG as positive control were administered to the mice, and the group receiving the (G2)₂ glycoform had the lowest

arthritis score and serum interleukin-6 levels among the groups (**Supplementary Figure 3**).

DISCUSSION

A rationale for the use of IVIG, at a high dose, and its mechanism of action in the treatment of autoimmune/inflammatory diseases remain to be elucidated. We have shown robust

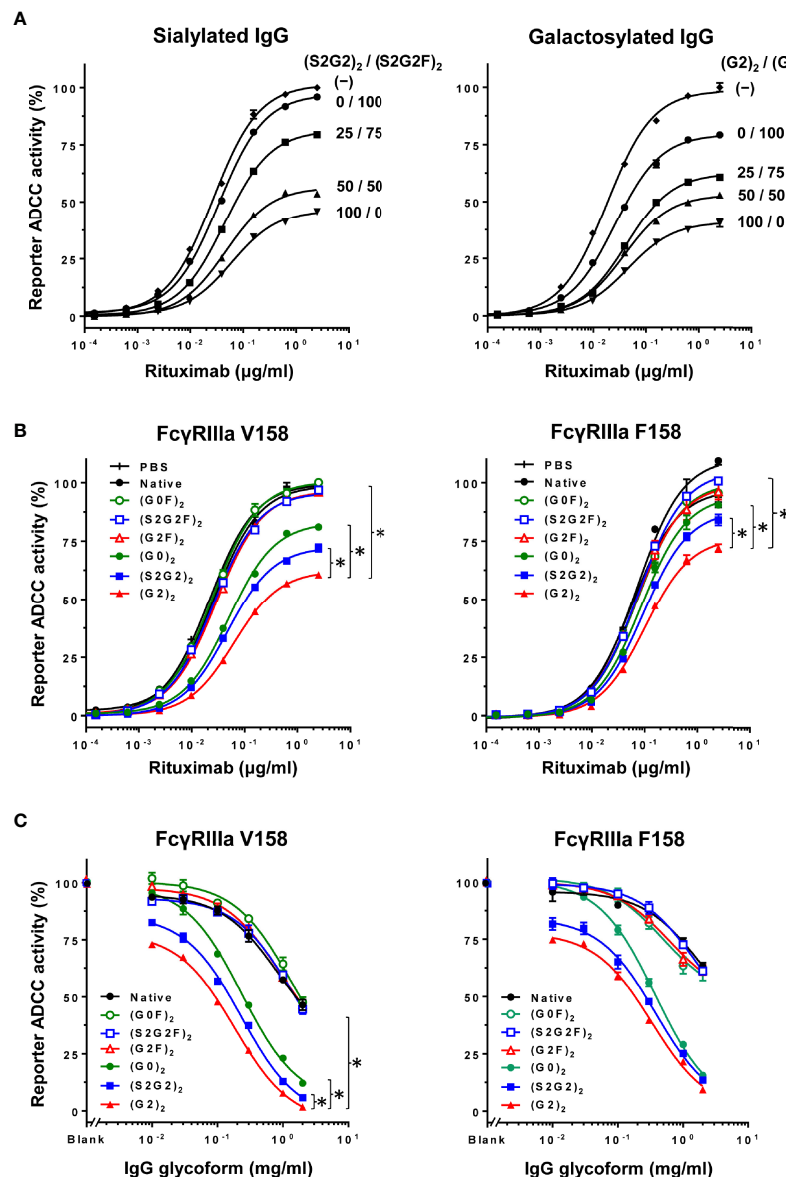


FIGURE 4 | Inhibition of ADCC with normal IgG is glycoform-dependent. **(A)** Influence of fucosylation of normal IgG on inhibition of ADCC was examined by titration of fucosylation levels of sialylated glycoforms (left) and galactosylated glycoforms (right) at the final concentration of 0.2 mg/ml. Error bars, mean \pm S.E. ($n = 3$). **(B)** Influence of the IgG glycoforms on inhibition of ADCC was examined at 0.1 mg/ml of each IgG glycoform. Error bars, mean \pm S.E. ($n = 3$). Note that the differences in EC_{50} between the (G2)₂ and other glycoforms were significant (asterisks) for both Fc γ RIIIa V158 and F158 ($p < 0.01$) as determined by extra sum of squares F -test. **(C)** Titration of the IgG glycoforms for comparison of the ADCC inhibitory capability at 0.1 $\mu\text{g/ml}$ rituximab. Error bars, mean \pm S.E. ($n = 3$). * $p < 0.05$.

immunomodulatory activity of the galactosylated, non-fucosylated (G2)₂ glycoform of human normal IgG as a minor but active component of IVIG. High affinity-binding of galactosylated, nonfucosylated IgG to Fc γ RIIIa that can modulate immune responses including ADCC is a novel mechanism of action of IVIG (Figure 5). This study provides insights into improved therapeutic strategies for autoimmune diseases and the involvement of endogenous galactosylated, nonfucosylated IgG in immune homeostasis.

The immunomodulatory effect of IVIG was Fc glycoform-dependent. The (G2)₂ glycoform of IVIG at a low dose (0.1 g/kg)

was as protective as the 10-fold higher dose of native IVIG in mice with collagen antibody-induced arthritis (Supplementary Figure 3). The robust anti-inflammatory activity of the (G2)₂ glycoform is consistent with the highest affinity to Fc γ RIIIa (38–40) and the strongest ADCC inhibitory activity among the six IgG glycoforms examined (Figures 2B, 4B, C). The mice in the (S2G2)₂ and (S2G2F)₂-treated groups were not protected (Supplementary Figure 3), which is consistent with previous reports that the anti-inflammatory activity of IVIG is independent of Fc sialylation (41–43) but not with the report

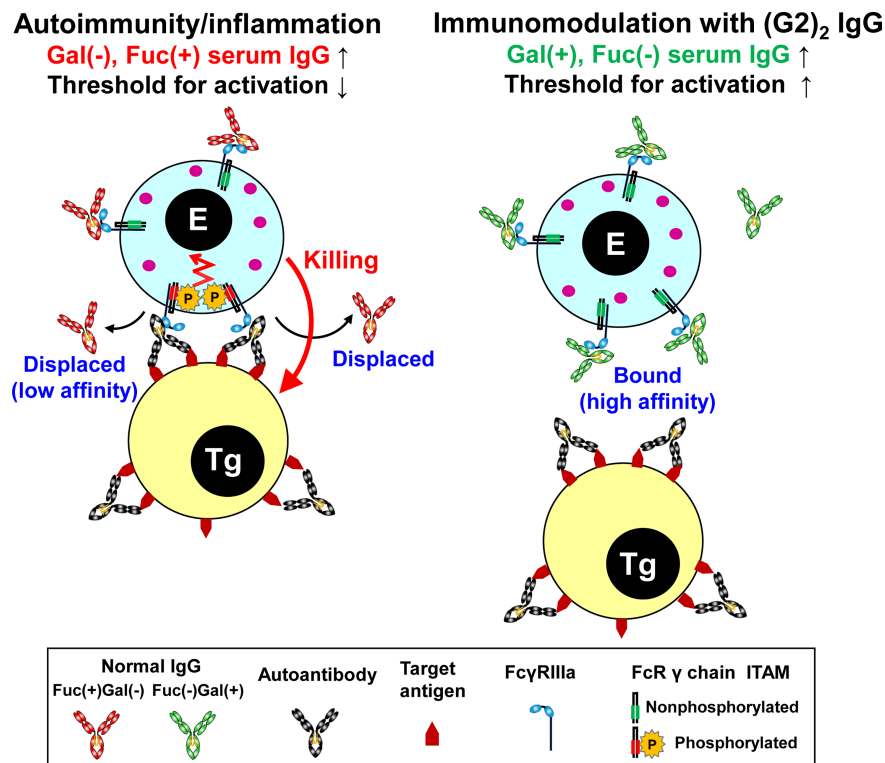


FIGURE 5 | Summary of the mechanism of immunomodulation by the (G2)₂ glycoform of IgG. In autoimmune/inflammatory state, hypogalactosylated, fucosylated serum IgG cannot compete with high-avidity multimeric IgG immune complexes on a target cell for FcγRIIIa binding, resulting in the activation of an effector cell (left). Increased levels of galactosylated, nonfucosylated serum IgG by administration of the (G2)₂ glycoform of IVIG result in saturation of FcγRIIIa with the (G2)₂ glycoform, inhibiting the activation of an effector cell (right). E, effector cell. Tg, target cell. Gal, galactose. Fuc, fucose.

by Washburn et al. about enhanced anti-inflammatory effects of hyper-sialylated Fc (44). However, the difference in the outcome between these studies might be attributed to different sialylated IgG/Fc preparations and experimental protocols.

Galactosylation and nonfucosylation influence FcγRIIIa binding independently because the α(1-6)-arm galactose interacts with the amino acid residues at the C_H2/C_H3 domain interface while core fucose is proximal to the lower hinge region. Lack of core fucose of IgG-Fc increases oligosaccharide-oligosaccharide and oligosaccharide-protein interactions between FcγRIIIa and IgG-Fc, thereby stabilizing complex formation (45, 46). On the other hand, the galactose residue(s) contribute to the stability of IgG-Fc structure, as evidenced by increased enthalpy for the unfolding of the galactosylated C_H2 domains (40, 47), increased mobility of the Fc oligosaccharide by removal of galactose (48), and lowered deuterium uptake in the hydrophobic surface of the galactosylated C_H2 domain spanning Phe241 to Met252 (49). By crystallographic analysis, the α(1-6)-arm galactose makes 27 non-covalent contacts with the protein structure of the C_H2 domain including a minimum of 2 hydrogen bonds (50). Additionally, the two C_H2 domains of the (G2F)₂ glycoform adopts an open conformation of the horseshoe-shaped Fc, which is favorable for FcγRIII binding (51, 52). In contrast, sialylation of the Fc had a minor but negative impact on FcγRIIIa

binding, resulting in lowered ADCC inhibitory activity as compared with the (G2)₂ glycoform (Figures 2B, 4B, C) (39, 40). Crystallographic studies of disialylated Fc reveal open and closed conformations (PDB ID codes: 4Q6Y and 5GSQ) (53, 54), and its closed conformation would be unfavorable for FcγR binding. Degalactosylation had further negative impact on FcγRIIIa binding and ADCC inhibition (Figures 2B, 4B, C), due to the net loss of stabilizing oligosaccharides/protein interactions as revealed by elevated B-factor of the nongalactosylated Fc glycoform (52).

Naturally occurring galactosylated, nonfucosylated IgG in serum may be involved in immune homeostasis. Galactosylation and nonfucosylation of IgG enhance FcγRIIIa binding by two orders of magnitude (Figure 2B) (23, 24, 45, 46, 55), which explains why the (G2)₂ glycoform of serum IgG bound to FcγRIIIa is not displaced by autoantibody-antigen complexes (Figures 2B, 5). In the ADCC reporter bioassay, ADCC was inhibited with the (G2)₂ glycoform of IgG at as low as 0.1 mg/ml (~0.6 μM) *in vitro* (Figure 4B). As the proportion of the G2 oligosaccharide released from IgG-Fc of the IVIG preparation was ~1% (Figure 1B, Supplementary Figure 1 and Supplementary Table 1), the serum level of IgG bearing at least one G2 oligosaccharide chain is estimated to be up to 0.2 mg/ml (~1.3 μM), which is higher than the IC₅₀ of the (G2)₂ glycoform for ADCC inhibition (Figure 4C) and the K_d for the binding of the (G2)₂ glycoform of IgG to FcγRIIIa

V158 (1.98 nM) and F158 (24.6 nM) as reported previously (56). It is likely that the equilibrium of the interaction between the (G2)₂ glycoform of serum IgG and FcγRIIIa on immune cells shifts toward association *in vivo*. In fact, the FcγRIIIa molecules isolated from circulating NK cells were shown to preferentially bind nonfucosylated IgG1 bearing G2, monosialylated G2, G1, and bisected G1 oligosaccharides while serum IgG is largely fucosylated in the same subjects (29). The imbalance of the IgG glycoform distribution between serum and FcγRIIIa on NK cells indicates that circulating galactosylated, nonfucosylated IgG glycoforms represents the tip of the iceberg. Thus, the majority of endogenous nonfucosylated IgG glycoforms are likely bound to FcγRIIIa, modulating immune cell responses in healthy conditions.

Under autoimmune and inflammatory conditions, it is conceived that circulating galactosylated, nonfucosylated IgG glycoforms decrease due to the binding to FcγRIIIa on expanding immune cells. In rheumatoid arthritis (RA), elevated hypogalactosylated IgG levels associate with disease activity (57, 58), and during pregnancy its galactosylation level can return to normal with disease symptoms being improved (58). The involvement of hypogalactosylation of serum IgG in the pathophysiology of RA remains uncertain probably because in early studies the impact of core fucosylation was not appreciated or quantitated (17). Importantly, the fucosylation level of serum IgG in RA was recently found to be elevated as compared with healthy control (58, 59), indicating a decrease of galactosylated and/or nonfucosylated IgG in serum. It should be noted that due to the asymmetry of the Fc–FcγRIIIa interaction nonfucosylation of one heavy chain is sufficient for tight binding (45, 46). Therefore, IgG bound to FcγRIIIa on immune cells may bear a pair of fucosylated and nonfucosylated oligosaccharides in the Fc portion, which may explain why a decrease of not only nonfucosylated but fucosylated oligosaccharides is observed in oligosaccharide profiles of serum IgG in RA (48). It has been reported in Guillain-Barré syndrome that the responses to IVIG therapy correlate with IgG glycosylation profiles where patients who failed to respond to IVIG were characterized by hypogalactosylation of serum IgG before and after the treatment (60). Thus, a better understanding of the relationship between glycosylation changes of IgG and disease activity will be helpful in the treatment and management of certain autoimmune diseases with IVIG and its (G2)₂ glycoform *via* the saturation of FcγRIIIa, blocking FcγRIIIa-mediated ADCC (Figure 5).

To conclude, elucidation of the mechanism of action of IVIG is essential to establish its clinical indication, as over 200 metric tons of IVIG per year are consumed worldwide for treatment of autoimmune and inflammatory diseases including off-label purposes (14, 61). Considering the prioritized use of IVIG for primary immunodeficiency, the Fc fragments should suffice for immunomodulatory therapy, which suggests clinical application of glycoengineered recombinant Fc proteins as an alternative to plasma-derived IVIG. Various recombinant Fc multimers have been designed to block effector molecules including FcγRs, C1q and neonatal Fc receptor (FcRn), and some Fc multimers including GL-2045 and M230 have been under clinical evaluation (62, 63). Recombinant Fc multimers are shown to block multiple effector

molecules while glycoengineered Fc monomers may not be useful to target C1q or FcRn due to low affinity to C1q ($K_a = 5 \times 10^4 \text{ M}^{-1}$) (64) and lack of the impact of Fc glycosylation on FcRn binding (40). Although recombinant Fc multimers are promising therapeutics, their broad immunomodulatory effects and unnatural antibody formats might be associated with potential risks during the long-term use in autoimmune diseases. On the other hand, galactosylated, nonfucosylated IgG glycoforms bearing human-type oligosaccharides are naturally occurring and likely devoid of immunogenicity *in vivo*. Further studies are needed to evaluate the efficacy of the (G2)₂ glycoform of IVIG and recombinant Fc in a range of autoimmune diseases and severe infections including coronavirus disease 2019 (Covid-19) (65, 66). The disease severities of certain viral infections including SARS-CoV-2 and dengue viruses have been reported to associate with elevated levels of nonfucosylated IgG against the pathogens (67–70); therefore, the (G2)₂ glycoform of IVIG and Fc are promising immunomodulatory agents for attenuation of antibody-dependent enhancement of infection *via* competition with antiviral nonfucosylated IgG.

DATA AVAILABILITY STATEMENT

The original contributions presented in the study are included in the article/**Supplementary Material**. Further inquiries can be directed to the corresponding author.

ETHICS STATEMENT

The animal study was reviewed and approved by The Animal Care and Use Committees of Yamaguchi Ube Medical Center and Unitech Co., Ltd.

AUTHOR CONTRIBUTIONS

YM and YM-K conceived the study, designed and performed experiments, and wrote the manuscript. RS performed the glycan analysis. RJ and PR analyzed the results and cowrote the manuscript. All authors approved the manuscript.

ACKNOWLEDGMENTS

We thank Drs. Feng Tang and Wei Huang (Chinese Academy of Sciences) for the generous gifts of expression vectors encoding EndoS D233Q and α-L-fucosidase AlfC.

SUPPLEMENTARY MATERIAL

The Supplementary Material for this article can be found online at: <https://www.frontiersin.org/articles/10.3389/fimmu.2022.818382/full#supplementary-material>

REFERENCES

- Burns JC, Franco A. The Immunomodulatory Effects of Intravenous Immunoglobulin Therapy in Kawasaki Disease. *Expert Rev Clin Immunol* (2015) 11:819–25. doi: 10.1586/1744666X.2015.1044980
- Galeotti C, Kaveri SV, Bayry J. IVIG-Mediated Effector Functions in Autoimmune and Inflammatory Diseases. *Int Immunol* (2017) 29:491–8. doi: 10.1093/intimm/dxx039
- Nagelkerke SQ, Kuijpers TW. Immunomodulation by IVIg and the Role of Fc-Gamma Receptors: Classic Mechanisms of Action After All? *Front Immunol* (2014) 5:674–674. doi: 10.3389/fimmu.2014.00674
- Schwab I, Nimmerjahn F. Intravenous Immunoglobulin Therapy: How Does IgG Modulate the Immune System? *Nat Rev Immunol* (2013) 13:176–89. doi: 10.1038/nri3401
- Debre M, Bonnet MC, Fridman WH, Carosella E, Philippe N, Reinert P, et al. Infusion of Fc Gamma Fragments for Treatment of Children With Acute Immune Thrombocytopenic Purpura. *Lancet* (1993) 342:945–9. doi: 10.1016/0140-6736(93)92000-J
- Imbach P, Barandun S, d'Apuzzo V, Baumgartner C, Hirt A, Morell A, et al. High-Dose Intravenous Gammaglobulin for Idiopathic Thrombocytopenic Purpura in Childhood. *Lancet* (1981) 1:1228–31. doi: 10.1016/s0140-6736(81)92400-4
- Bussell JB. Fc Receptor Blockade and Immune Thrombocytopenic Purpura. *Semin Hematol* (2000) 37:261–6. doi: 10.1016/s0037-1963(00)90104-5
- Gelfand EW. Intravenous Immune Globulin in Autoimmune and Inflammatory Diseases. *N Engl J Med* (2012) 367:2015–25. doi: 10.1056/NEJMr1009433
- Massoud AH, Yona M, Xue D, Chouiali F, Alturaihi H, Ablona A, et al. Dendritic Cell Immunoreceptor: A Novel Receptor for Intravenous Immunoglobulin Mediates Induction of Regulatory T Cells. *J Allergy Clin Immunol* (2014) 133:853–63.e5. doi: 10.1016/j.jaci.2013.09.029
- Maddur MS, Kaveri SV, Bayry J. Circulating Normal IgG as Stimulator of Regulatory T Cells: Lessons From Intravenous Immunoglobulin. *Trends Immunol* (2017) 38:789–92. doi: 10.1016/j.it.2017.08.008
- Cousens LP, Tassone R, Mazer BD, Ramachandiran V, Scott DW, De Groot AS. Tregitope Update: Mechanism of Action Parallels IVIg. *Autoimmun Rev* (2013) 12:436–43. doi: 10.1016/j.autrev.2012.08.017
- Anthony RM, Kobayashi T, Wermeling F, Ravetch JV. Intravenous Gammaglobulin Suppresses Inflammation Through a Novel T(H)2 Pathway. *Nature* (2011) 475:110–3. doi: 10.1038/nature10134
- Anthony RM, Wermeling F, Karlsson MC, Ravetch JV. Identification of a Receptor Required for the Anti-Inflammatory Activity of IVIG. *Proc Natl Acad Sci USA* (2008) 105:19571–8. doi: 10.1073/pnas.0810163105
- Joao C, Negi VS, Kazatchkine MD, Bayry J, Kaveri SV. Passive Serum Therapy to Immunomodulation by IVIG: A Fascinating Journey of Antibodies. *J Immunol* (2018) 200:1957–63. doi: 10.4049/jimmunol.1701271
- Bruggeman CW, Dekkers G, Visser R, Goes NWM, van den Berg TK, Rispens T, et al. IgG Glyco-Engineering to Improve IVIg Potency. *Front Immunol* (2018) 9:2442. doi: 10.3389/fimmu.2018.02442
- Kaneko Y, Nimmerjahn F, Ravetch JV. Anti-Inflammatory Activity of Immunoglobulin G Resulting From Fc Sialylation. *Science* (2006) 313:670–3. doi: 10.1126/science.1129594
- Mimura Y, Jefferis R. Human IgG Glycosylation in Inflammation and Inflammatory Disease. In: JJ Barchi, editor. *Comprehensive Glycoscience*. Oxford: Elsevier (2021). p. 215–32.
- Mimura Y, Katoh T, Saldova R, O'Flaherty R, Izumi T, Mimura-Kimura Y, et al. Glycosylation Engineering of Therapeutic IgG Antibodies: Challenges for the Safety, Functionality and Efficacy. *Protein Cell* (2018) 9:47–62. doi: 10.1007/s13238-017-0433-3
- Jefferis R. Recombinant Proteins and Monoclonal Antibodies. *Adv Biochem Eng Biotechnol* (2017) 1–36. doi: 10.1007/10_2017_32
- Zhang P, Woen S, Wang T, Liao B, Zhao S, Chen C, et al. Challenges of Glycosylation Analysis and Control: An Integrated Approach to Producing Optimal and Consistent Therapeutic Drugs. *Drug Discov Today* (2016) 21:740–65. doi: 10.1016/j.drudis.2016.01.006
- Jefferis R, Lund J, Mizutani H, Nakagawa H, Kawazoe Y, Arata Y, et al. A Comparative Study of the N-Linked Oligosaccharide Structures of Human IgG Subclass Proteins. *Biochem J* (1990) 268:529–37. doi: 10.1042/bj2680529
- Mimura Y, Saldova R, Mimura-Kimura Y, Rudd PM, Jefferis R. Importance and Monitoring of Therapeutic Immunoglobulin G Glycosylation. *Exp Suppl* (2021) 112:481–517. doi: 10.1007/978-3-030-76912-3_15
- Shinkawa T, Nakamura K, Yamane N, Shoji-Hosaka E, Kanda Y, Sakurada M, et al. The Absence of Fucose But Not the Presence of Galactose or Bisecting N-Acetylglucosamine of Human IgG1 Complex-Type Oligosaccharides Shows the Critical Role of Enhancing Antibody-Dependent Cellular Cytotoxicity. *J Biol Chem* (2003) 278:3466–73. doi: 10.1074/jbc.M210665200
- Shields RL, Lai J, Keck R, O'Connell LY, Hong K, Meng YG, et al. Lack of Fucose on Human IgG1 N-Linked Oligosaccharide Improves Binding to Human FcγRIII and Antibody-Dependent Cellular Toxicity. *J Biol Chem* (2002) 277:26733–40. doi: 10.1074/jbc.M202069200
- Ishida T, Joh T, Uike N, Yamamoto K, Utsunomiya A, Yoshida S, et al. Defucosylated Anti-CCR4 Monoclonal Antibody (KW-0761) for Relapsed Adult T-Cell Leukemia-Lymphoma: A Multicenter Phase II Study. *J Clin Oncol* (2012) 30:837–42. doi: 10.1200/JCO.2011.37.3472
- Sehn LH, Goy A, Offner FC, Martinelli G, Caballero MD, Gadeberg O, et al. Randomized Phase II Trial Comparing Obinutuzumab (GA101) With Rituximab in Patients With Relapsed CD20+ Indolent B-Cell Non-Hodgkin Lymphoma: Final Analysis of the GAUSS Study. *J Clin Oncol* (2015) 33:3467–74. doi: 10.1200/JCO.2014.59.2139
- Sehmi R, Lim HF, Mukherjee M, Huang C, Radford K, Newbold P, et al. Benralizumab Attenuates Airway Eosinophilia in Prednisone-Dependent Asthma. *J Allergy Clin Immunol* (2018) 141:1529–32.e8. doi: 10.1016/j.jaci.2018.01.008
- Frampton JE. Inebilizumab: First Approval. *Drugs* (2020) 80:1259–64. doi: 10.1007/s40265-020-01370-4
- Patel KR, Nott JD, Barb AW. Primary Human Natural Killer Cells Retain Proinflammatory IgG1 at the Cell Surface and Express CD16a Glycoforms With Donor-Dependent Variability. *Mol Cell Proteomics* (2019) 18:2178–90. doi: 10.1074/mcp.RA119.001607
- Tang F, Wang LX, Huang W. Chemoenzymatic Synthesis of Glycoengineered IgG Antibodies and Glycosite-Specific Antibody-Drug Conjugates. *Nat Protoc* (2017) 12:1702–21. doi: 10.1038/nprot.2017.058
- Tang F, Yang Y, Tang Y, Tang S, Yang L, Sun B, et al. One-Pot N-Glycosylation Remodeling of IgG With non-Natural Sialylglycopeptides Enables Glycosite-Specific and Dual-Payload Antibody-Drug Conjugates. *Org Biomol Chem* (2016) 14:9501–18. doi: 10.1039/c6ob01751g
- Sun B, Bao W, Tian X, Li M, Liu H, Dong J, et al. A Simplified Procedure for Gram-Scale Production of Sialylglycopeptide (SGP) From Egg Yolks and Subsequent Semi-Synthesis of Man3GlcNAc Oxazoline. *Carbohydr Res* (2014) 396:62–9. doi: 10.1016/j.carres.2014.07.013
- Calarese DA, Scanlan CN, Zwirk MB, Deechongkit S, Mimura Y, Kunert R, et al. Antibody Domain Exchange Is an Immunological Solution to Carbohydrate Cluster Recognition. *Science* (2003) 300:2065–71. doi: 10.1126/science.1083182
- Doherty M, McManus CA, Duke R, Rudd PM. High-Throughput Quantitative N-Glycan Analysis of Glycoproteins. *Methods Mol Biol* (2012) 899:293–313. doi: 10.1007/978-1-61779-921-1_19
- Hilliard M, Alley WR Jr., McManus CA, Yu YQ, Hallinan S, Gebler J, et al. Glycan Characterization of the NIST RM Monoclonal Antibody Using a Total Analytical Solution: From Sample Preparation to Data Analysis. *MAbs* (2017) 9:1349–59. doi: 10.1080/19420862.2017.1377381
- Pucic M, Knezevic A, Vidic J, Adamczyk B, Novokmet M, Polasek O, et al. High Throughput Isolation and Glycosylation Analysis of IgG-Variability and Heritability of the IgG Glycome in Three Isolated Human Populations. *Mol Cell Proteomics* (2011) 10:M111.010090. doi: 10.1074/mcp.M111.010090
- Yu X, Baruah K, Harvey DJ, Vasiljevic S, Alonzi DS, Song BD, et al. Engineering Hydrophobic Protein-Carbohydrate Interactions to Fine-Tune Monoclonal Antibodies. *J Am Chem Soc* (2013) 135:9723–32. doi: 10.1021/ja4014375
- Houde D, Peng Y, Berkowitz SA, Engen JR. Post-Translational Modifications Differentially Affect IgG1 Conformation and Receptor Binding. *Mol Cell Proteomics* (2010) 9:1716–28. doi: 10.1074/mcp.M900540-MCP200
- Dekkers G, Treffers L, Plomp R, Bentlage AEH, de Boer M, Koeleman CAM, et al. Decoding the Human Immunoglobulin G-Glycan Repertoire Reveals a Spectrum of Fc-Receptor- and Complement-Mediated-Effector Activities. *Front Immunol* (2017) 8:877. doi: 10.3389/fimmu.2017.00877

40. Wada R, Matsui M, Kawasaki M, Nishimura N. Influence of N-Glycosylation on Effector Functions and Thermal Stability of Glycoengineered IgG1 Monoclonal Antibody With Homogeneous Glycoforms. *MAbs* (2019) 11:350–72. doi: 10.1080/19420862.2018.1551044
 41. Campbell IK, Miescher S, Branch DR, Mott PJ, Lazarus AH, Han D, et al. Therapeutic Effect of IVIG on Inflammatory Arthritis in Mice is Dependent on the Fc Portion and Independent of Sialylation or Basophils. *J Immunol* (2014) 192:5031–8. doi: 10.4049/jimmunol.1301611
 42. Guhr T, Bloem J, Derksen NI, Wuhrer M, Koenderman AH, Aalberse RC, et al. Enrichment of Sialylated IgG by Lectin Fractionation Does Not Enhance the Efficacy of Immunoglobulin G in a Murine Model of Immune Thrombocytopenia. *PLoS One* (2011) 6:e21246. doi: 10.1371/journal.pone.0021246
 43. Leontyev D, Katsman Y, Ma XZ, Miescher S, Kasermann F, Branch DR. Sialylation-Independent Mechanism Involved in the Amelioration of Murine Immune Thrombocytopenia Using Intravenous Gammaglobulin. *Transfusion* (2012) 52:1799–805. doi: 10.1111/j.1537-2995.2011.03517.x
 44. Washburn N, Schwab I, Ortiz D, Bhatnagar N, Lansing JC, Medeiros A, et al. Controlled Tetra-Fc Sialylation of IVIg Results in a Drug Candidate With Consistent Enhanced Anti-Inflammatory Activity. *Proc Natl Acad Sci USA* (2015) 112:E1297–306. doi: 10.1073/pnas.1422481112
 45. Ferrara C, Grau S, Jager C, Sondermann P, Brunner P, Waldhauer I, et al. Unique Carbohydrate-Carbohydrate Interactions are Required for High Affinity Binding Between FcγRIIIb and Antibodies Lacking Core Fucose. *Proc Natl Acad Sci USA* (2011) 108:12669–74. doi: 10.1073/pnas.1108455108
 46. Mizushima T, Yagi H, Takemoto E, Shibata-Koyama M, Isoda Y, Iida S, et al. Structural Basis for Improved Efficacy of Therapeutic Antibodies on Defucosylation of Their Fc Glycans. *Genes Cells* (2011) 16:1071–80. doi: 10.1111/j.1365-2443.2011.01552.x
 47. Ghirlando R, Lund J, Goodall M, Jefferis R. Glycosylation of Human IgG-Fc: Influences on Structure Revealed by Differential Scanning Micro-Calorimetry. *Immunol Lett* (1999) 68:47–52. doi: 10.1016/S0165-2478(99)00029-2
 48. Wormald MR, Rudd PM, Harvey DJ, Chang SC, Scragg IG, Dwek RA. Variations in Oligosaccharide-Protein Interactions in Immunoglobulin G Determine the Site-Specific Glycosylation Profiles and Modulate the Dynamic Motion of the Fc Oligosaccharides. *Biochemistry* (1997) 36:1370–80. doi: 10.1021/bi9621472
 49. Aoyama M, Hashii N, Tsukimura W, Osumi K, Harazono A, Tada M, et al. Effects of Terminal Galactose Residues in Mannose Alpha1-6 Arm of Fc-Glycan on the Effector Functions of Therapeutic Monoclonal Antibodies. *MAbs* (2019) 11:826–36. doi: 10.1080/19420862.2019.1608143
 50. Deisenhofer J. Crystallographic Refinement and Atomic Models of a Human Fc Fragment and its Complex With Fragment B of Protein A From *Staphylococcus Aureus* at 2.9- and 2.8-Å Resolution. *Biochemistry* (1981) 20:2361–70. doi: 10.1021/bi00512a001
 51. Sondermann P, Huber R, Oosthuizen V, Jacob U. The 3.2-Å Crystal Structure of the Human IgG1 Fc Fragment-FcγRIIIb Complex. *Nature* (2000) 406:267–73. doi: 10.1038/35018508
 52. Krapp S, Mimura Y, Jefferis R, Huber R, Sondermann P. Structural Analysis of Human IgG-Fc Glycoforms Reveals a Correlation Between Glycosylation and Structural Integrity. *J Mol Biol* (2003) 325:979–89. doi: 10.1016/S0022-2836(02)01250-0
 53. Ahmed AA, Giddens J, Pincetic A, Lomino JV, Ravetch JV, Wang LX, et al. Structural Characterization of Anti-Inflammatory Immunoglobulin G Fc Proteins. *J Mol Biol* (2014) 426:3166–79. doi: 10.1016/j.jmb.2014.07.006
 54. Chen CL, Hsu JC, Lin CW, Wang CH, Tsai MH, Wu CY, et al. Crystal Structure of a Homogeneous IgG-Fc Glycoform With the N-Glycan Designed to Maximize the Antibody Dependent Cellular Cytotoxicity. *ACS Chem Biol* (2017) 12:1335–45. doi: 10.1021/acscchembio.7b00140
 55. Okazaki A, Shoji-Hosaka E, Nakamura K, Wakitani M, Uchida K, Kakita S, et al. Fucose Depletion From Human IgG1 Oligosaccharide Enhances Binding Enthalpy and Association Rate Between IgG1 and FcγRIIIa. *J Mol Biol* (2004) 336:1239–49. doi: 10.1016/j.jmb.2004.01.007
 56. Li T, DiLillo DJ, Bournazos S, Giddens JP, Ravetch JV, Wang LX. Modulating IgG Effector Function by Fc Glycan Engineering. *Proc Natl Acad Sci USA* (2017) 114:3485–90. doi: 10.1073/pnas.1702173114
 57. Parekh RB, Dwek RA, Sutton BJ, Fernandes DL, Leung A, Stanworth D, et al. Association of Rheumatoid Arthritis and Primary Osteoarthritis With Changes in the Glycosylation Pattern of Total Serum IgG. *Nature* (1985) 316:452–7. doi: 10.1038/316452a0
 58. Bondt A, Selman MH, Deelder AM, Hazes JM, Willemsen SP, Wuhrer M, et al. Association Between Galactosylation of Immunoglobulin G and Improvement of Rheumatoid Arthritis During Pregnancy is Independent of Sialylation. *J Proteome Res* (2013) 12:4522–31. doi: 10.1021/pr400589m
 59. Gornik I, Maravic G, Dumic J, Fogel M, Lauc G. Fucosylation of IgG Heavy Chains is Increased in Rheumatoid Arthritis. *Clin Biochem* (1999) 32:605–8. doi: 10.1016/s0009-9120(99)00060-0
 60. Fokkink WJ, Selman MH, Dordland JR, Durmus B, Kuitwaard K, Huizinga R, et al. IgG Fc N-Glycosylation in Guillain-Barre Syndrome Treated With Immunoglobulins. *J Proteome Res* (2014) 13:1722–30. doi: 10.1021/pr401213z
 61. Prevot J, Jolles S. Global Immunoglobulin Supply: Steaming Towards the Iceberg? *Curr Opin Allergy Clin Immunol* (2020) 20:557–64. doi: 10.1097/ACI.0000000000000696
 62. Zuercher AW, Spirig R, Baz Morelli A, Rowe T, Kasermann F. Next-Generation Fc Receptor-Targeting Biologics for Autoimmune Diseases. *Autoimmun Rev* (2019) 18:102366. doi: 10.1016/j.autrev.2019.102366
 63. Fitzpatrick EA, Wang J, Strome SE. Engineering of Fc Multimers as a Protein Therapy for Autoimmune Disease. *Front Immunol* (2020) 11:496:496. doi: 10.3389/fimmu.2020.00496
 64. Nezlín R, Ghetie V. Interactions of Immunoglobulins Outside the Antigen-Combining Site. *Adv Immunol* (2004) 82:155–215. doi: 10.1016/S0065-2776(04)82004-2
 65. Herth FJF, Sakoulas G, Haddad F. Use of Intravenous Immunoglobulin (Prevacen or Octagam) for the Treatment of COVID-19: Retrospective Case Series. *Respiration* (2020) 99:1145–53. doi: 10.1159/000511376
 66. Fajenbaum DC, June CH. Cytokine Storm. *N Engl J Med* (2020) 383:2255–73. doi: 10.1056/NEJMr2026131
 67. Chakraborty S, Gonzalez J, Edwards K, Mallajosyula V, Buzzanco AS, Sherwood R, et al. Proinflammatory IgG Fc Structures in Patients With Severe COVID-19. *Nat Immunol* (2021) 22:67–73. doi: 10.1038/s41590-020-00828-7
 68. Wang TT, Sewatanon J, Memoli MJ, Wrammert J, Bournazos S, Bhaumik SK, et al. IgG Antibodies to Dengue Enhanced for FcγRIIIa Binding Determine Disease Severity. *Science* (2017) 355:395–8. doi: 10.1126/science.aaa8128
 69. Bournazos S, Gupta A, Ravetch JV. The Role of IgG Fc Receptors in Antibody-Dependent Enhancement. *Nat Rev Immunol* (2020) 20:633–43. doi: 10.1038/s41577-020-00410-0
 70. Larsen MD, de Graaf EL, Sonneveld ME, Plomp HR, Nouta J, Hoepel W, et al. Afucosylated IgG Characterizes Enveloped Viral Responses and Correlates With COVID-19 Severity. *Science* (2021) 371:eabc8378. doi: 10.1126/science.abc8378
- Conflict of Interest:** The authors declare that the research was conducted in the absence of any commercial or financial relationships that could be construed as a potential conflict of interest.
- Publisher's Note:** All claims expressed in this article are solely those of the authors and do not necessarily represent those of their affiliated organizations, or those of the publisher, the editors and the reviewers. Any product that may be evaluated in this article, or claim that may be made by its manufacturer, is not guaranteed or endorsed by the publisher.
- Copyright © 2022 Mimura, Mimura-Kimura, Saldova, Rudd and Jefferis. This is an open-access article distributed under the terms of the Creative Commons Attribution License (CC BY). The use, distribution or reproduction in other forums is permitted, provided the original author(s) and the copyright owner(s) are credited and that the original publication in this journal is cited, in accordance with accepted academic practice. No use, distribution or reproduction is permitted which does not comply with these terms.

Conflict of Interest: The authors declare that the research was conducted in the absence of any commercial or financial relationships that could be construed as a potential conflict of interest.

Publisher's Note: All claims expressed in this article are solely those of the authors and do not necessarily represent those of their affiliated organizations, or those of the publisher, the editors and the reviewers. Any product that may be evaluated in this article, or claim that may be made by its manufacturer, is not guaranteed or endorsed by the publisher.

Copyright © 2022 Mimura, Mimura-Kimura, Saldova, Rudd and Jefferis. This is an open-access article distributed under the terms of the Creative Commons Attribution License (CC BY). The use, distribution or reproduction in other forums is permitted, provided the original author(s) and the copyright owner(s) are credited and that the original publication in this journal is cited, in accordance with accepted academic practice. No use, distribution or reproduction is permitted which does not comply with these terms.



GlycoFibroTyper: A Novel Method for the Glycan Analysis of IgG and the Development of a Biomarker Signature of Liver Fibrosis

Danielle A. Scott¹, Mengjun Wang², Stephane Grauzam², Sarah Pippin¹, Alyson Black², Peggi M. Angel², Richard R. Drake², Stephen Castellino¹, Yuko Kono³, Don C. Rockey⁴ and Anand S. Mehta^{2*}

¹ Glycopath, Inc., Charleston, SC, United States, ² Department of Cell and Molecular Pharmacology & Experimental Therapeutics, Medical University of South Carolina, Charleston, SC, United States, ³ Department of Medicine, Gastroenterology and Hepatology, University of California San Diego, San Diego, CA, United States, ⁴ Digestive Disease Research Center, Medical University of South Carolina, Charleston, SC, United States

OPEN ACCESS

Edited by:

Irena Trbojević-Akmačić,
Genos Glycoscience Research
Laboratory, Croatia

Reviewed by:

Frederico Alisson-Silva,
Federal University of Rio de Janeiro,
Brazil
Claire Carter,
Hackensack Meridian Health,
United States

*Correspondence:

Anand S. Mehta
mehtaa@musc.edu

Specialty section:

This article was submitted to
B Cell Biology,
a section of the journal
Frontiers in Immunology

Received: 18 October 2021

Accepted: 14 January 2022

Published: 07 February 2022

Citation:

Scott DA, Wang M, Grauzam S,
Pippin S, Black A, Angel PM,
Drake RR, Castellino S, Kono Y,
Rockey DC and Mehta AS (2022)
GlycoFibroTyper: A Novel Method
for the Glycan Analysis of IgG
and the Development of a Biomarker
Signature of Liver Fibrosis.
Front. Immunol. 13:797460.
doi: 10.3389/fimmu.2022.797460

Our group has recently developed the GlycoTyper assay which is a streamlined antibody capture slide array approach to directly profile N-glycans of captured serum glycoproteins including immunoglobulin G (IgG). This method needs only a few microliters of serum and utilizes a simplified processing protocol that requires no purification or sugar modifications prior to analysis. In this method, antibody captured glycoproteins are treated with peptide N-glycosidase F (PNGase F) to release N-glycans for detection by MALDI imaging mass spectrometry (IMS). As alterations in N-linked glycans have been reported for IgG from large patient cohorts with fibrosis and cirrhosis, we utilized this novel method to examine the glycosylation of total IgG, as well as IgG1, IgG2, IgG3 and IgG4, which have never been examined before, in a cohort of 106 patients with biopsy confirmed liver fibrosis. Patients were classified as either having no evidence of fibrosis (41 patients with no liver disease or stage 0 fibrosis), early stage fibrosis (10 METAVIR stage 1 and 18 METAVIR stage 2) or late stage fibrosis (6 patients with METAVIR stage 3 fibrosis and 37 patients with METAVIR stage 4 fibrosis (cirrhosis)). Several major alterations in glycosylation were observed that classify patients as having no fibrosis (sensitivity of 92% and a specificity of 90%), early fibrosis (sensitivity of 84% with 90% specificity) or significant fibrosis (sensitivity of 94% with 90% specificity).

Keywords: glycosylation, immunoglobulin, fibrosis, cirrhosis, biomarker

INTRODUCTION

Cirrhosis is the result of chronic liver injury and leads to replacement of the normal liver architecture by fibrotic scar tissue, and is associated with a concomitant decline of liver function and devastating clinical complications (1). Many different underlying processes cause cirrhosis: chronic viral infection by hepatitis B virus (HBV) and/or hepatitis C virus (HCV) have been

historically among the most common etiologies, but non-alcoholic fatty liver disease and ethanol are currently emerging as the leading causes of chronic liver disease worldwide.

For HBV and/or HCV infected patients, treatment decisions are based upon a variety of factors, including elevated levels of hepatic transaminases which may reflect the degree of hepatic inflammation and perhaps fibrosis when combined with other features such as platelet count (2, 3). Historically, in individuals with HBV or HCV, advanced fibrosis and cirrhosis are considered justifications to begin antiviral therapy (2, 4, 5). More importantly, the determination of hepatic fibrosis is critical to stage the severity of the liver disease and has been associated with prognosis (6). Therefore, it is extremely important to determine the presence of significant fibrosis and cirrhosis. Although liver biopsy has been historically the gold standard for assessment of fibrosis (7) noninvasive assessment of fibrosis is less intrusive and will allow for routine clinical monitoring.

Analysis of disease associated changes in total N-glycan compositions of serum and plasma in large patient cohorts has been previously reported (8, 9). There has also been extensive evaluation of disease-associated alterations of immunoglobulin G N-linked glycans in large sample cohorts in patients with rheumatoid arthritis, digestive diseases, heart disease, cancer and liver fibrosis (10–34). In the case of liver fibrosis, two analytical methods have identified alterations in N-linked glycosylation on both total IgG populations and on specific IgG molecules. Both methods can detect cirrhosis with a high degree of accuracy and are also able to detect intermediate levels of fibrosis (11, 16). However, both analytical methods have drawbacks. One approach utilizes a capillary electrophoresis-based analysis of N-linked glycans on total serum following release of glycans using PNGase F, labeling of the released glycans using a fluorescent dye, and electrophoresis of the released glycans for peak identification (11). While this method works well, it is both time and labor intensive. Another method for liver fibrosis identification from serum utilizes a plate-based ELISA format to detect altered glycosylation using a sugar binding protein called a lectin (16). This test is hampered by the poor specificity of lectins and the limited readout (i.e. binding or not). Both of these methods require specialized sample handling resources, extensive processing and purification prior to analysis, and are expensive in regard to reagents and processing.

Our group has recently developed the GlycoTyper, a streamlined antibody capture slide array approach to directly profile N-glycans of captured serum glycoproteins like IgG. The method needs only a few microliters of serum and utilizes simplified processing workflows that requires no purification or sugar derivatizations as a part of the analysis. In this method, N-linked glycans are released from antibody captured glycoproteins and are directly analyzed by MALDI IMS, building on the utility of MALDI MS glycan imaging developed in our laboratories (35–48). Here, we have used the GlycoTyper to demonstrate its ability to measure changes in the N-linked glycans on IgG subtypes and serve as a surrogate marker of liver disease.

MATERIALS AND METHODS

Patients

Samples were from two main sources. The first was from the University of California at San Diego and the second from the Medical University of South Carolina. In both cases, the study protocol was approved by the appropriate Institutional Review Board and written informed consent was obtained from each subject. Demographic and clinical information was obtained, and a blood sample was collected from each subject. All liver biopsies were graded using the METAVIR scoring system (49). The etiology of the liver disease for the patients without viral infection was determined as previously described (50) and cirrhosis was determined based on histologic and/or clinical findings (i.e., clinical features of portal hypertension, with no alternative cause of portal hypertension). Details on all patients are provided in **Table 1**. A group of individuals with no history of liver disease, alcohol consumption less than 40 g a week, and no risk factors for viral hepatitis were utilized as controls. All subjects in this control group were documented to have normal liver biochemistry and negative HCV antibodies or HBV.

Antibody Array Preparation

The serum assay used a 24-well slide module (Grace -Bio Labs, Bend, OR) that was mounted to a nitrocellulose-coated microscope slides (Grace-Bio Labs, Bend, OR). Antibodies: anti-human (IgG (Bethyl Labs, Montgomery, TX) anti-IgG1 (Abcam, Cambridge, UK), anti-IgG2, anti IgG-3, and anti-IgG 4 (Bio-Rad,

TABLE 1 | Description of control patients and those with liver fibrosis.

Variables	Controls	Stage of Fibrosis (METAVIR) ¹				
		0	1	2	3	4
Sample Size	38	3	10	18	6	37
Age ²	51 ± 11	56 ± 7	50 ± 6	51 ± 4	51 ± 7	55 ± 8
% NHW/AA/H/Asian ³	NA	100/0/0/0	98/1/1/0	96/2/1/1	100/0/0/0	98/0/1/0
ALT (IU/mL) ⁴	NA	75 ± 7	71 ± 11	78 ± 9	72 ± 12	85 ± 26
AST (IU/mL) ⁵	NA	73 ± 5	69 ± 8	77 ± 10	78 ± 13	108 ± 24
Total Bilirubin (mg/dL)	NA	0.3 ± 0.2	0.3 ± 0.4	0.5 ± 0.4	0.9 ± 1.2	1.2 ± 1.3

¹Fibrosis staging based upon METAVIR scoring system. ²Mean age in years. ³NHW, non-Hispanic White; AA, African American; H, Hispanic; ⁴ALT, alanine aminotransferase; ⁵AST, aspartate aminotransferase. NA, not applicable.

Hercules, CA), were diluted in PBS and manually spotted in wells at 200 ng per 1.5 μ L spot. Spots were then left to adhere overnight at 4°C in a humidity chamber made from cell culture dishes lined with a Wypall X 60 paper towel and two rolled KimWipes saturated with distilled water. Slides were then placed in a vacuum desiccator to dry at room temperature and rinsed for 1 minute with 200 μ L 0.1% octyl- β -D-glucopyranoside in PBS (referred to as PBS-OGS) per well to remove any unbound protein from the slide. More detail on slide preparation and the general GlycoTyper method can be found in (41, 42).

Sample Capture and N-Glycan Release

Antibody spots were blocked with 200 μ L of 2% BSA (prepared in PBS-OGS) per well for 1 h with gentle shaking, washed with 200 μ L PBS (3 min \times 2) and 200 μ L double distilled water (1 min \times 1) per well and dried in a desiccator. Pure protein (0.5 μ g in 100 μ L) or serum samples (diluted 1:100 in PBS to a total volume of 100 μ L) were added to wells and incubated at room temperature for 2 hours in a humidity chamber with gentle shaking. Pure proteins: human IgG (Jackson ImmunoResearch Laboratories, West Grove, PA), human IgG1, IgG2, IgG3 and IgG4 (Abcam, Cambridge, UK). Wells were then serially washed with 200 μ L of PBS-OGS (1 min \times 2), 200 μ L PBS (3 min \times 2), 200 μ L double distilled water (1 min \times 2), and dried. The well module was removed, and slides were dried in a vacuum desiccator. PNGase F Prime PRIME-LY (N-Zyme Scientifics, Doylestown, PA) (0.1 μ g/ μ L in HPLC grade water) was applied to the slides using an automated sprayer (M5 TM-Sprayer, HTX Technologies, Chapel Hill, NC). Spatial localization to each capture spot was accomplished using spraying parameters of 15 passes at 45°C, 10 psi, flow rate of 25 μ L/min, and 1200 mm/min velocity. Slides were incubated overnight at 37°C in humidity chambers made in cell culture dishes with Wypall X 60 paper towels and two rolled KimWipes saturated with distilled water.

MALDI MS Preparation and Imaging

MALDI matrix α -cyano-4-hydroxycinnamic acid (CHCA, 7 mg/mL in 50% acetonitrile/0.1% trifluoroacetic acid) (Cayman Chemical, Ann Arbor, MI) was applied to slides using the same automated sprayer. Matrix was sprayed for two passes at 77°C, 10 psi, 1300 mm/min velocity, and flow rate of 100 μ L/min. MALDI IMS data were acquired on a solariX Legacy 7T FT-ICR mass spectrometer (Bruker, Billerica, MA) equipped with a SmartBeam II laser operating at 2000 Hz and pixel dimension of 25 μ m. Images were collected using a smartwalk pattern at a 300 μ m raster with 200 laser shots per pixel. Samples were analyzed in positive ion with a mass range of 500–5000 m/z using a 512k word time domain. An on-slide resolving power of 58,000 at m/z 1501 was calculated.

Data Analysis

N-Glycan localization and intensity were visualized using FlexImaging v5.0 (Bruker), with data imported at a 0.98 ICR reduction noise threshold. Images were normalized to total ion current, and N-glycan peaks were selected manually based on their theoretical mass values. For quantification of peaks at individual spots, spectra were imported into SCiLS Lab

software 2017a (Bruker). Each spot was designated a unique region, and area under monoisotopic peak values were exported from each region and quantified by mean peak intensity. In all cases, glycan peaks (specific m/z values) were given a relative percentile of the total glycan profile. Glycan names are provided using the Oxford Nomenclature (51).

Statistical Analysis

Patients were grouped as those: i) without any liver disease (healthy and stage 0), ii) with early to moderate fibrosis (stage 1 & 2), and iii) with advanced fibrosis or cirrhosis (stage 3 & 4). One-way ANOVA and *Post hoc* tests were applied to inference any statistical difference among these three stages. Glycans with no statistical difference among stages ($p > 0.05$, F-test) were discarded from further model development.

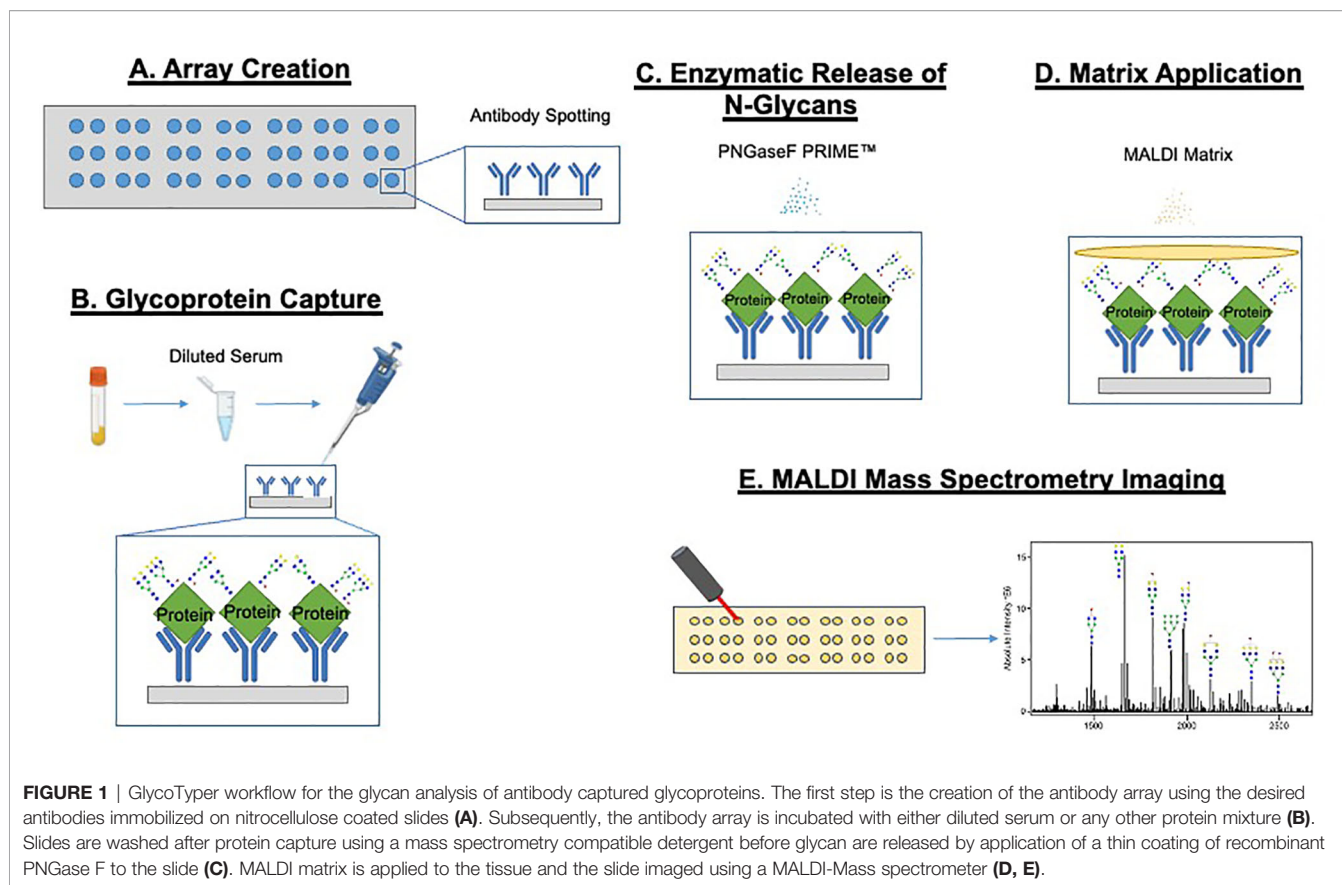
Subsequently, we applied the supervised learning algorithm random forest to determine the relative importance of the remaining features (glycans). Simultaneously, we applied variable clustering to perform a hierarchical cluster analysis, which is based on the similarity matrix that contains pairwise Hoeffding D statistics (52). From the variable clustering output, the most highly correlated two features were identified. These two features' relative importance were derived from random forest analysis. We discarded one of these pairs with lower importance. Then we utilized the remaining features in Apparent Cross-Validation, Leave-One-Out Cross-Validation, 3-Fold Random Subsampling Cross-Validation, and Repeated 3-Fold Cross-Validation to evaluate predictive performance of the current random forest model (simulation 200 times for 3-Fold Random Subsampling Cross-Validation and Repeated 3-Fold Cross-Validation). Predictive accuracy (%), related sensitivity, specificity, positive predictive value (PPV), and negative predictive value (NPV) were criteria of model selection. The entire procedure (random forest, variable clustering; cross-validations) was iterated until the removal of any additional features resulted in the predictive ability of the model to consistently and dramatically deteriorated. The final model had the best predictive ability with the fewest features and was composed of glycans (features) from four of the IgG subtypes. These were A2G2F and A2BG0F on IgG, A2G1F and A2G2S1 on IgG1, A2G1F and A2G0F on IgG2 and A2BG1F on IgG3.

Finally, we evaluated our final model's discriminating ability between the following groups: no fibrosis vs moderate fibrosis, moderate vs later fibrosis, and no fibrosis vs later fibrosis. Four Cross-Validations listed above was applied and the corresponding AUCs (area under the curve), specificities, sensitivities, PPVs, and NPVs were derived.

More detail on feature selection, cross validation and model development can be found in the **Supplementary Evidence File**.

RESULTS

The basic GlycoTyper workflow for the glycan analysis of antibody captured glycoproteins is shown in **Figure 1**. Briefly, the first step is the creation of the antibody array using the desired antibodies immobilized on nitrocellulose



coated slides (**Figure 1A**). Subsequently, the antibody array is incubated with either diluted serum or pure protein as shown in **Figure 1B**. Slides are washed after protein capture using a mass spectrometry compatible detergent before glycans are released by application of a thin coating of recombinant PNGase F PRIME™ to the slide (**Figure 1C**). This step is identical to what is performed in tissue glycan imaging (35, 42). Lastly, MALDI matrix is applied to the slide and is imaged using a MALDI Mass Spectrometer (**Figures 1D, E**). Importantly, the spatial localization provided by the IMS data link the detected glycans to their corresponding captured glycoproteins.

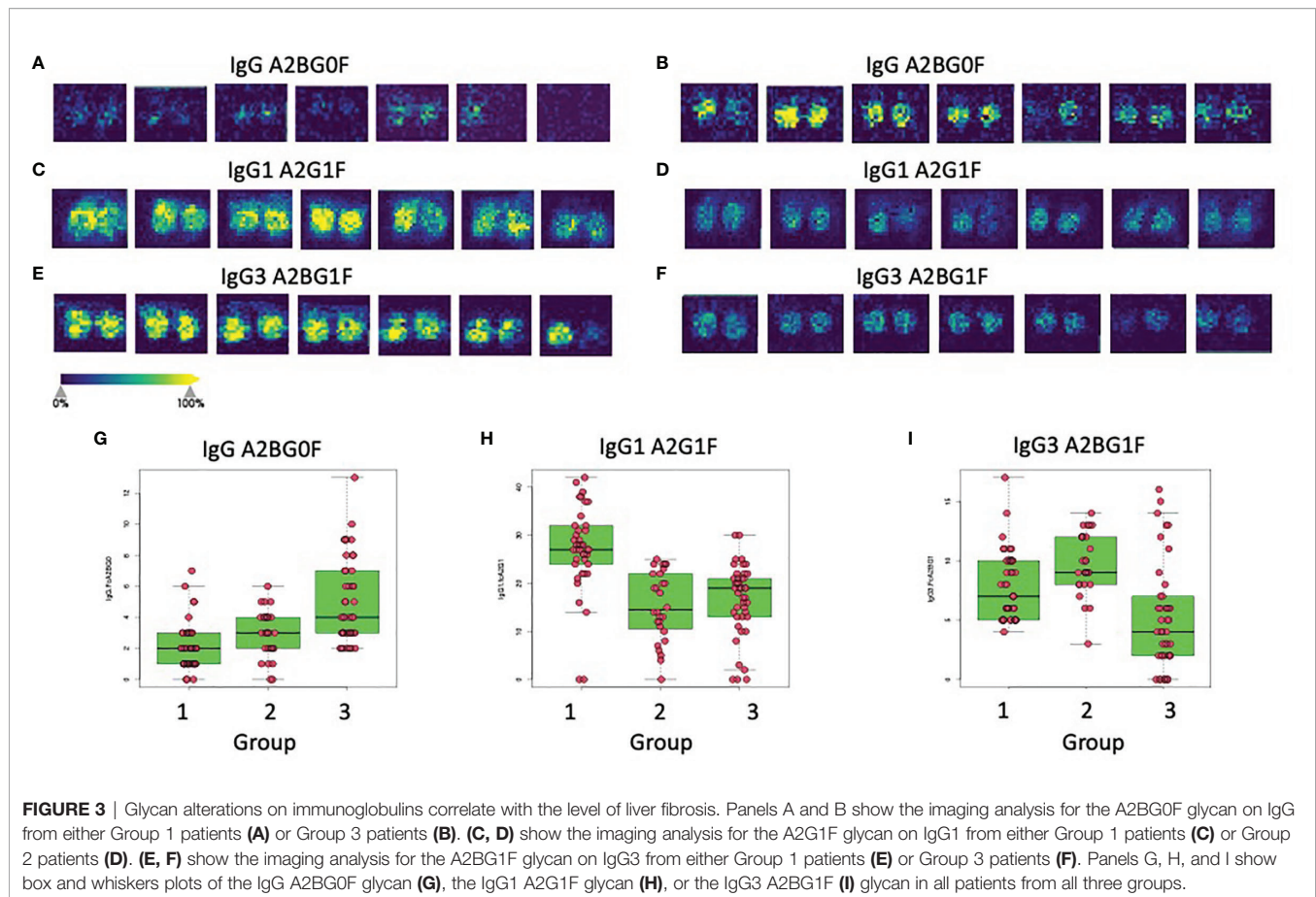
In initial studies, we examined the glycans on IgG, IgG1, IgG2, IgG3 and IgG4 captured *via* antibody from pure proteins spiked into PBS or from healthy serum diluted in PBS. As **Figure 2** shows for all proteins, the glycan observed from the pure protein was similar to that observed from captured human serum, with little difference in the glycosylation observed on the pure protein and that observed from the serum captured protein (with a single exception). The major exception was a glycan at m/z 1976.7822, which matches by accurate mass to a bi-antennary glycan with a single sialic acid (A2G2S1). In all cases, the level of this glycan was lower in the pure protein than that observed in human serum. In addition, a glycan at a glycan at m/z 1809.73273, which matches by accurate mass to a bi-antennary glycan with a single fucose residue was also varied in IgG2 and IgG3. **Supplementary Table S1** shows all the glycans found associated with IgG, IgG1, IgG2,

IgG3 or IgG4 and **Supplementary Figure S1** shows a column chart of the data in **Figure 1**.

The major glycan observed for each immunoglobulin subtype was a fucosylated biantennary glycan with single or double galactose residues, with or without a bisecting N-acetyl glucosamine (**Figure 2**). It is noted that the glycan profile observed from both samples was consistent with the glycan profile observed by other methods for these proteins (16, 53–59).

Simultaneous Analysis of the Glycans on IgG, IgG1, IgG2, IgG3 and IgG4 in Patients With Liver Fibrosis

As previously reported, the glycosylation of IgG is altered with the development of liver fibrosis and cirrhosis and therefore can be used as a non-invasive measure of liver disease (11, 16, 18, 20, 30). Thus, the GlycoTyper method described in **Figure 1** was used for the analysis of a cohort of patients with biopsy confirmed fibrosis (**Table 1**). In total, 38 healthy individuals with no evidence of liver disease, 3 patients with stage 0 fibrosis (METAVIR), 10 patients with stage 1 fibrosis (METAVIR), 18 patients with stage 2 fibrosis (METAVIR), 6 patients with stage 3 fibrosis (METAVIR) and 37 patients with stage 4 fibrosis (METAVIR) were analyzed using this method. Because of the limited patient number, we grouped samples into three categories: i) those who are healthy with no fibrosis (healthy & METAVIR stage 0; $n=41$), ii) those with early to moderate fibrosis (METAVIR stages 1&2, $n=28$), and iii) those



(Figures 3E, F). As Figures 3E, F demonstrate, this glycan was found at high levels in either healthy patients or patients with stage 0 fibrosis but was reduced dramatically in those with cirrhosis (Figure 3F).

The expression levels of both of these glycans also varied within the larger patient groups. In the case of IgG, the A2BG0F glycan increased from Group 1 to Group 2 and was the highest in Group 3, showing increased levels with increased fibrosis (Figure 3G). In contrast, IgG1 associated A2G1F glycan was reduced in patients with both limited and severe fibrosis and did not correlate with the state of fibrosis (Figure 3H). Other glycans such as the A2BG1F glycan on IgG3, was only reduced in patients with more significant fibrosis (Group 3, Figure 3I). A complete list of glycans that were altered in both those with mild to moderate fibrosis and those glycans altered with more significant fibrosis are shown in Table 2.

Development of a Model to Determine the Level of Liver Fibrosis in Individuals Based Upon the IgG Glycan Profile

Based on our previous algorithm development work for the early detection of HCC (34, 60–62), we developed a random forest algorithm that could be used to differentiate individuals with early fibrosis (Group 2) from healthy controls (Group 1) as well as identify late fibrosis patients (Group 3) from those with early

fibrosis (Group 2). **Supplementary Table S2** shows the glycans that were found to be associated with IgG, IgG1, IgG2, IgG3 or IgG4 in all patient groups along with the results following ANOVA analysis. Although there were 50 glycans on the five subtypes of IgG that were altered with the development of liver fibrosis, many of these were associated and thus, only seven glycans on four glycoproteins were used to build and test the model. These are shown in **Supplementary Tables S3, S4** and include, A2G2F and A2BG0F on IgG, A2G1F and A2G2S1 on IgG1, A2G1F and A2G0F on IgG2 and A2BG1F on IgG3. **Figure 4A** shows the AUC (area under the curve) of the model following leave one out cross validation (LOOCV) when differentiating Group 1 (healthy and stage 0) from those with early or moderate fibrosis (Group 2; METAVIR stage 1 or 2). The AUC was 0.9530 (95%CI: 0.9008–1.0) for differentiating these two groups with a sensitivity of 94% at 90% specificity. Similar results were obtained using three-fold cross validation (3CV) (data not shown). When we compared those with early to moderate fibrosis (stage 1&2) to those with severe fibrosis or cirrhosis (stage 3 & 4), the AUC was 0.9377 (95%CI: 0.8819–0.9935) with a sensitivity of 84% at 90% specificity (Figure 4B). A further comparison was made to demonstrate that the AUC for differentiating those with no liver disease from those with significant fibrosis/cirrhosis (Figure 4C) and in this case, the AUC was 0.9745 (95%CI: 0.9415–1) with 98% sensitivity at 90% specificity. The

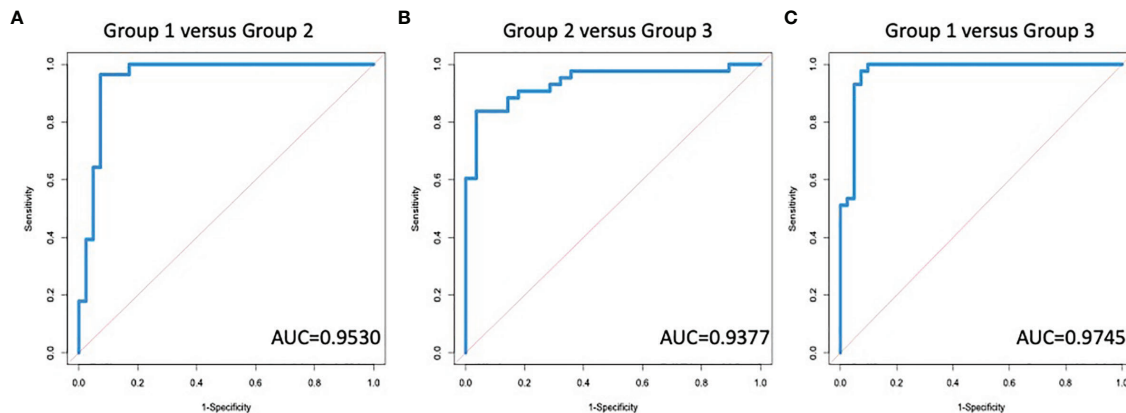


FIGURE 4 | A Diagnostic algorithm based upon IgG glycans can identify the degree of fibrosis in patients with liver disease. AUROC for the differentiation of **(A)** group 1 (no fibrosis) versus group 2 (early to moderate fibrosis); **(B)** group 2 versus group 3 (significant fibrosis or cirrhosis); or **(C)** group 1 versus group 3.

sensitivity, specificity, positive and negative predictive values of the assay for differentiating the different groups are shown in **Supplementary Tables S5–S7**. In addition, a comparison between our assay and other noninvasive assays for the detection of liver fibrosis is shown in **Supplementary Table S8**. It is noted that in **Supplementary Table S8** the assay performance for the detection of ≥ 2 fibrosis or ≥ 4 fibrosis is compared, as these are the data most often presented for other markers.

We also examined the ability of these glycans (**Supplementary Figure S1**) to differentiate different groups of patients, specifically, those with no or early fibrosis (healthy and stage 0&1) from those with moderate to significant fibrosis (stage 2&3) and those with cirrhosis (stage 4) from those with moderate to significant fibrosis (stage 2&3). The AUC was 0.8464 (95%CI: 0.7576–0.9352) for differentiating those with no or early fibrosis (healthy versus stage 0&1) from those with moderate to significant fibrosis (stage 2&3) but 0.9673 (95%CI: 0.93–1.0) when differentiating cirrhosis from moderate to significant fibrosis. These findings highlight that changes in IgG glycosylation can be observed *via* the GlycoTyper method and used to determine the level of liver fibrosis in individuals with liver disease.

DISCUSSION

The GlycoTyper is an imaging mass spectrometry platform for the multiplexed detection of N-glycans from individual glycoproteins. This method is suitable for the analysis of immunoglobulin molecules from a wide variety of biological samples. The development of this technique was based on a well-established protocol for enzymatic release of N-glycans from tissue sections for MALDI IMS (63). In this platform, antibodies are essential for the specific capture of glycoprotein targets from a complex biological mixture, similar to an ELISA. However, unlike an ELISA, no secondary antibody or lectin is needed for this methodology as mass spectrometry provides sensitive and molecular specific detection of distinct N-glycans. Antibody capture also negates the

need for sample cleanup prior to MS analysis, which can be extensive (64).

We applied the GlycoTyper platform to the analysis of IgG glycans from patients with liver disease. As stated, changes in the glycosylation of immunoglobulins have been associated with liver fibrosis and cirrhosis previously and in many cases, those changes were detected with lectins or other indirect or laborious methods (16, 56). The results presented here show that these changes can be observed *via* the GlycoTyper method and furthermore, that these can be used to determine the level of liver fibrosis in individuals with liver disease. One of the major changes observed was an increase in the level of IgG associated glycans devoid of terminal galactose residues (**Figure 3**). This is a change that has been observed before and exploited with lectins (16). However, this was only one of numerous subtype specific glycan changes that were observed (**Figure 3**). These subtype specific glycan changes were used to create a diagnostic algorithm that could classify the level of fibrosis in individuals with high accuracy and specificity. It is noted that other glycoproteins have altered glycans in liver fibrosis and the methods described here could easily be applied to the analysis of those glycoproteins as well (65–69).

Our study was limited in part by the relatively small number of patients with histologically proven early stage liver disease (**Table 1**). This required clustering multiple patient groups together for further analysis. Consequently, patients were grouped into those with no fibrosis (Group 1), those with early to moderate fibrosis (Group 2) or late-stage fibrosis or cirrhosis (Group 3). We also attempted to classify patients into those with no to early fibrosis (healthy, stage 0&1), moderate to severe fibrosis (stage 2&3) and cirrhosis (stage 4). However, as shown in **Supplementary Figure S2**, diagnostic performance was poor in differentiating those with zero to early fibrosis from those with moderate to severe fibrosis. This was primarily the result of the stage 1 patients having an immunoglobulin glycan profile that was more similar to stage 2 patients than to stage 0 or healthy patients. This is an important point and clearly indicates that the

changes in glycosylation observed on immunoglobulins occurs early in fibrosis development. It is also noted that excellent discriminatory ability was observed between those with moderate to severe fibrosis and cirrhosis. However, this is most likely driven by the small number of patients with severe fibrosis ($n=6$) and the large glycan difference observed in patients with cirrhosis and moderate fibrosis. Larger, more diverse studies that include patients with different types of clinical liver diseases and a direct comparison to other non-invasive tests for cirrhosis required (3, 11, 70–73)

In conclusion, this study establishes a clinical rationale for integrating direct analysis of IgG glycans for the active management of people with liver disease. The diagnostic performance of this method was dramatically greater than other non-invasive tests for liver fibrosis (**Supplementary Table S8**), such as FIB4, APRI and even tests that look at IgG glycans (11, 16, 74). One reason for this is the ability to not just look at total IgG but also the specific IgG sub-classes, which has not been performed before, as such studies were not technically feasible for large patient cohorts. Thus, the methods described here are not only useful as a research tool for the analysis of protein specific glycosylation but also represents a new diagnostic platform that will allow for the true diagnostic potential of N-linked glycans to be developed.

DATA AVAILABILITY STATEMENT

The original contributions presented in the study are included in the article/**Supplementary Material**. Further inquiries can be directed to the corresponding author.

ETHICS STATEMENT

The studies involving human participants was reviewed and approved by the University of South California at San Diego and Medical University of South Carolina Review Board. The patients/participants provided their written informed consent to participate in research studies.

REFERENCES

1. Rockey DC, Bell PD, Hill JA. Fibrosis—a Common Pathway to Organ Injury and Failure. *N Engl J Med* (2015) 372:1138–49. doi: 10.1056/NEJMra1300575
2. Fung SK, Lok AS. Management of Hepatitis B Patients With Antiviral Resistance. *Antivir Ther* (2004) 9:1013–26.
3. Sterling RK, Lissen E, Clumeck N, Sola R, Correa MC, Montaner J, et al. Development of a Simple Noninvasive Index to Predict Significant Fibrosis in Patients With HIV/HCV Coinfection. *Hepatology* (2006) 43:1317–25. doi: 10.1002/hep.21178
4. Kweon YO, Goodman ZD, Dienstag JL, Schiff ER, Brown NA, Burchardt E, et al. Decreasing Fibrogenesis: An Immunohistochemical Study of Paired Liver Biopsies Following Lamivudine Therapy for Chronic Hepatitis B. *J Hepatol* (2001) 35:749–55. doi: 10.1016/S0168-8278(01)00218-5
5. Sherman M. Hepatocellular Carcinoma: Epidemiology, Risk Factors, and Screening. *Semin Liver Dis* (2005) 25:143–54. doi: 10.1055/s-2005-871194
6. Liaw YF. Results of Lamivudine Trials in Asia. *J Hepatol* (2003) 39(Suppl 1): S111–5. doi: 10.1016/S0168-8278(03)00155-7

AUTHOR CONTRIBUTIONS

DS was involved in performance of assay, assay design, data analysis and writing of manuscript. MW was responsible of statistics and algorithm development. SG and SP were involved in performance of assay. AB was responsible for experimental design and assay development. PA, RD, and SC were involved in conceptualization of assay, data analysis and writing of manuscript. YK and DR provided samples for patient analysis, data analysis, editing of manuscript. AM was involved with conceptualization of assay design, data analysis and writing of manuscript. All authors contributed to the article and approved the submitted version.

FUNDING

NIH/NIDDK: R41 DK124058. The goal is to develop a mass spectrometry based method for the detection of liver fibrosis. NIH/NCI: U01 CA242096. The goals of the grant are to develop rapid glycan analysis workflows using basic MALDI-TOF MS instrumentation common to most institutions. Slide-based analysis of N-glycans from immunoglobulin classes, immune cells and cells grown in culture on slides is emphasized. NIH/NCI: R01CA237659. The goal of this grant is to develop and validate a promising biomarker for the early detection of hepatocellular carcinoma. NIH/NCI: U01 CA226052. The goals are to determine the genetic basis of alterations in N-linked glycosylation observed (fucose or tetra-antennary glycan) in liver cancer typed by genetic classifications, and determine serum glycoproteins that directly reflect these changes for use as cancer biomarkers.

SUPPLEMENTARY MATERIAL

The Supplementary Material for this article can be found online at: <https://www.frontiersin.org/articles/10.3389/fimmu.2022.797460/full#supplementary-material>

7. Rockey DC, Caldwell SH, Goodman ZD, Nelson RC, Smith AD American Association for the Study of Liver, D. Liver Biopsy. *Hepatology* (2009) 49:1017–44. doi: 10.1002/hep.22742
8. Mehta A, Block TM. Fucosylated Glycoproteins as Markers of Liver Disease. *Dis Markers* (2008) 25:259–65. doi: 10.1155/2008/264594
9. Gudeli I, Lauc G, Pezer M. Immunoglobulin G Glycosylation in Aging and Diseases. *Cell Immunol* (2018) 333:65–79. doi: 10.1016/j.cellimm.2018.07.009
10. Callewaert N, Schollen E, Vanhecke A, Jaeken J, Matthijs G, Contreras R. Increased Fucosylation and Reduced Branching of Serum Glycoprotein N-Glycans in All Known Subtypes of Congenital Disorder of Glycosylation I. *Glycobiology* (2003) 13:367–75. doi: 10.1093/glycob/cwg040
11. Callewaert N, Van Vlierberghe H, Van Hecke A, Laroy W, Delanghe J, Contreras R. Noninvasive Diagnosis of Liver Cirrhosis Using DNA Sequencer Based Total Serum Protein Glycomics. *Nat Med* (2004) 10:429–34. doi: 10.1038/nm1006
12. Block TM, Comunale MA, Lowman M, Steel LF, Romano PR, Fimmel C, et al. Use of Targeted Glycoproteomics to Identify Serum Glycoproteins That Correlate With Liver Cancer in Woodchucks and Humans. *Proc Natl Acad Sci USA* (2005) 102:779–84. doi: 10.1073/pnas.0408928102

13. Marrero JA, Romano PR, Nikolaeva O, Steel L, Mehta A, Fimmel CJ, et al. GP73, a Resident Golgi Glycoprotein, Is a Novel Serum Marker for Hepatocellular Carcinoma. *J Hepatol* (2005) 43:1007–12. doi: 10.1016/j.jhep.2005.05.028
14. Comunale MA, Lowman M, Long RE, Krakover J, Philip R, Seeholzer S, et al. Proteomic Analysis of Serum Associated Fucosylated Glycoproteins in the Development of Primary Hepatocellular Carcinoma. *J Proteome Res* (2006) 5:308–15. doi: 10.1021/pr050328x
15. Liu XE, Desmyter L, Gao CF, Laroy W, Dewaele S, Vanhooren V, et al. N-Glycomic Changes in Hepatocellular Carcinoma Patients With Liver Cirrhosis Induced by Hepatitis B Virus. *Zhonghua gan zang Bing Za Zhi = Zhonghua Ganzangbing Zazhi = Chin J Hepatol* (2008) 16:74–5. doi: 10.1002/hep.21855
16. Mehta AS, Long RE, Comunale MA, Wang M, Rodemich L, Krakover J, et al. Increased Levels of Galactose-Deficient Anti-Gal Immunoglobulin G in the Sera of Hepatitis C Virus-Infected Individuals With Fibrosis and Cirrhosis. *J Virol* (2008) 82:1259–70. doi: 10.1128/JVI.01600-07
17. Norton PA, Comunale MA, Krakover J, Rodemich L, Pirog N, D'amelio A, et al. N-Linked Glycosylation of the Liver Cancer Biomarker GP73. *J Cell Biochem* (2008) 104:136–49. doi: 10.1002/jcb.21610
18. Blomme B, Van Steenkiste C, Callewaert N, Van Vlierberghe H. Alteration of Protein Glycosylation in Liver Diseases. *J Hepatol* (2009) 50:592–603. doi: 10.1016/j.jhep.2008.12.010
19. Comunale MA, Wang M, Hafner J, Krakover J, Rodemich L, Kopenhagen B, et al. Identification and Development of Fucosylated Glycoproteins as Biomarkers of Primary Hepatocellular Carcinoma. *J Proteome Res* (2009) 8:595–602. doi: 10.1021/pr800752c
20. Vanderschaeghe D, Laroy W, Sablon E, Halfon P, Van Hecke A, Delanghe J, et al. GlycoFibrotest Is a Highly Performant Liver Fibrosis Biomarker Derived From DNA Sequencer-Based Serum Protein Glycomics. *Mol Cell Proteomics: MCP* (2009) 8:986–94. doi: 10.1074/mcp.M800470-MCP200
21. Wang M, Long RE, Comunale MA, Junaidi O, Marrero J, Di Bisceglie AM, et al. Novel Fucosylated Biomarkers for the Early Detection of Hepatocellular Carcinoma: A Publication of the American Association for Cancer Research, Cosponsored by the American Society of Preventive Oncology. *Cancer Epidemiol Biomarkers Prev* (2009) 18:1914–21. doi: 10.1158/1055-9965.EPI-08-0980
22. Comunale MA, Rodemich-Betesh L, Hafner J, Wang M, Norton P, Di Bisceglie AM, et al. Linkage Specific Fucosylation of Alpha-1-Antitrypsin in Liver Cirrhosis and Cancer Patients: Implications for a Biomarker of Hepatocellular Carcinoma. *PLoS One* (2010) 5:e12419. doi: 10.1371/journal.pone.0012419
23. Debruyne EN, Vanderschaeghe D, Van Vlierberghe H, Vanhecke A, Callewaert N, Delanghe JR. Diagnostic Value of the Hemopexin N-Glycan Profile in Hepatocellular Carcinoma Patients. *Clin Chem* (2010) 56:823–31. doi: 10.1373/clinchem.2009.139295
24. Vanderschaeghe D, Szekrenyes A, Wenz C, Gassmann M, Naik N, Bynum M, et al. High-Throughput Profiling of the Serum N-Glycome on Capillary Electrophoresis Microfluidics Systems: Toward Clinical Implementation of Glycohepatotest. *Anal Chem* (2010) 82:7408–15. doi: 10.1021/ac101560a
25. Blomme B, Van Steenkiste C, Grassi P, Haslam SM, Dell A, Callewaert N, et al. Alterations of Serum Protein N-Glycosylation in Two Mouse Models of Chronic Liver Disease Are Hepatocyte and Not B Cell Driven. *Am J Physiol Gastrointest Liver Physiol* (2011) 300:G833–42. doi: 10.1152/ajpgi.00228.2010
26. Comunale MA, Wang M, Rodemich-Betesh L, Hafner J, Lamontagne A, Klein A, et al. Novel Changes in Glycosylation of Serum Apo-J in Patients With Hepatocellular Carcinoma. *Cancer Epidemiol Biomarkers Prev* (2011) 20:1222–9. doi: 10.1158/1055-9965.EPI-10-1047
27. Blomme B, Francque S, Trepo E, Libbrecht L, Vanderschaeghe D, Verrijken A, et al. N-Glycan Based Biomarker Distinguishing Non-Alcoholic Steatohepatitis From Steatosis Independently of Fibrosis. *Dig Liver Dis* (2012) 44:315–22. doi: 10.1016/j.dld.2011.10.015
28. Mehta A, Norton P, Liang H, Comunale MA, Wang M, Rodemich-Betesh L, et al. Increased Levels of Tetra-Antennary N-Linked Glycan But Not Core Fucosylation Are Associated With Hepatocellular Carcinoma Tissue. *Cancer Epidemiol Biomarkers Prev* (2012) 21:925–33. doi: 10.1158/1055-9965.EPI-11-1183
29. Comunale MA, Wang M, Anbarasan N, Betesh L, Karabudak A, Moritz E, et al. Total Serum Glycan Analysis Is Superior to Lectin-FLISA for the Early Detection of Hepatocellular Carcinoma. *Proteomics Clin Appl* (2013) 7:690–700. doi: 10.1002/prca.201200125
30. Lamontagne A, Long RE, Comunale MA, Hafner J, Rodemich-Betesh L, Wang M, et al. Altered Functionality of Anti-Bacterial Antibodies in Patients With Chronic Hepatitis C Virus Infection. *PLoS One* (2013) 8:e64992. doi: 10.1371/journal.pone.0064992
31. Vanderschaeghe D, Debruyne E, Van Vlierberghe H, Callewaert N, Delanghe J. CE Analysis of Gamma-Globulin Mobility and Potential Clinical Utility. *Methods Mol Biol* (2013) 919:249–57. doi: 10.1007/978-1-62703-029-8_22
32. Betesh L, Comunale MA, Wang M, Liang H, Hafner J, Karabudak A, et al. Identification of Fucosylated Fetuin-a as a Potential Biomarker for Cholangiocarcinoma. *Proteomics Clin Appl* (2017) 11:9–10. doi: 10.1002/prca.201600141
33. Verhelst X, Vanderschaeghe D, Castera L, Raes T, Geerts A, Francoz C, et al. A Glycomics-Based Test Predicts the Development of Hepatocellular Carcinoma in Cirrhosis. *Clin Cancer Res* (2017) 23:2750–8. doi: 10.1158/1078-0432.CCR-16-1500
34. Wang M, Sanda M, Comunale MA, Herrera H, Swindell C, Kono Y, et al. Changes in the Glycosylation of Kininogen and the Development of a Kininogen-Based Algorithm for the Early Detection of HCC. *Cancer Epidemiol Biomarkers Prev* (2017) 26:795–803. doi: 10.1158/1055-9965.EPI-16-0974
35. Powers TW, Neely BA, Shao Y, Tang H, Troyer DA, Mehta AS, et al. MALDI Imaging Mass Spectrometry Profiling of N-Glycans in Formalin-Fixed Paraffin Embedded Clinical Tissue Blocks and Tissue Microarrays. *PLoS One* (2014) 9:e106255. doi: 10.1371/journal.pone.0106255
36. Powers TW, Holst S, Wuhrer M, Mehta AS, Drake RR. Two-Dimensional N-Glycan Distribution Mapping of Hepatocellular Carcinoma Tissues by MALDI-Imaging Mass Spectrometry. *Biomolecules* (2015) 5:2554–72. doi: 10.3390/biom5042554
37. Drake RR, Powers TW, Jones EE, Bruner E, Mehta AS, Angel PM. MALDI Mass Spectrometry Imaging of N-Linked Glycans in Cancer Tissues. *Adv Cancer Res* (2017) 134:85–116. doi: 10.1016/bs.acr.2016.11.009
38. Drake RR, Powers TW, Norris-Caneda K, Mehta AS, Angel PM. *In Situ* Imaging of N-Glycans by MALDI Imaging Mass Spectrometry of Fresh or Formalin-Fixed Paraffin-Embedded Tissue. *Curr Protoc Protein Sci* (2018) 94:e68. doi: 10.1002/cpps.68
39. Drake RR, West CA, Mehta AS, Angel PM. MALDI Mass Spectrometry Imaging of N-Linked Glycans in Tissues. *Adv Exp Med Biol* (2018) 1104:59–76. doi: 10.1007/978-981-13-2158-0_4
40. West CA, Wang M, Herrera H, Liang H, Black A, Angel PM, et al. N-Linked Glycan Branching and Fucosylation Are Increased Directly in Hcc Tissue as Determined Through *In Situ* Glycan Imaging. *J Proteome Res* (2018) 17:3454–62. doi: 10.1021/acs.jproteome.8b00323
41. Black AP, Angel PM, Drake RR, Mehta AS. Antibody Panel Based N-Glycan Imaging for N-Glycoprotein Biomarker Discovery. *Curr Protoc Protein Sci* (2019) 98:e99. doi: 10.1002/cpps.99
42. Black AP, Liang H, West CA, Wang M, Herrera HP, Haab BB, et al. A Novel Mass Spectrometry Platform for Multiplexed N-Glycoprotein Biomarker Discovery From Patient Biofluids by Antibody Panel Based N-Glycan Imaging. *Anal Chem* (2019) 91:8429–35. doi: 10.1021/acs.analchem.9b01445
43. Scott DA, Casadonte R, Cardinali B, Spruill L, Mehta AS, Carli F, et al. Increases in Tumor N-Glycan Polylactosamines Associated With Advanced HER2-Positive and Triple-Negative Breast Cancer Tissues. *Proteomics Clin Appl* (2019) 13:e1800014. doi: 10.1002/prca.201800014
44. Scott DA, Norris-Caneda K, Spruill L, Bruner E, Kono Y, Angel PM, et al. Specific N-Linked Glycosylation Patterns in Areas of Necrosis in Tumor Tissues. *Int J Mass Spectrom* (2019) 437:69–76. doi: 10.1016/j.ijms.2018.01.002
45. Blaschke CRK, Black AP, Mehta AS, Angel PM, Drake RR. Rapid N-Glycan Profiling of Serum and Plasma by a Novel Slide-Based Imaging Mass Spectrometry Workflow. *J Am Soc Mass Spectrom* (2020) 12:2511–20. doi: 10.1021/jasms.0c00213
46. Drake RR, McDowell C, West C, David F, Powers TW, Nowling T, et al. Defining the Human Kidney N-Glycome in Normal and Cancer Tissues Using MALDI Imaging Mass Spectrometry. *J Mass Spectrom* (2020) 55:e4490. doi: 10.1002/jms.4490

47. West CA, Liang H, Drake RR, Mehta AS. New Enzymatic Approach to Distinguish Fucosylation Isomers of N-Linked Glycans in Tissues Using MALDI Imaging Mass Spectrometry. *J Proteome Res* (2020) 19(8):2989–96. doi: 10.1021/acs.jproteome.0c00024
48. Delacourt A, Black A, Angel P, Drake R, Hoshida Y, Singal A, et al. N-Glycosylation Patterns Correlate With Hepatocellular Carcinoma Genetic Subtypes. *Mol Cancer Res* (2021) 19(11):1686–77. doi: 10.1158/1541-7786.MCR-21-0348
49. Goodman ZD. Grading and Staging Systems for Inflammation and Fibrosis in Chronic Liver Diseases. *J Hepatol* (2007) 47:598–607. doi: 10.1016/j.jhep.2007.07.006
50. Marrero JA, Fontana RJ, Su GL, Conjeevaram HS, Emick DM, Lok AS. NAFLD may be a Common Underlying Liver Disease in Patients With Hepatocellular Carcinoma in the United States. *Hepatology* (2002) 36:1349–54. doi: 10.1002/hep.1840360609
51. Harvey DJ, Merry AH, Royle L, Campbell MP, Dwek RA, Rudd PM. Proposal for a Standard System for Drawing Structural Diagrams of N- and O-Linked Carbohydrates and Related Compounds. *Proteomics* (2009) 9:3796–801. doi: 10.1002/pmic.200900096
52. Hoeffding W. A Non-Parametric Test of Independence. *Ann Math Stat* (1948) 19:546–57. doi: 10.1214/aoms/1177730150
53. Malhotra R, Wormald MR, Rudd PM, Fischer PB, Dwek RA, Sim RB. Glycosylation Changes of IgG Associated With Rheumatoid Arthritis can Activate Complement via the Mannose-Binding Protein. *Nat Med* (1995) 1:237–43. doi: 10.1038/nm0395-237
54. Wormald MR, Rudd PM, Harvey DJ, Chang SC, Scragg IG, Dwek RA. Variations in Oligosaccharide-Protein Interactions in Immunoglobulin G Determine the Site-Specific Glycosylation Profiles and Modulate the Dynamic Motion of the Fc Oligosaccharides. *Biochemistry* (1997) 36:1370–80. doi: 10.1021/bi9621472
55. Saphire EO, Stanfield RL, Crispin MD, Morris G, Zwick MB, Pantophlet RA, et al. Crystal Structure of an Intact Human IgG: Antibody Asymmetry, Flexibility, and a Guide for HIV-1 Vaccine Design. *Adv Exp Med Biol* (2003) 535:55–66. doi: 10.1007/978-1-4615-0065-0_4
56. Saldova R, Royle L, Radcliffe CM, Abd Hamid UM, Evans R, Arnold JN, et al. Ovarian Cancer Is Associated With Changes in Glycosylation in Both Acute-Phase Proteins and IGG. *Glycobiology* (2007) 17:1344–56. doi: 10.1093/glycob/cwm100
57. Bones J, Mittermayr S, O'donoghue N, Guttman A, Rudd PM. Ultra Performance Liquid Chromatographic Profiling of Serum N-Glycans for Fast and Efficient Identification of Cancer Associated Alterations in Glycosylation. *Anal Chem* (2010) 82:10208–15. doi: 10.1021/ac102860w
58. Pucic M, Knezevic A, Vidic J, Adamczyk B, Novokmet M, Polasek O, et al. High Throughput Isolation and Glycosylation Analysis of IgG-Variability and Heritability of the IGG Glycome in Three Isolated Human Populations. *Mol Cell Proteomics* (2011) 10:M111 010090. doi: 10.1074/mcp.M111.010090
59. Coss KP, Byrne JC, Coman DJ, Adamczyk B, Abrahams JL, Saldova R, et al. IgG N-Glycans as Potential Biomarkers for Determining Galactose Tolerance in Classical Galactosaemia. *Mol Genet Metab* (2012) 105:212–20. doi: 10.1016/j.ymgme.2011.10.018
60. Wang M, Block TM, Marrero J, Di Bisceglie AM, Devarajan K, Mehta A. (2012). Improved Biomarker Performance for the Detection of Hepatocellular Carcinoma by Inclusion of Clinical Parameters. *Proc IEEE Int Conf Bioinformatics Biomed* (2012) 10.1109/BIBM.2012.6392612. doi: 10.1109/BIBM.2012.6392612
61. Wang M, Mehta A, Block TM, Marrero J, Di Bisceglie AM, Devarajan K. A Comparison of Statistical Methods for the Detection of Hepatocellular Carcinoma Based on Serum Biomarkers and Clinical Variables. *BMC Med Genomics* (2013) 6:S9. doi: 10.1186/1755-8794-6-S3-S9
62. Wang M, Devarajan K, Singal AG, Marrero JA, Dai J, Feng Z, et al. The Doylestown Algorithm: A Test to Improve the Performance of AFP in the Detection of Hepatocellular Carcinoma. *Cancer Prev Res (Phila)* (2016) 9:172–9. doi: 10.1158/1940-6207.CAPR-15-0186
63. Powers TW, Jones EE, Betesh LR, Romano PR, Gao P, Copland JA, et al. Matrix Assisted Laser Desorption Ionization Imaging Mass Spectrometry Workflow for Spatial Profiling Analysis of N-Linked Glycan Expression in Tissues. *Anal Chem* (2013) 85:9799–806. doi: 10.1021/ac402108x
64. Ruhaak LR, Huhn C, Waterreus WJ, De Boer AR, Neuss C, Hokke CH, et al. Hydrophilic Interaction Chromatography-Based High-Throughput Sample Preparation Method for N-Glycan Analysis From Total Human Plasma Glycoproteins. *Anal Chem* (2008) 80:6119–26. doi: 10.1021/ac800630x
65. Shirabe K, Bekki Y, Gantumur D, Araki K, Ishii N, Kuno A, et al. Mac-2 Binding Protein Glycan Isomer (M2bpgi) Is a New Serum Biomarker for Assessing Liver Fibrosis: More Than a Biomarker of Liver Fibrosis. *J Gastroenterol* (2018) 53:819–26. doi: 10.1007/s00535-017-1425-z
66. Cao X, Shang QH, Chi XL, Zhang W, Xiao HM, Sun MM, et al. Serum N-Glycan Markers for Diagnosing Liver Fibrosis Induced by Hepatitis B Virus. *World J Gastroenterol* (2020) 26:1067–79. doi: 10.3748/wjg.v26.i10.1067
67. Higashi M, Yoshimura T, Usui N, Kano Y, Deguchi A, Tanabe K, et al. A Potential Serum N-Glycan Biomarker for Hepatitis C Virus-Related Early-Stage Hepatocellular Carcinoma With Liver Cirrhosis. *Int J Mol Sci* (2020) 21:8913–25. doi: 10.3390/ijms21238913
68. Ogawa K, Kobayashi T, Furukawa JI, Hanamatsu H, Nakamura A, Suzuki K, et al. Tri-Antennary Tri-Sialylated Mono-Fucosylated Glycan of Alpha-1 Antitrypsin as a Non-Invasive Biomarker for Non-Alcoholic Steatohepatitis: A Novel Glycobiomarker for Non-Alcoholic Steatohepatitis. *Sci Rep* (2020) 10:321. doi: 10.1038/s41598-019-56947-1
69. Verhelst X, Dias AM, Colombel JF, Vermeire S, Van Vlierberghe H, Callewaert N, et al. Protein Glycosylation as a Diagnostic and Prognostic Marker of Chronic Inflammatory Gastrointestinal and Liver Diseases. *Gastroenterology* (2020) 158:95–110. doi: 10.1053/j.gastro.2019.08.060
70. Myers RP, Ratziu V, Imbert-Bismut F, Charlotte F, Poynard T. Biochemical Markers of Liver Fibrosis: A Comparison With Historical Features in Patients With Chronic Hepatitis C. *Am J Gastroenterol* (2002) 97:2419–25. doi: 10.1111/j.1572-0241.2002.05997.x
71. Myers RP, Benhamou Y, Imbert-Bismut F, Thibault V, Bochet M, Charlotte F, et al. Serum Biochemical Markers Accurately Predict Liver Fibrosis in HIV and Hepatitis C Virus Co-Infected Patients. *Aids* (2003) 17:721–5. doi: 10.1097/00002030-200303280-00010
72. Myers RP, De Torres M, Imbert-Bismut F, Ratziu V, Charlotte F, Poynard T. Biochemical Markers of Fibrosis in Patients With Chronic Hepatitis C: A Comparison With Prothrombin Time, Platelet Count, and Age-Platelet Index. *Dig Dis Sci* (2003) 48:146–53. doi: 10.1023/A:1021702902681
73. Rossi E, Adams L, Prins A, Bulsara M, De Boer B, Garas G, et al. Validation of the Fibrotest Biochemical Markers Score in Assessing Liver Fibrosis in Hepatitis C Patients. *Clin Chem* (2003) 49:450–4. doi: 10.1373/49.3.450
74. Younes R, Caviglia GP, Govaere O, Rosso C, Armandi A, Sanavia T, et al. Long-Term Outcomes and Predictive Ability of Non-Invasive Scoring Systems in Patients With Non-Alcoholic Fatty Liver Disease. *J Hepatol* (2021) 75:786–94. doi: 10.1016/j.jhep.2021.05.008

Conflict of Interest: DS, SC, and SP all work for GlycoPath Inc, who have licensed technology from AM, PA, and RD for the glycan analysis of antibody captured glycoproteins.

The remaining authors declare that the research was conducted in the absence of any commercial or financial relationships that could be construed as a potential conflict of interest.

Publisher's Note: All claims expressed in this article are solely those of the authors and do not necessarily represent those of their affiliated organizations, or those of the publisher, the editors and the reviewers. Any product that may be evaluated in this article, or claim that may be made by its manufacturer, is not guaranteed or endorsed by the publisher.

Copyright © 2022 Scott, Wang, Grauzam, Pippin, Black, Angel, Drake, Castellino, Kono, Rocky and Mehta. This is an open-access article distributed under the terms of the Creative Commons Attribution License (CC BY). The use, distribution or reproduction in other forums is permitted, provided the original author(s) and the copyright owner(s) are credited and that the original publication in this journal is cited, in accordance with accepted academic practice. No use, distribution or reproduction is permitted which does not comply with these terms.



Changes of IgG N-Glycosylation in Thyroid Autoimmunity: The Modulatory Effect of Methimazole in Graves' Disease and the Association With the Severity of Inflammation in Hashimoto's Thyroiditis

Sara Trzos¹, Paweł Link-Lenczowski², Grzegorz Sokołowski³ and Ewa Pocheć^{1*}

¹ Department of Glycoconjugate Biochemistry, Institute of Zoology and Biomedical Research, Faculty of Biology, Jagiellonian University, Kraków, Poland, ² Department of Medical Physiology, Faculty of Health Sciences, Jagiellonian University Medical College, Kraków, Poland, ³ Department of Endocrinology, Faculty of Medicine, Jagiellonian University Medical College, Kraków, Poland

OPEN ACCESS

Edited by:

David Falck,
Leiden University Medical Center,
Netherlands

Reviewed by:

Eleonore Fröhlich,
Medical University of Graz, Austria
Markus Biburger,
Friedrich-Alexander-University
Erlangen-Nürnberg, Germany

*Correspondence:

Ewa Pocheć
ewa.pochec@uj.edu.pl

Specialty section:

This article was submitted to
B Cell Biology,
a section of the journal
Frontiers in Immunology

Received: 22 December 2021

Accepted: 18 February 2022

Published: 15 March 2022

Citation:

Trzos S, Link-Lenczowski P, Sokołowski G and Pocheć E (2022) Changes of IgG N-Glycosylation in Thyroid Autoimmunity: The Modulatory Effect of Methimazole in Graves' Disease and the Association With the Severity of Inflammation in Hashimoto's Thyroiditis. *Front. Immunol.* 13:841710. doi: 10.3389/fimmu.2022.841710

The N-glycome of immunoglobulin G (IgG), the most abundant glycoprotein in human blood serum, reflects pathological conditions of autoimmunity and is sensitive to medicines applied in disease therapy. Due to the high sensitivity of N-glycosylation, the IgG N-glycan profile may serve as an indicator of an ongoing inflammatory process. The IgG structure and its effector functions are strongly dependent on the composition of N-glycans attached to the Fc fragment, and the binding of antigens is regulated by Fab sugar moieties. Because of the crucial role of N-glycans in IgG function, remodeling of its N-oligosaccharides can induce pathological changes that ultimately contribute to the development of autoimmunity; restoration of their physiological structure is critical to the reduction of disease symptoms. Our recently published data have shown that the pathology of autoimmune thyroid diseases (AITDs), including Hashimoto's thyroiditis (HT) and Graves' disease (GD), is accompanied by alterations of the composition of IgG N-glycans. The present study is a more in-depth investigation of IgG glycosylation in both AITDs, designed to determine the relationship between the severity of thyroid inflammation and IgG N-glycan structures in HT, and to assess the impact of immunosuppressive therapy on the N-glycan profile in GD patients. The study material consisted of human serum samples collected from donors with elevated anti-thyroglobulin (Tg) and/or anti-thyroperoxidase (TPO) IgGs without symptoms of hypothyroidism (n=68), HT patients characterized by high autoantibody titers and advanced destruction of the thyroid gland (n=113), GD patients with up-regulated IgG against thyroid-stimulating hormone receptor (TSHR) before (n=62) and after (n=47) stabilization of TSH level as a result of methimazole therapy (study groups), and healthy donors (control group, n=90). IgG was isolated from blood serum using protein G affinity chromatography. N-glycans were released from IgG by PNGase F digestion and analyzed by ultra-performance liquid

chromatography-mass spectrometry (UPLC-MS) after 2-aminobenzamide (2-AB) labeling. UPLC-MS chromatograms were integrated into 25 peaks (GP) in the Waters UNIFI Scientific Information System, and *N*-glycans were assigned based on the glucose unit values and mass-to-charge ratios (*m/z*) of the detected ions. The Kruskal-Wallis non-parametric test was used to determine the statistical significance of the results ($p < 0.05$). The obtained results suggest that modifications of IgG sialylation, galactosylation and core-fucosylation are associated with the severity of HT symptoms. Methimazole therapy implemented in GD patients affected the IgG *N*-glycan profile; as a result, the content of the sialylated and galactosylated oligosaccharides with core fucose differed after treatment. Our results suggest that *N*-glycosylation of IgG undergoes dynamic changes during the intensification of thyroiditis in HT, and that in GD autoimmunity it is affected significantly by immunosuppressive therapy.

Keywords: immunoglobulin G (IgG), N-glycosylation, Graves' disease (GD), Hashimoto's thyroiditis (HT), immunosuppressive therapy, ultraperformance liquid chromatography - mass spectrometry (UPLC-MS)

1 INTRODUCTION

Class G immunoglobulins (IgGs), produced by plasma cells and B cells, are the most abundant human serum glycoproteins. They are an essential component of humoral immune responses and are involved in the recognition, neutralization, and elimination of pathogens and toxic antigens (1). The antigen-binding fragment (Fab) of IgG binds specifically antigens, while the crystallizable fragment (Fc) is responsible for mediating the antibody effector functions. Due to its great importance in immune response, IgG is one of the best-studied glycoproteins, i.e. proteins modified post-translationally by covalent attachment of various oligosaccharide structures, called glycans (2, 3).

Oligosaccharides represent up to 15% of IgG molecular weight (4). They are attached to both Fc and Fab fragments and belong to the *N*-glycans characterized by the presence of an *N*-glycosidic bond linking an *N*-acetylglucosamine (GlcNAc) in sugar structure with asparagine (Asn) within the Asn-X-Ser/Thr amino acid sequence. Each IgG molecule has two highly conserved *N*-glycosylation sites located at Asn297 within the CH2 domains of the Fc fragment (5–7). Mature IgG Fc glycoforms possess mainly diantennary complex-type structures differing in the number of monosaccharides building the antennae, namely GlcNAc, galactose (Gal), and sialic acid (SA) as well as in the number of bisecting GlcNAc residue, and the presence of core fucose (Fuc) (8, 9). Fab fragments have also been found to be *N*-glycosylated but only in 10–30% of IgGs (7, 10, 11). It has been demonstrated that altering the oligosaccharide composition in the IgG Fc region affects its secretion, tertiary structure, half-life, and effector functions (10, 12–15). Interestingly, a complete deletion of Fc *N*-glycans results in loss of pro- and anti-inflammatory IgG activity (16).

The composition of the IgG glycome is influenced by both genetic and environmental factors, making it an excellent biomarker of overall human health. It seems likely that the IgG *N*-glycosylation process in healthy individuals undergoes little

change during homeostasis, while its disruption may be influenced by sex hormones, age, and stress (6, 17, 18). Furthermore, changes in IgG *N*-oligosaccharide patterns have been implicated in disease progression and remission, representing both predisposition and functional mechanisms involved in the pathogenesis of diseases, including autoimmune diseases (6, 19). Some of the most common autoimmune disorders are autoimmune thyroid diseases (AITDs), which include Graves' disease (GD) and Hashimoto's thyroiditis (HT) (20).

The development of AITD follows a loss of immune tolerance and reactivity to thyroid autoantigens, leading to infiltration of thyroid gland by T cells and B cells that produce characteristic antibodies. An activity of autoantibodies against thyrotropic hormone receptor (TSHR) expressed on thyroid follicular cells (thyrocytes) initiates the development of GD. Intense stimulation of TSHR by anti-TSHR antibodies (TRAb) leads to increased secretion of thyroid hormones, thyroxine (T4) and triiodothyronine (T3), resulting in hyperthyroidism. As a result, GD-associated autoimmunity can cause goiter, ophthalmopathy or thyroid dermopathy. TSHR activation by anti-TSHR can also stimulate the growth of thyrocytes and causes the development of thyroid vascularization (21). In the HT immune tolerance to thyroid self-antigens is lost, resulting in the destruction of thyrocytes by activated T lymphocytes which leads to hypothyroidism. HT is diagnosed based on the elevated levels of circulating antibodies against thyroid antigens: thyroperoxidase (TPO) and thyroglobulin (Tg), and is supported by the decreased thyroid echogenicity on ultrasound (22). In HT patients, a Th1 immune response predominates, promoting cellular immunity and thyroid follicular apoptosis (23, 24). Proapoptotic ligands and death receptors such as FasL, TNF and TRAIL, present on thyrocytes, remain inactive under physiological conditions (23). Fas/FasL expression induced in Th1 response by infiltration of pro-inflammatory cytokines TNF- α and IL-1 β activates thyroid follicular cell apoptosis in HT (24). In GD, the predominance of Th2 cells promotes a

humoral response, with increased production of TRAb antibodies by B cells. The presence of autoantibodies and the increased level of cytokines produced by Th2 lymphocytes, inhibits Fas/FasL expression and results in the activation of anti-apoptotic molecule Bcl-2, which protects thyroid cells from apoptosis, but increases the death of T cells infiltrating the gland tissue (25, 26). Apart from apoptosis, thyroid cells are destroyed by anti-TPO IgG, present in serum of about 80–95% of patients (27). Anti-TPO IgG is involved in thyrocyte destruction through antibody-dependent cellular cytotoxicity (ADCC) (28, 29) and complement-dependent cytotoxicity (CDC) (29). Environmental factors, mainly nuclear radiation, iodine, smoking, infections, stress, alcohol and drugs, contribute approximately to 20% of all AITDs (30). Genetic factors are also implicated in the development of diseases. Studies conducted over many years have identified several genes and chromosome regions that are associated with the development of GD and HT (30, 31).

Changes in IgG N-glycans have been demonstrated in chronic inflammation, including autoimmune diseases. The altered N-glycan profile of IgG has been proven to be a valuable indicator of systemic lupus erythematosus (SLE) and rheumatoid arthritis (RA) (32, 33). Reduced galactosylation of IgG in RA, described for the first time by Parekh et al. (1985), has been repeatedly confirmed in subsequent analyses by numerous research groups (32, 34, 35). Currently it is the best-characterized modification of IgG glycosylation, used as a serum glycomarker of RA progression and remission (36). Alteration of α 1,6-fucosylation is, after agalactosylation, one of the most common modifications of IgG N-glycans observed in inflammatory diseases (37). The vast majority of human IgG Fc glycoforms (over 90%) are core fucosylated (6, 34), and this modification plays a crucial role in the modulation of IgG biological activity. Up-regulation of N-glycans with core Fuc on IgG heavy chains has been demonstrated in RA patients compared to healthy individuals (38) and the higher exposure of Fuc residues on IgG N-oligosaccharides has been shown in the blood of SLE donors than in healthy people (19). Reduced α 1,6-fucosylation has been observed in SLE IgG during remission compared to patients with acute SLE (19). The further study performed with the use of the UPLC method showed a decreased galactosylation, sialylation, and core fucosylation of IgG accompanied by an increase of bisecting GlcNAc in IgG N-glycans from three independent populations of SLE patients in comparison to healthy donors (39). Our recent study performed on three European cohorts revealed a reduced core fucosylation of IgG in AITD patients compared to a population of healthy donors and a correlation of this IgG modification with anti-TPO serum titer (40). Terminally located sialic acid is another monosaccharide building IgG N-glycans that fundamentally regulates the activity of this glycoprotein. Down-regulation of IgG sialylation, which is usually followed by agalactosylation in inflammatory conditions, significantly promotes the pro-inflammatory potential of antibodies (6, 36).

The mechanisms underlying the impact of IgG Fc N-glycan fucosylation and sialylation on this protein physiological property have been widely described. Several studies have

demonstrated for example the higher cytotoxicity in antibody-dependent cell-mediated (ADCC) and complement-dependent cytotoxicity (CDC) mediated by IgG with reduced sialylation and fucosylation (41–43). Attachment of SA to glycans affects the structure of the Fc fragment in IgG and leads to a 10-fold reduction in the affinity of antibodies for Fc γ R, thereby impairing their effector functions (44). Increased sialylation reduces cytotoxic activity in ADCC (45). The inhibitory effect of sialic acid in IgG N-oligosaccharides on ADCC may be due to reduced binding of IgG to its receptor as a result of impaired antigen binding caused by the lack of flexibility of the IgG hinge region (46). Fucosylation of the core of IgG N-glycans is also crucial for the control of ADCC, as IgG lacking α 1,6-linked Fuc on Fc has been found to have up to 100-fold increased ADCC activity (42).

Until recently, it was thought that each step of N-glycosylation could only occur intracellularly in the rough endoplasmic reticulum (RER) and Golgi apparatus (GA). However, it has been found that α 2,6-sialylation can also occur in the bloodstream in a reaction catalyzed by β -galactoside α 2,6-sialyltransferase 1 (ST6Gal1) which transfers sialic acid from nucleotide sugar donor cytidine monophosphate (CMP)-SA, secreted by platelet α granules, to Gal in IgG N-glycan and creates between them α 2,6-glycosidic bond. ST6Gal1 is produced by hepatic central veins and secreted into the bloodstream. This discovery sheds new light on the process of IgG sialylation and may explain the great dynamics of inflammatory processes mediated by antibodies (47).

N-glycans on IgG are rebuilt not only during disease development and progression, but their composition is also sensitive to medications used during the treatment of patients, including immunosuppressive drugs. Up-regulation of IgG galactosylation was observed in patients with RA who have been treated with methotrexate (48–50) and infliximab (chimeric anti-tumour necrosis factor α monoclonal antibodies, anti-TNF α IgG) (51). Moreover, restoration of N-glycan galactosylation correlated with significant clinical improvement following infliximab therapy (51). Nonsteroidal anti-inflammatory drugs (NSAIDs), i.e. aspirin, and also glucocorticosteroids, were shown to influence the glycosylation of human plasma proteins. NSAIDs and corticosteroids reduced core-fucosylation of di- and triantennary complex-type structures, together with oligomannose oligosaccharide levels in plasma N-glycome (52).

Our recently published study showed the changes of IgG N-glycome are characteristic for AITD patients (40). The present study aimed to investigate the IgG N-glycosylation in thyroid autoimmunity in more depth by determining the relationship between thyroiditis severity and IgG N-glycan structure in HT and by evaluating the effect of methimazole therapy on the N-oligosaccharide profile in GD patients. A comparative analysis of the IgG N-glycome was performed by ultra-performance liquid chromatography combined with mass spectrometry (UPLC-MS). We also examined B-cell independent α 2,6-sialylation of IgG in AITD blood sera considering it as a particularly interesting mechanism of N-glycan modification.

2 MATERIALS AND METHODS

2.1 Bioethical Statement

The study was conducted in accordance with the Declaration of Helsinki and approved by the Bioethics Committee of the Jagiellonian University in Krakow, Poland (1072.6120.99.2021). All individuals donating blood for the experiment signed informed consent. Blood samples were collected between May 2014 and March 2021.

2.2 Characteristics of the Study Groups

The study was conducted in cooperation with the Department of Endocrinology of the Jagiellonian University Hospital in Krakow. Recruitment of adult patients with AITDs without any other concomitant autoimmune diseases, and healthy volunteers was performed by an endocrinologist based on thyrotropic hormone (TSH) and thyroid autoantibody levels, thyroid gland ultrasonography and medical history of donors. Patients with AITD affected by other diseases, taking other drugs than those associated with AITD, donors suffering from alcoholism and taking other stimulants as well as pregnant women were excluded.

Human serum samples were collected from donors with the elevated IgG anti-thyroglobulin (TgAb) and/or anti-thyroperoxidase (anti-TPO) levels without symptoms of hypothyroidism (HT1, n=68), from Hashimoto's thyroiditis patients characterized by the high autoantibody titers, advanced thyroid destruction and with the stabilized TSH level as a result of L-thyroxine treatment (HT2, n=113), GD patients with the elevated thyrotropic hormone receptor IgG (TRAb) levels before (GD, n=62) and after (GD/T, n=47) stabilization of TSH level as a result of the treatment with methimazole (1-methyl-2-mercaptoimidazole), an anti-thyroid agent with immunosuppressive activity. Healthy donors with the serum titers of TSH and autoantibodies within the normal range constituted a control group (CTR, n=90). The control group was age-matched to the study groups. **Table 1** contains the demographic and clinical characteristics of donors with AITDs and healthy volunteers, and **Figure 1** shows a graphical comparison of TSH and autoantibody (anti-TPO, TgAb, and TRAb) levels between the groups.

2.3 Collection of Serum Samples

Blood samples were collected by venipuncture into the tubes containing a clotting activator (S-Monovette, Sarstedt, 04.1934.001), left for 5 h at room temperature (RT) for blood clotting, and centrifuged at 2500 rpm for 10 min at 4°C (Heraeus). Serum samples were stored at -80°C until IgG isolation.

2.4 IgG Purification

IgGs were isolated by affinity chromatography with G-protein conjugated to the deposit grains. Serum samples (100 µl) were diluted 1:1 with a binding buffer (0.1 M Na₂HPO₄, 0.15 M NaCl, pH 7.2), applied to 96-well Protein G Spin Plates (Thermo Fisher Scientific, 45204), and incubated for 30 min at RT on an orbital shaker (Biosan). After incubation, the plates were centrifuged (1000 rpm, 1 min, RT) and the fraction containing IgG-depleted serum was discarded. Agarose resin was washed with the binding buffer until the ballast proteins were removed which was monitored by measuring the protein absorbance at 280 nm against the binding buffer (NanoDrop 2000, Thermo Fisher Scientific). Then IgGs were eluted with 200 µl of 0.1 M glycine, pH 2.5 into the collection plates containing 20 µl per well of a neutralization buffer (1 M Tris). IgG concentration was determined at 280 nm against a reagent blank (NanoDrop 2000, Thermo Fisher Scientific). IgG samples were stored at -80°C for further analyses.

The efficiency of IgG isolation from human serum was evaluated by SDS-PAGE. Purified IgG (10 µl) was separated on 10% gels under reducing conditions and then stained with colloidal Coomassie Brilliant Blue G-250 (CBB) (Sigma-Aldrich, B2025) according to the manufacturer's protocol. The molecular masses of the light (25 kDa) and heavy chains (50 kDa) were verified using PageRuler™ Prestained Protein Ladder (Thermo Fisher Scientific, 26616).

2.5 Sample Preparation for UPLC-MS Analysis

2.5.1 Buffer Exchange After IgG Isolation

Before deglycosylation, the glycine buffer was exchanged for ammonium formate (AmF) buffer using an Acroprep Advance

TABLE 1 | Characteristics of healthy donors (CTR, control group) and patients with elevated TgAb and/or anti-TPO levels without symptoms of hypothyroidism (HT1), patients with Hashimoto's thyroiditis (HT2) and patients with Graves' disease before (GD) and after (GD/T) TSH normalization (study groups).

status	age	sex (F/M)	TSH 0.27-4.20 µIU/ml	TRAb 0.0-1.0 IU/ml	anti-TPO <34.0 IU/ml	TgAb <115.0 IU/ml
CTR	18-64 34±8.75	67/8	2.22±1.04	0.47±0.26	19.60±18.54	10.63±1.55
HT1	18-66 35±10.55	53/2	3.10±1.93	0.63±0.36	140.78±174.24	310.22±358.76
HT2	20-62 36±10.17	88/0	2.46±2.34	1.49±4.61	294.57±605.09	233.32±231.21
GD	22-55 35±9.08	46/15	0.01±0.02	8.47±5.90	207.33±175.61	311.37±270.29
GD/T	23-56 37±9.46	33/13	3.29±2.18	8.27±15.31	146.26±149.66	170.12±184.02

Mean ± SD is given for age, TSH and antibody levels. anti-TPO, anti-thyroperoxidase antibodies; TgAb, thyroglobulin antibodies; TSH, thyrotropic hormone; TRAb, antibodies directed against the receptor for thyrotropin; F, female; M, male.

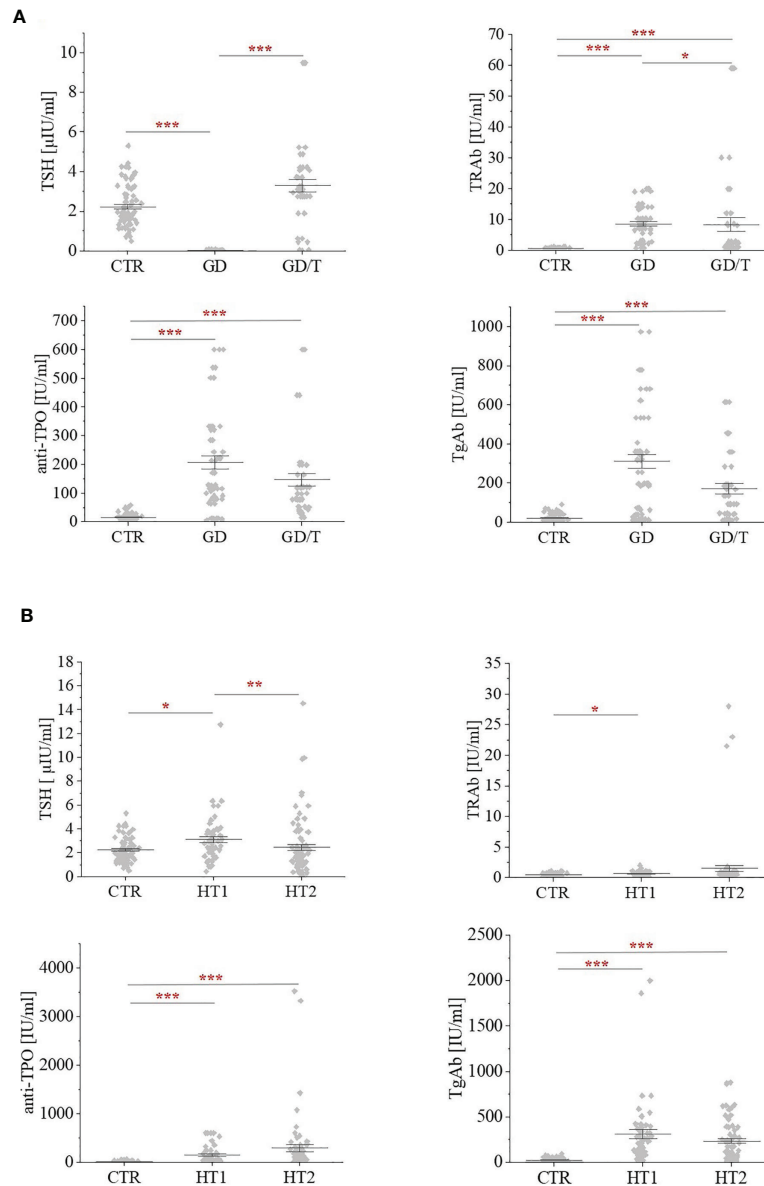


FIGURE 1 | The levels of thyrotropic hormone (TSH) and autoantibodies: against the receptor for thyrotropin (TRAb); anti-thyroperoxidase (anti-TPO); thyroglobulin antibodies (TgAb) within **(A)** Graves' disease groups: before (GD) and after (GD/T) TSH normalization, and **(B)** Hashimoto's thyroiditis groups: the donors with the elevated TgAb and/or anti-TPO (HT1), Hashimoto's thyroiditis patients (HT2) relative to the control group (CTR). Statistically significant differences were determined at $p < 0.05$ (*), $p < 0.01$ (**), and $p < 0.001$ (***).

96 10 MWCO filter plate (Pall Corporation). The membrane of the plate was prewashed three times with 100 μ l of deionized water (Milli-Q, Millipore) by filtration on a microplate vacuum manifold (Waters). After the last wash, 50 μ g or 100 μ g of IgG was applied to the wells followed by the addition of 100 μ l of 100 mM AmF buffer pH 7.5, and the solution was filtered to a minimum volume. The plate was then washed three times with 100 μ l of AmF buffer by filtration. Finally, 25 μ l AmF buffer was added to the wells and the samples were transferred by pipetting to a PCR plate (Thermo Fisher Scientific), which was repeated twice

for each well to maximize the recovery of the IgGs. Finally, the samples were lyophilized to dryness (Labconco) and stored at -80°C .

2.5.2 Enzymatic De-N-Glycosylation of IgG

Samples after lyophilization were resuspended in 19 μ l of Rapid PNGase F buffer (New England Biolabs). They were then denatured for 15 min at 80°C . After cooling the plate to RT, 0.9 μ l of Rapid PNGase F (New England Biolabs, P0710S) was added to each well and the plate was incubated for 25 min at 50°C . After deglycosylation, samples were diluted with 100 μ l

Milli-Q. IgG-released N-glycans were desalted by solid-phase extraction on HyperSep™ Hypercarb™ SPE 96-Well Plates with 10 mg bed weight (Thermo Fisher Scientific, 60302-606). The plate was prewashed three times with 400 µl of 80% acetonitrile (AcN) with 0.1% trifluoroacetic acid (TFA) and then three times with 400 µl of Milli-Q, on the vacuum filtration manifold. The samples were then applied and the columns were washed three times with 400 µl of Milli-Q. In the next step, N-oligosaccharides were eluted with 25% AcN + 0.05% TFA into a 96-well Sample Collection Plate (Waters, 186005837). The collected fractions were dried-down by lyophilization (Labconco).

2.5.3 Fluorescent Labeling of N-Glycans

N-glycan labeling with 2-aminobenzamide (2-AB) was performed according to the procedure previously described by Link-Lenczowski et al. (53). Briefly, the labeling solution consisting of 2-AB (60 mg/mL, Sigma-Aldrich, A89804) and sodium cyanoborohydride (60 mg/mL, Fluka, 156159) in acetic acid:DMSO (3:5) was added to the lyophilized N-glycan samples and incubated for 3 h at 65°C. After cooling the plate to RT, the excess dye was removed on a BioZen N-Glycan Clean-Up Microelution Plate (Phenomenex, 8M-S009-NGA) according to the manufacturer's instructions. Elution of labeled sugar structures was performed using 200 mM ammonium acetate in AcN:water (5:95). Eluted glycan samples were lyophilized (Labconco) and stored at -80°C for further analysis.

2.5.4 UPLC-MS Analysis

2-AB labeled N-glycans were analyzed by liquid chromatography-mass spectrometry (LC-MS) on Aquity I-Class Plus UPLC system with an in-line fluorescent detector coupled through electrospray ion source to the Vion® IMS-QToF high-resolution mass spectrometer (Waters). N-glycans were loaded in 50% AcN and separated by HILIC-UPLC on ACQUITY UPLC Glycan BEH Amide Column, 130Å, 1.7 µm, 2.1 mm X 150 mm (Waters) at 60°C with the following gradient conditions: solvent A was 50 mM ammonium formate pH 4.4, solvent B was 100% acetonitrile (Chemsolv), time = 0 min (t = 0.0), 25% A, 0.4 mL/min; t = 35.0, 46% A, 0.4 mL/min; t = 36.0, 100% A, 0.2 mL/min; t = 39.5, 100% A, 0.2 mL/min; t = 43.5, 25% A, 0.2 mL/min; t = 47.6, 25% A, 0.4 mL/min; t = 55.0, 25% A, 0.4 mL/min. The fluorescence detector was set at Exλ 330 nm and Emλ 420 nm and for electrospray ionization the following parameters were used: capillary voltage: 3.0 kV, source temperature: 120°C, desolvation temperature 350°C, desolvation gas flow: 800 L/h. The mass spectrometer was operated in positive ion ToF MS mode and the ions from m/z 600 to m/z 2000 were registered with the mass correction by sampling the reference mass standard once every 60 seconds. The UPLC runs were externally calibrated with a 2-AB-labeled glucose homopolymer standard (Waters, 186006841). The resulting chromatograms were automatically integrated with manual correction into 25 peaks to which glycans were assigned based on glucose unit (GU) values and exact mass. The chromatographic and mass data were analyzed with the use

of the Waters UNIFI scientific information system with the integrated Waters Glycan GU Scientific Library.

2.6 Statistical Analysis

Based on the relative intensity of the glycan peaks (GPs), expressed as percent (%) of the total area of all GPs, statistical analysis was performed using the Kruskal-Wallis nonparametric test with significance at p<0.05. All statistical interpretations of the results were performed in Origin Pro 2021b software (Origin Lab).

2.7 Evaluation of Serum ST6Gal1 Activity Using Desialylated IgG

To assess the catalytic activity of serum ST6Gal1, desialylated IgG heavy chains immobilized on PVDF membrane were incubated with human sera from control and study groups according to the protocol by Jones et al. (47) with the minor modifications. The purified IgGs were digested with *Arthrobacter ureafaciens* sialidase with a wide specificity (ABS, 1 U in 100 mL, Roche, 10269611001) to remove sialic acid (SA) from the antibody N-glycans. IgG samples (0.5 µg) were incubated with 1 µl of ABS in 8 µl of 50 mM sodium acetate, pH 5.2 overnight at 37°C (Biosan thermoblock). Desialylated and untreated IgG samples were separated under reducing conditions on 10% gels in SDS-PAGE, electrotransferred onto a PVDF membrane (Millipore, 88518), which was cut into small pieces containing IgG heavy chains based on PageRuler™ Prestained Protein Ladder (Thermo Fisher Scientific, 26616), and blocked overnight in 1% BSA (Sigma-Aldrich, A7906) at 4°C. The selected PVDF sections were incubated with human sera from each study and control group diluted 1:1 with TBST (50 mM Tris-HCl, 150 mM NaCl, and 10% Tween) overnight at 4°C. Then the membranes were probed 1 h at RT with biotinylated *Sambucus nigra* agglutinin (SNA, Vector Lab., B-1305) diluted 1:4000 in TBS containing 0.1 mM CaCl₂ and 0.01 mM MgCl₂ or with SNA preincubated with 1 M acetic acid as a negative control to check nonspecific binding of SNA *via* protein domains but not to α2,6-sialylated N-glycans. After washing three times with TBST, alkaline phosphatase (AP)-conjugated avidin (Sigma-Aldrich, E2636) diluted 1:4000 in TBST was applied for 1 h at RT. IgG heavy chain was visualized by a colorimetric reaction using 5-bromo-4-chloro-3-indolylphosphate (BCIP, Roche, 11383221001) and nitro-blue-tetrazolium (NBT, Roche, 11383213001).

ABS re-digestion of IgG N-glycans sialylated by serum ST6Gal1 on PVDF membrane was used as an additional control. Membrane fragments with IgG heavy chains sialylated by serum ST6Gal1 were placed in 4-well plates (Nunc, 176740), and incubated with 3 µl of ABS in 27 µl of 50 mM sodium acetate, pH 5.2 overnight at 37°C (Forma Steri-Cycle i160 CO₂ incubator, Thermo Fisher Scientific). Then the membranes have been subjected to incubation with SNA and visualized by colorimetric reaction as described above.

3 RESULTS

The analysis of N-glycosylation was performed on IgG purified from human serum samples according to standard protocol with

agarose-linked protein G as a ligand for IgG capturing. IgG was isolated from the sera of patients with Graves' disease before and after normalization of TSH level as the result of thyrostatic therapy, the donors with the elevated antithyroid Abs without hypothyroidism, and the patients with Hashimoto's thyroiditis (GD, GD/T, HT1, and HT2 respectively). The control group consisted of healthy individuals (CTR). The characteristic of healthy donors and patients with AITDs is shown in **Table 1** and **Figure 1**. As expected, TSH level was significantly down-regulated in GD patients in relation to CTR and normalized during methimazole therapy. TRAb serum level, an immunological marker of Graves' disease, was markedly increased in GD and partially normalized during therapy. GD donors showed also enhanced anti-TPO and TgAb titers, which remained elevated during treatment (**Table 1** and **Figure 1A**). The level of TSH was significantly higher in HT1 than CTR, but still within the normal range and these donors recruited to HT1 group did not show hypothyroidism, like the patients with Hashimoto's thyroiditis. Anti-TPO and TgAb levels were significantly up-regulated in both HT1 and HT2 donors (**Table 1** and **Figure 1B**).

To verify the efficiency of IgG isolation, the eluted samples were resolved on SDS-PAGE under reducing conditions and IgG chains were visualized by CBB staining. CBB profiles showed the highest intensity of the bands corresponding to IgG heavy chain of ca. 50 kDa and a light chain of about 25 kDa. The staining revealed also the presence of a small portion of other proteins in the eluates, but with much weaker staining intensities than IgG chains, indicating their non-specific binding to the G protein which was also previously shown by Croce et al., who estimated IgG purity to be higher than 90% (54). CBB staining of the eluted proteins is shown in **Supplementary Figure 1**.

The structure and the amount of N-glycans released enzymatically from IgG molecules were analyzed by the UPLC-MS method. PNGase F digested N-glycans were fluorescently labeled with 2-AB. The obtained resulting chromatograms were integrated into 25 glycan peaks. N-oligosaccharide structures were assigned based on the GU values and m/z ratios using Waters UNIFI scientific information system software (**Figures 2, 3** and **Supplementary Table 1**). The chromatographic pattern of resolved glycans with dominant GP3 was similar for all analyzed groups. The identified N-glycans were predominantly partially core-fucosylated diantennary complex-type species, and sialylated structures, some of them with bisecting GlcNAc residue. Based on the relative peak intensity, expressed as a percentage of the area of a given GP, statistical analysis was performed using the Kruskal-Wallis nonparametric test with a significance level of $p < 0.05$.

3.1 Immunosuppressive Treatment Affects IgG N-Glycosylation in Graves' Disease

The statistically significant differences in IgG N-glycan profiles between patients with Graves' disease before and during immunosuppressive therapy and healthy donors were demonstrated for the twelve out of 25 GP-matched N-glycan structures (**Figure 2**). A content of agalactosylated structures

with proximal fucose (F(6)A1, F(6)A2, F(6)A2B) and oligomannose (M5) increases in GD (all structures) and GD/T (F(6)A2B and M5) compared with CTR. Statistically significant quantitative differences were also found in galactosylated (A2G(4)2) and fucosylated (F(6)A2[6]BG(4)1) N-oligosaccharides with their up-regulation in GD/T patients compared to GD. In contrast to the above-mentioned changes in the case of N-glycans with a bisecting GlcNAc (A2BG(4)2), α 1,6-fucosylated (F(6)A2BG(4)2), monosialylated (A2G(4)2S1 and F(6)A2G(4)2S1), and disialylated (A2G(4)2S2) structures we observed their statistically significant down-regulation in GD (all structures) and GD/T (A2G(4)2S2) relatively to CTR.

The effect of N-glycosylation on the development of AITD compared with CTR after UPLC-MS analysis was further verified by performing statistical analysis with the Kruskal-Wallis test for glycan groups (non-sialylated, monosialylated, disialylated, non-fucosylated, fucosylated, nongalactosylated, galactosylated, monoantennary, and diantennary). The results showing statistically significant differences are presented in **Figure 4**. Non-sialylated and monoantennary glycans showed an increase in both GD groups compared with healthy volunteers, whereas diantennary structures showed an increasing trend in GD compared with CTR. Statistically significant decreases were shown for monosialylated (in GD and GD/T), and disialylated (in GD) glycans compared with healthy subjects. The relative content of galactosylated structures was lower in GD while in GD/T this group of glycans normalized partly which was related to a decline of agalactosylated structures. The reduced IgG galactosylation was accompanied by an increase of agalactosylated structures in GD (**Figure 4A**).

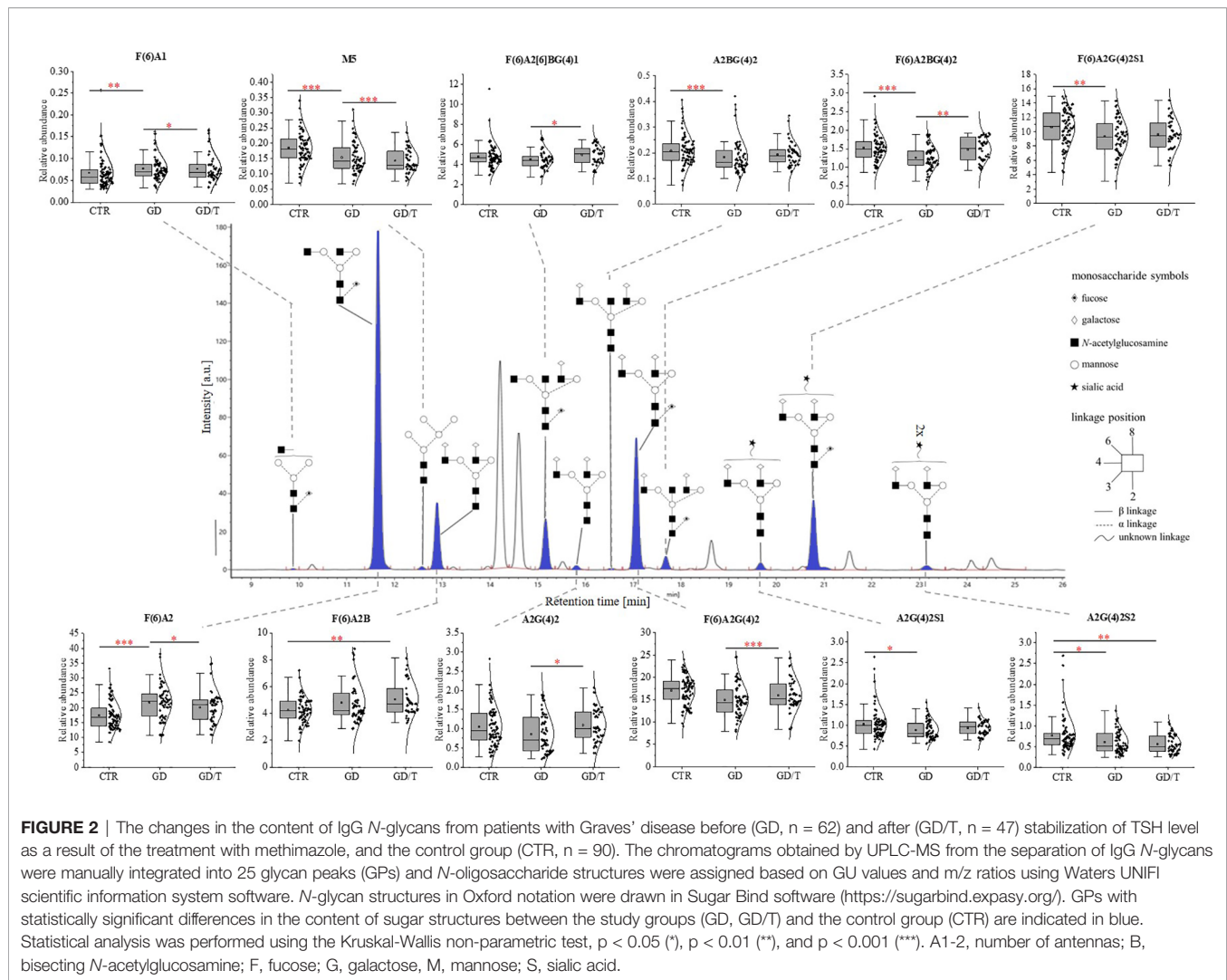
3.2 The Severity of Inflammation in Hashimoto's Thyroiditis Is Accompanied by Changes of IgG N-Glycosylation

Statistically significant quantitative differences were also found for 8 N-oligosaccharide structures between patients without hypothyroidism, patients with HT after L-thyroxine treatment, and healthy volunteers (**Figure 4**). For agalactosylated (F(6)A1, A2, F(6)A2), mono- (A2G(4)2S1) and disialylated (A2BG(4)2S2) structures, an increase was shown in HT2 compared to CTR (A2, A2BG(4)2S2) and HT1 (other structures). In contrast, some fucosylated (F(6)A2G(4)2) and monosialylated (F(6)A2G(4)2S1) structures were increased in HT1 relative to HT2. HT1 also indicated a statistically significant decrease in oligomannose-type N-glycan (M5) compared to CTR.

A statistically quantitative increase in the content of monoantennary oligosaccharides was observed in HT2 compared to HT1. The amount of diantennary sugar structures was significantly higher in HT1 compared to HT2 and CTR. We identified also a relationship between the alterations of galactosylated and agalactosylated N-glycans in HT patients, parallel with the lowering of galactosylation, agalactosylated structures increased in HT2 vs. HT1 donors (**Figure 4B**).

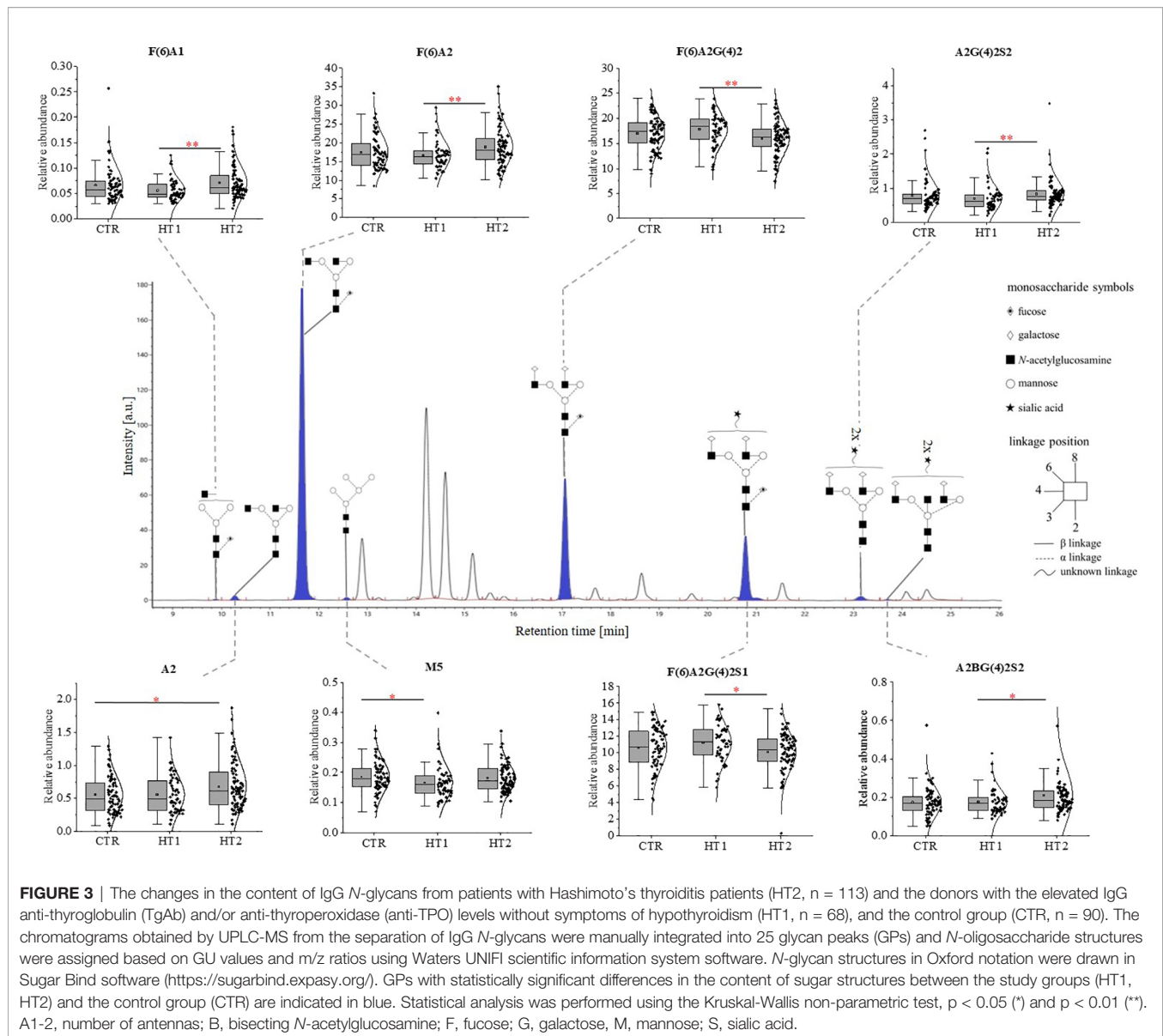
3.3 ST6Gal1 Is Active in AITD Patients' Sera and Can Modify IgG Sialylation

Due to the changes of mono- and disialylated IgG N-glycans in both HT and GD sera detected by UPLC-MS analysis (**Figure 4**),



we evaluated an activity of ST6Gal1 in sera of AITD patients and healthy individuals using SNA lectin blotting method described by Jones et al. (47) with some modifications. We observed a positive reaction of α 2,6-sialylated *N*-glycans on the heavy chain with SNA for IgG isolated from control and AITD sera. Desialylation of IgG using the neuraminidase with a wide specificity resulted in an almost complete attenuation of the reaction with SNA (Figure 5A). A weak signal observed for neuraminidase + samples (Figure 5A) was a result of non-specific SNA binding to IgG polypeptides as determined by the reaction with SNA preincubated with acetic acid which abolishes SNA binding to SA (Figure 5D). Incubation of desialylated IgG heavy chain with human sera restored SNA-positive reaction which resulted from re-sialylation of IgG by ST6Gal1 present in donor sera (Figure 5B). To verify reversibility of this sialylation on PVDF membrane-bound IgG heavy chain we used again neuraminidase to remove SA attached by serum ST6Gal1 which led to an almost complete loss of the reaction with SNA (Figure 5C).

The detailed characteristic of IgG *N*-glycome obtained by UPLC-MS showed the statistically significant quantitative differences in sugar structures in the course of immunosuppressive treatment of GD patients, and during the development of thyroiditis. The obtained results allow us to support the previous observation that IgG *N*-glycosylation is a particularly dynamic process, reflecting the course of the diseases, and conclude that IgG *N*-glycan alterations accompany the inflammatory processes in AITD and the applied therapy. The changes occur early in the development of the disease when the synthesis of autoantibodies is triggered, and the thyroid structure has not yet undergone the destruction that accompanies chronic inflammation at later stages of the disease. Methimazole therapy significantly changes the structure of the IgG glycome in patients with GD. We have also shown that ST6Gal1, responsible for the attachment of α 2,6-SA, is active in the sera of AITD patients and healthy donors and has the potential to modify IgG sialylation independently from the classical pathway of cellular glycosylation.



4 DISCUSSION

The research area that has been little addressed so far is the glycoimmunobiology of AITDs. Changes in *N*-glycosylation of immune system molecules in AITDs have only been analyzed concerning serum proteins present in the context of differences between healthy controls and patients (40, 55, 56), while the impact of treatment and the severity of thyroiditis on protein glycosylation has never been focused on. Previous studies have shown that the sialylation and core fucosylation of TgAb *N*-glycans in Hashimoto's thyroiditis patients were lowered compared to GD donors (56), but elevated in HT compared to healthy individuals (57). Also, oligomannose type structures in TgAb antibodies were increased in HT versus the control group (57). In contrast, our recent study has demonstrated the reduced core fucosylation of IgG in AITD patients compared to healthy donors which

correlated of the reduced Fuc content with serum anti-TPO titers (40). On the other hand, the study of Ząbczyńska et al. revealed the up-regulation of disialylated, diantennary complex *N*-glycans and monosialylated, triantennary structures in IgG-depleted sera from patients with HT compared to healthy donors (55).

To explore the glycoimmunology of AITD more deeply, in the present study, we focused on changes in IgG *N*-glycan structures in donors with Graves' disease before (GD) and after (GD/T) TSH normalization as the result of thyrostatic and immunosuppressive therapy, patients with the elevated titer of antithyroid autoantibodies (HT1), and subjects with Hashimoto's thyroiditis treated with L-thyroxine (HT2) in comparison to healthy volunteers (CTR).

Our present results are partially in accordance with the previous one by Martin et al. (40). Obtaining full compliance of the results of glycosylation analysis seems to be impossible, because of diverse

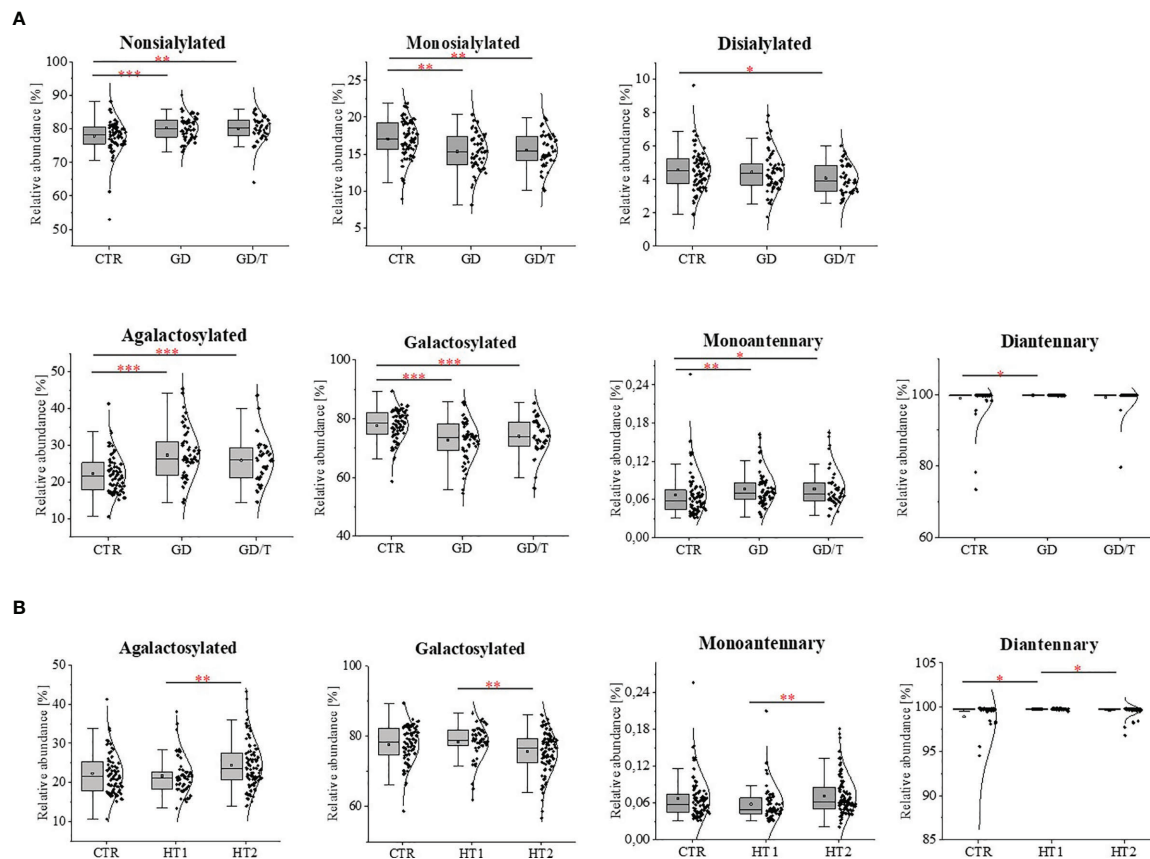


FIGURE 4 | IgG *N*-glycosylation changes in sera of **(A)** the patients with Graves' disease before (GD, $n = 62$) and after (GD/T, $n = 47$) stabilization of TSH level, **(B)** the subjects with the elevated IgG anti-thyroglobulin (TgAb) and/or anti-thyroperoxidase (anti-TPO) levels (HT1, $n = 68$), Hashimoto's disease patients (HT2, $n = 113$) (study groups) relative to the healthy donors (CTR, control group, $n = 90$). Quantitative comparison of derived glycan traits (nonsialylated, monosialylated, disialylated, galactosylated, agalactosylated, monoantennary, diantennary) between control and study groups was performed by Kruskal-Wallis test assuming a significance level for $p < 0.05$ (*), $p < 0.01$ (**), and $p < 0.001$ (***).

monosaccharide composition, asymmetric glycosylation in both Fc glycosylation sites, *N*-glycosylation of Fab variable regions, and variant glycosylation of IgG1-4 subclasses, which result in a huge heterogeneity of IgG glycome in a given person (4). It means that drawing reliable conclusions requires verification of the results for various populations and analysis for large study groups.

4.1 Methimazole Therapy Impact on IgG *N*-Glycosylation in Graves' Diseases

The effect of immunosuppressive drugs used in the treatment of autoimmune diseases on *N*-glycosylation of IgG and other serum proteins has been demonstrated in previous studies. This issue has been the most explored in RA, the autoimmune disorders with the best characterized IgG *N*-glycan alterations. It is well documented that one of the effects of immunosuppressive agents administrated in RA is the altered IgG glycosylation reversing the antibody activity towards the anti-inflammatory response (48–51, 58).

GD patients recruited to our study were treated with methimazole (1-methyl-2-mercaptoimidazole; Polish brand names: Thyrozol or Metizol), which affects thyroid hormone

synthesis as thyrostatics. Methimazole was shown also to have an immunosuppressive effect resulting from a decrease of TRAb serum level, triggering of intrathyroidal T cell apoptosis, reduction of HLA class II expression as well as up-regulation of circulating Tregs and reduction of the number of Th cells, NK, and activated intrathyroidal T cells (59–61). TRAb concentration in the sera of methimazole-treated GD patients was partly reduced (Table 1 and Figure 1A), which confirms the immunosuppressive activity of this antithyroid agent. Taking into account that the blood was taken in the relatively short term after stabilization of TSH levels, it can be assumed that in the longer term TRAb titer was further stabilized.

The normalisation of TRAb level in GD/T (Table 1 and Figure 1A) was accompanied by the altered intensity of the individual UPLC-MS peaks to which agalactosylated (F(6)A2), monogalactosylated (F(6)A2(5)BG(4)1), and digalactosylated (A2G(4)2, F(6)A2G(4)2 and F(6)A2BG(4)2) glycans were assigned. The amount of both digalactosylated *N*-glycans was up-regulated while the content of agalactosylated structure was reduced as the result of methimazole therapy in GD patients

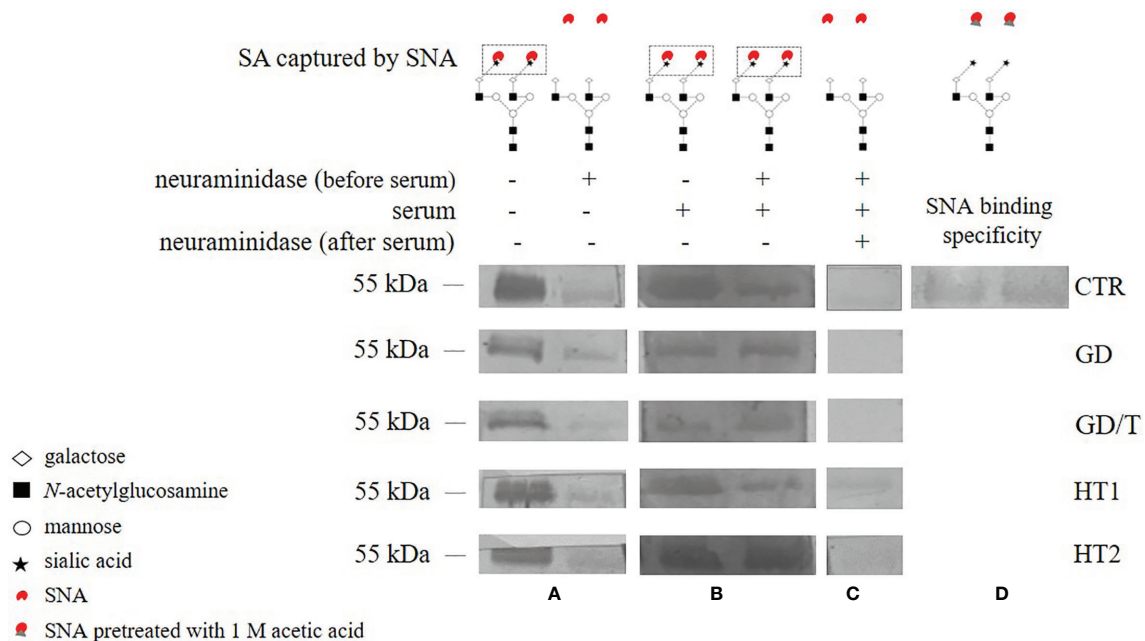


FIGURE 5 | The activity of serum ST6Gal1 assessed by SNA lectin blotting on IgG heavy chain *N*-glycans. IgGs isolated from the sera of the patients with Graves' disease before (GD) and after (GD/T) TSH normalization, the subjects with the elevated anti-thyroglobulin (TgAb) and/or anti-thyroperoxidase (TPO) antibodies (HT1), Hashimoto's thyroiditis patients (HT2), and healthy volunteers (CTR, control group) were used. **(A)** IgG heavy chain sialylated (neuraminidase -) and desialylated by neuraminidase from *Arthrobacter ureafaciens* (neuraminidase +), both untreated with serum, **(B)** IgG heavy chain sialylated by serum ST6Gal1 from control and study groups after desialylation by neuraminidase, **(C)** IgG heavy chain redsialylated after serum ST6Gal1 sialylation performed to verify the reversibility of ST6Gal1 sialylation, **(D)** control of SNA binding specificity verified by lectin blotting with SNA preincubated with 1 M acetic acid. More details are described in the section Materials and Methods.

(Figures 2, 4A). This part of our observations is following the previous experiments on IgG *N*-oligosaccharides from RA patients undergoing treatment with methotrexate and infliximab. In addition to suppressing inflammatory processes confirmed by a reduced level of C-reactive protein (CRP) (58), both antirheumatic drugs were shown to enhance IgG galactosylation (48–51, 58). In turn, in immune thrombocytopenia galactosylation of IgG1 and IgG4 subclasses in the blood of anti-CD20 monoclonal antibody (rituximab)-treated patients was slightly reduced, while IgG1, IgG2/3, and IgG4 showed the higher content of *N*-glycans with bisected GlcNAc (62). Therefore we can conclude that the effect of immunosuppressive therapy on *N*-glycosylation depends on the applied therapeutic agent and autoimmune disorder.

Apart from the significantly increased galactosylation of *N*-glycans in inflammatory arthritis patients treated with anti-TNF IgG, Collins et al. observed an up-regulation of *N*-glycan core-fucosylation (58), which is well known to contribute to IgG anti-inflammatory activity (6). Our study demonstrated that the amount of IgGs with core-fucosylated structures F(6)A2(6)BG(4)1, F(6)A2G(4)2, and F(6)A2BG(4)2 is higher in GD patients after TSH normalization as the result of methimazole therapy (GD/T) in relation to the untreated donors (Figure 2) which can also contribute to attenuating of the immune response.

According to the literature data, reduced sialylation favors the pro-inflammatory properties of IgG (63, 64). Our UPLC-MS

analysis showed that the sialylation status of IgG was not affected by methimazole treatment. The intensity of the sialylated *N*-glycans was not altered in GD patients during immunosuppressive therapy in relation to the state before this drug implementation (GD/T vs. GD) (Figure 2). However, the entire pool of IgG monosialylated and disialylated *N*-oligosaccharides was significantly reduced in both GD groups in comparison to healthy donors (Figure 4A). Sialic acid is terminally linked to Gal residues in IgG *N*-glycans, and its attachment requires the presence of galactosylated structures. We presently show that galactosylation of IgG is normalized during methimazole administration (Figure 4A) while *N*-glycans are still undersialylated in relation to healthy donors (Figure 2), which can be an effect of too short drug administration. To resolve this, studies on a long-term treatment cohort would be necessary.

Methimazole therapy partially reversed the changes of IgG *N*-glycosylation by the up-regulation of galactosylation and reduction of agalactosylation (Figure 4A). Down-regulated galactosylation is well known to promote the proinflammatory potential of IgG (34). Without detailed functional studies, we can only speculate that this effect of anti-inflammatory treatment may reduce clinical symptoms of the disease also by affecting galactosylation of antibodies in GD.

Due to the documented activity of serum ST6Gal1 from AITD patients on desialylated IgG *N*-glycans (Figure 5), we

suppose that this serum sialyltransferase may contribute to IgG sialylation in the bloodstream in thyroid autoimmunity. SNA lectin blotting used in our study to assess ST6Gal1 activity provided the qualitative data but did not allow for quantitative analysis and determination of possible differences between groups. A quantitative assessment of the effects of ST6Gal1 activity would be interesting to interpret the UPLC-MS results, and is worth pursuing in future studies. Anti-inflammatory activity of IgG sialylation is also considered as a therapeutic strategy in terms of the usage of intravenous immunoglobulins (IVIGs) for the treatment of autoimmune diseases (65, 66). Pagan et al. used the mechanism of extracellular sialylation to target IgG N-glycan remodeling. They confirmed the attaching of SA by the extracellular enzyme to Fc of IgGs deposited at sites of inflammation. The activity of recombinant human galactosyltransferase B4GALT1 and ST6Gal1 on a single Fc fragment of IgG1 attenuated inflammation in a K/BxN arthritis model. The increased IgG sialylation resulted from *in vivo* administration of a soluble ST6GAL1 converted IgG activity into anti-inflammatory in autoimmune disease (67).

In the previous study, we have also demonstrated the altered glycosylation on human leukocytes activated *in vitro* in a two-way mixed leukocyte reaction (MLR) in the presence of two immunosuppressive agents commonly used to induce immune tolerance after organ transplantation: cyclosporin A (CsA), an inhibitor of calcineurin, and rapamycin (Rapa), which blocks mammalian target of rapamycin mTOR. Oligomannose/hybrid-type N-glycans on human leukocytes in MLR model were significantly down-regulated by CsA, while the synergistic action of both immunosuppressive drugs enhanced the amount of these structures on leukocyte proteins (68).

Based on the previous literature data and the presently obtained results, it seems that immunosuppressive agents-triggered changes of glycosylation are a wider phenomenon, which can concern drugs with various mechanisms of action, and different targeted proteins. Functional consequences of the observed changes in IgG N-glycosylation isolated from methimazole-treated patients for Graves' disease course need further study.

4.2 Altered IgG N-Glycosylation in Autoimmune Thyroiditis May Contribute to Thyroid Destruction

The crucial role of Asn297-linked N-glycans attached to IgG Fc fragment in ADCC and CDC has been demonstrated on various research models (69), and was shown to be important in autoimmune disease development (70, 71), including thyrocyte destruction in Hashimoto's thyroiditis (72). Forming of immune complexes of IgG autoantibodies with self-antigens gathers innate immune effector cells, like NK and myeloid cells, which express Fcγ receptors (FcγR) and/or recruits complement proteins. Activation of effector cells and complement cascade results in target cell apoptosis and finally tissue damage (34, 73).

Martin et al. detected the reduced level of core Fuc in IgG N-glycans from AITD subjects and depletion of antenna fucosylation in peripheral blood mononuclear cells (PBMCs)

isolated from the whole blood of HT patients (40). The current analysis showed that the content of two core-fucosylated IgG structures (F(6)A2G(4)2 and F(6)A2G(4)2S) was decreased in Hashimoto's thyroiditis patients, while the level of F(6)A2 N-glycan assigned the most abundant UPLC peak was up-regulated in these patients (HT2) compared to the donors with the higher level of anti-Tg/anti-TPO (HT1) (**Figure 3**). In effect, the group analysis did not show statistically significant changes in the whole pool of core-fucosylated N-glycans between the patients with thyroiditis at different stages of the disease severity and healthy subject (**Figure 4**). Taking into account the significantly different number of the recruited participants in both studies, not complete reproducibility of the obtained results seems to be understandable.

Core-fucosylation of immune system proteins, including IgG, plays an important role in their activity. Alterations in IgG core-fucosylation are, right after galactosylation, one of the most common modifications detected in inflammatory diseases, including autoimmune diseases (37). Based on the previous results which demonstrated that core-fucosylation impeded FcγRIIIA binding and inhibited ADCC (47), we can speculate that the reduced core-fucosylation of IgG N-glycans in AITD described by Martin et al. (40), and the currently observed decrease of the two core-fucosylated structures in HT2 (**Figure 3**) may contribute to inflammation and thyroid tissue damage in the course of Hashimoto's thyroiditis.

Sialic acid is a component of glycans crucially important in the regulation of immune glycoprotein function, due to its negative charge, and terminal localization in oligosaccharide structures. Autoimmunity is usually accompanied by down-regulation of IgG sialylation (74, 75). The reduced sialylation of IgG1 and IgG2 occurs in granulomatosis with vasculitis (GPA) (64). Kemna et al. showed that the level of total IgG sialylation has a prognostic value in GPA relapse, as the SA content of IgG1 in patients with granulomatosis decreased during relapse and remains unchanged in remission (63). Collins et al. demonstrated a decrease in sialylated triantennary N-glycans in inflammatory arthritis patients, strongly correlated with reduced CRP level in the silenced inflammatory process (73).

Our recent study has demonstrated more intensive thyrocyte lysis in the presence of IgG isolated from HT patients than from healthy donors, which resulted from the higher anti-TPO content in the whole IgG pool of HT donors and the altered IgG N-glycosylation in HT autoimmunity (72). The present analysis demonstrated that the content of F(6)A2G(4)2S1 structure, the most intensely sialylated N-glycan in IgG glycoprofile, was lowered in Hashimoto's thyroiditis in comparison to HT1 group (**Figure 3**), which may explain the results obtained in the previous functional analysis performed with IgG from HT patients in the *in vitro* model (72). The study by Ząbczyńska et al. indicated also that IgGs with desialylated N-glycans were more potent to induce ADCC in human thyrocytes (72).

In summary, N-glycans are involved in fundamental cellular and molecular processes that stimulate and inhibit immune system pathways. Detailed characterization of the IgG

N-glycans obtained by UPLC-MS revealed statistically significant quantitative differences in sugar structure during immunosuppressive treatment of GD patients and during the development of Hashimoto's thyroiditis. The results show that changes in IgG *N*-oligosaccharides contribute to the development of inflammation in autoimmune thyroid diseases. These changes begin in the early stages of the disease, where autoantibodies are overproduced, but hypothyroidism and thyroid gland destruction, which are associated with later stages of pathology, are not observed. The use of immunosuppressive therapy significantly alters the process of *N*-glycosylation in patients with Graves' disease. Further studies are needed to evaluate the changes in IgG *N*-glycosylation in AITD to see how relevant it is to determine the contribution of altered oligosaccharide content to antibody-mediated autoimmunity in these autoimmune diseases. It is also worth noting, that similarly as in the case of vast majority of glycomic studies of this kind, we compare only relative quantities of glycan structures in tested samples. By its nature, the relative content of a given sugar structure in a sample depends not only on the increase or decrease in its expression, but also on the simultaneous quantitative changes of other glycans. Being aware of these limitations, we used this approach in the described studies and we believe that it is, however, a specific description of the phenotype of the patients and enables comparative analysis. On the one hand, it gives less room for interpretation of the biological contexts and mechanisms causing the observed changes, but on the other hand, when applied according to the same criteria for all analysed samples, it can be a useful parameter for patient stratification.

5 CONCLUDING REMARKS

N-glycosylation of immune proteins fundamentally affects their structure, half-life, activity and interaction with protein partners on other cells or soluble ones present in body fluids (76). For a long time the sugar part of glycoproteins has been considered only as an insignificant decoration, until the results of glycoanalysis obtained for IgG showed, how essential sugar structures are for the proper biochemical properties, and biological activity of this molecule. Thanks to the development of new research technologies, we are increasingly aware of the great role played by glycans under physiological conditions. In turn, determining how structure of oligosaccharides is remodeled in human pathologies, and what the consequences of these changes are for the course of disease has not been well studied (8, 9, 12). *N*-glycosylation of IgG in AITDs was relatively poorly studied, although HT and GD are among the most common autoimmune diseases. Our present study provides new data on IgG remodeling in the course of AITD. The questions are how the observed changes of IgG *N*-glycosylation affect its activity, and what consequences these oligosaccharide modifications have for the development of the disease or, in the case of treatment, for the recovery or the reduction of symptoms, remain to be answered in further studies.

DATA AVAILABILITY STATEMENT

The original contributions presented in the study are included in the article/**Supplementary Material**. Further inquiries can be directed to the corresponding author.

ETHICS STATEMENT

The studies involving human participants were reviewed and approved by Bioethics Committee of the Jagiellonian University in Kraków, Poland. The patients/participants provided their written informed consent to participate in this study.

AUTHOR CONTRIBUTIONS

EP designed the study and secured grant funding. GS recruited blood donors. ST and PL-L performed experiments, and analyzed data. ST drafted the manuscript. EP and PL-L revised the manuscript. All authors contributed to the article and approved the submitted version.

FUNDING

The study was supported by a grant from the Polish National Science Centre (grant no. 2015/18/E/NZ6/00602).

ACKNOWLEDGMENTS

The publication was created with the use of equipment co-financed by the qLIFE Priority Research Area under the program "Excellence Initiative - Research University" at Jagiellonian University in Kraków, Poland. The open-access publication of this article was funded by the programme "Excellence Initiative - Research University" at Jagiellonian University in Kraków, Poland.

SUPPLEMENTARY MATERIAL

The Supplementary Material for this article can be found online at: <https://www.frontiersin.org/articles/10.3389/fimmu.2022.841710/full#supplementary-material>

Supplementary Figure 1 | Protein profiles of IgG separated by SDS-PAGE under reducing conditions after Coomassie Brilliant Blue (CBB) staining. IgG heavy and light chains are indicated by red boxes. MW, molecular weight marker (Page Ruler Prestained Protein Ladder, Thermo Scientific, 26616).

Supplementary Table 1 | UPLC-MS *N*-glycan peaks annotation. Glycan structures were identified in Waters UNIFI Scientific Information System based on glucose unit values (GU) and the exact mass. The Oxford notation was used for glycan names and symbolic representations. Observed GU and observed masses were calculated as averages of all samples analysed. The structures of *N*-glycans in Oxford notation (UOXF) were prepared in Sugar Bind software (<https://sugarbind.expaty.org/>).

REFERENCES

- Schroeder H, Cavacini L. Structure and Function of Immunoglobulins. *J Allergy Clin Immunol* (2010) 125(2 Suppl 2):S41–52. doi: 10.1016/j.jaci.2009.09.046
- Krapp S, Mimura Y, Jefferis R, Huber R, Sondermann P. Structural Analysis of Human IgG-Fc Glycoforms Reveals a Correlation Between Glycosylation and Structural Integrity. *J Mol Biol* (2003) 325(5):979–89. doi: 10.1016/s0022-2836(02)01250-0
- Seeling M, Bruckner C, Nimmerjahn F. Differential Antibody Glycosylation in Autoimmunity: Sweet Biomarker or Modulator of Disease Activity? *Nat Rev Rheumatol* (2017) 13(10):621–30. doi: 10.1038/nrheum.2017.146
- Gudelf I, Lauc G, Pezer M. Immunoglobulin G Glycosylation in Aging and Diseases. *Cell Immunol* (2018) 333:65–79. doi: 10.1016/j.cellimm.2018.07.009
- Kozłowska K, Rydlewska M, Ząbczyńska M, Pocheć E. IgG Glycosylation in Autoimmune Diseases. *Postepy Hig Med Dosw* (2018) 72:975–90. doi: 10.5604/01.3001.0012.7351
- Shade K, Anthony M. Antibody Glycosylation and Inflammation. *Antibodies* (2013) 2(3):392–414. doi: 10.3390/antib2030392
- van de Bovenkamp F, Hafkenschied L, Rispeus T, Rombouts Y. The Emerging Importance of IgG Fab Glycosylation in Immunity. *J Immunol* (2016) 196(4):1435–41. doi: 10.1049/jimmunol.1502136
- Cobb B. The History of IgG Glycosylation and Where We are Now. *Glycobiology* (2020) 30(4):202–13. doi: 10.1093/glycob/cwz065
- Wang T. IgG Fc Glycosylation in Human Immunity. *Curr Top Microbiol Immunol* (2019) 423:63–75. doi: 10.1007/82_2019_152
- Bowden T, Baruah K, Coles C, Harvey D, Yu X, Song B, et al. Chemical and Structural Analysis of an Antibody Folding Intermediate Trapped During Glycan Biosynthesis. *J Am Chem Soc* (2012) 134(42):17554–63. doi: 10.1021/ja306068g
- Dunn-Walters D, Boursier L, Spencer J. Effect of Somatic Hypermutation on Potential N-Glycosylation Sites in Human Immunoglobulin Heavy Chain Variable Regions. *Mol Immunol* (2000) 37(3-4):107–13. doi: 10.1016/s0161-5890(00)00038-9
- Alter G, Ottenhoff T, Joosten S. Antibody Glycosylation in Inflammation, Disease and Vaccination. *Semin Immunol* (2018) 39:102–10. doi: 10.1016/j.smim.2018.05.003
- Dwek R. Biological Importance of Glycosylation. *Dev Biol Stand* (1998) 96:43–7. doi: 10.1007/978-94-011-5288-4_1
- Mimura Y, Church S, Ghirlando R, Ashton P, Dong S, Goodall M, et al. The Influence of Glycosylation on the Thermal Stability and Effector Function Expression of Human IgG1-Fc: Properties of a Series of Truncated Glycoforms. *Mol Immunol* (2000) 37(12-13):697–706. doi: 10.1016/s0161-5890(00)00105-x
- Mimura Y, Sondermann P, Ghirlando R, Lund J, Young S, Goodall M, et al. Role of Oligosaccharide Residues of IgG1-Fc in Fc Gamma RIIB Binding. *J Biol Chem* (2001) 276(49):45539–47. doi: 10.1074/jbc.M107478200
- Schwab I, Nimmerjahn F. Intravenous Immunoglobulin Therapy: How Does IgG Modulate the Immune System? *Nat Rev Immunol* (2013) 13(3):176–89. doi: 10.1038/nri3401
- Pučić Baković M, Selman M, Hoffmann M, Rudan I, Campbell H, Deelder A, et al. High-Throughput IgG Fc N-Glycosylation Profiling by Mass Spectrometry of Glycopeptides. *J Proteome Res* (2013) 12(2):821–31. doi: 10.1021/pr300887z
- Novokmet M, Lukic E, Vuckovic F, Duric Z, Keser T, Rajsl K, et al. Changes in IgG and Total Plasma Protein Glycomes in Acute Systemic Inflammation. *Sci Rep* (2014) 4:4347. doi: 10.1038/srep04347
- Sjöwall C, Zapf J, von Lohneysen S, Magorivska I, Biermann M, Janko C, et al. Altered Glycosylation of Complexed Native IgG Molecules is Associated With Disease Activity of Systemic Lupus Erythematosus. *Lupus* (2015) 24(6):569–81. doi: 10.1177/0961203314558861
- Fröhlich E, Wahl R. Thyroid Autoimmunity: Role of Anti-Thyroid Antibodies in Thyroid and Extra-Thyroidal Diseases. *Front Immunol* (2017) 8:521. doi: 10.3389/fimmu.2017.00521
- Chen C, Pichurin P, Nagayama Y, Latrofa F, Rapoport B, McLachlan S. The Thyrotropin Receptor Autoantigen in Graves' Disease is the Culprit as Well as the Victim. *J Clin Invest* (2003) 111(12):1897–904. doi: 10.1172/JCI17069
- Caturegli P, De Remigis A, Rose N. Hashimoto Thyroiditis: Clinical and Diagnostic Criteria. *Autoimmun Rev* (2014) 13(4-5):391–7. doi: 10.1016/j.autrev.2014.01.007
- Wang S, Baker J. The Role of Apoptosis in Thyroid Autoimmunity. *Thyroid* (2007) 17(10):975–9. doi: 10.1089/thy.2007.0208
- Stassi G, De Maria R. Autoimmune Thyroid Disease: New Models of Cell Death in Autoimmunity. *Nat Rev Immunol* (2002) 2(3):195–204. doi: 10.1038/nri750
- Bretz J, Baker J. Apoptosis and Autoimmune Thyroid Disease: Following a TRAIL to Thyroid Destruction? *Clin Endocrinol (Oxf)* (2001) 55(1):1–11. doi: 10.1046/j.1365-2265.2001.01345.x
- Salmaso C, Bagnasco M, Pesce G, Montagna P, Brizzolara R, Altrinetti V, et al. Regulation of Apoptosis in Endocrine Autoimmunity: Insights From Hashimoto's Thyroiditis and Graves' Disease. *Ann NY Acad Sci* (2002) 966:496–501. doi: 10.1111/j.1749-6632.2002.tb04253.x
- Chardès T, Chapal N, Bresson D, Bès C, Giudicelli V, Lefranc M, et al. The Human Anti-Thyroid Peroxidase Autoantibody Repertoire in Graves' and Hashimoto's Autoimmune Thyroid Diseases. *Immunogenetics* (2002) 54:141–57. doi: 10.1007/s00251-002-0453-9
- Bogner U, Schleusener H, Wall J. Antibody-Dependent Cell Mediated Cytotoxicity Against Human Thyroid Cells in Hashimoto's Thyroiditis But Not Graves' Disease. *J Clin Endocrinol Metab* (1984) 59(4):734–58. doi: 10.1210/jcem-59-4-734
- Rebuffat S, Nguyen B, Robert B, Castex F, Peraldi-Roux S. Antithyroperoxidase Antibody-Dependent Cytotoxicity in Autoimmune Thyroid Disease. *J Clin Endocrinol Metab* (2008) 93(3):929–34. doi: 10.1210/jc.2007-2042
- Antonelli A, Ferrari S, Corrado A, Di Domenicantonio A, Fallahi P. Autoimmune Thyroid Disorders. *Autoimmun Rev* (2015) 14(2):174–80. doi: 10.1016/j.autrev.2014.10.016
- Yeşilkaya E, Koç A, Bideci A, Camurdana O, Boyraz M, Erkal O, et al. CTLA4 Gene Polymorphisms in Children and Adolescents With Autoimmune Thyroid Diseases. *Genet Test* (2008) 12(3):461–4. doi: 10.1089/gte.2008.0053
- Ercan A, Cui J, Chatterton D, Deane K, Hazen M, Brintnella W, et al. IgG Galactosylation Aberrancy Precedes Disease Onset, Correlates With Disease Activity and is Prevalent in Autoantibodies in Rheumatoid Arthritis. *Arthritis Rheumatol* (2010) 62(8):2239–48. doi: 10.1002/art.27533
- Parekh R, Dwek R, Suttona B, Fernandes D, Leung A, Stanworth D, et al. Association of Rheumatoid Arthritis and Primary Osteoarthritis With Changes in the Glycosylation Pattern of Total Serum IgG. *Nature* (1985) 316(6027):452–7. doi: 10.1038/316452a0
- Dekkers G, Rispeus T, Vidarsson G. Novel Concepts of Altered Immunoglobulin G Galactosylation in Autoimmune Diseases. *Front Immunol* (2018) 9:553. doi: 10.3389/fimmu.2018.00553
- Grinżewska-Sieškiewicz E, Klimiuk P, Kisiel D, Gindziński A, Sierakowski S. The Changes in Monosaccharide Composition of Immunoglobulin G in the Course of Rheumatoid Arthritis. *Clin Rheumatol* (2007) 26(5):685–90. doi: 10.1007/s10067-006-0370-7
- Ząbczyńska M, Link-Lenczowski P, Pocheć E. "Glycosylation in Autoimmune Diseases." In: G Lauc and I Trbojević-Akmačić, editors. *The Role of Glycosylation in Health and Disease*, vol. 1325 (2021). p. 205–18. *Adv. Exp. Med. Biol.* Springer. Cham. doi: 10.1007/978-3-030-70115-4_10
- Knopf J, Biermann M, Muñoz L, Herrmann M. Antibody Glycosylation as a Potential Biomarker for Chronic Inflammatory Autoimmune Diseases. *AIMS Genet* (2016) 3:280–91. doi: 10.3934/gene.2016.4.280
- Gornik I, Maravić G, Dumić J, Flögel M, Lauc G. Fucosylation of IgG Heavy Chains is Increased in Rheumatoid Arthritis. *Clin Biochem* (1999) 32(8):605–8. doi: 10.1016/s0009-9120(99)00060-0
- Vučković F, Krištić J, Gudelf I, Teruel M, Keser T, Pezer M, et al. Association of Systemic Lupus Erythematosus With Decreased Immunosuppressive Potential of the IgG Glycome. *Arthritis Rheumatol* (2015) 67(11):2978–89. doi: 10.1002/art.39273
- Martin T, Simurina M, Ząbczyńska M, Kavr M, Rydlewska M, Pezer M, et al. Decreased Immunoglobulin G Core Fucosylation, A Player in Antibody-Dependent Cell-Mediated Cytotoxicity, is Associated With Autoimmune Thyroid Diseases. *Mol Cell Proteomics* (2020) 19(5):774–92. doi: 10.1074/mcp.RA119.001860
- Scallan B, Tam S, McCarthy S, Cai A, Raju T. Higher Levels of Sialylated Fc Glycans in Immunoglobulin G Molecules can Adversely Impact Functionality. *Mol Immunol* (2007) 44(7):1524–34. doi: 10.1016/j.molimm.2006.09.005
- Shields R, Lai J, Keck R, O'Connell L, Hong K, Meng Y, et al. Lack of Fucose on Human IgG1 N-Linked Oligosaccharide Improves Binding to Human

- Fcγ3 and Antibody-Dependent Cellular Toxicity. *J Biol Chem* (2002) 277(30):26733–40. doi: 10.1074/jbc.M202069200
43. Quast I, Keller C, Maurer M, Giddens J, Tackenberg B, Wang L, et al. Sialylation of IgG Fc Domain Impairs Complement-Dependent Cytotoxicity. *J Clin Invest* (2015) 125(11):4160–70. doi: 10.1172/JCI82695
 44. Anthony R, Wermeling F, Ravetch J. Novel Roles for the IgG Fc Glycan. *Ann NY Acad Sci* (2012) 1253:170–80. doi: 10.1111/j.1749-6632.2011.06305.x
 45. Thomann M, Reckermann K, Reusch D, Prasser J, Tejada M. Fc-Galactosylation Modulates Antibody-Dependent Cellular Cytotoxicity of Therapeutic Antibodies. *Mol Immunol* (2016) 73:69–75. doi: 10.1016/j.molimm.2016.03.002
 46. Li T, DiLillo D, Bournazos S, Giddens J, Ravetch J, Wang L. Modulating IgG Effector Function by Fc Glycan Engineering. *Proc Natl Acad Sci U S A* (2017) 114:3485–90. doi: 10.1073/pnas.1702173114
 47. Jones M, Oswald D, Joshi S, Whiteheart S, Orlando R, Cobb B. B-Cell-Independent Sialylation of IgG. *Proc Natl Acad Sci U S A* (2016) 113(26):7207–12. doi: 10.1073/pnas.1523968113
 48. Gindzińska-Sieškiewicz E, Radziejewska I, Domysławska I, Klimiuk P, Sulik A, Rojewski J. Changes of Glycosylation of IgG in Rheumatoid Arthritis Patients Treated With Methotrexate. *Adv Med Sci* (2016) 61(2):193–7. doi: 10.1016/j.advms.2015.12.009
 49. Lundström S, Hensvold A, Rutishauser D, Klareskog L, Ytterberg A, Zubarev R, et al. IgG Fc Galactosylation Predicts Response to Methotrexate in Early Rheumatoid Arthritis. *Arthritis Res Ther* (2017) 19(1):182. doi: 10.1186/s13075-017-1389-7
 50. Pasek M, Duk M, Podbielska M, Sokolik R, Szechiński J, Lisowska E, et al. Galactosylation of IgG From Rheumatoid Arthritis (RA) Patients - Changes During Therapy. *Glycoconj J* (2006) 23(7-8):463–71. doi: 10.1007/s10719-006-5409-0
 51. Van Beneden K, Coppieters K, Laroy W, De Keyser F, Hoffman IE, Van den Bosch F. Reversible Changes in Serum Immunoglobulin Galactosylation During the Immune Response and Treatment of Inflammatory Autoimmune Arthritis. *Ann Rheumatol Dis* (2009) 68(8):1360–5. doi: 10.1136/ard.2008.089292
 52. Saldova R, Huffman J, Adamczyk B, Muzinic A, Kattla J, Pucic M, et al. Association of Medication With the Human Plasma N-Glycome. *J Proteome Res* (2012) 11(3):1821–31. doi: 10.1021/pr2010605
 53. Link-Lenczowski P, Bubka M, Balog C, Koeleman C, Butters T, Wührer M, et al. The Glycomic Effect of N-Acetylglucosaminyltransferase III Overexpression in Metastatic Melanoma Cells. *GnT-III modifies highly branched N-glycans Glycoconj J* (2018) 35(2):217–31. doi: 10.1007/s10719-018-9814-y
 54. Croce A, Firuzi O, Altieri F, Eufemi M, Agostino R, Priori R, et al. Effect of Infliximab on the Glycosylation of IgG of Patients With Rheumatoid Arthritis. *J Clin Lab Anal* (2007) 21(5):303–14. doi: 10.1002/jcla.20191
 55. Ząbczyńska M, Link-Lenczowski P, Novokmet M, Martin T, Turek-Jabrocka R, Trofimiuk-Möldner M, et al. Altered N-Glycan Profile of IgG-Depleted Serum Proteins in Hashimoto's Thyroiditis. *Biochim Biophys Acta Gen Subj* (2020) 1864(3):129464. doi: 10.1016/j.bbagen.2019.129464
 56. Zhao L, Liu M, Gao Y, Huang Y, Lu G, Gao Y, et al. Glycosylation of Sera Thyroglobulin Antibody in Patients With Thyroid Diseases. *Eur J Endocrinol* (2013) 168(4):585–92. doi: 10.1530/EJE-12-0964
 57. Yuan S, Li Q, Zhang Y, Huang C, Wu H, Li Y, et al. Changes in Anti-Thyroglobulin IgG Glycosylation Patterns in Hashimoto's Thyroiditis Patients. *J Clin Endocrinol Metab* (2015) 100(2):717–24. doi: 10.1210/jc.2014-2921
 58. Collins E, Galligan M, Saldova R, Adamczyk B, Abrahams J, Campbell M, et al. Glycosylation Status of Serum in Inflammatory Arthritis in Response to Anti-TNF Treatment. *Rheumatol (Oxford)* (2013) 52(9):1572–82. doi: 10.1093/rheumatology/ket189
 59. Balazs C, Kiss E, Leóvey A, Farid N. The Immunosuppressive Effect of Methimazole on Cell-Mediated Immunity is Mediated by its Capacity to Inhibit Peroxidase and to Scavenge Free Oxygen Radicals. *Clin Endocrinol (Oxf)* (1986) 25(1):7–16. doi: 10.1111/j.1365-2265.1986.tb03590.x
 60. Cooper D. Antithyroid Drugs. *N Engl J Med* (2005) 352(9):905–17. doi: 10.1056/NEJMr042972
 61. Kendall-Taylor P. Are Antithyroid Drugs Immunosuppressive? *Br Med J (Clin Res Ed.)* (1984) 288(6416):509–11. doi: 10.1136/bmj.288.6416.509
 62. Schmidt D, de Haan N, Sonneveld M, Porcelijn L, van der Schoot C, de Haas M, et al. IgG-Fc Glycosylation Before and After Rituximab Treatment in Immune Thrombocytopenia. *Sci Rep* (2020) 10(1):3051. doi: 10.1038/s41598-020-59651-7
 63. Kemna M, Plomp R, van Paassen I, Koeleman C, Jansen B, Damoiseaux J, et al. Galactosylation and Sialylation Levels of IgG Predict Relapse in Patients With PR3-ANCA Associated Vasculitis. *E Bio Med* (2017) 17:108–18. doi: 10.1016/j.ebiom.2017.01.033
 64. Wührer M, Stavenhagen K, Koeleman C, Selman M, Harper L, Jacobs B, et al. Skewed Fc Glycosylation Profiles of Anti-Proteinase 3 Immunoglobulin G1 Autoantibodies From Granulomatosis With Polyangiitis Patients Show Low Levels of Bisection, Galactosylation, and Sialylation. *J Proteome Res* (2015) 14(4):1657–65. doi: 10.1021/pr500780a
 65. Li D, Lou Y, Zhang Y, Liu S, Li J, Tao J. Sialylated Immunoglobulin G: A Promising Diagnostic and Therapeutic Strategy for Autoimmune Diseases. *Theranostics* (2021) 11(11):5430–46. doi: 10.7150/thno.53961
 66. Schwab I, Nimmerjahn F. Role of Sialylation in the Anti-Inflammatory Activity of Intravenous Immunoglobulin - F(Ab')₂ Versus Fc Sialylation. *Clin Exp Immunol* (2014) 178 Suppl 1(Suppl 1):97–9. doi: 10.1111/cei.12527
 67. Pagan J, Kitaoka M, Anthony A. Engineered Sialylation of Pathogenic Antibodies *In Vivo* Attenuates Autoimmune Disease. *Cell* (2018) 172(3):564–77. doi: 10.1016/j.cell.2017.11.041
 68. Pocheć E, Bocian K, Ząbczyńska M, Korczak-Kowalska G, Lityńska A. Immunosuppressive Drugs Affect High-Mannose/Hybrid N-Glycans on Human Allostimulated Leukocytes. *Anal Cell Pathol (Amst.)* (2015) 2015:324980. doi: 10.1155/2015/324980
 69. Polak K, Ząbczyńska M, Pocheć E. The Role of IgG Fc N-Glycosylation in Antibody-Dependent Cell-Mediated Cytotoxicity (ADCC). *Post Biol Kom* (2019) 46(1):75–92.
 70. Bogner U, Wall J, Schleusener H. Cellular and Antibody Mediated Cytotoxicity in Autoimmune Thyroid Disease. *Acta Endocrinol Suppl (Copenh.)* (1987) 281:133–8. doi: 10.1530/acta.0.114s133
 71. Kucuksezar U, Cetin E, Esen F, Tahrili I, Akdeniz N, Gelmez M, et al. The Role of Natural Killer Cells in Autoimmune Disease. *Front Immunol* (2021) 12:622306. doi: 10.3389/fimmu.2021.622306
 72. Ząbczyńska M, Polak K, Kozłowska K, Sokołowski G, Pocheć E. The Contribution of IgG Glycosylation to Antibody-Dependent Cell-Mediated Cytotoxicity (ADCC) and Complement-Dependent Cytotoxicity (CDC) in Hashimoto's Thyroiditis: An *In Vitro* Model of Thyroid Autoimmunity. *Biomolecules* (2020) 10(2):171. doi: 10.3390/biom10020171
 73. Collin M, Ehlers M. The Carbohydrate Switch Between Pathogenic and Immunosuppressive Antigen-Specific Antibodies. *Exp Dermatol* (2013) 22(8):511–4. doi: 10.1111/exd.12171
 74. Mavarakis E, Kim K, Shimoda M, Gershwin M, Patel F, Wilken R. Glycans in the Immune System and The Altered Glycan Theory of Autoimmunity: A Critical Review. *J Autoimmun* (2015) 57:1–13. doi: 10.1016/j.jaut.2014.12.002
 75. Mahajan V, Pillai S. Sialic Acids and Autoimmune Disease. *Immunol Rev* (2016) 269(1):145–61. doi: 10.1111/imr.12344
 76. Ząbczyńska M, Pocheć E. The Role of Protein Glycosylation in Immune System. *Post Biochem* (2015) 61(2):129–37.

Conflict of Interest: The authors declare that the research was conducted in the absence of any commercial or financial relationships that could be construed as a potential conflict of interest.

Publisher's Note: All claims expressed in this article are solely those of the authors and do not necessarily represent those of their affiliated organizations, or those of the publisher, the editors and the reviewers. Any product that may be evaluated in this article, or claim that may be made by its manufacturer, is not guaranteed or endorsed by the publisher.

Copyright © 2022 Trzos, Link-Lenczowski, Sokołowski and Pocheć. This is an open-access article distributed under the terms of the Creative Commons Attribution License (CC BY). The use, distribution or reproduction in other forums is permitted, provided the original author(s) and the copyright owner(s) are credited and that the original publication in this journal is cited, in accordance with accepted academic practice. No use, distribution or reproduction is permitted which does not comply with these terms.



Distinct N-Linked Immunoglobulin G Glycosylation Patterns Are Associated With Chronic Pathology and Asymptomatic Infections in Human Lymphatic Filariasis

Tomabu Adjobimey^{1,2*} and Achim Hoerauf^{1,3}

¹ Institute of Medical Microbiology, Immunology and Parasitology Institut für Medizinische Mikrobiologie, Immunologie und Parasitologie (IMMIP), University Hospital Bonn, Bonn, Germany, ² Faculté des Sciences et Techniques (FAST), Université d'Abomey Calavi, Abomey Calavi, Bénin, ³ Bonn-Cologne Site, German Center for Infectious Disease Research Deutsches Zentrum für Infektionsforschung (DZIF), Bonn, Germany

OPEN ACCESS

Edited by:

Irena Trbojević-Akmačić,
Genos Glycoscience Research
Laboratory, Croatia

Reviewed by:

Joana Gaífem,
Universidade do Porto, Portugal
Miriam Laura Fichtner,
Yale Medicine, United States

*Correspondence:

Tomabu Adjobimey
Tomabu.Adjobimey@ukb-uni-bonn.de

Specialty section:

This article was submitted to
B Cell Biology,
a section of the journal
Frontiers in Immunology

Received: 07 October 2021

Accepted: 03 March 2022

Published: 25 March 2022

Citation:

Adjobimey T and Hoerauf A
(2022) Distinct N-Linked
Immunoglobulin G Glycosylation
Patterns Are Associated With
Chronic Pathology and
Asymptomatic Infections in
Human Lymphatic Filariasis.
Front. Immunol. 13:790895.
doi: 10.3389/fimmu.2022.790895

Lymphatic filariasis presents a complex spectrum of clinical manifestations ranging from asymptomatic microfilariaemic (MF+) to chronic pathology (CP), including lymphedema and elephantiasis. Emerging evidence suggests a link between the physiopathology of filarial infections and antibody properties. Post-translational glycosylation has been shown to play a key role in the modulation of antibodies' effector functions. Here, we investigated the link between total IgG-N-glycosylation patterns and the physiopathology of human lymphatic filariasis using UPLC-FLD/ESI-MS comparison of N-glycan profiles of total IgG purified from endemic normals (EN), MF+, and CP patients. We detected a total of 19 glycans released from all IgG samples. Strikingly, agalactosylated glycan residues were more prominent in EN, whereas sialylation and bisecting GlcNac correlated with asymptomatic infections. While IgG from all three clinical groups expressed high levels of fucosylated residues, significantly lower expressions of afucosylated IgG were seen in MF+ individuals compared to EN and CP. Our data reveal distinct N-linked IgG glycan profiles in EN, MF+, and CP and suggest that IgG galactosylation and sialylation are associated with chronic pathology, whereas agalactosylation correlates with putative immunity. The results also indicate a role for sialylation, fucosylation, and bisecting GlcNac in immune tolerance to the parasite. These findings highlight the link between N-glycosylation and the physiopathology of lymphatic filariasis and open new research avenues for next-generation therapeutic formulations against infectious diseases.

Keywords: IgG, filariasis, UPLC-FLD/ESI-MS, N-glycosylation, galactosylation, fucosylation, sialylation, GlcNac

Abbreviations: EN, endemic normals; MF, microfilariae; CP, chronic pathology; IgG, immunoglobulin G; GlcNac, N-Acetylglucosamine; CFA, circulating microfilaria antigen; UPLC-FLD/ESI-MS, ultra-performance liquid chromatography-fluorescence detector/electrospray ionization-mass spectrometry.

INTRODUCTION

Lymphatic filariasis, commonly known as elephantiasis, is a neglected tropical disease caused by vector-borne filarial parasites *Wuchereria bancrofti*, *Brugia malayi*, and *Brugia timori* (1). Recent estimations of the WHO indicate that 859 million people in 50 countries live in areas requiring chemotherapy to stop the spread of the infection. The global baseline estimate of people affected by lymphatic filariasis is 25 million men with hydrocele and over 15 million people with lymphoedema (2). In endemic areas, most infected individuals remain asymptomatic, showing no external signs of the infection while bearing microfilaria (MF+) and contributing to the transmission of the parasite (2). In contrast, putatively immune individuals, also known as endemic normals (EN), remain infection-free despite continuous exposition to the vector (3). In some of the exposed individuals, the infection develops into chronic pathology (CP), manifesting as lymphoedema (tissue swelling), elephantiasis (skin/tissue thickening) of limbs, or hydrocele (scrotal swelling). Besides morbidity and its economic drawbacks, the disfiguring sequels of LF often lead to social stigma and considerable psychological burden (4). The clinical outcomes of the infection are tightly linked to the host's immune reactivity. Typically, alongside classical parasite-induced Th2 immune responses, asymptomatic patients present a strong immune-regulated profile with high levels of regulatory cells, anti-inflammatory cytokines. This immune-regulated environment is associated with elevated levels of the non-cytolytic antibody IgG4 (3, 5, 6). It is well established that antibodies play a key role in protection and pathology across infectious diseases. While the antibody variable domain facilitates antibody binding to antigens and the blockade of infection, the constant, crystallizable fragment (Fc) mediates cross-talk with the innate immune system. The biological activity of the Fc region is controlled genetically *via* class switch recombination, resulting in the selection of distinct antibody isotypes and subclasses (7). In helminth infections, the IgG4 subclass was seen to be associated with tolerance of the parasite, whereas IgG1 and IgG3 are associated with parasite clearance and/or pathology (5). New pieces of evidence suggest a second level of control *via* post-translational changes in antibody glycosylation. Fc glycans were shown to be critical for maintaining both the proinflammatory and the anti-inflammatory effector functions of IgG (8). Indeed N-glycan moieties of IgG-Fc were shown to significantly impact antibody stability and effector functions (7, 9). All four human IgG subclasses exhibit two variable bi-antennary glycans in their Fc region, attached at the conserved Asn297 site (10). The Fc glycans in the IgG molecule are bi-antennary glycans with varying fucose content, bisecting N-acetylglucosamine (GlcNAc), galactose (Gal), and sialic acid; most IgG molecules are fucosylated. These glycan structures have profound impacts on antibody functions and thereby on health. Agalactosylated and asialylated IgG glycoforms, for example, were seen to be particularly abundant in chronic inflammatory diseases such as rheumatoid arthritis, systemic lupus erythematosus, inflammatory bowel disease (IBD), HIV, and mycobacterial

infections (11–16). Global immune activation studies reveal that IgG1 galactose deficiency correlated with parasitic infections or asthma (17). Conversely, sialylation has been associated with anti-inflammatory properties and has, for example, been seen to reduce pathogenic properties of IgG autoantibodies (18). Recent data from our group have suggested that helminths modulate both the quantity and the function of antibodies secreted in their host (19). This qualitative modulation of antibodies' properties may have a profound impact on the ability of the host to tolerate or eliminate adult worms and microfilaria. Here we analyzed the link between different antibody-glycosylation patterns and the physiopathology of human lymphatic filariasis using mass spectrometry. Ultimately, this work provides critical new insights into the functional roles of antibody glycosylation and lays initial foundations for leveraging antibody glycosylation to drive prevention and control across diseases.

MATERIALS AND METHODS

Study Population and Ethic Statement

The present study used archived material from previous projects. Patients and endemic controls' samples were collected between 2009 and 2010 in the Nzema East District in the western region of Ghana endemic for LF. No other human filarial species were endemic in the region. Written informed consent was obtained from all participants. Exclusion criteria included abnormal hepatic and renal enzyme levels (γ -glutamyltransferase > 28 U/L, glutamyl pyruvic transaminase > 30 U/L, creatinine > 1.2 mg/100 mL) assessed by dipstick chemistry, alcohol, drug abuse, or antifilarial therapy in the past 10 months. The participants in the study were examined by a clinician using physical methods and a portable ultrasound machine (180 Plus; SonoSite, Bothell, WA) as described previously (20). Ethical clearance was given by the Committee on Human Research Publication and Ethics at the University of Science and Technology in Kumasi and the Ethics Committee at the University Hospital Bonn. Microfilaremia was determined by microscopic examination of fingerprick night blood samples as published (20). Endemic normals (EN) were defined as residing in the endemic region but free of infection (CFA-, MF-, n=10), clinically asymptomatic microfilaremic (CFA+, MF+, n=10) chronic pathology patients (CP) with lymphedema or elephantiasis (n=10), negative for filarial antigen. Since IgG-glycosylation patterns can be affected by aging and estrogens levels (21, 22), only middle-aged males (41–48 years) were included in the analysis (Table 1). Patients receiving any other medical treatments were excluded from the analysis.

IgG Isolation by Protein G Agarose Beads

Complete plasma samples (500 μ g–1 mg) were diluted in 0.4 mL of PBS (Fisher Scientific) and filtered with Amicon ultrafiltration filters (1.5 mL, 30 kDa cutoff) at 12,500 r.p.m. (Allegra bench centrifuge) for 3 minutes at 25°C to remove buffer and stabilization media. This washing was repeated twice. Filtered

TABLE 1 | Clinical characteristics of patients and controls.

N°	Age in years	Gender	MF/10 ml	CFA	LE/Hy	Antifilarial antibody titer	Clinical classification
1	45	M	0	-	-	-	EN
2	48	M	0	-	-	-	EN
3	43	M	0	-	-	-	EN
4	44	M	0	-	-	-	EN
5	42	M	0	-	-	-	EN
6	40	M	0	-	-	-	EN
7	41	M	0	-	-	-	EN
8	43	M	0	-	-	-	EN
9	45	M	0	-	-	-	EN
10	43	M	0	-	-	-	EN
11	47	M	1101	+	-	+	MF+
12	46	M	2710	+	-	+	MF+
13	44	M	4264	+	-	+	MF+
14	41	M	2182	+	-	+	MF+
15	44	M	5166	+	-	+	MF+
16	46	M	1182	+	-	+	MF+
17	40	M	271	+	-	+	MF+
18	42	M	3864	+	-	+	MF+
19	46	M	354	+	-	+	MF+
20	44	M	608	+	-	+	MF+
21	48	M	0	-	+	+	LE
22	46	M	0	-	+	+	LE
23	47	M	0	-	+	+	LE
24	43	M	0	-	+	+	LE
25	41	M	0	-	+	+	LE
26	45	M	0	-	+	+	Hy
27	41	M	0	-	+	+	Hy
28	46	M	0	-	+	+	Hy
29	47	M	0	-	+	+	Hy
30	40	M	0	-	+	+	Hy

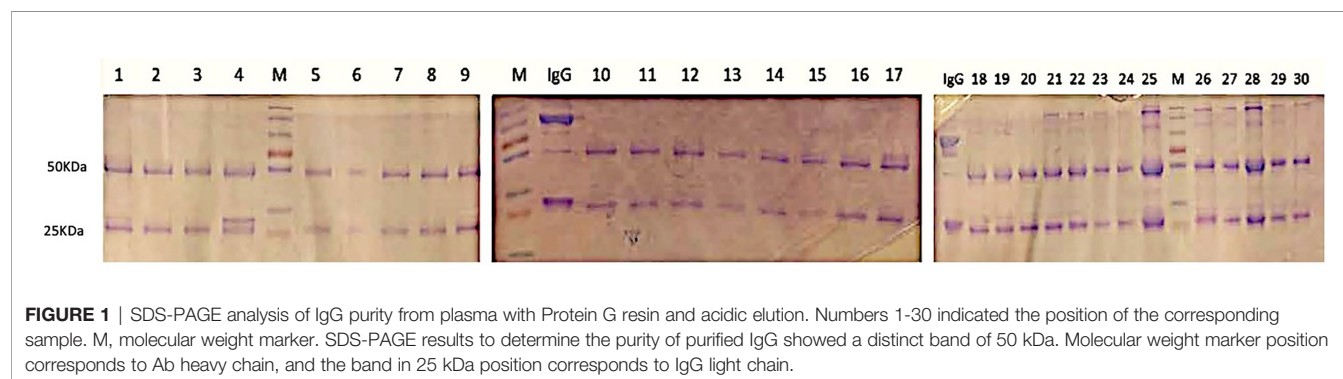
M, Male; MF, Microfilaria; CFA, Circulating Filarial Antigen; EN, Endemic Normal; LE, Lymphedema; Hy, Hydrocele.

plasma solutions in PBS were incubated with 30μL of protein G beads solutions for 60 minutes for antibody immobilization by IgG-G protein binding. After binding, the solution containing the beads was centrifuged at 12.500 r.p.m. (Allegra bench centrifuge) for 3 minutes at 25°C to remove any unbound excess protein. Centrifugation was repeated three times with 200μL of PBS. Subsequently, the IgG fraction (150μL in PBS) was released from the protein G beads by incubation with 200μL of HCL 100 mM solution (acidic conditions) for 15 minutes. The samples were centrifuged again, and the supernatant containing the IgG was recovered. Each purified IgG solution was neutralized with 40μL of a NaOH 500 mM solution, and the resulting solutions were analyzed by SDS-PAGE for assessing the

purification yield (**Figure 1**). IgG samples were then used directly for the next deglycosylation step.

Deglycosylation and Glycan Isolation

IgG samples (25μg-200μg) were diluted in 300μL ultrapure water and filtered with Amicon® Ultra 0.5mL Centrifugal filters (10,000 NMWL) at 4,500 r.p.m on an Allegra™ X-22R Benchtop Centrifuge for 12 minutes at 25°C to remove metabolites from media. The protein samples were concentrated to 150μL and immediately denatured using 150μL of 1% SDS and under heating at 60°C for 30 minutes. The solutions of denatured IgG were diluted with 350μL of deionized water and concentrated, using Amicon® Ultra 0.5mL



Centrifugal filters as described above to remove SDS. The concentrated/denatured protein solutions were treated with 4 μ L of PNGase F and incubated for 90 minutes at 60°C. After deglycosylation, released N-glycans were isolated from the protein fraction by filtration using Amicon Ultra-0.5 mL Centrifugal filters (10,000 NMWL) at 12,500 r.p.m. (Allegra™ X-22R Benchtop Centrifuge) for 5 minutes at 25°C. The filtrate solutions containing released N-glycans were lyophilized on a TELSTAR LyoQuest Plus -55 freeze dryer (TELSTAR, Terrassa, Spain). The retained fractions were recovered by inverting the filter and transferred by centrifugation (at 1,500 r.p.m. for 1 minute at 25°C) to a second receiver vial and stored at -20°C.

Procainamide Labeling

Recent reports on LC-FLR/MS reveal glycans labeling with procainamide (4-amino-N- (2-diethylaminoethyl) benzamide) as an effective method to improve MS ionization efficiency without compromising LC separation (23). A procainamide labeling solution was prepared following the Waters Application Note. UPLC/FLR/QTof (MS Analysis of Procainamide-Labeled N-glycans). Briefly, 12mg of procainamide and 6mg of sodium cyanoborohydride were dissolved in 0.5mL of a dimethyl sulfoxide (DMSO)/Acetic acid (7/3) mixture. The lyophilized N-glycan samples were reconstituted in 10 μ L of ultrapure water. The obtained solutions were treated with 50 μ L of procainamide labeling solution at 65°C for 3 hours under gentle shaking on a Thermomixer (Eppendorf). After labeling, the labeling solutions were diluted with 200 μ L Acetonitrile and directly analyzed by UPLC-FLD/ESI-MS under standard conditions (Waters, Application Note. UPLC/FLR/QTof MS Analysis of Procainamide-Labeled N- glycans).

UPLC-FLD/MS Analysis of Procainamide Labeled N-Glycans

Profiles of procainamide-labeled fluorescent N-glycans from isolated IgG samples were obtained by HILIC UPLC-FLD/ESI-MS. Labeled glycans were separated by UPLC on a HILIC (hydrophilic interaction liquid chromatography) column, and labeled glycans were detected by online fluorescence and ESI-TOF mass detection. Fluorescence detection allowed us to quantify the uniformly labeled glycans peaks with very high sensitivity. In contrast, mass detection was employed to provide structural data for the assignment of peaks to glycan structures based on mass. For quantification, peaks areas were integrated and converted into relative percentages of the total glycan amount defined as the sum of all peaks and normalized to 100%. The UPLC analysis was performed following the standard procedures from Waters (Application Note. UPLC/FLR/QTof MS Analysis of Procainamide-Labeled N-glycans).

Peak Assignment - Methodology

Mass distribution spectrum assigned to the glycan; ESI-MS spectrum confirming the mass found; and the fluorescence chromatogram of the sample, containing all peaks, with their corresponding retention times, total integration, and relative

abundance. As an example, **Figure 2** shows the chromatogram of sample 30 for G0 glycan with a retention time of 20.9 and ESI+ mass 768.8.

Statistical Analysis

All statistical analyses were performed using Prism 5.03 software (GraphPad Software, Inc., La Jolla, USA). Comparative analyses among groups were conducted using the Kruskal-Wallis test with a Dunn's nonparametric posthoc test (> 2 groups). Significance was accepted when $p < 0.05$.

RESULTS

Characterization of Glycans of IgG

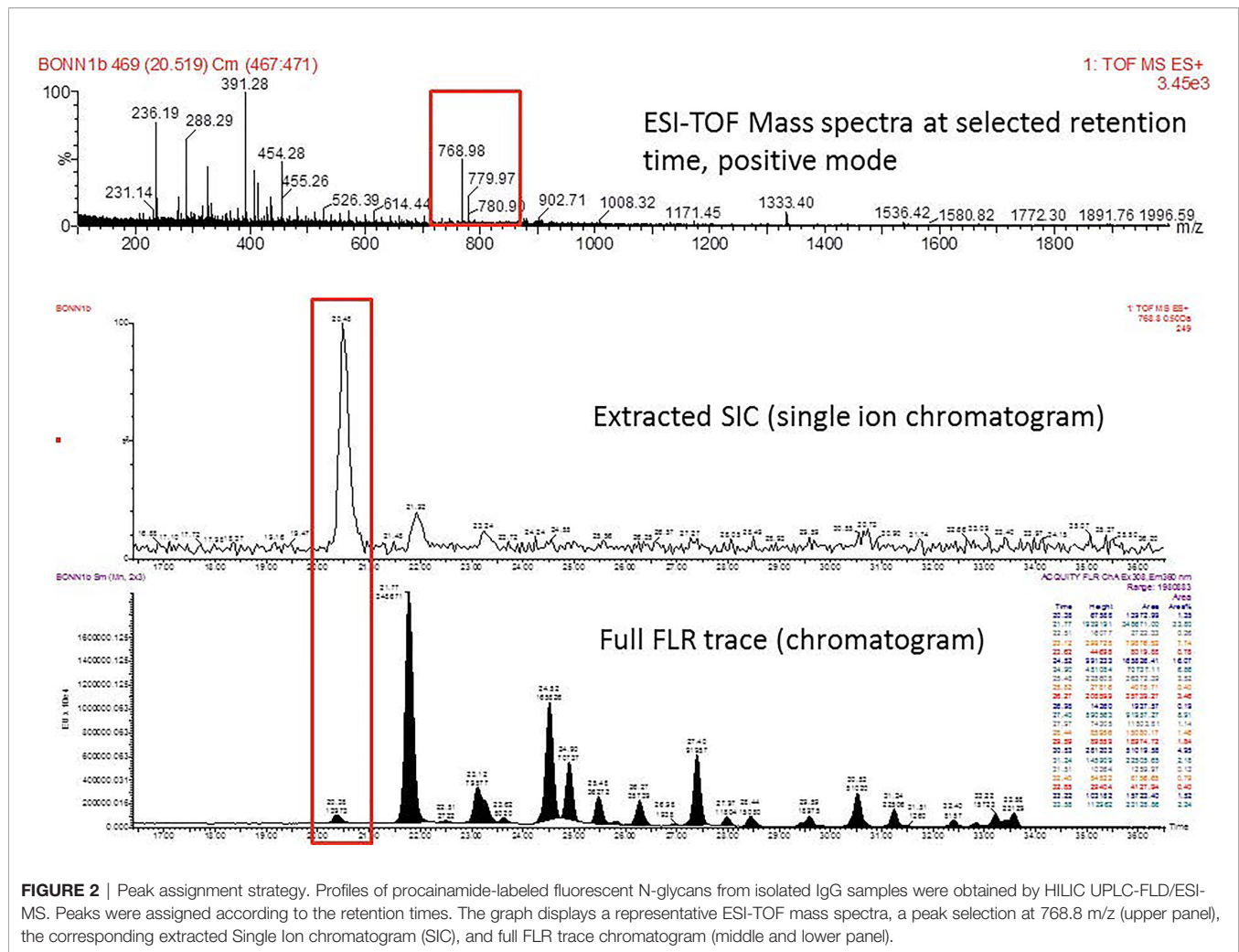
We detected a total 19 glycans released from IgG purified from all tested samples. **Table 2** summarizes the proposed structures for all 19 glycans and the code used. The identified IgG-glycoforms can be separated according to the presence or not of a galactose residue. 3 glycans were agalactosylated (G0). 6 were monogalactosylated (G1), 8 glycans digalactosylated (G2) and 13 were fucosylated (F), and 6 were afucosylated. 4 glycans were monosialylated (A1), 3 glycans were disialylated (A2), whereas 12 were asialylated. 7 glycans had a bisecting GlcNAc arm (bG0F, bG1Fa, bG1Fb, bG2, bG2F, bG2A1F, bA2F).

Higher Heterogeneity in Antibody Glycosylation Patterns in Chronic Pathology Patients

To determine whether the level of complexity in glycosylation patterns of total IgG differed between EN, CP, and MF+ donors, N-linked glycosylation patterns of total IgG were compared between the different groups. The data suggest that CP patients presented significantly more glycan residues compared to MF+ and EN. No significant difference was seen between EN and MF+ individuals regarding the number of IgG-N-linked glycan residues (**Figure 3**). This higher number of glycan residues may be linked with a more pronounced inflammatory state observed in CP patients.

Agalactosylation Correlates With Putative Immunity

Fc-galactosylation is known to improve binding to C1q in human IgG without affecting antigen-binding affinities (24). To determine the importance of IgG-N-linked galactose residues in the physiopathology of lymphatic filariasis, we analyzed the importance of lack of galactose residue on IgG of EN, MF+, and CP. Our data indicate that IgG from EN presented the highest numbers of agalactosylated residues (**Figure 4A**). This trend is confirmed when the most abundant agalactosylated residue G0F is considered (**Figure 4B**). However, the second most abundant agalactosylated residue (bG0F) was predominant in IgG of MF+ individuals (**Figure 4C**). No substantial difference was seen when considering other agalactosylated residues.



Galactosylation Correlates With Chronic Pathology (CP)

Next, we analyzed the importance of IgG-N-linked mono and bigalactosylated residues in the physiopathology of lymphatic filariasis. The relative abundance of mono (G1, G1Fa, G1Fb, bG1Fb, G1A1F) and bigalactosylated (G2, bG2, G2F, bG2F, G2A1, G2A1F, G2A2) residues was therefore investigated on IgG of EN, MF+, and CP. The results indicate that IgG from CP patients presented the highest levels of both mono- and bigalactosylated residues. This trend was confirmed when the 3 most abundant bi and monogalactosylated residues, G2F, G1Fa, G1Fb are considered (**Figures 5B, E**). MF+ individuals generally expressed significantly higher levels of galactosylated residues compared to EN (**Figures 5A, D**), suggesting that galactosylation of IgG is primarily associated with the infection. However, IgG from MF+ individuals expressed slightly lower levels of G1Fb, a less abundant glycomer of G1Fa, compared to EN. In contrast, the afucosylated and asialylated, bigalactosylated residue G2 was found to be more abundant of IgG of MF+ individuals compared to EN and CP.

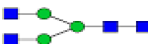






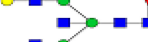





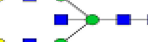

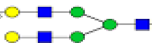



Lower Level of Afucosylation in IgG of Asymptomatic Microfilaremic (MF+)


IgG fucosylation in the Fc domain has been attributed anti-inflammatory properties. To investigate the role of IgG-fucosylation in the physiopathology of lymphatic filariasis, we analyzed the relative abundance of fucose residues in EN, MF+, and CP individuals. Interestingly, even though high levels of fucosylated glycans were found on IgG of all groups, significantly lower amounts of afucosylated residues (and higher amounts of fucosylated residues) were found in MF+ individuals. (**Figure 6**).

Higher Level of Sialylated Residues in IgG of Asymptomatic Microfilaremic Individuals

We next analyzed the expression of IgG-N-linked sialic acid residues on IgG of EN, MF+, and CP. Interestingly, MF+ individuals expressed the highest amounts of sialic acid-containing residues. This increased amount is mainly due to abundant residues like G1A1F, G2A1, G2A1F, bG2A1F. All these residues are galactosylated, and apart of G2A1, are fucosylated (**Figure 7**).

TABLE 2 | Detected glycan structures.

N-glycan	Structure	Ret. Time	ESI +
GO		20.9	768.8
GOF		22.29	841.8
bGOF		23.65	943.4
G1		24.1	849.8
G1Fa		25.05	922.9
G1Fb		25.44	922.9
bG1Fa		26.02	1024.4
bG1Fb		26.41	1024.4
G2		26.82	930.9
G2F		27.11	1032.5
bG2		27.95	1003.8
bG2F		28.54	1105
G1A1F		29.05	1068.5
G2A1		30.18	1076.5
G2A1F		31.12	1149
bG2A1f		31.84	1251
G2A2		32.56	1222
A2F		33.85	1295
bA2F		34.23	1396.6

 19 different glycan structures were detected in all tested IgG samples. 3 were agalactosylated (GO), 6 were monogalactosylated (G1), 8 were digalactosylated (G2). 13 were fucosylated (F), and 6 afucosylated. 4 glycans were monosialylated (A1), 3 glycans were disialylated (A2) whereas 12 were asialylated. 7 glycans had a bisecting GlcNAc arms (b...).

Bisecting GlcNAc Is Predominant in Asymptomatic Microfilaremic Individuals (MF+)

Attachment of bisecting GlcNAc to the Fc glycan was shown to play a critical role in antibody-dependent cell-mediated cytotoxicity (ADCC). To determine the role of IgG-N-linked bisecting GlcNAc residues in the physiopathology of lymphatic filariasis, we analyzed the presence of bisecting GlcNAc residues on IgG of EN, MF+, and CP. Surprisingly, MF+ patients expressed the highest amounts of bisecting GlcNAc containing residues (**Figure 8**). This predominance is mainly due to the most abundant residue with bisecting arm bG0F. However, the same trend is observed when bG1F, a monogalactosylated residue with the same core structure, is considered (**Figure 8C**).

DISCUSSION

The composition of the Fc N-glycan modulates the magnitude of antibodies' effector functions, such as the antibody-dependent cell-mediated cytotoxicity (ADCC) and the complement-dependent cytotoxicity (CDC) (9). Our data suggest a higher expression in antibody glycosylation in CP patients compared to the EN and MF+ individuals. This higher level of glycosylation might be associated with the well-known pronounced inflammatory state in CP patients (19). This finding is in line with previous investigations reporting an association between the levels of Fc and Fab immunoglobulin-G-related glycosylation with inflammation (25, 26).

The present study also demonstrates that IgG-galactosylation patterns significantly differ from one lymphatic filariasis clinical

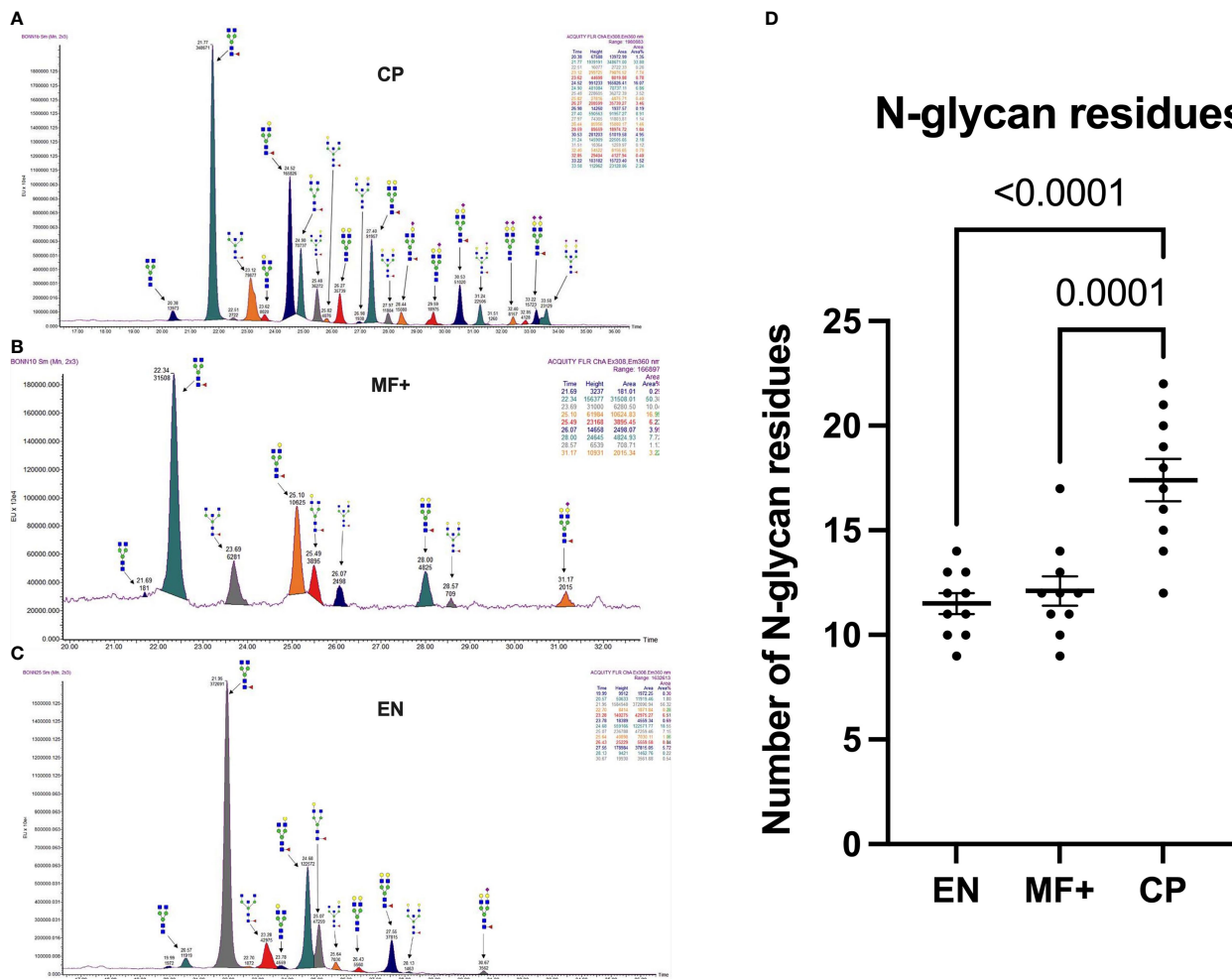


FIGURE 3 | Higher IgG-Glycan heterogeneity in CP patients. **(A–C)** Representative electropherograms from a CP **(A)**, MF+ **(B)**, and EN **(C)** indicating all structures present in the Fc region of IgG. **(D)** Relative abundance of IgG molecules carrying different glycan residues in total IgG purified from EN, MF+, and CP patients. Dots represent individual donors. Bars represent means \pm SEM. The indicated p-values refer to the significance level among all groups according to Kruskal-Wallis test. Indicated p values reflect the level of differences after Dunn's multiple comparisons test. Significance is accepted when $P < 0.05$.

group to the other. Indeed, IgG-agalactosylation correlates with putative immunity, whereas galactosylation was associated with chronic pathology. These data are in line with those obtained in a canine filaria infection model, where IgG N-galactosylation was increased as a result of infection with *Dirofilaria immitis*, a filarial nematode closely related to *Onchocerca volvulus*, *Wuchereria bancrofti*, and *Brugia malayi* (27). Even though our results converge with part of the literature, they differ from those obtained by O'Regan et al. in India, who demonstrated that IgG N-galactosylation was similar in EN, CP, and asymptotically infected donors (28). This divergence might be associated with different factors, including the nature of the pathogens and the study population. Indeed, LF is caused in Africa mainly by *Wuchereria bancrofti*, whereas *Brugia malayi* is the causative agent in India, Malaysia, and other parts of Southeast Asia (29). Whether these two main LF parasites have

different impacts on antibody galactosylation remains to be clarified. Nevertheless, additional investigations with larger and multiregional cohorts are required to precisely define the relationship between galactosylation and the physiopathology of helminth infections. In addition, it is well established that large variability in IgG glycome exists across multiple geographical locations (30).

Higher IgG-galactosylation linked with inflammation was also seen in patients with ankylosing spondylitis, a rare form of arthritis that primarily affects the spine. In this model, the ratio of galactosylated IgG was seen to be twice higher in patients than in controls (31). The presence of terminal galactose on recombinant monoclonal antibodies was reported to enhance their capacity to induce complement-dependent cytotoxicity (CDC) by affecting their affinity to C1q (32). CDC being a key mechanism associated with the killing of microfilaria (33), the

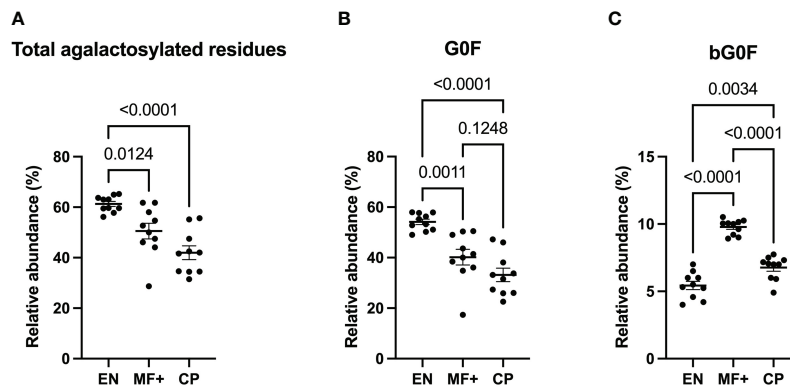


FIGURE 4 | Higher levels of agalactosylated residues in EN. Graphs represent the relative abundance of all IgG-bound glycan structures lacking galactose molecules (**A**), agalactosylated and fucosylated (**B**) or agalactosylated, fucosylated with a bisecting GlcNAc residue (**C**) in IgG purified from EN, MF+, and CP patients. Dots represent individual donors. Bars represent means \pm SEM. The indicated p-values refer to the significance level among all groups according to the Kruskal-Wallis test and Dunn's multiple comparisons test. Significance is accepted when $P < 0.05$.

predominance of galactosylated IgG molecules in CP may explain the absence of microfilaria in this clinical group.

Regarding fucosylation, our data suggest that fucosylation was high in all clinical groups. However, when considering the

relative abundance of afucosylated residues, CP patients expressed significantly higher levels of afucosylated IgG compared to both EN and MF+. Interestingly, MF+ individuals, known to have a more pronounced regulatory

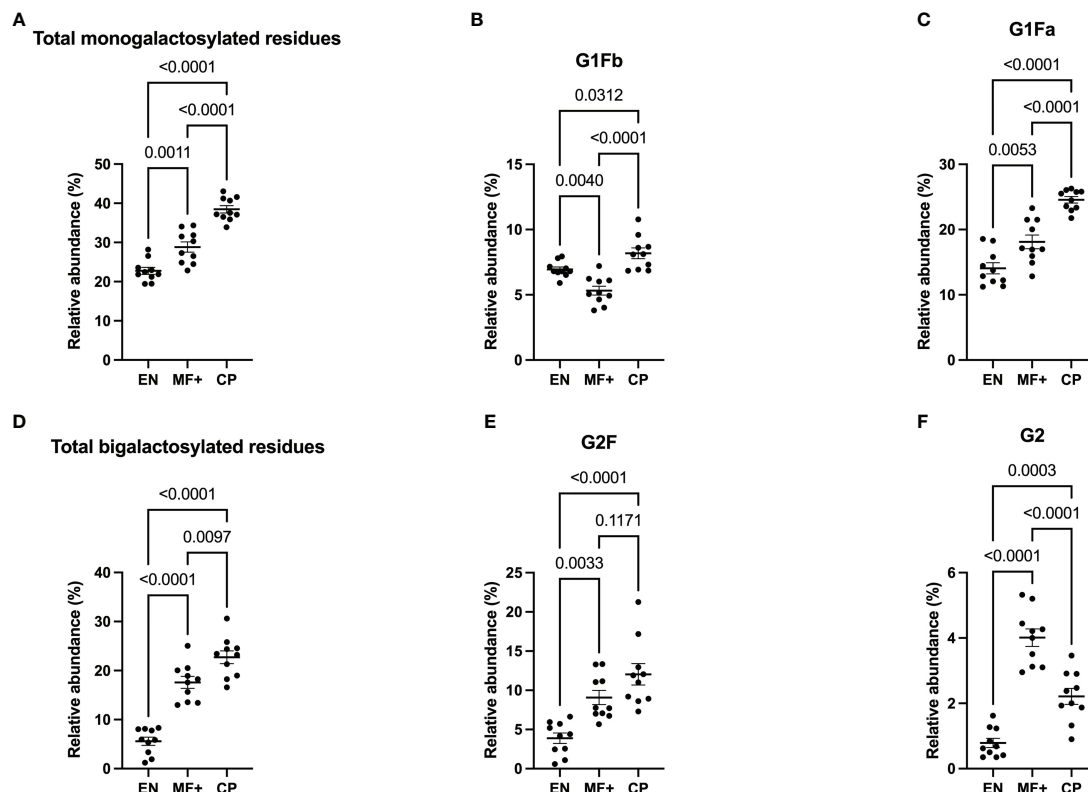


FIGURE 5 | Elevated IgG- galactosylation correlates with chronic pathology. Graphs represent the relative abundance of IgG-bound glycan structures with one (**A–C**) or two galactose molecules (**D–F**) in IgG purified from EN, MF+, and CP patients. Dots represent individual donors. Bars represent means \pm SEM. Statistical analyses were performed using the Kruskal-Wallis nonparametric test with Dunn's multiple comparison post-test. Significance is accepted when $P < 0.05$.

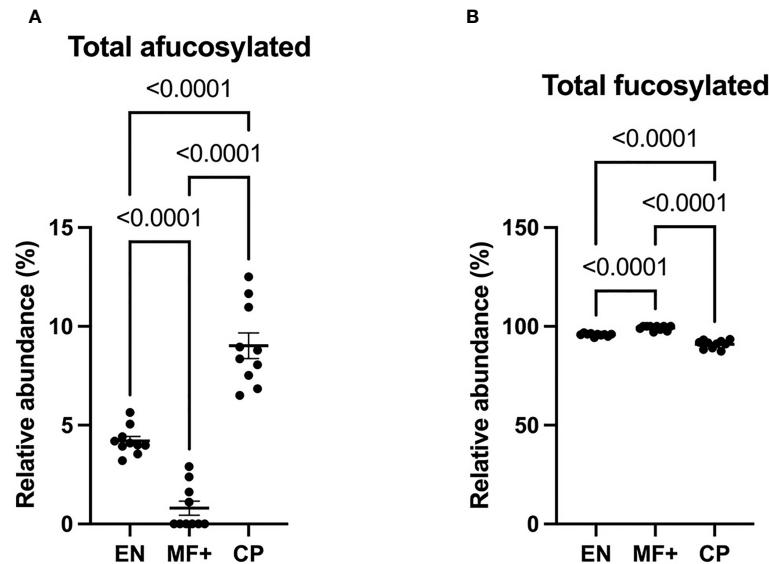


FIGURE 6 | Higher levels of afucosylated IgG are associated with CP. Graphs represent the relative abundance of IgG-bound glycan structures without **(A)** or with **(B)** fucose residues **(A)** in total IgG purified from EN, MF+, and CP patients. Dots represent individual donors. Bars represent means \pm SEM. Statistical analyses were performed using the Kruskal–Wallis nonparametric test with Dunn’s multiple comparison post-test. Significance is accepted when $P < 0.05$.

immune profile, presented the lowest levels of afucosylated IgG compared to EN and CP. While little data exist on IgG fucosylation in filarial infections, similar results were seen in severe acute respiratory syndrome coronavirus 2 (SARS-CoV-2) infections, where recent investigations suggest that afucosylated IgG responses promote the exacerbation of COVID-19 (34, 35). Hyperreactive immune responses being the hallmark of CP, our data confirm that excessive immune reactivity in both helminth

and viral infections might be associated with elevated amounts of afucosylated IgG.

Our results also showed a significantly higher expression of sialylation in total IgG of MF+ individuals. Sialylated IgG Fc domains were shown to have the ability to increase the activation threshold of innate effector cells to immune complexes by stimulating the upregulation of the inhibitory Fc-gamma-RIIb (36, 37). MF+ individuals being well known to have more

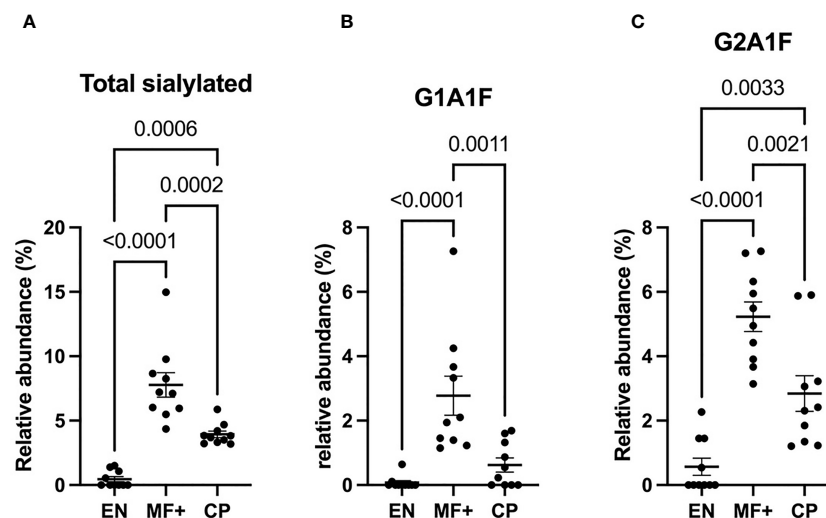


FIGURE 7 | Higher levels of IgG-sialylation are associated with asymptomatic infection during LF. Graphs represent the relative abundance of IgG-bound glycan structures with sialic acid residues in total IgG purified from EN, MF+, and CP patients **(A–C)**. Dots represent individual donors. Bars represent means \pm SEM. Statistical analyses were performed using the Kruskal–Wallis nonparametric test with Dunn’s multiple comparison post-test. Significance is accepted when $P < 0.05$.

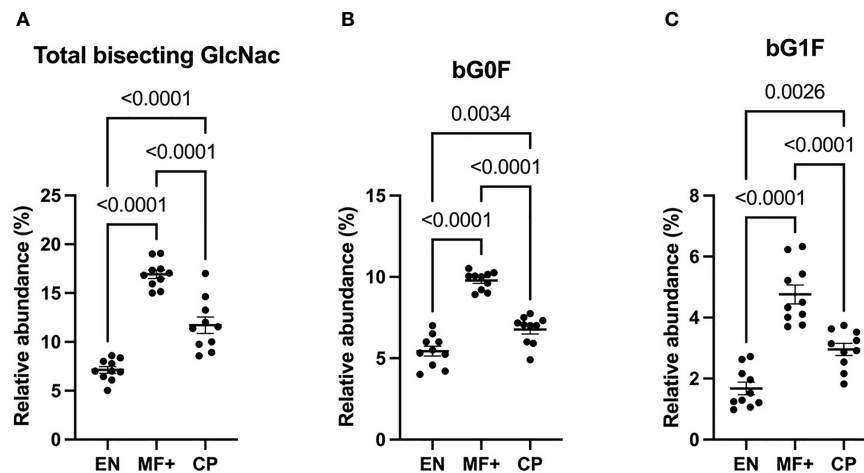


FIGURE 8 | Higher levels of N-linked GlcNac are associated with asymptomatic infection during LF. Graphs represent the relative abundance of IgG bound glycan structures with bisecting GlcNac, total (A), or in combination with fucose (B) or a galactose and fucose molecule (C). Dots represent individual donors. Bars represent means \pm SEM. Statistical analyses were performed using the Kruskal–Wallis nonparametric test with Dunn’s multiple comparison post-test. Significance is accepted when $P < 0.05$.

pronounced anti-inflammatory profiles, the higher expression of sialylated-IgG fits with the immune-regulated milieu in MF+ individuals (5). Our data confirmed previous findings suggesting that total IgG sialylation may be involved in asymptomatic infection during bancroftian filariasis (28).

When it comes to bisecting GlcNac, our data suggest that this feature is more pronounced in MF+ individuals compared to EN and CP. The impact of bisecting GlcNac on antibody functions is not well documented. Nonetheless, the combination of bisecting GlcNac on G0 was seen to enhance antibodies’ capacity to induce ADCC (38). ADCC being a proinflammatory process, the higher expression of IgG with bisecting GlcNac in MF+ individuals seems on the first sight to be controversial. However, the most abundant IgG glycoforms with bisecting GlcNac in MF+ individuals in our settings were also fucosylated. These findings suggest that IgG-fucosylation may interfere with the proinflammatory properties conferred by bisecting GlcNac in MF+ individuals. Indeed, branching fucose residues at the core of the biantennary glycan structure was shown to inhibit the binding affinity of the IgG-Fc to the proinflammatory receptor Fc- γ -RIIIa (10), known to play a key role in the induction of ADCC (39).

Our data highlighted the link between immune reactivity in lymphatic filariasis and IgG glycosylation. However, the main limitation of the present study is the fact that investigations were done at total IgG level. Indeed, the glycan-mediated fine-tuning of IgG functions at subclasses and antigen-specific levels may have a more direct impact on clinical outcomes of the infection. In addition, since Fc and Fab fragments were not purified in our settings, our results encompass glycosylation patterns of both Fc and Fab fragments. It can therefore not be excluded that Fab and Fc glycosylation have distinct effects on the physiopathology of lymphatic filariasis. Recent data suggest that Fab glycan patterns

are variable and play key roles in inflammation and immune regulation (26, 40). The present study focuses solely on N-glycosylation. However, in addition to N-glycosylation, O-glycosylation is also known to impact antibody effector functions (41). Given the delicate balance of protective versus pathological IgG glycosylation profiles across infectious diseases, further investigations are required to better define the implication of antibody Fab and Fc N and O-glycosylation profiles in disease outcomes. Technical limitations might also influence the results. Indeed, lower intensities were observed in some of the chromatograms. This is likely associated with the intrinsic quality of the samples. In addition, the amounts of protein obtained after protein G purification of sample 6 (EN) and 13 (MF+) were much lower compared to the other samples. For these two samples, 25 and 150 μ g of protein were used respectively for deglycosylation and glycan isolation, whereas 200 μ g was used for all other samples. Nonetheless, excluding these two samples would have no impact on the overall outcome.

Ultimately, the present study has identified clear differences in IgG glycan profiles between CP, MF+ individuals, and EN and suggests that IgG glycome alterations might potentially be useful as biomarkers for disease severity prediction in lymphatic filariasis. A better understanding of the impact of antibody glycosylation may also provide critical insights for next-generation therapeutic formulations and vaccines.

DATA AVAILABILITY STATEMENT

The original contributions presented in the study are included in the article/supplementary material. Further inquiries can be directed to the corresponding author.

ETHICS STATEMENT

The studies involving human participants were reviewed and approved by Ethics Committee of the University Hospital Bonn, University of Bonn, Germany. Committee on Human Research Publication and Ethics, University of Science and Technology in Kumasi, Ghana. The patients/participants provided their written informed consent to participate in this study.

AUTHOR CONTRIBUTIONS

All authors contributed to the article and approved the submitted version.

REFERENCES

1. 489 Global Programme to Eliminate Lymphatic Filariasis: Progress Report, 2014. *Wkly Epidemiol Rec* (2015) 90(38):489–504.
2. WHO. *Lymphatic Filariasis 2021*. Available at: <https://www.who.int/health-topics/lymphatic-filariasis>.
3. Maizels RM, Yazdanbakhsh M. Immune Regulation by Helminth Parasites: Cellular and Molecular Mechanisms. *Nat Rev Immunol* (2003) 3(9):733–44. doi: 10.1038/nri1183
4. Hofstraat K, van Brakel WH. Social Stigma Towards Neglected Tropical Diseases: A Systematic Review. *Int Health* (2016) 8(Suppl 1):i53–70. doi: 10.1093/inthealth/ihv071
5. Adjibimey T, Hoerauf A. Induction of Immunoglobulin G4 in Human Filariasis: An Indicator of Immunoregulation. *Ann Trop Med Parasitol* (2010) 104(6):455–64. doi: 10.1179/136485910X12786389891407
6. Babu S, Blauvelt CP, Kumaraswami V, Nutman TB. Regulatory Networks Induced by Live Parasites Impair Both Th1 and Th2 Pathways in Patent Lymphatic Filariasis: Implications for Parasite Persistence. *J Immunol* (2006) 176(5):3248–56. doi: 10.4049/jimmunol.176.5.3248
7. Irvine EB, Alter G. Understanding the Role of Antibody Glycosylation Through the Lens of Severe Viral and Bacterial Diseases. *Glycobiology* (2020) 30(4):241–53. doi: 10.1093/glycob/cwaa018
8. Arnold JN, Wormald MR, Sim RB, Rudd PM, Dwek RA. The Impact of Glycosylation on the Biological Function and Structure of Human Immunoglobulins. *Annu Rev Immunol* (2007) 25:21–50. doi: 10.1146/annurev.immunol.25.022106.141702
9. Kiyoshi M, Caaveiro JMM, Tada M, Tamura H, Tanaka T, Terao Y, et al. Assessing the Heterogeneity of the Fc-Glycan of a Therapeutic Antibody Using an Engineered FcγRIIIa-Immobilized Column. *Sci Rep* (2018) 8(1):3955.
10. Reily C, Stewart TJ, Renfrow MB, Novak J. Glycosylation in Health and Disease. *Nat Rev Nephrol* (2019) 15(6):346–66. doi: 10.1038/s41581-019-0129-4
11. Biermann MH, Griffante G, Podolska MJ, Boeltz S, Sturmer J, Munoz LE, et al. Sweet But Dangerous - The Role of Immunoglobulin G Glycosylation in Autoimmunity and Inflammation. *Lupus* (2016) 25(8):934–42. doi: 10.1177/0961203316640368
12. Go MF, Schrohenloher RE, Tomana M. Deficient Galactosylation of Serum IgG in Inflammatory Bowel Disease: Correlation With Disease Activity. *J Clin Gastroenterol* (1994) 18(1):86–7. doi: 10.1097/00004836-199401000-00021
13. Moore JS, Wu X, Kulhavy R, Tomana M, Novak J, Moldoveanu Z, et al. Increased Levels of Galactose-Deficient IgG in Sera of HIV-1-Infected Individuals. *AIDS* (2005) 19(4):381–9. doi: 10.1097/01.aids.0000161767.21405.68
14. Tomana M, Schrohenloher RE, Koopman WJ, Alarcon GS, Paul WA. Abnormal Glycosylation of Serum IgG From Patients With Chronic Inflammatory Diseases. *Arthritis Rheum* (1988) 31(3):333–8. doi: 10.1002/art.1780310304

FUNDING

This study was supported by the German Research Foundation (DFG): Project number 392112800, reference: HO 2009/13-1. AH is funded by the Deutsche Forschungsgemeinschaft (DFG, German Research Foundation) under Germany's Excellence Strategy – EXC2151 – 390873048”.

ACKNOWLEDGMENTS

We thank the Ghana-based team for their support during the recruitment of LF patients. We thank Asparia Glycomics' teams for the technical support.

15. Tomana M, Schrohenloher RE, Reveille JD, Arnett FC, Koopman WJ. Abnormal Galactosylation of Serum IgG in Patients With Systemic Lupus Erythematosus and Members of Families With High Frequency of Autoimmune Diseases. *Rheumatol Int* (1992) 12(5):191–4. doi: 10.1007/BF00302151
16. van Zeben D, Rook GA, Hazes JM, Zwinderman AH, Zhang Y, Ghelani S, et al. Early Agalactosylation of IgG Is Associated With a More Progressive Disease Course in Patients With Rheumatoid Arthritis: Results of a Follow-Up Study. *Br J Rheumatol* (1994) 33(1):36–43. doi: 10.1093/rheumatology/33.1.36
17. de Jong SE, Selman MH, Adegnik AA, Amoah AS, van Riet E, Kruize YC, et al. IgG1 Fc N-Glycan Galactosylation as a Biomarker for Immune Activation. *Sci Rep* (2016) 6:28207. doi: 10.1038/srep28207
18. Markina YV, Gerasimova EV, Markin AM, Glanz VY, Wu WK, Sobenin IA, et al. Sialylated Immunoglobulins for the Treatment of Immuno-Inflammatory Diseases. *Int J Mol Sci* (2020) 21(15):5472. doi: 10.3390/ijms21155472
19. Prodjinotho UF, von Horn C, Debrah AY, Batsa Debrah L, Albers A, Layland LE, et al. Pathological Manifestations in Lymphatic Filariasis Correlate With Lack of Inhibitory Properties of IgG4 Antibodies on IgE-Activated Granulocytes. *PLoS Negl Trop Dis* (2017) 11(7):e0005777. doi: 10.1371/journal.pntd.0005777
20. Debrah AY, Mand S, Marfo-Debrekyei Y, Batsa L, Pfarr K, Lawson B, et al. Reduction in Levels of Plasma Vascular Endothelial Growth Factor-A and Improvement in Hydrocele Patients by Targeting Endosymbiotic Wolbachia Sp. In *Wuchereria Bancrofti* With Doxycycline. *Am J Trop Med Hyg* (2009) 80(6):956–63. doi: 10.4269/ajtmh.2009.80.956
21. Gudeli I, Lauc G, Pezer M. Immunoglobulin G Glycosylation in Aging and Diseases. *Cell Immunol* (2018) 333:65–79. doi: 10.1016/j.cellimm.2018.07.009
22. Ercan A, Kohrt WM, Cui J, Deane KD, Pezer M, Yu EW, et al. Estrogens Regulate Glycosylation of IgG in Women and Men. *JCI Insight* (2017) 2(4):e89703. doi: 10.1172/jci.insight.89703
23. Klapoetke S, Zhang J, Becht S, Gu X, Ding X. The Evaluation of a Novel Approach for the Profiling and Identification of N-Linked Glycan With a Procainamide Tag by HPLC With Fluorescent and Mass Spectrometric Detection. *J Pharm BioMed Anal* (2010) 53(3):315–24. doi: 10.1016/j.jpba.2010.03.045
24. Peschke B, Keller CW, Weber P, Quast I, Lunemann JD. Fc-Galactosylation of Human Immunoglobulin Gamma Isotypes Improves C1q Binding and Enhances Complement-Dependent Cytotoxicity. *Front Immunol* (2017) 8:646. doi: 10.3389/fimmu.2017.00646
25. Ferrantelli E, Farhat K, Ederveen ALH, Reiding KR, Beelen RHJ, van Ittersum FJ, et al. Effluent and Serum Protein N-Glycosylation Is Associated With Inflammation and Peritoneal Membrane Transport Characteristics in Peritoneal Dialysis Patients. *Sci Rep* (2018) 8(1):979. doi: 10.1038/s41598-018-19147-x
26. Koers J, Derksen N, Falkenburg W, Ooijevaar-de Heer P, Nurmohamed MT, Wolbink GJ, et al. Elevated Fab Glycosylation of Anti-Hinge Antibodies. *Scand J Rheumatol* (2021) 50:1–8. doi: 10.1080/03009742.2021.1986959

27. Behrens AJ, Duke RM, Petralia LMC, Lehoux S, Carlow CKS, Taron CH, et al. Changes in Canine Serum N-Glycosylation as a Result of Infection With the Heartworm Parasite *Dirofilaria immitis*. *Sci Rep* (2018) 8(1):16625. doi: 10.1038/s41598-018-35038-7
28. O'Regan NL, Steinfelder S, Schwedler C, Rao GB, Srikantham A, Blanchard V, et al. Filariasis Asymptomatically Infected Donors Have Lower Levels of Disialylated IgG Compared to Endemic Normals. *Parasite Immunol* (2014) 36(12):713–20. doi: 10.1111/pim.12137
29. Small ST, Labbe F, Coulibaly YI, Nutman TB, King CL, Serre D, et al. Human Migration and the Spread of the Nematode Parasite *Wuchereria bancrofti*. *Mol Biol Evol* (2019) 36(9):1931–41. doi: 10.1093/molbev/msz116
30. Stambuk J, Nakic N, Vuckovic F, Pucic-Bakovic M, Razdorov G, Trbojevic-Akmacic I, et al. Global Variability of the Human IgG Glycome. *Aging (Albany NY)* (2020) 12(15):15222–59. doi: 10.18632/aging.103884
31. Liu J, Zhu Q, Han J, Zhang H, Li Y, Ma Y, et al. The IgG Galactosylation Ratio Is Higher in Spondyloarthritis Patients and Associated With the MRI Score. *Clin Rheumatol* (2020) 39(8):2317–23. doi: 10.1007/s10067-020-04998-5
32. Hodoniczky J, Zheng YZ, James DC. Control of Recombinant Monoclonal Antibody Effector Functions by Fc N-Glycan Remodeling In Vitro. *Biotechnol Prog* (2005) 21(6):1644–52. doi: 10.1021/bp050228w
33. Hamada A, Young J, Chmielewski RA, Greene BM. C1q Enhancement of Antibody-Dependent Granulocyte-Mediated Killing of Nonphagocytosable Targets In Vitro. *J Clin Invest* (1988) 82(3):945–9. doi: 10.1172/JCI113702
34. Hoepel W, Chen HJ, Geyer CE, Allahverdiyeva S, Manz XD, de Taeye SW, et al. High Titers and Low Fucosylation of Early Human Anti-SARS-CoV-2 IgG Promote Inflammation by Alveolar Macrophages. *Sci Transl Med* (2021) 13(596):eabf8654. doi: 10.1126/scitranslmed.abf8654
35. Larsen MD, de Graaf EL, Sonneveld ME, Plomp HR, Nouta J, Hoepel W, et al. Afucosylated IgG Characterizes Enveloped Viral Responses and Correlates With COVID-19 Severity. *Science* (2021) 371(6532):eabc8378. doi: 10.1126/science.abc8378
36. Anthony RM, Ravetch JV. A Novel Role for the IgG Fc Glycan: The Anti-Inflammatory Activity of Sialylated IgG Fcs. *J Clin Immunol* (2010) 30(Suppl 1):S9–14. doi: 10.1007/s10875-010-9405-6
37. Quast I, Keller CW, Maurer MA, Giddens JP, Tackenberg B, Wang LX, et al. Sialylation of IgG Fc Domain Impairs Complement-Dependent Cytotoxicity. *J Clin Invest* (2015) 125(11):4160–70. doi: 10.1172/JCI82695
38. Dekkers G, Plomp R, Koeleman CA, Visser R, von Horsten HH, Sandig V, et al. Multi-Level Glyco-Engineering Techniques to Generate IgG With Defined Fc-Glycans. *Sci Rep* (2016) 6:36964. doi: 10.1038/srep36964
39. de Taeye SW, Bentlage AEH, Mebius MM, Meesters JI, Lissenberg-Thunnissen S, Falck D, et al. FcγR Binding and ADCC Activity of Human IgG Allotypes. *Front Immunol* (2020) 11:740. doi: 10.3389/fimmu.2020.00740
40. van de Bovenkamp FS, Hafkenscheid L, Rispens T, Rombouts Y. The Emerging Importance of IgG Fab Glycosylation in Immunity. *J Immunol* (2016) 196(4):1435–41. doi: 10.4049/jimmunol.1502136
41. de Haan N, Falck D, Wuhrer M. Monitoring of Immunoglobulin N- and O-Glycosylation in Health and Disease. *Glycobiology* (2020) 30(4):226–40. doi: 10.1093/glycob/cwz048

Conflict of Interest: The authors declare that the research was conducted in the absence of any commercial or financial relationships that could be construed as a potential conflict of interest.

Publisher's Note: All claims expressed in this article are solely those of the authors and do not necessarily represent those of their affiliated organizations, or those of the publisher, the editors and the reviewers. Any product that may be evaluated in this article, or claim that may be made by its manufacturer, is not guaranteed or endorsed by the publisher.

Copyright © 2022 Adjobimey and Hoerauf. This is an open-access article distributed under the terms of the Creative Commons Attribution License (CC BY). The use, distribution or reproduction in other forums is permitted, provided the original author(s) and the copyright owner(s) are credited and that the original publication in this journal is cited, in accordance with accepted academic practice. No use, distribution or reproduction is permitted which does not comply with these terms.



Core Fucosylation Regulates the Function of Pre-BCR, BCR and IgG in Humoral Immunity

Yuhan Sun^{1,2†}, Xueying Li^{3†}, Tiantong Wang¹ and Wenzhe Li^{1*}

¹ College of Basic Medical Science, Dalian Medical University, Dalian, China, ² Division of Regulatory Glycobiology, Institute of Molecular Biomembrane and Glycobiology, Tohoku Pharmaceutical University, Sendai, Japan, ³ Research Institute for Microbial Diseases and World Premier International Immunology Frontier Research Center, Osaka University, Suita, Japan

OPEN ACCESS

Edited by:

Irena Trbojević-Akmačić,
Genos Glycoscience Research
Laboratory, Croatia

Reviewed by:

József Prechl,
Diagnosticum Zrt., Hungary
Anja Lux,
University of Erlangen
Nuremberg, Germany

*Correspondence:

Wenzhe Li
liwenzhe@dmu.edu.cn

[†]These authors have contributed
equally to this work

Specialty section:

This article was submitted to
B Cell Biology,
a section of the journal
Frontiers in Immunology

Received: 28 December 2021

Accepted: 25 February 2022

Published: 25 March 2022

Citation:

Sun Y, Li X, Wang T and Li W (2022)
Core Fucosylation Regulates the
Function of Pre-BCR, BCR
and IgG in Humoral Immunity.
Front. Immunol. 13:844427.
doi: 10.3389/fimmu.2022.844427

Most of the membrane molecules involved in immune response are glycosylated. N-glycans linked to asparagine (Asn) of immune molecules contribute to the protein conformation, surface expression, stability, and antigenicity. Core fucosylation catalyzed by core fucosyltransferase (FUT8) is the most common post-translational modification. Core fucosylation is essential for evoking a proper immune response, which this review aims to communicate. First, FUT8 deficiency suppressed the interaction between μ HC and λ 5 during pre-BCR assembly is given. Second, we described the effects of core fucosylation in B cell signal transduction via BCR. Third, we investigated the role of core fucosylation in the interaction between helper T (T_H) cells and B cells. Finally, we showed the role of FUT8 on the biological function of IgG. In this review, we discussed recent insights into the sites where core fucosylation is critical for humoral immune responses.

Keywords: core fucosylation, pre-B cell, BCR, IgG, humoral immune response

INTRODUCTION

Humoral immune response relies on intrinsic B cell development. The gradual stages of B lymphocyte differentiation are marked by the arrangement and expression of immunoglobulin (Ig) genes in the bone marrow (BM) (1). Early B lymphocytes are produced in the BM, in which there is a stepwise subgroup from hematopoietic stem cells (HSC) to immature B cells. The middle steps are composed of pro-B cells and pre-B cells. The V(D)J rearrangement of the μ -heavy chain (μ HC) gene occurs in pro-B cells, and the gene rearrangement of light chains begins in the pre-B cell stage. Once a light chain gene is assembled and a completed IgM is expressed on the surface of immature B cells, the B cells differentiate further to become mature B cells expressing IgD and IgM. The mature B cells recirculate through secondary lymphoid tissues, where they may encounter foreign antigens (Ags). Ag-binding B cells are trapped in the T-cell zone of lymphoid tissue and activated by encounter with helper T (T_H) cells, and differentiated into plasma cells, which secrete large amounts of antibodies (Abs) to provide lasting protective immunity (2, 3).

Almost all of the immunological molecules are glycosylated (4, 5). Glycosylation is one of the most common post-translational modifications of eukaryotic proteins. The glycans attached to these proteins can be classified into two major types: O-linked glycosylation, whose glycan chains are linked to the oxygen atom of serine or threonine residues in the Golgi, and N-linked glycosylation, whose glycan chains are covalently linked to the amide nitrogen of asparagine (Asn) residues of an

Asn-X-Ser/Thr sequence (where X is not proline) by an N-glycosidic bond in the endoplasmic reticulum (ER). Despite their microheterogeneity, most N-glycans share a common N-glycan precursor, 14 monosaccharide residues (i.e., $\text{Glc}_3\text{Man}_9\text{GlcNAc}_2$) that is pre-assembled on the ER membrane before it is transferred to protein. After the attachment of the N-glycan precursor to Asn-X-Ser/Thr in a protein, a series of processing reactions trim the N-glycan in the ER. After sequential trimming of the terminal monosaccharide residues (glucose and mannose), the glycoproteins exiting the ER en route to the Golgi carry N-glycans with a $\text{Man}_8\text{GlcNAc}_2$ isomer. Then, the glycoprotein undergoes further sugar chain elongation and “glycan maturation” (e.g., fucosylation, galactosylation, and terminal sialylation) by a suite of glycosyltransferases (6). The glycosyltransferases that assemble monosaccharide moieties of a simple nucleotide sugar donor substrate (e.g., UDP-Gal, GDP-Fuc, or CMP-Sia) into the acceptor substrate (linear and branched glycan chains). The ER-Golgi pathway harbors many glycan-modifying enzymes in eukaryotic cells. In the *medial*-Golgi, the N-glycan has two branches, which are initiated by the addition of two-terminalA006C N-acetylglucosamine (GlcNAc) residues by N-acetylglucosaminyltransferase-I (GnT-I) and GnT-II. Additional branches can be initiated at C-4 of the core mannose $\alpha 1,3$ (by GnT-IV) and C-6 of the core mannose $\alpha 1,6$ (by GnT-V) to yield tri- and tetra-antennary N-glycans. N-glycans may carry a “bisecting” GlcNAc residue that is catalyzed by GnT-III. Further sugar additions, such as galactosylation by galactosyltransferases (GalT), fucosylation by fucosyltransferases

(FUTs), and sialylation by sialyltransferases (STs), mostly occur in the *trans*-Golgi. FUTs consist of 13 members, including FUT1 to FUT11, protein O-fucosyltransferase 1 (POFUT1), and POFUT2. Core fucosylation is catalyzed by core fucosyltransferase (FUT8). **Figure 1** depicts a bisecting N-GlcNAc on a tetra-antennary N-glycan, which may be present in all of the more highly branched structures. Glycosylation regulates several glycoprotein functions, including half-life on the membrane, sorting to specific subcellular sites, and folding in the ER (7).

We have been devoted to the study that core fucosylation is an essential segment in the early B cell differentiation (8, 9), B cell activation (10, 11), Ab production (11, 12), systemic lupus erythematosus (SLE) development (11), infection (12, 13) and antitumor activity (14). The critical physiological function of the fucosylation is characterized by leukocyte adhesion deficiency II, which emphasizes the physiological significance of the fucosylation due to immunodeficiency caused by fucosylation deficiency (15). This review focuses on the unique roles of core fucosylation in adaptive humoral immune responses.

CORE FUCOSYLATION AND ITS FUNCTION

In mammalian cells, the core fucosylation catalyzed by FUT8 is a common post-translational modification (**Figure 2**) (16, 17). FUT8 is the only glycosyltransferase that catalyzes the transfer

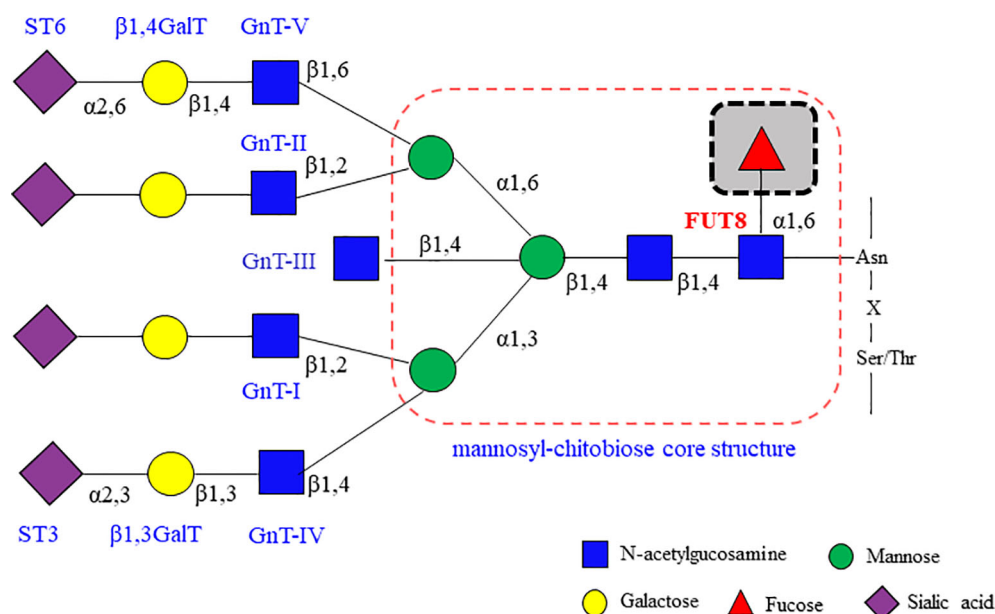


FIGURE 1 | Glycosyltransferases involving in the biosynthesis of branching N-glycans. $\alpha 2,6$ sialyltransferases (ST6) and/or $\alpha 2,3$ sialyltransferases (ST3) that act on galactose, $\beta 1,4$ galactosyltransferases ($\beta 1,4$ GalT) and/or $\beta 1,3$ galactosyltransferases ($\beta 1,3$ GalT) that act on N-acetylglucosamine (GlcNAc), and the family of N-acetylglucosamine transferases (GnT-I, GnT-II, GnT-III, GnT-IV, GnT-V and so on) that participate in GlcNAc synthesis. Fucosyltransferases (FUT3, FUT4, FUT5, FUT6, FUT7, FUT8, FUT9) can attach fucose in either $\alpha 1,3/\alpha 1,4$ or $\alpha 1,6$ linkage. These enzymes act sequentially, so that the product of one enzyme yields a preferred acceptor substrate for the subsequent action of another. Different proteins may have different subsets of N-glycans, which is referred to as microheterogeneity. All N-glycans share a common core sugar sequence, $\text{Man}\alpha 1-6(\text{Man}\alpha 1-3)\text{Man}\beta 1-4\text{GlcNAc}\beta 1-4\text{GlcNAc}\beta 1$.

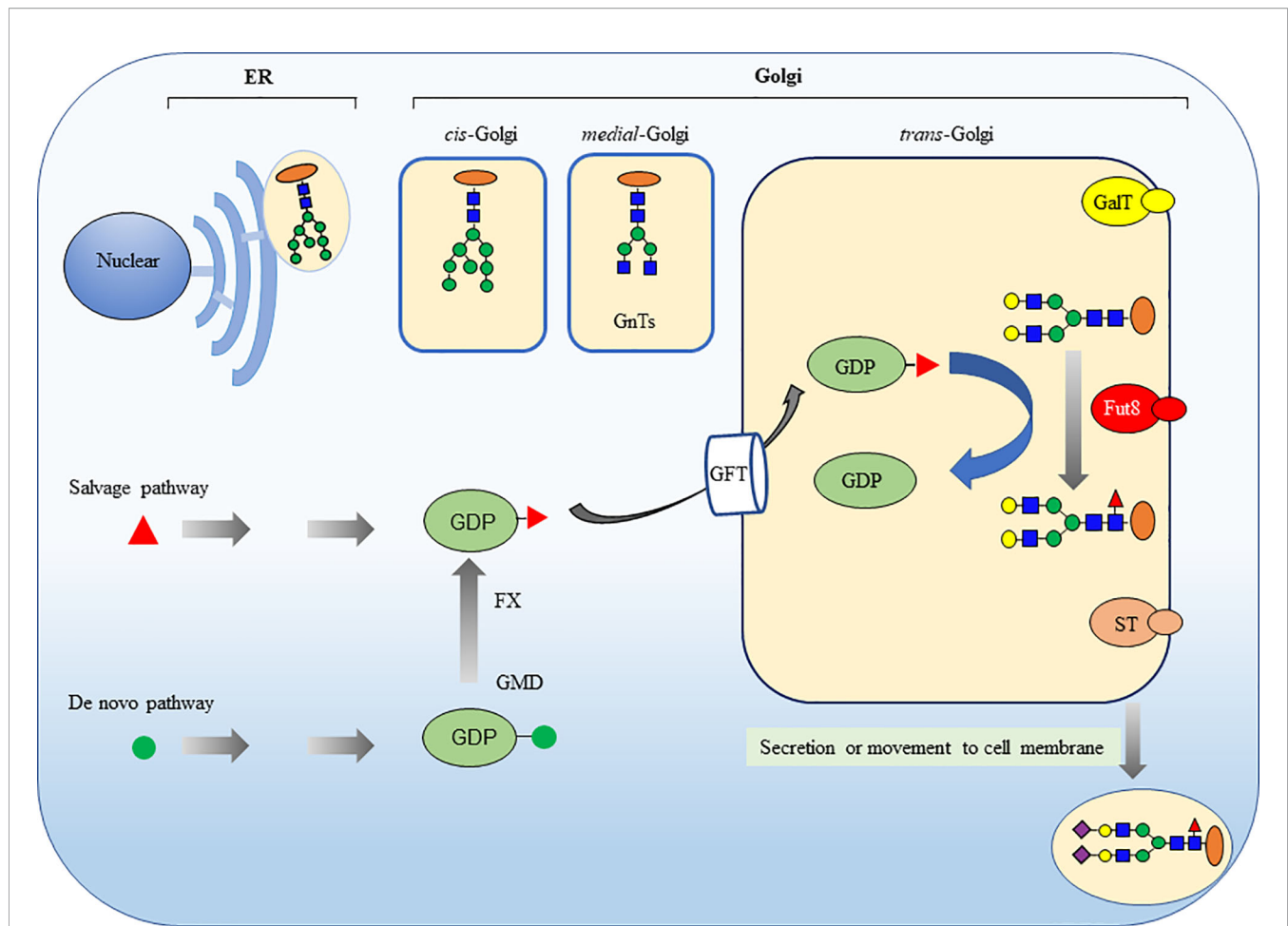


FIGURE 2 | Core fucosylation modification in mammalian N-glycans is catalyzed by FUT8. The ER-Golgi pathway harbors many glycan-modifying enzymes in eukaryotic cells. The glycosyltransferases that operate in the ER are woven into the ER membrane. In contrast, the glycosyltransferases in Golgi compartments are generally type II membrane proteins with a small cytoplasmic amino-terminal domain, a single transmembrane domain, and a large luminal domain that has an elongated stem region and a globular catalytic domain. FUT8 is a typical type II membrane protein and a Golgi apparatus-resident glycosyltransferase to catalyze the transfer of a fucose from GDP-fucose to the inner GlcNAc of N-glycans through $\alpha 1,6$ -linkage (core fucosylation). There are two different pathways for producing GDP-fucose, namely salvage pathway and *de novo* pathway. The GDP-fucose is transferred from the cytosol into the Golgi apparatus by GDP-fucose transporter (GFT). The sugar additions, such as galactosylation by GalT, fucosylation by FUTs and sialylation by STs, mostly occurring in the *trans*-Golgi.

of fucose from GDP-fucose to the inner GlcNAc of N-glycans through $\alpha 1,6$ -linkage (core fucosylation) in the Golgi apparatus. There are two different pathways for producing GDP-fucose, namely the salvage and *de novo* pathways. The salvage pathway utilizes free fucose derived from dietary sources. The *de novo* pathway (the major way) synthesizes GDP-fucose from GDP-mannose through oxidation, epimerization, and reduction catalyzed by two enzymes, including GDP-mannose 4,6-dehydratase (GMD) and GDP-4-keto-6-deoxy-mannose-3,5-epimerase-4-reductase (FX). Then, the GDP-fucose transporter (GFT) transfers the GDP-fucose from the cytosol into the Golgi apparatus.

Previous studies have observed relationships between protein structures and the N-glycan repertoires (18). The underlying pentasaccharide (mannosyl-chitobiose: Man3GlcNAc2) core structure of all eukaryotic N-glycans serves as scaffolding. The flexible glycosidic linkages are often found in the pentasaccharide

core structure of the N-glycans. The antenna flexibility could play a specific role in directing precise recognition in carbohydrate-protein interactions. N-linked glycosylation does not induce any secondary structure of proteins but that it does alter their conformational preferences in the vicinity of the glycosylation site, increasing the probability of more compact conformations (19). These effects seem to involve only the monosaccharide units of the N-glycan and are probably mediated by steric and hydrophobic or hydrophilic interactions between the N-glycan and the neighboring amino acid sidechains (20). Most glycoproteins are expressed on the cell surface. Each interaction between such proteins involved in cell-cell recognition events are frequently weak. Strong cell-cell interactions are obtained from many of these interactions occurring simultaneously on cell surface molecules. The N-glycans on these molecules influence their orientation and their packing of glycoproteins on the cell surface.

It has been reported that the core fucose influences the conformational flexibility of the core-fucosylated biantenna of N-glycans (21). The core fucose also plays a crucial role in the binding of an N-glycan to a plant lectin (22). As shown in the **Table 1**, core fucosylation regulates the conformation, stability and expression of immune molecules, such as pre-BCR, BCR, IgG, T cell receptor (TCR), CD276(B7H3), CD14, CD41a, hemagglutinin (HA), PD-1 and VLA-4. The association between an N-glycan and its Asn sidechain is relatively rigid and planar, with a tendency to extend the core sugar structure (24). Conversely, core fucosylation is strongly influenced by the structure of the proteins. The glycosylation sites of the proteins and their subcellular location determine whether the conjugated N-glycans will be modified by core fucosylation. It is reasonable to propose that core fucosylation could affect the glycosidic linkage flexibility and conformation of proteins, resulting in modification of protein interactions or assembly. Core fucosylation is ubiquitously expressed in mammalian tissues and participate in the regulation of numerous biological events of physiological and pathological conditions (25), including cell growth (8, 26), cell signal transduction (9, 10), protein-protein interaction (9, 10), cell-cell interaction (11, 12) and tumorigenesis (23, 27, 28). FUT8 knockout (FUT8^{-/-}) mice exhibit early postnatal death (29), retardant growth (26, 30), emphysema-like changes (29, 31), schizophrenia-like phenotype (32) and so on.

CORE FUCOSYLATION REGULATES PRE-BCR ASSEMBLY

During early B cell differentiation, the formation of pre-BCR complex allows progression from the pro-B cell stage to pre-B cell stage (33). The assembly of the pre-BCR on the cell membrane is a critical checkpoint for B cell growth and differentiation in humans and mice (34–38). Suppression of pre-BCR complex formation inhibits the transition of B lymphocyte development from pro-B cell stage to pre-B cell stage (39, 40). The functional pre-BCR complex consists of immunoglobulin (Ig) μ HC, surrogate light chain (SLC), and Ig α /Ig β (CD79a/CD79b) (41). The μ HCS assembled with SLC are classically obligatory for pre-BCR trafficking to the surface (42). The μ HC (GI:90956) comprises the variable region of Ig

μ HC (V_H) and the constant portion of the Ig μ HC (C_H). The λ 5 (GI:54887631) and Vpre-B are non-covalently associated to form SLC. In a pre-BCR complex, λ 5 binds to the C_{H1} domain of μ HC, while Vpre-B interacted with the V_H domain. Vpre-B is stabilized by a salt bridge between Glu¹⁰⁶ residue of Vpre-B and Arg⁵⁹ residue of V_H (33). The N-glycans on μ HC are of the high-mannose type (43). Ubelhart et al. (44) also discovered that μ HC of mouse and human Igs contains the N-linked glycosylation site N⁴⁶ and that a conserved N⁴⁶-glycan at the C_{H1} domain of μ HC was necessary for the interaction of μ HC and λ 5, followed by the formation of pre-BCR. There are no N-glycosylated sites on λ 5, and it is covalently coupled to the C_{H1} domain of μ HC *via* a carboxyl-terminal cysteine (42). Only pre-B cells that express the pre-BCR complex undergo the following clonal expansion.

In FUT8^{-/-} BM, we found a profound and selective suppression in pre-B cell generations without a concomitant change in the pro-B cell population (8). To address the impairment of the pre-B cell population in FUT8^{-/-} mice, we investigated the role of FUT8 in pre-BCR assembly. Indeed, μ HC is a core fucosylated protein, and loss of core fucosylation of μ HC reduces the binding affinity between μ HC and λ 5. Consistent with this result, the formation of pre-BCR is down-regulated in the FUT8 knockdown pre-B cell line (70Z/3-KD cells) and has been recovered in 70Z/3-KD-re cells (9). Indeed, the subpopulation of μ HC⁺ λ 5⁺ cells is lower in FUT8^{-/-} BM than in FUT8^{+/+} BM. Early pre-B cells expressing both μ HC and SLC are in the BM and fetal liver; one produces SLC-pairing μ HC, and the other produces SLC-nonpairing μ HC (36). Only half of the in-frame rearranges μ HCS pair correctly with SLCs (45). Subsequently, μ HCS that bind poorly to SLCs are subsequently poorly represented among μ HC families (46). The μ HC undergoes glycosylation modification and is transported to the cell surface. The newly synthesized membrane form of μ HC is Endo H-resistant, which reaches the cell surface, while the secretory form is Endo H-sensitive (47). Since FUT8 expression is significantly increased during the transition from pro-B to pre-B cell development (8), and since the core fucosylation is required for pre-BCR complex assembly (9), it is conceivable that FUT8 controls the core fucosylation of μ HC, followed by pre-BCR complex assembly. There are no N-glycosylation sites in λ 5, Vpre-B, and V_H domains of μ HC. When the binding of V_H of μ HC to Vpre-B is a protein-protein

TABLE 1 | Core fucosylated immune molecules and their crucial functions.

Immune molecules	Functions	References
pre-BCR	Loss of core fucosylation of μ HC reduced the binding affinity between μ HC and λ 5.	(13, 14)
BCR	Loss of core fucosylation reduced the lipid raft formation of B cells.	(15)
IgG	Loss of core fucosylation promotes the ADCC of nature killer cells.	(6–8)
TCR	Core fucosylation of the TCR is necessary for T-cell of nature killer cells.	(3–5)
CD276(B7H3)	FUT8-B7H3 axis is a promising strategy for improving anti-tumor immune responses.	(9)
CD14	Core fucose is critical for CD14-dependent Toll-like receptor 4 signaling.	(1)
CD41a	The enzyme activity of FUT8 is involved in the megakaryocytes differentiation.	(16)
Hemagglutinin (HA)	Loss of core fucosylation reduces the binding of influenza A virus HA to IgE.	(12)
PD-1	Loss of core fucosylation enhanced the PD-1 expression in CD8 ⁺ cytotoxic T lymphocytes.	(23)
VLA-4	Loss of core fucosylation decreased binding between pre-B cells and stromal cells.	(13)

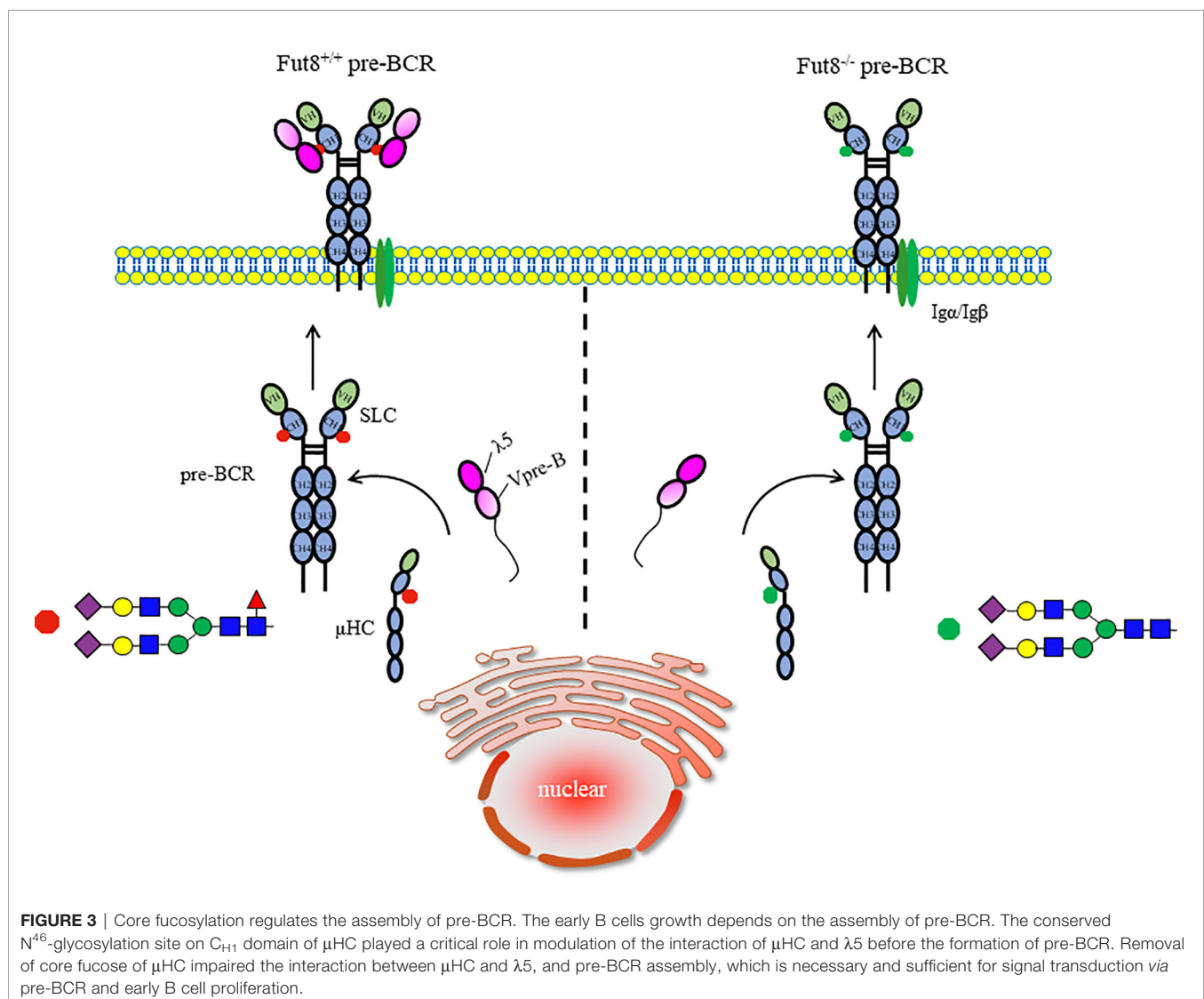
interaction by ionic bonding between Glu¹⁰⁶ of Vpre-B and Arg⁵⁹ residue of V_H region, and the binding of C_{H1} of μ HC to λ 5 is a protein-glycoprotein interaction. It is reasonable to propose that the FUT8 regulated the interaction between C_{H1} of μ HC and λ 5, but did not influence the interaction between Vpre-B and μ HC during pre-BCR assembly (Figure 3). The pre-BCR tunes pre-B cell repertoire by driving the preferential differentiation and expansion of cells with a higher quality of μ HC (37). Thus, we propose a mechanism in which core fucosylated μ HC has a higher potential to assemble with SLC and amplify the pre-B cell repertoire.

Pre-BCR expression is sufficient and required for constitutive cell signaling (48). Mutations of genes associated with the pre-BCR signal pathway culminate in agammaglobulinemia (35–38, 49). Core fucosylation is required for the appropriate binding of μ HC to λ 5, as well as pre-BCR assembly (9). Except for the signal transduction *via* pre-BCR, integrins bind to vascular adhesion molecule-1 (VCAM-1), thereby facilitating signaling with stimulation of IL-7 from stromal cells, which plays a significant

role in the generation of B cell precursors (50). Integrins on pre-B cells, together with pre-BCR and galectin-1, could form a homogeneous lattice at the contact area between pre-B cells and stromal cells (51). FUT8 ablation reduces binding affinity between very late antigen 4 (VLA-4, α 4 β 1 integrin) on pre-B cells and VCAM-1 on stromal cells, which impaired the colony expansion of pre-B cells in FUT8^{-/-} BM (8).

CORE FUCOSYLATION REGULATES THE SIGNAL TRANSDUCTION VIA BCR

Upon B cell activation, B cells recognize both soluble and membrane-associated Ags by B-cell receptor (BCR), and respond to them (3). After the recognition of Ags, BCRs on B cells trigger signaling that eventually induced B cell activation and Abs production (52). First identified in 1970 (53), the BCR and Ab consisted of two heavy (H) chains and two light (L)



chains, which are linked by disulfide bonds. Each H chain is composed of an N-terminal variable domain (V_H) and three constant domains (C_{H1} , C_{H2} , C_{H3}); the L chains consist of an N-terminal variable domain (V_L) and one constant domain (C_L). The “fragment antigen-binding” (Fab) domains, which mediate antigen recognition, contain the complementarity determining regions (CDRs), located in the N-terminal region of C_H and C_L , which define the antigen-specificity. The “fragment crystallizable” (Fc) of the C-terminal regions is composed of the two C_H (C_{H2} , C_{H3}), which bind to the immune effector molecules, including Fc receptors. The BCR complex contains a membrane-bound immunoglobulin (mIg) with a small cytoplasmic domain and a disulfide-linked heterodimer Ig α –Ig β (CD79a–CD79b), which contains the immunoreceptor tyrosine-based activation motif, ITAMs (54, 55).

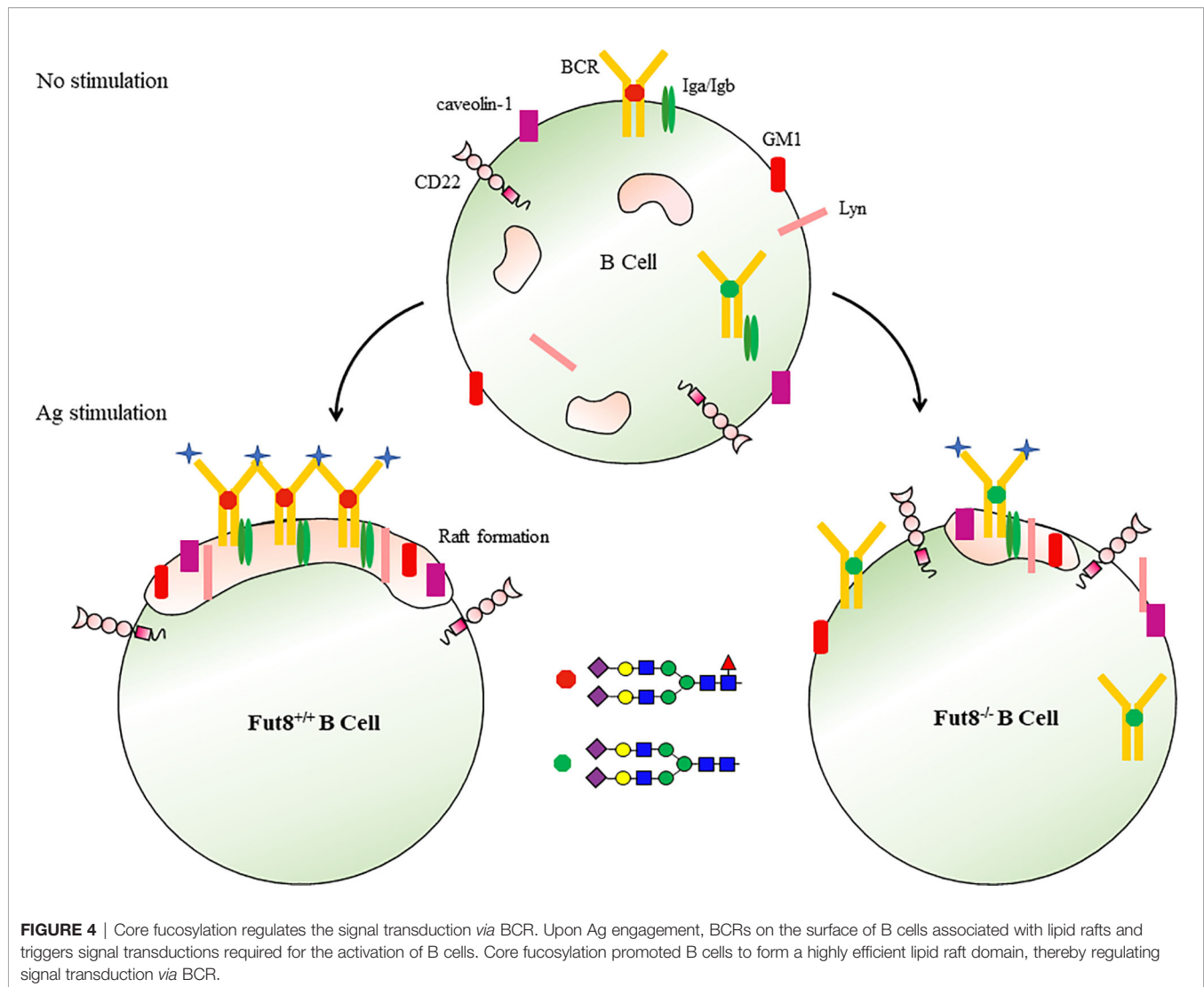
There are glycosylation sites at Asn²⁹⁷ of the Fc region but not in the V_H of IgG–BCR. Microheterogeneity of N-glycans on IgG is detected by the linkage of galactose–sialic acid or galactose at one or both of the terminal GlcNAc or linkage of a third GlcNAc arm. The profile of N-glycans at Asn²⁹⁷ on BCR is of the complex type (51). Furthermore, BCR is a highly core fucosylated glycoprotein, and the core fucosylation regulates the function of BCR to distinguish Ag (10). Indeed, FUT8 ablation impaired the binding affinity of IgG–BCRs to their ligands. Since core fucosylation could modulate the conformation and ligand affinity of the membrane receptors (8–11, 26, 29) and could influence the flexibility of N-glycans antenna (21), it is suggested that core fucosylation could control the axial rotation of the Fab arms and the recognition of BCR to Ag. Core fucosylation of μ HC impaired the interaction between μ HC and λ 5 of the SLC. However, FUT8 gene knockout/knockdown does not influence the BCR expression on the cell surface. It is conceivable that the difference of N-glycan in heavy chains is attributed to the distinct assembly between pre-BCR and BCR.

Lipid rafts are heterogeneous, dynamic and transient plasma membrane entities enriched in saturated phospho-, sphingo- and glycolipids, cholesterol, lipidated proteins and glycosylphosphatidylinositol (GPI)-anchored proteins (56). The BCR is found in detergent-soluble membrane fractions in resting cells, but is acquired in detergent-resistant membrane fractions (raft domains) after receptor activation (57–59). Fluorescence resonance energy transfer confocal microscopy revealed that the association of BCR with lipid raft occurred within seconds, resulting in the cross-linking of BCR (60). Upon Ag stimulation, core fucosylation influences the binding of BCR to Ag peptide at 30 seconds, the formation of lipid raft at 3 min, and signal transduction *via* BCR after 5 min (10). FUT8 ablation suppresses the together with BCR, Lyn, and GM1 or caveolin-1 in lipid raft domains. Except for their role in signaling molecules concentrating, lipid rafts play a significant role in protein internalization through the endocytic pathway (60). The FUT8 gene disruption significantly reduces the Ag endocytosis of B cells (10). Several mechanisms may contribute to the reduced lipid raft formation by FUT8 ablation. First, because of the conformation with an increasing affinity for lipid rafts caused by Ag-driven oligomerization of the BCR (58), the failed

oligomerizations of BCR by afucosylation result in reduced lipid raft formation. Second, caveolin-1 is a scaffolding protein of cholesterol-rich caveolae lipid rafts (57), the inhibited recruitment of caveolin-1 by FUT8 ablation influences the efficient coalescing of the lipid raft in the plasma membrane. Third, the depletion of core fucose increased the hydrophilicity of immune molecules and impaired lipid raft formation (61) (**Figure 4**). Core fucosylation controls several parameters associated with B cell activation, including Ag recognition, BCR oligomerization, signal transduction *via* BCR, and lipid raft cluster formation.

CORE FUCOSYLATION REGULATES THE T_H -B CELL INTERACTION

Upon Ag engagement by BCR, B cells process and present the Ag peptide in association with the major histocompatibility complex class II (MHC-II) molecules *via* BCR-mediated endocytosis (3). Then, the peptide-loaded MHC-II complex (pMHC-II) on B cells can be recognized by Ag-specific armed T_H cells *via* T cell receptor (TCR) (62). During T_H -B cell interaction, activated T_H cells produce cytokines for the B lymphocytes clonal expansion and differentiate into Ab-secreting cells (58). Several studies revealed the contribution of glycosylation in the T_H -B cell interaction (20). Loss of GlcNAcT-V glycosyltransferase (GnT-V), for example, could promote the recruitment of TCR to the synapse and enhance TCR internalization (63). FUT1 overexpressed T cells enhance the signaling pathway *via* TCR and apoptosis required for thymocyte maturation arrest (64). The α 2,6-sialyltransferase (ST6Gal-1) is required for the development of humoral immunity (65, 66). The removal of N-glycan in T cells improves the functional avidity of TCR to Ag recognition (67). Notably, the most immune molecules participated in T and B cell activation are core-fucosylated glycoproteins. To assess the function of FUT8 in the T–B cell interactions, we obtained FUT8^{+/+}OT-II and FUT8^{-/-}OT-II mice by crossing FUT8^{+/+} mice with OT-II mice (these transgenic mice express CD4⁺ TCR specific for chicken ovalbumin 323–339, OVA_{323–339}). Most key proteins associated with Ag recognition and the orchestration including MHC-I and MHC-II, are glycosylated (68). Although I-A^d has a single N-glycan (69), core fucosylation cannot change the OVA_{323–339} presentation abilities of MHC-II (11, 12). However, compared to FUT8^{+/+}OT-II cells, the communication of T–B cells (MHC-II⁺ TCR β ⁺ cells) is significantly decreased in FUT8^{-/-}OT-II cells (11). Also, ZAP-70 and Syk phosphorylation was significantly reduced in FUT8^{-/-}OT-II cells with interaction by OVA_{323–339}-loaded B cells. Given that the pMHC on B cells induces a particular conformational change of TCR on T cells (70, 71), and the core fucose is expressed on the cell surface of T and B cells and could affect the flexibility and the conformation of proteins (21). It is reasonable to propose that core fucosylation would influence the conformational stability and geometry of any TCR–pMHC clusters in the T_H -B cell interactions. Alternatively, a diverse range of glycan-binding proteins, such as galectins and siglecs, bind to the sugar chains on these glycoproteins, thereby modulating cell signaling and cell-cell



interactions (21). Galectin-1^{-/-} mice show abnormal thymocyte selection, causing alteration in T cell responses (72). CD22 selectin, which recognizes α 2,6-linked sialylated glycans, is a B cell co-receptor that decreases the signaling via BCR (73). Fucose-specific lectins (74) enable to participate the events in the interactions between T and B cells.

Ab production is one of the major events in the adaptive humoral immune response. The titer of anti-OVA IgG is markedly decreased after the OVA immunization in FUT8^{-/-} mice (11). Moreover, compared to FUT8^{+/+} SPLs, the number of IgG-producing cells is obviously decreased in FUT8^{-/-} SPLs. During *S. typhimurium* infection, the production of IgG and sIgA specific for bacteria is also decreased in FUT8^{-/-} mice with attenuated the T_H-B cell interactions, but not in communication between T cells and DCs (12), indicating that core fucosylation is essential for the efficient Ab production. Ig class-switching recombination generates an isotype-switched Abs, which are essential for mediating effective humoral immunity (75). The isotype switching of a mature B cell via its BCR from one class to

another depends upon the interaction of Ag-stimulated B cells with T_H cells. To assess FUT8 function in Ig class-switching, IgGs of different subclasses (class-switched) and IgM (non-switched) are measured in the sera of FUT8^{-/-} mice. The amounts of IgG subclasses, IgG₁, IgG_{2a}, IgG_{2b}, and IgG₃ are significantly reduced in FUT8^{-/-} mice due to low levels of cytokines, such as IL-4, IL-5, IL-6, IFN γ , and TGF secreted by FUT8^{-/-} T_H cells, while amounts of IgM are relatively normal (11). Core fucosylation plays a crucial role in all steps required for Abs production. First, in the T_H-B cell interactions, core fucosylation regulates the geometry and conformation of TCR-pMHC clusters in lipid rafts. Second, in cytokine production, core fucosylation controls the expression level of T_{H2}-type cytokines (IL-4, IL-6) associated with the activation of T_H and B cells (12). Third, in B cell generation, FUT8 affects the population of CD19⁺ B cells.

Several studies have been reported that aberrant cues of glycosylation contribute to autoimmune disease (AD) pathogenesis (76–78). For example, the low levels of sialylated

IgG are detected in the sera of rheumatoid arthritis and Wegener's granulomatosis patients, while the sialylated IgG is increased during remission (78, 79). Galactosylated IgG1 is significantly reduced in the sera of rheumatoid arthritis patients (77). GnT-V ablation induces the coclustering of TCRs at the cell surface, reducing the threshold for T cell activation and causing multiple sclerosis (63). SLE is a typical autoimmune disease whose characteristics are inflammatory disorders and autoantibodies production (80). The level of core fucosylated IgG is significantly increased in the sera of SLE patients (11, 76, 81). Indeed, T_H cell activation in the peripheral blood of SLE patients plays a crucial role in SLE pathogenesis, and the hyperactivity of B cells is T_H cell-dependent in SLE (82, 83). The remarkable differences of glycosylation on T_H cells have been observed in active SLE patients (84). Core fucosylation is required for TCR activation in T_H cells (61). Increased-core fucosylation induces T_H cell hyper-activation and contributes to the SLE severity and pathogenesis.

CORE FUCOSYLATION REGULATES THE FUNCTION OF IGGs

Glycosylation occurs normally in human IgGs, and plays a significant role in IgG function (85–87). Structural evidence

proved that each IgG molecule has a highly conserved N-glycan at Asn²⁹⁷ in the C_{H2}/C_{H3} domain of Fc regions, and plays a crucial role in sustaining the conformation of Fc domain of IgGs. Multiple sugar chain moieties extend from Fc domains toward each other into the interchain region of IgG, and then they stabilize the IgG framework (88). Differences in the sugar chains determine the variances in the orientation of the protein surface (88).

Several functions of IgGs are mediated through Fc γ receptors (Fc γ Rs) on the effector cells. Because the N-glycan at Asn²⁹⁷ on the Fc domain is located next to the Fc γ Rs binding interface, glycosylation controls the biological function of IgGs (88). The Fc domain sialylation triggers conformational changes in IgG1 that enable interactions with type II Fc γ Rs, while core fucose alters type I Fc γ Rs binding of IgG1 by modulating the Fc's affinity for Fc γ RIIIa. Core fucosylated N-glycans attached to the Fc region is a critical determinant of antibody-dependent cell-mediated cytotoxicity (ADCC), as the deletion of core fucose from the Fc region enhances its binding affinity to the Fc γ Rs and significantly improves ADCC (**Figure 5**) (89–92). The highly de-fucosylated (~60%) IgG₁ exhibits 100-fold ADCC compared to hyper fucosylated (~10% defucosylated) IgG₁, without any difference for Ag binding. Dengue virus infection increases the afucosylation level of IgG₁, and the level of afucosylated IgG₁ could predict the severity of dengue disease (93). Moreover,

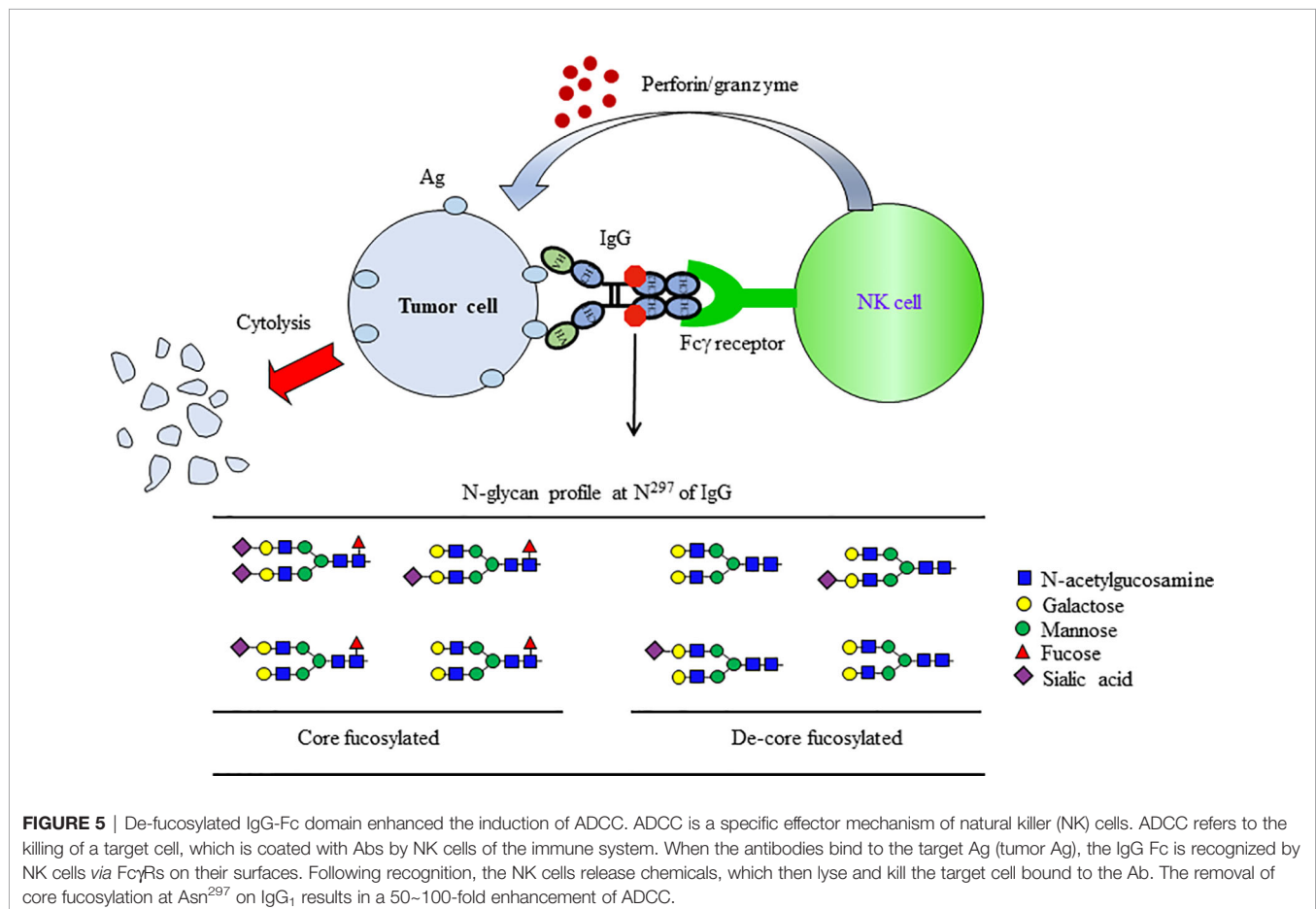


FIGURE 5 | De-fucosylated IgG-Fc domain enhanced the induction of ADCC. ADCC is a specific effector mechanism of natural killer (NK) cells. ADCC refers to the killing of a target cell, which is coated with Abs by NK cells of the immune system. When the antibodies bind to the target Ag (tumor Ag), the IgG Fc is recognized by NK cells via Fc γ Rs on their surfaces. Following recognition, the NK cells release chemicals, which then lyse and kill the target cell bound to the Ab. The removal of core fucosylation at Asn²⁹⁷ on IgG₁ results in a 50–100-fold enhancement of ADCC.

afucosylated IgG₁ plays a critical role in immune responses to enveloped viruses, including COVID-19 (94). Also, afucosylated IgG efficiently induced FcγRs-dependent natural killer (NK) cell degranulation in malaria (95). As a result of these advances, Ab “glycoengineering” is currently gaining attention as an approach to enhance the effects of therapeutic Abs for tumor and virus infection (96).

In human serum, FUT8 is derived in about 95% from blood platelets (97). Platelets release the FUT8 with components of vesicles during blood coagulation (98). Serum IgG contains more than 30 different N-glycan profiles, and all of the major N-glycans were core fucosylated (99). Core fucosylated glycans is increased on the IgG of SLE patients (81). The hyper-core fucosylation frequently occurs in the sera of epithelial ovarian cancer patients with cisplatin resistance (23) and lung adenocarcinoma patients (14), but the core fucosylation level is down-regulated in the sera of patients with cervical cancer (100). Core fucosylation is also increased in intestinal tissues of patients with inflammatory bowel disease (61).

CONCLUSION AND PERSPECTIVES

Appropriate B cell responses are critical for adaptive humoral immunity. Early B cell differentiation, activation and population of B cells, T_H-B cell interaction and Ab production are processes carefully orchestrated by a complex network of immune molecules. During B cell development, approximately 90% of B cells are eliminated due to the greatly restricting mature immune repertoire of BCR available for Ag recognition (101). Hence, the mechanisms regulating B cell development are crucial in treating of ADs and improving vaccination strategies.

FUT8 can modify multiple proteins, and core fucosylation of N-glycans of the immune molecules could significantly alter their functions (14). Based on our previous study, core fucosylation is not only associated with pre-BCR assembly and Ag recognition of BCR but also plays a crucial role in effective lipid raft formation, T_H-B cell interaction, and Ab production in guiding B lymphopoiesis to shape humoral immunity. It is worth noting that the loss of FUT8 inhibits effective Ab production, while hyper-activation of these cells results in SLE pathogenesis. There are 2937 single-nucleotide polymorphisms

(SNPs) in the FUT8 gene region, and the FUT8 gene rs35949016 SNP could affect FUT8 expression (51, 102). Given that the balance between specific and degenerate immune responses holds a vital illumination for protective immunity versus autoimmunity, the relevance of FUT8 SNPs with immune regulatory activity will be considered. Several core fucosylated immune molecules have been identified thus far, and their significance in immune responses is becoming clear. However, the following points seem to be limitations of the research on core fucosylation. First, because FUT8 could regulate multiple glycoproteins, the widespread changes in core fucosylated proteins in FUT8^{-/-} cells make it difficult to discern the role of core fucosylation in individual core fucosylated proteins. Second, very few core fucosylated glycoproteins crystallize for the entire N-glycan due to glycan microheterogeneity and flexibility. Third, due to the potential of flexibility in glycosidic linkages, the conformational requirements for efficient binding of core fucosylated N-glycans to proteins are difficult to analyze. The future ability to determine the sugar chains of immune receptors combined with the ability to selectively modulate cellular glycomes is expected to offer exciting chances to regulate adaptive immune responses. With a better understanding of how FUT8 regulates the adaptive immune system, its use in therapy for autoimmunity proves to be a helpful intervention from glycoimmunological aspects.

AUTHOR CONTRIBUTIONS

YS and XL were mainly responsible to write the review and complete the Figures. TW collected and checked the References. WL designed the research and modified the manuscript. All authors reviewed and approved the final version of the manuscript.

FUNDING

WL is supported by grants from the National Nature Science Foundation of China (32171279, 31870797, 31570797, 31270864, 30972675) and Liaoning Provincial Program for Top Discipline of Basic Medical Sciences.

REFERENCES

- Azagra A, Marina-Zárate E, Ramiro AR, Javierre BM, Parra M. From Loops to Looks: Transcription Factors and Chromatin Organization Shaping Terminal B Cell Differentiation. *Trends Immunol* (2020) 41:46–60. doi: 10.1016/j.it.2019.11.006
- Hardy RR, Hayakawa K. B Cell Development Pathways. *Annu Rev Immunol* (2001) 19:595–621. doi: 10.1146/annurev.immunol.19.1.595
- Batista FD, Harwood NE. The Who, How and Where of Antigen Presentation to B Cells. *Nat Rev Immunol* (2009) 9:15–27. doi: 10.1038/nri2454
- Baum LG, Cobb BA. The Direct and Indirect Effects of Glycans on Immune Function. *Glycobiology* (2017) 27:619–24. doi: 10.1093/glycob/cwx036
- Wolfert MA, Boons GJ. Adaptive Immune Activation: Glycosylation Does Matter. *Nat Chem Biol* (2013) 9:776–84. doi: 10.1038/nchembio.1403
- Ohtsubo K, Marth JD. Glycosylation in Cellular Mechanisms of Health and Disease. *Cell* (2006) 126:855–67. doi: 10.1016/j.cell.2006.08.019
- Varki A. Biological Roles of Glycans. *Glycobiology* (2017) 27:3–49. doi: 10.1093/glycob/cww086
- Li W, Ishihara K, Yokota T, Nakagawa T, Koyama N, Jin J, et al. Reduced Alpha4beta1 Integrin/VCAM-1 Interactions Lead to Impaired Pre-B Cell Repopulation in Alpha 1,6-Fucosyltransferase Deficient Mice. *Glycobiology* (2008) 18:114–24. doi: 10.1093/glycob/cwm107
- Li W, Liu Q, Pang Y, Jin J, Wang H, Cao H, et al. Core Fucosylation of μ Heavy Chains Regulates Assembly and Intracellular Signaling of Precursor B Cell Receptors. *J Biol Chem* (2012) 287:2500–8. doi: 10.1074/jbc.M111.303123

10. Li W, Yu R, Ma B, Yang Y, Jiao X, Liu Y, et al. Core Fucosylation of IgG B Cell Receptor Is Required for Antigen Recognition and Antibody Production. *J Immunol (Baltimore Md)* (2015) 194:2596–606. doi: 10.4049/jimmunol.1402678
11. Liang W, Mao S, Sun S, Li M, Li Z, Yu R, et al. Core Fucosylation of the T Cell Receptor Is Required for T Cell Activation. *Front Immunol* (2018) 9:78. doi: 10.3389/fimmu.2018.00078
12. Zahid D, Zhang N, Fang H, Gu J, Li M, Li W. Loss of Core Fucosylation Suppressed the Humoral Immune Response in Salmonella Typhimurium Infected Mice. *J Microbiol Immunol Infect = Wei mian yu gan ran za zhi* (2020) 606–15. doi: 10.1016/j.jmii.2020.02.006
13. Hao S, Fan Q, Bai Y, Fang H, Zhou J, Fukuda T, et al. Core Fucosylation of Intestinal Epithelial Cells Protects Against Salmonella Typhi Infection via Up-Regulating the Biological Antagonism of Intestinal Microbiota. *Front Microbiol* (2020) 11:1097. doi: 10.3389/fmicb.2020.01097
14. Zhang N, Li M, Xu X, Zhang Y, Liu Y, Zhao M, et al. Loss of Core Fucosylation Enhances the Anticancer Activity of Cytotoxic T Lymphocytes by Increasing PD-1 Degradation. *Eur J Immunol* (2020) 1820–33. doi: 10.1002/eji.202048543
15. Sturla L, Fruscione F, Noda K, Miyoshi E, Taniguchi N, Contini P, et al. Core Fucosylation of N-Linked Glycans in Leukocyte Adhesion Deficiency/ Congenital Disorder of Glycosylation IIc Fibroblasts. *Glycobiology* (2005) 15:924–34. doi: 10.1093/glycob/cwi081
16. Cai D, Xun C, Tang F, Tian X, Yang L, Ding K, et al. Glycoconjugate Probes Containing a Core-Fucosylated N-Glycan Trisaccharide for Fucose Lectin Identification and Purification. *Carbohydr Res* (2017) 449:143–52. doi: 10.1016/j.carres.2017.07.011
17. Ihara H, Ikeda Y, Toma S, Wang X, Suzuki T, Gu J, et al. Crystal Structure of Mammalian Alpha1,6-Fucosyltransferase, FUT8. *Glycobiology* (2007) 17:455–66. doi: 10.1093/glycob/cwl079
18. Thaysen-Andersen M, Packer NH. Site-Specific Glycoproteomics Confirms That Protein Structure Dictates Formation of N-Glycan Type, Core Fucosylation and Branching. *Glycobiology* (2012) 22:1440–52. doi: 10.1093/glycob/cws110
19. De Boeck H, Looftens FG, Lis H, Sharon N. Binding of Simple Carbohydrates and Some N-Acetylglucosamine-Containing Oligosaccharides to Erythrina Cristagalli Agglutinin as Followed With a Fluorescent Indicator Ligand. *Arch Biochem Biophys* (1984) 234:297–304. doi: 10.1016/0003-9861(84)90352-7
20. Wormald MR, Dwek RA. Glycoproteins: Glycan Presentation and Protein-Fold Stability. *Struct (London England: 1993)* (1999) 7:R155–60. doi: 10.1016/S0969-2126(99)80095-1
21. Stubbs HJ, Lih JJ, Gustafson TL, Rice KG. Influence of Core Fucosylation on the Flexibility of a Biantennary N-Linked Oligosaccharide. *Biochemistry* (1996) 35:937–47. doi: 10.1021/bi9513719
22. Bourne Y, Mazurier J, Legrand D, Rougé P, Montreuil J, Spik G, et al. Structures of a Legume Lectin Complexed With the Human Lactotransferrin N2 Fragment, and With an Isolated Biantennary Glycopeptide: Role of the Fucose Moiety. *Struct (London Engl)* (1994) 2:209–19. doi: 10.1016/S0969-2126(00)00022-8
23. Lv X, Song J, Xue K, Li Z, Li M, Zahid D, et al. Core Fucosylation of Copper Transporter 1 Plays a Crucial Role in Cisplatin-Resistance of Epithelial Ovarian Cancer by Regulating Drug Uptake. *Mol Carcinog* (2019) 58:794–807. doi: 10.1002/mc.22971
24. Wormald MR, Wooten EW, Bazzo R, Edge CJ, Feinstein A, Rademacher TW, et al. The Conformational Effects of N-Glycosylation on the Tailpiece From Serum IgM. *Eur J Biochem* (1991) 198:131–9. doi: 10.1111/j.1432-1033.1991.tb15995.x
25. Schneider M, Al-Shareffi E, Haltiwanger RS. Biological Functions of Fucose in Mammals. *Glycobiology* (2017) 27:601–18. doi: 10.1093/glycob/cwx034
26. Li W, Nakagawa T, Koyama N, Wang X, Jin J, Mizuno-Horikawa Y, et al. Down-Regulation of Trypsinogen Expression Is Associated With Growth Retardation in Alpha1,6-Fucosyltransferase-Deficient Mice: Attenuation of Proteinase-Activated Receptor 2 Activity. *Glycobiology* (2006) 16:1007–19. doi: 10.1093/glycob/cwl023
27. Osumi D, Takahashi M, Miyoshi E, Yokoe S, Lee SH, Noda K, et al. Core Fucosylation of E-Cadherin Enhances Cell-Cell Adhesion in Human Colon Carcinoma WiDr Cells. *Cancer Sci* (2009) 100:888–95. doi: 10.1111/j.1349-7006.2009.01125.x
28. Ito Y, Miyauchi A, Yoshida H, Uruno T, Nakano K, Takamura Y, et al. Expression of Alpha1,6-Fucosyltransferase (FUT8) in Papillary Carcinoma of the Thyroid: Its Linkage to Biological Aggressiveness and Anaplastic Transformation. *Cancer Lett* (2003) 200:167–72. doi: 10.1016/S0304-3835(03)00383-5
29. Wang X, Inoue S, Gu J, Miyoshi E, Noda K, Li W, et al. Dysregulation of TGF-Beta1 Receptor Activation Leads to Abnormal Lung Development and Emphysema-Like Phenotype in Core Fucose-Deficient Mice. *Proc Natl Acad Sci USA* (2005) 102:15791–6. doi: 10.1073/pnas.0507375102
30. Wang X, Gu J, Ihara H, Miyoshi E, Honke K, Taniguchi N. Core Fucosylation Regulates Epidermal Growth Factor Receptor-Mediated Intracellular Signaling. *J Biol Chem* (2006) 281:2572–7. doi: 10.1074/jbc.M510893200
31. Gao C, Maeno T, Ota F, Ueno M, Korekane H, Takamatsu S, et al. Sensitivity of Heterozygous α 1,6-Fucosyltransferase Knock-Out Mice to Cigarette Smoke-Induced Emphysema: Implication of Aberrant Transforming Growth Factor- β Signaling and Matrix Metalloproteinase Gene Expression. *J Biol Chem* (2012) 287:16699–708. doi: 10.1074/jbc.M111.315333
32. Fukuda T, Hashimoto H, Okayasu N, Kameyama A, Onogi H, Nakagawasai O, et al. Alpha1,6-Fucosyltransferase-Deficient Mice Exhibit Multiple Behavioral Abnormalities Associated With a Schizophrenia-Like Phenotype: Importance of the Balance Between the Dopamine and Serotonin Systems. *J Biol Chem* (2011) 286:18434–43. doi: 10.1074/jbc.M110.172536
33. Bankovich AJ, Raunser S, Juo ZS, Walz T, Davis MM, Garcia KC. Structural Insight Into Pre-B Cell Receptor Function. *Science (New York NY)* (2007) 316:291–4. doi: 10.1126/science.1139412
34. Wasserman R, Li YS, Shinton SA, Carmack CE, Manser T, Wiest DL, et al. A Novel Mechanism for B Cell Repertoire Maturation Based on Response by B Cell Precursors to Pre-B Receptor Assembly. *J Exp Med* (1998) 187:259–64. doi: 10.1084/jem.187.2.259
35. Hess J, Werner A, Wirth T, Melchers F, Jäck HM, Winkler TH. Induction of Pre-B Cell Proliferation After *De Novo* Synthesis of the Pre-B Cell Receptor. *Proc Natl Acad Sci USA* (2001) 98:1745–50. doi: 10.1073/pnas.98.4.1745
36. Mårtensson IL, Almqvist N, Grimsholm O, Bernardi AI. The Pre-B Cell Receptor Checkpoint. *FEBS Lett* (2010) 584:2572–9. doi: 10.1016/j.febslet.2010.04.057
37. Kawano Y, Yoshikawa S, Minegishi Y, Karasuyama H. Selection of Stereotyped VH81X-[Micro]H Chains via Pre-B Cell Receptor Early in Ontogeny and Their Conservation in Adults by Marginal Zone B Cells. *Int Immunol* (2005) 17:857–67. doi: 10.1093/intimm/dxh265
38. Kawano Y, Yoshikawa S, Minegishi Y, Karasuyama H. Pre-B Cell Receptor Assesses the Quality of IgH Chains and Tunes the Pre-B Cell Repertoire by Delivering Differential Signals. *J Immunol (Baltimore Md)* (2006) 177:2242–9. doi: 10.4049/jimmunol.177.4.2242
39. Zhang M, Srivastava G, Lu L. The Pre-B Cell Receptor and Its Function During B Cell Development. *Cell Mol Immunol* (2004) 1:89–94.
40. Conley ME, Rohrer J, Rapalus L, Boylin EC, Minegishi Y. Defects in Early B-Cell Development: Comparing the Consequences of Abnormalities in Pre-BCR Signaling in the Human and the Mouse. *Immunol Rev* (2000) 178:75–90. doi: 10.1034/j.1600-065X.2000.17809.x
41. Espeli M, Rossi B, Mancini SJ, Roche P, Gauthier L, Schiff C. Initiation of Pre-B Cell Receptor Signaling: Common and Distinctive Features in Human and Mouse. *Semin Immunol* (2006) 18:56–66. doi: 10.1016/j.smim.2005.11.002
42. Corcos D, Dunda O, Butor C, Cesbron JY, Lorès P, Buchini D, et al. Pre-B-Cell Development in the Absence of Lambda 5 in Transgenic Mice Expressing a Heavy-Chain Disease Protein. *Curr Biol: CB* (1995) 5:1140–8. doi: 10.1016/S0960-9822(95)00230-2
43. Haimovich J, Ben Moshe N, Raviv Y, Hollander N. All Oligosaccharide Moieties of the μ Chains in the Pre-BCR Are of the High-Mannose Type. *Mol Immunol* (2010) 48:351–5. doi: 10.1016/j.molimm.2010.07.005
44. Ubelhart R, Bach MP, Eschbach C, Wossning T, Reth M, Jumaa H. N-Linked Glycosylation Selectively Regulates Autonomous Precursor BCR Function. *Nat Immunol* (2010) 11:759–65. doi: 10.1038/ni.1903

45. ten Boekel E, Melchers F, Rolink AG. Changes in the V(H) Gene Repertoire of Developing Precursor B Lymphocytes in Mouse Bone Marrow Mediated by the Pre-B Cell Receptor. *Immunity* (1997) 7:357–68. doi: 10.1016/S1074-7613(00)80357-X
46. Marshall AJ, Wu GE, Paige GJ. Frequency of VH81x Usage During B Cell Development: Initial Decline in Usage Is Independent of Ig Heavy Chain Cell Surface Expression. *J Immunol (Baltimore Md)* (1996) 150:156:2077–84.
47. Rabinovich E, Bar-Nun S, Amitay R, Shachar I, Gur B, Taya M, et al. Different Assembly Species of IgM Are Directed to Distinct Degradation Sites Along the Secretory Pathway. *J Biol Chem* (1993) 268:24145–8. doi: 10.1016/S0021-9258(20)80503-1
48. Gauthier L, Rossi B, Roux F, Termine E, Schiff C. Galectin-1 Is a Stromal Cell Ligand of the Pre-B Cell Receptor (BCR) Implicated in Synapse Formation Between Pre-B and Stromal Cells and in Pre-BCR Triggering. *Proc Natl Acad Sci USA* (2002) 99:13014–9. doi: 10.1073/pnas.202323999
49. Lopez Granados E, Porpiglia AS, Hogan MB, Matamoros N, Krasovec S, Pignata C, et al. Clinical and Molecular Analysis of Patients With Defects in Micro Heavy Chain Gene. *J Clin Invest* (2002) 110:1029–35. doi: 10.1172/JCI0215658
50. Hynes RO. Integrins: Versatility, Modulation, and Signaling in Cell Adhesion. *Cell* (1992) 69:11–25. doi: 10.1016/0092-8674(92)90115-S
51. Rossi B, Espeli M, Schiff C, Gauthier L. Clustering of Pre-B Cell Integrins Induces Galectin-1-Dependent Pre-B Cell Receptor Relocalization and Activation. *J Immunol (Baltimore Md)* (2006) 177:796–803. doi: 10.4049/jimmunol.177.2.796
52. Gauld SB, Dal Porto JM, Cambier JC. B Cell Antigen Receptor Signaling: Roles in Cell Development and Disease. *Science (New York NY)* (2002) 296:1641–2. doi: 10.1126/science.1071546
53. Raff MC, Sternberg M, Taylor RB. Immunoglobulin Determinants on the Surface of Mouse Lymphoid Cells. *Nature* (1970) 225:553–4. doi: 10.1038/225553a0
54. Gomes de Castro MA, Wildhagen H, Sograte-Idrissi S, Hitzing C, Binder M, Trepel M, et al. Differential Organization of Tonic and Chronic B Cell Antigen Receptors in the Plasma Membrane. *Nat Commun* (2019) 10:820. doi: 10.1038/s41467-019-08677-1
55. Hagman J. Conveying the Message: Identification of Ig-Alpha and Ig-Beta as Components of the B Cell Receptor Complex. *J Immunol (Baltimore Md: 1950)* (2009) 183:1503–4. doi: 10.4049/jimmunol.0990055
56. Sezgin E, Levental I, Mayor S, Eggeling C. The Mystery of Membrane Organization: Composition, Regulation and Roles of Lipid Rafts. *Nat Rev Mol Cell Biol* (2017) 18:361–74. doi: 10.1038/nrm.2017.16
57. Cheng PC, Dykstra ML, Mitchell RN, Pierce SK. A Role for Lipid Rafts in B Cell Antigen Receptor Signaling and Antigen Targeting. *J Exp Med* (1999) 190:1549–60. doi: 10.1084/jem.190.11.1549
58. Pierce SK. Lipid Rafts and B-Cell Activation. *Nat Rev Immunol* (2002) 2:96–105. doi: 10.1038/nri726
59. Gupta N, DeFranco AL. Visualizing Lipid Raft Dynamics and Early Signaling Events During Antigen Receptor-Mediated B-Lymphocyte Activation. *Mol Biol Cell* (2003) 14:432–44. doi: 10.1091/mbc.02-05-0078
60. Sohn HW, Tolar P, Jin T, Pierce SK. Fluorescence Resonance Energy Transfer in Living Cells Reveals Dynamic Membrane Changes in the Initiation of B Cell Signaling. *Proc Natl Acad Sci USA* (2006) 103:8143–8. doi: 10.1073/pnas.0509858103
61. Fujii H, Shinzaki S, Iijima H, Wakamatsu K, Iwamoto C, Sobajima T, et al. Core Fucosylation on T Cells, Required for Activation of T-Cell Receptor Signaling and Induction of Colitis in Mice, Is Increased in Patients With Inflammatory Bowel Disease. *Gastroenterology* (2016) 150:1620–32. doi: 10.1053/j.gastro.2016.03.002
62. Reinherz EL, Tan K, Tang L, Kern P, Liu J, Xiong Y, et al. The Crystal Structure of a T Cell Receptor in Complex With Peptide and MHC Class II. *Science (New York NY)* (1999) 286:1913–21. doi: 10.1126/science.286.5446.1913
63. Demetriou M, Granovsky M, Quaggin S, Dennis JW. Negative Regulation of T-Cell Activation and Autoimmunity by Mgat5 N-Glycosylation. *Nature* (2001) 409:733–9. doi: 10.1038/35055582
64. Moore GT, Brown SJ, Winterhalter AC, Lust M, Salvaris EJ, Selan C, et al. Glycosylation Changes in Hfuit1 Transgenic Mice Increase TCR Signaling and Apoptosis Resulting in Thymocyte Maturation Arrest. *Mol Immunol* (2008) 45:2401–10. doi: 10.1016/j.molimm.2007.11.006
65. Hennot T, Chui D, Paulson JC, Marth JD. Immune Regulation by the ST6Gal Sialyltransferase. *Proc Natl Acad Sci USA* (1998) 95:4504–9. doi: 10.1073/pnas.95.8.4504
66. Irons EE, Lau JTY. Systemic ST6Gal-1 Is a Pro-Survival Factor for Murine Transitional B Cells. *Front Immunol* (2018) 9:2150. doi: 10.3389/fimmu.2018.02150
67. Kuball J, Hauptrock B, Malina V, Antunes E, Voss RH, Wolff M, et al. Increasing Functional Avidity of TCR-Redirected T Cells by Removing Defined N-Glycosylation Sites in the TCR Constant Domain. *J Exp Med* (2009) 206:463–75. doi: 10.1084/jem.20082487
68. Johnson JL, Jones MB, Ryan SO, Cobb BA. The Regulatory Power of Glycans and Their Binding Partners in Immunity. *Trends Immunol* (2013) 34:290–8. doi: 10.1016/j.it.2013.01.006
69. Scott CA, Peterson PA, Teyton L, Wilson IA. Crystal Structures of Two I-Ad-Peptide Complexes Reveal That High Affinity can be Achieved Without Large Anchor Residues. *Immunity* (1998) 8:319–29. doi: 10.1016/S1074-7613(00)80537-3
70. Alam SM, Davies GM, Lin CM, Zal T, Nasholds W, Jameson SC, et al. Qualitative and Quantitative Differences in T Cell Receptor Binding of Agonist and Antagonist Ligands. *Immunity* (1999) 10:227–37. doi: 10.1016/S1074-7613(00)80023-0
71. Schamel WW, Arechaga I, Risueño RM, van Santen HM, Cabezas P, Risco C, et al. Coexistence of Multivalent and Monovalent TCRs Explains High Sensitivity and Wide Range of Response. *J Exp Med* (2005) 202:493–503. doi: 10.1084/jem.20042155
72. Perillo NL, Pace KE, Seilhamer JJ, Baum LG. Apoptosis of T Cells Mediated by Galectin-1. *Nature* (1995) 378:736–9. doi: 10.1038/378736a0
73. Poe JC, Tedder TF. CD22 and Siglec-G in B Cell Function and Tolerance. *Trends Immunol* (2012) 33:413–20. doi: 10.1016/j.it.2012.04.010
74. Manabe Y, Marchetti R, Takakura Y, Nagasaki M, Nihei W, Takebe T, et al. The Core Fucose on an IgG Antibody Is an Endogenous Ligand of Dectin-1. *Angewandte Chemie (International Ed English)* (2019) 58:18697–702. doi: 10.1002/anie.201911875
75. Chen Z, Wang JH. Signaling Control of Antibody Isotype Switching. *Adv Immunol* (2019) 141:105–64. doi: 10.1016/b.sai.2019.01.001
76. Vučković F, Krištić J, Gudelj I, Teruel M, Keser T, Pezer M, et al. Association of Systemic Lupus Erythematosus With Decreased Immunosuppressive Potential of the IgG Glycome. *Arthritis Rheumatol (Hoboken NJ)* (2015) 67:2978–89. doi: 10.1002/art.39273
77. Ercan A, Cui J, Chatterton DE, Deane KD, Hazen MM, Brintnell W, et al. Aberrant IgG Galactosylation Precedes Disease Onset, Correlates With Disease Activity, and Is Prevalent in Autoantibodies in Rheumatoid Arthritis. *Arthritis Rheum* (2010) 62:2239–48. doi: 10.1002/art.27533
78. Matsumoto A, Shikata K, Takeuchi F, Kojima N, Mizuuchi T. Autoantibody Activity of IgG Rheumatoid Factor Increases With Decreasing Levels of Galactosylation and Sialylation. *J Biochem* (2000) 128:621–8. doi: 10.1093/oxfordjournals.jbchem.a022794
79. Espy C, Morelle W, Kaviani N, Grange P, Goulvestre C, Viallon V, et al. Sialylation Levels of Anti-Proteinase 3 Antibodies Are Associated With the Activity of Granulomatosis With Polyangiitis (Wegener's). *Arthritis Rheum* (2011) 63:2105–15. doi: 10.1002/art.30362
80. Yin Y, Choi SC, Xu Z, Perry DJ, Seay H, Croker BP, et al. Normalization of CD4+ T Cell Metabolism Reverses Lupus. *Sci Trans Med* (2015) 7:274ra18. doi: 10.1126/scitranslmed.aaa0835
81. Sun Y, Li Z, Liang W, Zhang Y, Song W, Song J, et al. A Novel Immunochromatographic Strips Assay for Rapid and Simple Detection of Systemic Lupus Erythematosus. *Sci Rep* (2020) 10:14178. doi: 10.1038/s41598-020-71137-0
82. Rupanagudi KV, Kulkarni OP, Lichtnekert J, Darisipudi MN, Mulay SR, Schott B, et al. Cathepsin S Inhibition Suppresses Systemic Lupus Erythematosus and Lupus Nephritis Because Cathepsin S Is Essential for MHC Class II-Mediated CD4 T Cell and B Cell Priming. *Ann Rheum Dis* (2015) 74:452–63. doi: 10.1136/annrheumdis-2013-203717
83. Mao L, Hou H, Wu S, Zhou Y, Wang J, Yu J, et al. TIGIT Signalling Pathway Negatively Regulates CD4(+) T-Cell Responses in Systemic Lupus Erythematosus. *Immunology* (2017) 151:280–90. doi: 10.1111/imm.12715

84. Ramos-Martínez E, Lascurain R, Tenorio EP, Sánchez-González A, Chávez-Rueda K, Chávez-Sánchez L, et al. Differential Expression of O-Glycans in CD4(+) T Lymphocytes From Patients With Systemic Lupus Erythematosus. *Tohoku J Exp Med* (2016) 240:79–89. doi: 10.1620/tjem.240.79
85. Donadel G, Calabro A, Sigounas G, Hascall VC, Notkins AL, Harindranath N. Human Polyreactive and Monoreactive Antibodies: Effect of Glycosylation on Antigen Binding. *Glycobiology* (1994) 4:491–6. doi: 10.1093/glycob/4.4.491
86. Krapp S, Mimura Y, Jefferis R, Huber R, Sonderrmann P. Structural Analysis of Human IgG-Fc Glycoforms Reveals a Correlation Between Glycosylation and Structural Integrity. *J Mol Biol* (2003) 325:979–89. doi: 10.1016/S0022-2836(02)01250-0
87. Burton DR, Dwek RA. Immunology. Sugar Determines Antibody Activity. *Science (New York NY)* (2006) 313:627–8. doi: 10.1126/science.1131712
88. Radaev S, Motyka S, Fridman WH, Sautes-Fridman C, Sun PD. The Structure of a Human Type III Fcγ Receptor in Complex With Fc. *J Biol Chem* (2001) 276:16469–77. doi: 10.1074/jbc.M100350200
89. Shinkawa T, Nakamura K, Yamane N, Shoji-Hosaka E, Kanda Y, Sakurada M, et al. The Absence of Fucose But Not the Presence of Galactose or Bisecting N-Acetylglucosamine of Human IgG1 Complex-Type Oligosaccharides Shows the Critical Role of Enhancing Antibody-Dependent Cellular Cytotoxicity. *J Biol Chem* (2003) 278:3466–73. doi: 10.1074/jbc.M210665200
90. Ferrara C, Grau S, Jäger C, Sonderrmann P, Brünker P, Waldhauer I, et al. Unique Carbohydrate-Carbohydrate Interactions Are Required for High Affinity Binding Between FcγRIII and Antibodies Lacking Core Fucose. *Proc Natl Acad Sci USA* (2011) 108:12669–74. doi: 10.1073/pnas.1108455108
91. Niwa R, Natsume A, Uehara A, Wakitani M, Iida S, Uchida K, et al. IgG Subclass-Independent Improvement of Antibody-Dependent Cellular Cytotoxicity by Fucose Removal From Asn297-Linked Oligosaccharides. *J Immunol Methods* (2005) 306:151–60. doi: 10.1016/j.jim.2005.08.009
92. Lu J, Chu J, Zou Z, Hamacher NB, Rixon MW, Sun PD. Structure of FcγRI in Complex With Fc Reveals the Importance of Glycan Recognition for High-Affinity IgG Binding. *Proc Natl Acad Sci USA* (2015) 112:833–8. doi: 10.1073/pnas.1418812112
93. Bournazos S, Vo HTM, Duong V, Auerswald H, Ly S, Sakuntabhai A, et al. Antibody Fucosylation Predicts Disease Severity in Secondary Dengue Infection. *Science (New York NY)* (2021) 372:1102–5. doi: 10.1126/science.abc7303
94. Larsen MD, de Graaf EL, Sonneveld ME, Plomp HR, Nouta J, Hoepel W, et al. Afucosylated IgG Characterizes Enveloped Viral Responses and Correlates With COVID-19 Severity. *Science (New York NY)* (2021) 371: eabc8378. doi: 10.1126/science.abc8378
95. Larsen MD, Lopez-Perez M, Dickson EK, Ampomah P, Tuikue Ndam N, Nouta J, et al. Afucosylated Plasmodium Falciparum-Specific IgG Is Induced by Infection But Not by Subunit Vaccination. *Nat Commun* (2021) 12:5838. doi: 10.1038/s41467-021-26118-w
96. Le NP, Bowden TA, Struwe WB, Crispin M. Immune Recruitment or Suppression by Glycan Engineering of Endogenous and Therapeutic Antibodies. *Biochim Biophys Acta* (2016) 1860:1655–68. doi: 10.1016/j.bbagen.2016.04.016
97. Kościelak J, Pacuska T, Miller-Podraza H, Zdziechowska H. Activities of Fucosyltransferases in Sera of Leukaemic Patients: Platelet Origin of Serum Alpha-6-L-Fucosyltransferase. *Biochem Soc Trans* (1987) 15:603–6. doi: 10.1042/bst0150603
98. Antoniewicz J, Bykowska K, Zdebska E, Kościelak J. Human Platelets Release Alpha-6-L-Fucosyltransferase Upon Activation. *FEBS Lett* (1989) 244:388–90. doi: 10.1016/0014-5793(89)80569-1
99. Lu G, Holland LA. Profiling the N-Glycan Composition of IgG With Lectins and Capillary Nanogel Electrophoresis. *Anal Chem* (2019) 91:1375–83. doi: 10.1021/acs.analchem.8b03725
100. Fan Q, Wu Y, Li M, An F, Yao L, Wang M, et al. Lactobacillus spp. Create a Protective Micro-Ecological Environment Through Regulating the Core Fucosylation of Vaginal Epithelial Cells Against Cervical Cancer. *Cell Death Dis* (2021) 12:1094. doi: 10.1038/s41419-021-04388-y
101. Chung JB, Silverman M, Monroe JG. Transitional B Cells: Step by Step Towards Immune Competence. *Trends Immunol* (2003) 24:343–9. doi: 10.1016/S1471-4906(03)00119-4
102. Yamada M, Ishii T, Ikeda S, Naka-Mieno M, Tanaka N, Arai T, et al. Association of Fucosyltransferase 8 (FUT8) Polymorphism Thr267Lys With Pulmonary Emphysema. *J Hum Genet* (2011) 56:857–60. doi: 10.1038/jhg.2011.118

Conflict of Interest: The authors declare that the research was conducted in the absence of any commercial or financial relationships that could be construed as a potential conflict of interest.

Publisher's Note: All claims expressed in this article are solely those of the authors and do not necessarily represent those of their affiliated organizations, or those of the publisher, the editors and the reviewers. Any product that may be evaluated in this article, or claim that may be made by its manufacturer, is not guaranteed or endorsed by the publisher.

Copyright © 2022 Sun, Li, Wang and Li. This is an open-access article distributed under the terms of the Creative Commons Attribution License (CC BY). The use, distribution or reproduction in other forums is permitted, provided the original author(s) and the copyright owner(s) are credited and that the original publication in this journal is cited, in accordance with accepted academic practice. No use, distribution or reproduction is permitted which does not comply with these terms.



Sialylation as an Important Regulator of Antibody Function

Ravi Vattepu, Sunny Lyn Sneed and Robert M. Anthony*

Center for Immunology and Inflammatory Diseases, Division of Rheumatology, Allergy and Immunology, Department of Medicine, Massachusetts General Hospital, Harvard Medical School, Boston, MA, United States

OPEN ACCESS

Edited by:

David Falck,
Leiden University Medical Center,
Netherlands

Reviewed by:

Richard John Pleass,
Liverpool School of Tropical Medicine,
United Kingdom
Steven William De Taeye,
Academic Medical Center,
Netherlands

*Correspondence:

Robert M. Anthony
robert.anthony@mgh.harvard.edu

Specialty section:

This article was submitted to
B Cell Biology,
a section of the journal
Frontiers in Immunology

Received: 19 November 2021

Accepted: 17 March 2022

Published: 07 April 2022

Citation:

Vattepu R, Sneed SL and Anthony RM
(2022) Sialylation as an Important
Regulator of Antibody Function.
Front. Immunol. 13:818736.
doi: 10.3389/fimmu.2022.818736

Antibodies play a critical role in linking the adaptive immune response to the innate immune system. In humans, antibodies are categorized into five classes, IgG, IgM, IgA, IgE, and IgD, based on constant region sequence, structure, and tropism. In serum, IgG is the most abundant antibody, comprising 75% of antibodies in circulation, followed by IgA at 15%, IgM at 10%, and IgD and IgE are the least abundant. All human antibody classes are post-translationally modified by sugars. The resulting glycans take on many divergent structures and can be attached in an N-linked or O-linked manner, and are distinct by antibody class, and by position on each antibody. Many of these glycan structures on antibodies are capped by sialic acid. It is well established that the composition of the N-linked glycans on IgG exert a profound influence on its effector functions. However, recent studies have described the influence of glycans, particularly sialic acid for other antibody classes. Here, we discuss the role of glycosylation, with a focus on terminal sialylation, in the biology and function across all antibody classes. Sialylation has been shown to influence not only IgG, but IgE, IgM, and IgA biology, making it an important and unappreciated regulator of antibody function.

Keywords: antibody, glycosylation, sialylation, *in vitro* glycoengineering, *in vivo* glyco engineering, sialic acid, immunoglobulins

INTRODUCTION

Antibodies are critical mediators of host defense and homeostasis. Further, the therapeutic potential of antibodies has been fundamental in advancing basic immunology and biotechnology. Antibodies have two unique functions that are responsible for their biological function. They can recognize specific structures with high affinity and specificity, and simultaneously engage with cells of the innate immune system. Antibodies can be passively transferred across individuals or species, which gives them therapeutic utility. Indeed, polyclonal IgG from tens of thousands of healthy individuals, intravenous immunoglobulin (IVIG), is administered as IgG replacement therapy to immunocompromised individuals, and as an anti-inflammatory agent to some patients suffering from inflammatory and autoimmune diseases (1–3). Hybridoma technologies enable generation of monoclonal antibody preparations. The molecular biology revolution following the invention of PCR enabled cloning and recombinant production of monoclonal antibodies. Currently, there are 100 monoclonal antibodies (mAbs) approved by the FDA and monoclonal antibodies are the fastest growing class of therapeutics (4).

The monomeric structures of antibodies are composed of two identical heavy chains and two identical light chains connected by disulfide bonds (5, 6). In humans, antibodies are categorized into

five classes: IgG, IgM, IgA, IgE, and IgD, based on constant region structure, properties, and oligomerization (**Figure 1A**) (7). In serum, IgG is the most abundant antibody comprising 75% of all antibodies in circulation, followed by IgA at 15%, IgM at 10%, and IgD and IgE are the least abundant (6, 8). These antibodies are structurally different and elicit different effector functions through interactions between their fragment crystallizable (Fc) portion and different Fc receptors (6).

Therapeutic antibodies currently used in the clinic belong only to the IgG class because of their functional characteristics such as long half-life, strong antigen binding, and effector functions such as antibody-dependent cellular cytotoxicity (ADCC) and complement-dependent cytotoxicity (CDC). There is interest in developing therapeutic IgM, IgE, and IgA antibodies to explore novel targets and harness the effector functions of different immune cells. In contrast to IgG antibodies, IgM antibodies do not bind to Fc gamma receptors (FcγRs), but do bind the Fc mu receptor (FcμR) and can trigger potent CDC activity by binding to C1q (9). Currently, there are some IgM antibodies in clinical development (9). Further, IgE-based therapeutic antibodies are being evaluated in different studies (10). Advantages of using IgE include higher affinity interactions with the Fc epsilon receptor I (FcεRI), longer tissue residence time, and ability to infiltrate the tumor microenvironment (10). Similarly, the development of IgA therapeutics poses advantages such as the ability to recruit neutrophils to kill tumors cells, targeting IgA interactions with the Fc alpha receptor FcαRI, and mucosal applications (11). However, there are numerous challenges in the expression, purification, and characterization of IgE, IgM, and IgA, including heterogeneous products and low yields following

production, due in part to complex structures and multiple glycosylation sites (9, 11–13).

Studies over the last several years have revealed that glycosylation, both N-linked and O-linked, can play profound roles in modifying the effector functions for each antibody class. This ranges from maintaining the structure, tuning effector functions, engaging co-receptors and co-factors, improving their stability, and modifying antigenicity (14, 15). In this review, we will focus on the impact of glycosylation across the antibody classes, with a particular focus on the impact of sialic acid.

ANTIBODY N-LINKED AND O-LINKED GLYCOSYLATION

Glycosylation of antibodies is initiated in the endoplasmic reticulum (ER) of antibody-producing cells and further trimming and remodeling steps are processed by glycosidases and glycosyltransferases in the Golgi apparatus (16). N-linked glycosylation occurs on the amino acid asparagine within the consensus sequence of Asn-X-Ser/Thr, where X is any amino acid except proline. The glycosylation process starts with the transfer of the preassembled, lipid-linked glycan precursor, triglycosylated high-mannose-type tetradecasaccharide, to the asparagine residue by oligosaccharyl transferase in the ER (17). The glycan precursor undergoes further processing by glycosidases, which remove the glucose residues, one mannose residue, and three N-acetylglucosamine (GlcNAc) residues. Once the antibody is translocated into the cis-Golgi, the glycan undergoes further trimming by glycosidases and further

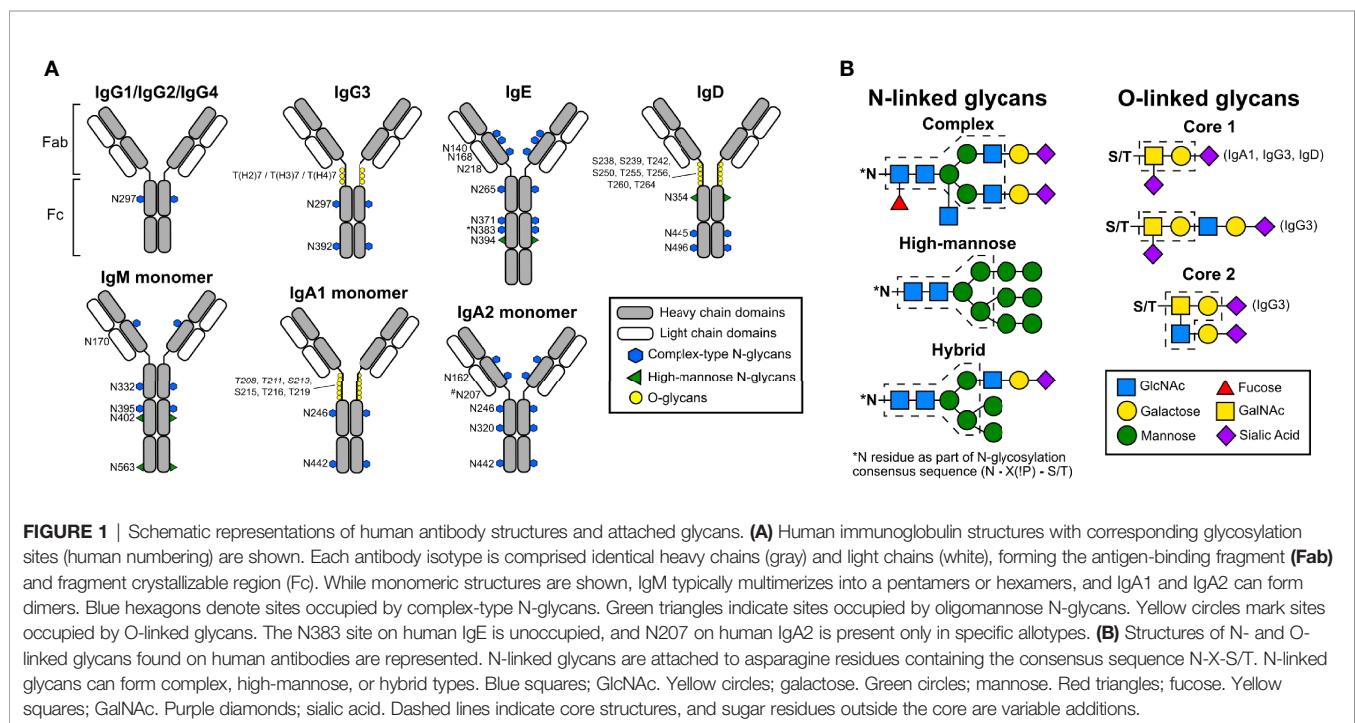


FIGURE 1 | Schematic representations of human antibody structures and attached glycans. **(A)** Human immunoglobulin structures with corresponding glycosylation sites (human numbering) are shown. Each antibody isotype is comprised identical heavy chains (gray) and light chains (white), forming the antigen-binding fragment (Fab) and fragment crystallizable region (Fc). While monomeric structures are shown, IgM typically multimerizes into a pentamers or hexamers, and IgA1 and IgA2 can form dimers. Blue hexagons denote sites occupied by complex-type N-glycans. Green triangles indicate sites occupied by oligomannose N-glycans. Yellow circles mark sites occupied by O-linked glycans. The N383 site on human IgE is unoccupied, and N207 on human IgA2 is present only in specific allotypes. **(B)** Structures of N- and O-linked glycans found on human antibodies are represented. N-linked glycans are attached to asparagine residues containing the consensus sequence N-X-S/T. N-linked glycans can form complex, high-mannose, or hybrid types. Blue squares; GlcNAc. Yellow circles; galactose. Green circles; mannose. Red triangles; fucose. Yellow squares; GalNAc. Purple diamonds; sialic acid. Dashed lines indicate core structures, and sugar residues outside the core are variable additions.

remodeling is performed by the glycosyltransferases in the median Golgi.

Based on their composition, glycans are classified into three types: oligomannose, hybrid, and complex (**Figure 1B**) (16–18). Oligomannose glycans contain 5 to 9 branching mannose residues which are not further cleaved during processing. Complex glycans possess a core structure composed of two inner GlcNAc residues, three mannose residues, and two outer GlcNAc residues each β -1,2-linked to the α -3 and the α -6 mannose residues, forming two antennae (19). The innermost GlcNAc can be further modified by addition of an α -1,6 linked fucose, which is catalyzed by α -1,6 fucosyltransferase (FUT8) (16, 20). One galactose residue may be added to each of the β -1,2 GlcNAc by β -1,4 galactosyl transferase-1, and this addition can be further extended by the addition of sialic acid by α -2,6 sialyltransferase (16, 21). Hybrid type glycans are a combination of the high-mannose and complex types, with one antenna possessing only mannose residues and the other arm including one GlcNAc residue with further addition of galactose and then sialic acid. Variations in antibody glycosylation depend on substrate availability, steric hindrance, and expression level of glycosyltransferases (22). This leads to heterogeneity in glycosylation, which the immune system uses to fine-tune immune responses, and certain glycosylation patterns can be used as biomarkers for certain diseases.

O-linked glycosylation is present in the hinge region of IgA1, IgG3, and in the Fc portions of human IgD (23–25). O-linked glycosylation occurs on serine and threonine residues, but the consensus sequence for this modification has not yet been identified, the regulation of O-linked glycosylation is less well understood compared to the N-linked pathways, and it occurs exclusively in the Golgi. In the first step, GalNAc is attached to serine or threonine by UDP-N-acetylgalactosaminyl transferase 2 (GalNAc-T2) in the *cis*-Golgi. Next, the addition of galactose is catalyzed by β 1,3-galactosyltransferase (C1GalT1), an enzyme which also requires the molecular chaperone COSMC for stability and function. O-linked glycans are further extended by the addition of sialic acid to the GalNAc and/or galactose residues by α 2,6-sialyltransferase (ST6GalNAc-I) or α 2,3-sialyltransferase (ST3Gal-1), respectively (26–29) in *medial*- and *trans*-Golgi.

ANTIBODY STRUCTURE, GLYCOSYLATION ACROSS CLASSES AND SUBCLASSES

IgG Antibodies

The monomeric structures of all antibodies, including IgG, contain two functional domains. The antigen-binding region (Fab) is involved in the recognition of antigens and the fragment crystallizable region (Fc) interacts with Fc γ Rs and other effector proteins, including complement component C1q to mediate effector functions. The Fab region is composed of one variable and one constant domain (CH1) of both the heavy and light chains, while the Fc domain is a homodimer consisting of the

heavy chain constant domains (CH2 and CH3). A flexible hinge region connects the Fab and Fc domains.

The four subclasses of IgG antibodies are numbered based on their prevalence in the serum: IgG1, IgG2, IgG3, and IgG4 (30–32). These four IgG subclasses share more than 90% sequence similarity, but each subclass has a distinct functional profile in mediating effector function, complement activation, half-life, and placental transport (33, 34). The Fc domain of each subclass carries a conserved N-linked glycosylation site at asparagine 297 (N297) in the CH2 domain. The glycan occupying this site has a complex biantennary structure. Several studies have shown roles for Fc glycosylation in mediating immune effector functions, including anti-inflammatory responses, ADCC, CDC, and antibody-dependent cell-mediated phagocytosis (ADCP) (34–38). Structural studies showed Fc glycans play a crucial role in maintaining an open conformation of the Fc domain and mediating interaction with Fc γ Rs and C1q (39, 40). Removal of this glycosylation site abrogates effector functions and abolishes binding to Fc γ Rs and C1q (41–43). Intriguingly, IgG Fc glycans are highly heterogeneous with more than 30 distinct glycoforms detected on IgG in healthy individuals (44, 45). The composition of the IgG Fc glycan has been demonstrated to significantly impact effector functions, pharmacokinetics, immunogenicity, stability, and aggregation (46–48).

IgG Sialylation

In a healthy individuals, approximately 10–15% of serum IgG are sialylated, with the majority of those possessing monosialylated glycoforms (49). Indeed, this percentage is reduced during inflammation and autoimmune disease flares (49, 50). IVIG is a therapeutic preparation of monomeric IgG pooled from the plasma of thousands of donors. It is administered as an IgG-replacement to immunocompromised individuals at 400–600mg/kg. Paradoxically, it is used to treat autoimmune and inflammatory diseases such as Myasthenia gravis (MG), immune thrombocytopenia (ITP), multiple sclerosis (MS), systemic lupus erythematosus (SLE), chronic inflammatory demyelinating neuropathy, and Kawasaki disease at a high dose of 1–2g/kg (51–53). Multiple studies support α -2,6 sialylated IgG as the biologically active component of immunomodulatory high dose IVIG (**Figure 2**) (36, 37, 54, 55). A series of mechanistic studies revealed that the immunomodulatory and anti-inflammatory activity of IVIG requires the inhibitory receptor Fc γ RIIB, and that Fc γ RIIB surface expression is increased on macrophages, dendritic cells, and B cells following IVIG infusion (56–58).

Further studies revealed terminal α -2,6 sialic acid on the IgG Fc glycans were required for anti-inflammatory activity, and C type lectins Specific ICAM-3 Grabbing Non-Integrin-Related 1 (SIGN-R1) and Dendritic Cell-Specific ICAM-3 Grabbing Non-Integrin (DC-SIGN) in mice and humans, respectively, were also required (36, 37, 39, 54). Administration of sialylated IgG Fc induces IL-33 production, which in turn triggers the expansion of IL-4-producing basophils and T regulatory cells, culminating in upregulation of Fc γ RIIB expression on effector cells (59, 60). While functional models support a role for DC-SIGN in the anti-

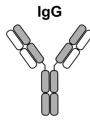
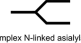
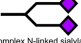
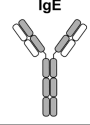
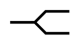
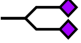
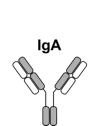
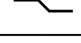


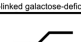
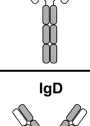
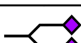
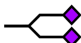
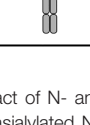
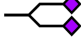

Antibody class	Glycoform	Function	Receptors & Cofactors	Effects
	 (Complex N-linked sialylated)	Pro-inflammatory	FcγRI FcγRIIA FcγRIIB C1q	↑ ADCC ↑ CDC ↑ Opsonization (ADCP) ↑ Antigen presentation
	 (Complex N-linked sialylated)	Anti-inflammatory, Improved vaccine responses	FcγRI FcγRIIA FcγRIIB FcγRIIA DCIR DC-SIGN	↑ IL-33 production ↑ Breadth of antigen-specific IgG responses ↑ FcγRIIB expression ↓ IgG-mediated anaphylaxis
	 (Complex N-linked sialylated)	Non-atopic	FcεRI FcεRII (CD23) Galectins Others?	↓ Effector cell degranulation ↓ Anaphylaxis
	 (Complex N-linked sialylated)	Pro-allergy	FcεRI FcεRII (CD23) Galectins	↑ Effector cell degranulation ↑ Anaphylaxis ↑ Antigen presentation
	 (Complex N-linked sialylated)	Pro-inflammatory	FcαRI Fcα/μR DC-SIGN	↑ NET formation by neutrophils (IgA1) ↑ IL-8 production by macrophages (IgA1) (IgA2 activity unaltered)
	 (Complex N-linked sialylated)	Mucosal immunity, Homeostasis	FcαRI Fcα/μR DC-SIGN FcRL4	↓ NET formation by neutrophils (IgA1) ↓ IL-8 production by macrophages (IgA1) (IgA2 activity unaltered)
	 (O-linked core 1 sialylated)	Native IgA1	FcαRI Fcα/μR DC-SIGN FcRL4	See pro-inflammatory IgA1 functions above
	 (O-linked galactose-deficient)	IgA nephropathy	Transferrin receptor (CD71)	↑ Targeted by anti-galactose-deficient IgA1 IgG antibodies ↑ Immune complex deposits in kidney
	 (Complex N-linked sialylated)	B Cell hyperactivity	Fcα/μR pIgR C1q	↑ T-cell responses & activity ↑ B-cell responses & activity
	 (Complex N-linked sialylated)	Host defense, Homeostasis	Fcα/μR pIgR C1q Siglec 2 (CD22)	↑ Complement fixation ↓ T-cell responses & activity ↓ B-cell responses & activity
	 (Complex N-linked sialylated)	Unknown	IgDR	Unknown
	 (Complex N-linked sialylated)	Unknown	IgDR	Unknown

FIGURE 2 | The impact of N- and O-linked sialylation across antibody classes. Antibody schematics are shown, along with skeleton sialylated (terminating in purple diamonds) or asialylated N-linked glycans. O-glycans and IgA1 are comprised of GalNAc (Yellow squares), galactose (yellow circles), and sialic acid (purple diamonds).

inflammatory activity of sialylated IgG, whether there is a direct interaction between these entities is under debate (61, 62). Insertion of additional N-linked glycosylation sites in the hinge region of IgG1 Fc *via* mutants D221N/N297A/N563A and D221N/N563A increases sialylation 75% and 44% respectively, resulting in increased binding to Siglec-1 (Sialoadhesion), and these mutants also inhibited demyelination by anti-MOG antibodies in an *ex vivo* model when multimerized (63–65). Another study demonstrated that sialylated IVIG mediates anti-inflammatory activity by induction of T regulatory cells through engagement of the dendritic cell immunoreceptor (DCIR) (66).

IgG sialylation is emerging as a therapeutic option to treat autoimmune diseases. A phase 1/2 clinical trial (NCT03866577) reported sialylated IVIG offered protection to patients with ITP (67). Confirmation of previous murine studies came following IVIG infusion in chronic inflammatory demyelinating polyneuropathy (CIDP) patients, which led to increased surface expression of FcγRIIB (68, 69). Further, IL-33 has been detected in the serum following IVIG infusion (70). Finally, sialylated IgG attenuated IgG-mediated anaphylaxis in murine models, but additional experiments are required to determine

whether sialylated IgG is a viable therapeutic for allergic disease (71, 72).

While sialylation conveys anti-inflammatory activity to monomeric IgG, it imparts unique functions to antigen-specific IgG. Indeed, increased antigen-specific IgG was detected following vaccination to *Streptococcus pneumonia* and SARS-CoV-2, and administration of sialylated IgG immune complexes led to an enhanced breadth of IgG responses in a FcεRII (CD23)-dependent manner (73–75). IgG sialylation appears to have little impact on ADCC, or FcγRI and FcγRIIA binding, and a only small enhancement of binding to FcγRIIB (76). Some functional studies have reported that sialylation impairs IgG-mediated ADCC and CDC (77–80). Consistently, asialylated IgG1 displayed enhanced C1q binding and CDC activity compared to sialylated IgG1 (80). In fact, a randomized clinical trial of patients with CIDP receiving high dose IVIG showed increased IgG sialylation and significantly lower levels of complement activation associated with disease remission (80). One contrasting study reported IgG1 Fc sialylation resulted in increased C1q binding (81). Further characterization of the role of IgG Fc sialylation and other glycoforms in FcγR

binding, C1q binding, and functional assays is needed to resolve some of these discrepancies.

IgG Fucosylation, Galactosylation, and Bisecting GlcNAc

It is well-established that non-sialic acid sugars also exert important and profound influence over IgG effector functions, as has been reviewed extensively elsewhere (82–85). Briefly, more than 90% of IgG glycans in human serum contain a fucose residue attached to the innermost GlcNAc core structure (86). Antibody fucosylation is catalyzed by FUT8 in the *medial/trans*-Golgi. Several studies have demonstrated that removal of the core fucose residue increases IgG binding affinity to the human FcγRIIIA receptor expressed on macrophages, dendritic cells, and natural killer cells, resulting in enhanced ADCC (87, 88). This generated tremendous interest in the roles of IgG glycosylation in Fc receptor binding and antibody function. Afucosylated therapeutic antibodies, including anti-HER2 and anti-CD20 IgG1, show 100-fold higher ADCC compared to fucosylated anti-HER2 antibodies (89). Thus, there is a huge potential in immunotherapy for afucosylated antibodies with increased ADCC activity (90–92). Further, the severity of viral diseases caused by Dengue virus and SARS-CoV-2 are associated with the percentage and titers of viral-specific afucosylated IgG (93, 94).

The IgG N-glycan may be agalactosylated (G0F), mono-galactosylated (G1F), or di-galactosylated (G2F), and the effector functions of each glycoform can vary significantly. In the serum of a healthy individual, G0F, G1F, and G2F each account for approximately 35%, 35%, and 15% of IgG glycoforms, respectively (49, 95). A decrease in IgG galactosylation in human serum is associated with chronic inflammatory and autoimmune diseases, such as SLE, MS, rheumatoid arthritis (RA), auto-immune vasculitis, active spondyloarthritis, Crohn's disease, inflammatory bowel disease, and psoriatic arthritis (49, 96–100). IgG galactosylation level also decreases with age and inflammation, but the rate of change is faster during the development of inflammatory conditions compared to typical aging (49). Galactosylated IgG1 immune complexes showed anti-inflammatory activity in mice through interactions with FcγRIIB and the receptor Dectin-1 (101). Galactosylated IgG have also been shown to bind complement effectively (102).

In healthy individuals, only a small fraction (10–15%) of antibodies contain bisecting GlcNAc (biGlcNAc) (49). In the Golgi, β-1,4-N-acetylglucosaminyltransferase III (GnT-III) catalyzes the addition of biGlcNAc to the internal mannose residue. Recombinant IgG Fcs with biGlcNAc possess an increase in ADCC activity and FcγRIIIA binding (103). However, the addition of biGlcNAc inhibits the addition of a core fucose residue due to steric hinderance, and increased ADCC is also attributed to the inhibition of fucose attachment (83).

IgE Antibodies

In comparison with other antibodies, IgE is the least abundant antibody in serum with a concentration of 50–100 ng/ml, and a

half-life of only two to three days; binding to the high affinity receptor FcεRI expressed on mast cells extends tissue half-life to three weeks (104). IgE is involved in triggering allergic reactions to food and pollen, and is involved in atopic diseases such as asthma and atopic dermatitis. The incidence of allergic disease is significantly increasing worldwide, with an estimated of 30–40% of the population having one or more allergic diseases. Thus, there has been significant interest in developing IgE-targeted therapeutic antibodies to treat IgE-mediated allergies. For example, Xolair (Omalizumab) is an FDA approved monoclonal antibody to treat IgE-mediated allergic disease. On the other hand, IgE antibodies also provide a defense against parasite infections and insect venoms (105–107).

IgE is composed of two identical heavy chains and two light chains. Each heavy chain consists of a single variable domain and four constant domains, and the light chain is composed of one variable and one constant domain. IgE is a heavily glycosylated monomeric antibody, with seven N-linked glycosylation sites spread across the four constant domains of the heavy chain. N394 is a conserved glycosylation site with an oligomannose glycan, N383 is unoccupied, and the other five sites (N140, N168, N218, N265, N371) are occupied by complex type biantennary glycans (108–111). The major structural differences of IgE compared to IgG are a shorter hinge region, the presence of an extra constant region, and an increased number of glycosylation sites.

Similar to IgG, the constant region of IgE mediates various effector functions through binding to the high-affinity and low-affinity receptors expressed on innate immune cells. The IgE high affinity receptor FcεRI is expressed on mast cells and basophils shows a significantly high binding affinity, approximately 10^{11} M^{-1} (112). The binding of an allergen to IgE followed by crosslinking the FcεRI receptors triggers cellular degranulation and symptoms of allergic inflammation (113). The low-affinity IgE receptor, FcεRII (CD23), has a binding affinity coefficient of 10^6 M^{-1} . Interactions with FcεRI or FcεRII depend on IgE's Fc conformation. In the open conformation, IgE binds to FcεRI at the CH3 domain, while in the closed conformation IgE binds to FcεRII at both the CH3 and CH4 domains (114, 115). Binding to the high affinity and low affinity receptors is mutually exclusive; conformation changes upon binding to one receptor hinder the binding to another receptor (116).

IgE Sialylation

With the emergence of glycosylation's role in regulating IgG structure and function, there is growing interest in the role of glycosylation across other antibody classes. Initial work indicated that IgE glycosylation is critical for FcεRI binding and effector functions (117–119). Subsequently, other studies showed that aglycosylated IgE produced in *E. coli* binds to FcεRI and can trigger effector functions, suggesting a null effect of glycosylation (120–122). However, studies coupling *in vitro*, cell-based, and mice model experiments have shown an important role for IgE glycosylation. The point mutation N384Q in murine IgE (mIgE), equivalent to human N383Q, abolished binding to FcεRI in ear mast cells and cell-based assays, and similar results were also observed with the enzymatic treatment of mIgE using PNGaseF

to remove all N-glycans (123). These results suggest an absolute requirement of mIgE N384 glycosylation for the initiation of anaphylaxis. Further, circular dichroism results showed enzymatic removal of N-linked glycans altered the secondary structure of IgE and abrogated binding to FcεRI (123). These results highlight the role of glycosylation in binding to the high-affinity receptor similar to the role of IgG glycosylation in FcγR binding. This also suggests that IgE produced in *E. coli* might adopt a different conformation when refolding than a glycosylated IgE and thus can still result in FcεRI binding.

Disease-specific IgE glycosylation patterns have been characterized in allergic and atopic cohorts (111). Between the two cohorts, mannose, fucose, and biGlcNAc content in complex bi-antennary type glycans were largely similar. However, terminal galactose was enriched on atopic total IgE while increased sialylation was observed in allergic IgE. Functional experiments revealed increased mast cell degranulation was observed after sensitization with peanut-allergic IgE compared to the atopic IgE. The role of IgE sialylation was further confirmed by the passive cutaneous anaphylaxis model. Indeed, sialylated IgE increased anaphylaxis compared to asialylated IgE (111). The emerging patterns of the effects of antibody sialylation are intriguing; IgG sialylation mediates anti-inflammatory activity, but IgE sialylation promotes allergy (Figure 2).

IgM Antibodies

There are generally thought to be two types of IgM produced, called natural IgM and immune IgM. Natural IgM antibodies are produced spontaneously and act as the first line of defense during microbial infections, prior to the adaptive immune response; its repertoire is largely unaffected by external antigens (124, 125). In humans, natural IgM antibodies are produced by B1 cells without exposure to exogenous antigens, are polyreactive, and constitute the majority of circulating IgM in serum (126, 127). Natural IgM antibodies can recognize specific neoepitopes on apoptotic cells to remove them selectively and to maintain tissue homeostasis. Antigens recognized by natural IgM include specific carbohydrates, phospholipids, and double-stranded DNA (128–130). The other IgM class, immune IgM, is produced after exposure to external antigens (131). While the source of the two IgM classes is different, the differences in their structural and functional properties are minimal (132).

IgM antibodies are found in a pentamer or hexamer format, in which each monomer is composed of a heavy chain with one variable region and four constant regions (CH1, CH2, CH3, CH4), and a light chain (133). In contrast to IgG, the molecular structure of IgM possesses a short hinge region, similar to IgE. A short peptide sequence of 18 amino acids, called a tailpiece, is essential for IgM multimerization. The tailpiece of each heavy chain forms disulfide bonds with each heavy chain monomer to form IgM and another disulfide bond between C414 residues in the CH3 region of each heavy chain is involved in the formation of the multimer (134, 135). Tailpiece multimerization has also been successfully used to form IgG hexamers (136, 137). IgM also contains a J chain in the pentameric structure which is involved in the transportation of IgM through binding to specific receptors (9, 138, 139).

Apart from multimerization, glycosylation sites add further complexity to the IgM structure. IgM is heavily glycosylated in comparison with IgG; it has five N-linked glycosylation sites in the heavy chain (N171 (CH1), N332 (CH2), N395, N402 (both in CH3)), one in the tailpiece (N563), and one on the J chain (140, 141). The N-linked glycosylation pattern of IgM includes complex type and high-mannose type glycans; as shown in Figure 1A, N171, N332, and N395 are occupied by complex type glycans and N402 and N563 contain high-mannose type glycans (141, 142). Similar to IgG, IgM complex type glycans also may contain terminal sialic acid.

IgM Sialylation

Natural anti-T lymphocyte IgM antibody levels are increased in patients with inflammatory conditions, HIV infections, and SLE compared to healthy individuals (143, 144). These antibodies mediate the inhibitory effects on anti-CD3-induced T cell activation but for a time the mechanism was not completely understood (145, 146). A recent study by Colucci *et al.* shows that IgM's inhibitory effects depend on antibody glycosylation (147). Five different IgM antibodies purified from healthy donors (n=2) or myeloma patients (n=3) were incubated with human PBMCs. Results showed that the IgM antibody from healthy donors (IgMh) bound to the T cells and were then internalized and inhibited T cell proliferation. Meanwhile, IgM from myeloma patients (IgMm) remained on the surface and did not inhibit T cell proliferation. Glycosylation analysis of these antibodies showed only the IgMh, which mediated the inhibitory effects, contained sialic acid but the IgMm antibodies did not. Furthermore, removal of sialic acid using neuraminidase enzyme completely abrogated internalization of IgM and this asialylated IgM did not inhibit T-cell proliferation. The proposed mechanism is that both sialylated and asialylated IgM bind to FcμR, but only the sialylated antibody is internalized and triggers the inhibitory pathways (147, 148).

IgA Antibodies

In the serum, IgA is the second most prevalent circulating antibody after IgG and it is the predominant antibody found in external secretions such as those that bathe mucosal surfaces (8). Interestingly, the molecular form of IgA varies between the serum and mucosal surfaces. In the serum IgA exists in the monomeric form, but on mucosal surfaces IgA exists as a dimer called secretory IgA (SIgA). SIgA contains two IgA molecules joined by a J chain, similarly to IgM, to form a dimer, and this complex is also bound to a secretory component (149). Serum IgA contains two heavy chains composed of one variable region and three constant regions, and two light chains.

Based on its structure, IgA is divided into subclasses IgA1 and IgA2. IgA1 contains a hinge region with six O-linked glycosylation sites and two N-Linked glycosylation sites on each heavy chain as shown in Figure 1A. In contrast, IgA2 lacks O-linked glycosylation due to a shortened hinge region and has two N-linked glycosylation sites per heavy chain. The glycosylation pattern of the O-linked glycans may vary, but the majority of the O-linked glycans contain GalNAc and galactose with one or two sialic acids (11, 26).

IgA blocks the entry of pathogens through antigen-binding sites and the IgA-specific receptor Fc α RI mediates the clearance mechanism (150). The SIgA molecule, with its multiple antigen-binding sites, provides high avidity to cross-link antigens in a highly efficient manner, which can block pathogen activity. Both serum IgA and secretory SIgA bind to the Fc α RI receptor with similar binding affinity but cause divergent downstream effects. To evade the immune system, pathogenic bacteria such as *Staphylococcus aureus* produce IgA binding proteins to inhibit IgA and Fc α RI (151). In another strategy, pathogenic bacteria produce specific bacterial proteases against IgA, which specifically cleaves inside the hinge region of IgA leading to the inefficient clearance of pathogens (11, 150).

Several studies have shown that variations in IgA1 O-linked glycosylation play a crucial role in the pathogenesis of IgA Nephropathy (IgAN) and kidney failure (152). Analysis of IgAN patient samples showed a galactose deficiency in O-linked glycans, resulting in immune complex formation stimulated by anti-IgA1 IgG antibodies specific for this O-linked glycan. The large immune complexes escape clearance mechanisms and deposit in the renal mesangium, leading to glomerular injury (26, 152–154). As mentioned previously, glycosylation patterns are driven by the availability of substrate and enzyme expression during biosynthesis. In the case of a IgAN, there is deficiency in the galactosyltransferase enzyme C1GALT1, resulting in IgA1 with galactose-deficient O-linked glycosylation in the hinge region (26).

IgA Sialylation

Recent studies have shown IgA subclasses isolated from serum display different effector functions (**Figure 2**). IgA2 elicits pro-inflammatory effects on macrophages and neutrophils, but this is not observed with IgA1. These differences are attributed to variations in N-linked glycosylation, where IgA2 has 25% less sialylation compared to IgA1. These results were further confirmed by the enzymatic removal of total sialic acid using neuraminidase and the complete removal of N-linked glycans using PNGaseF, both of which resulted in increased pro-inflammatory activity (155). Another study showed IgA mediates anti-viral activity through sialic acid from the complex N-linked glycan at N459, where sialic acid interfered with cell surface attachment of influenza A (156).

GLYCOENGINEERING

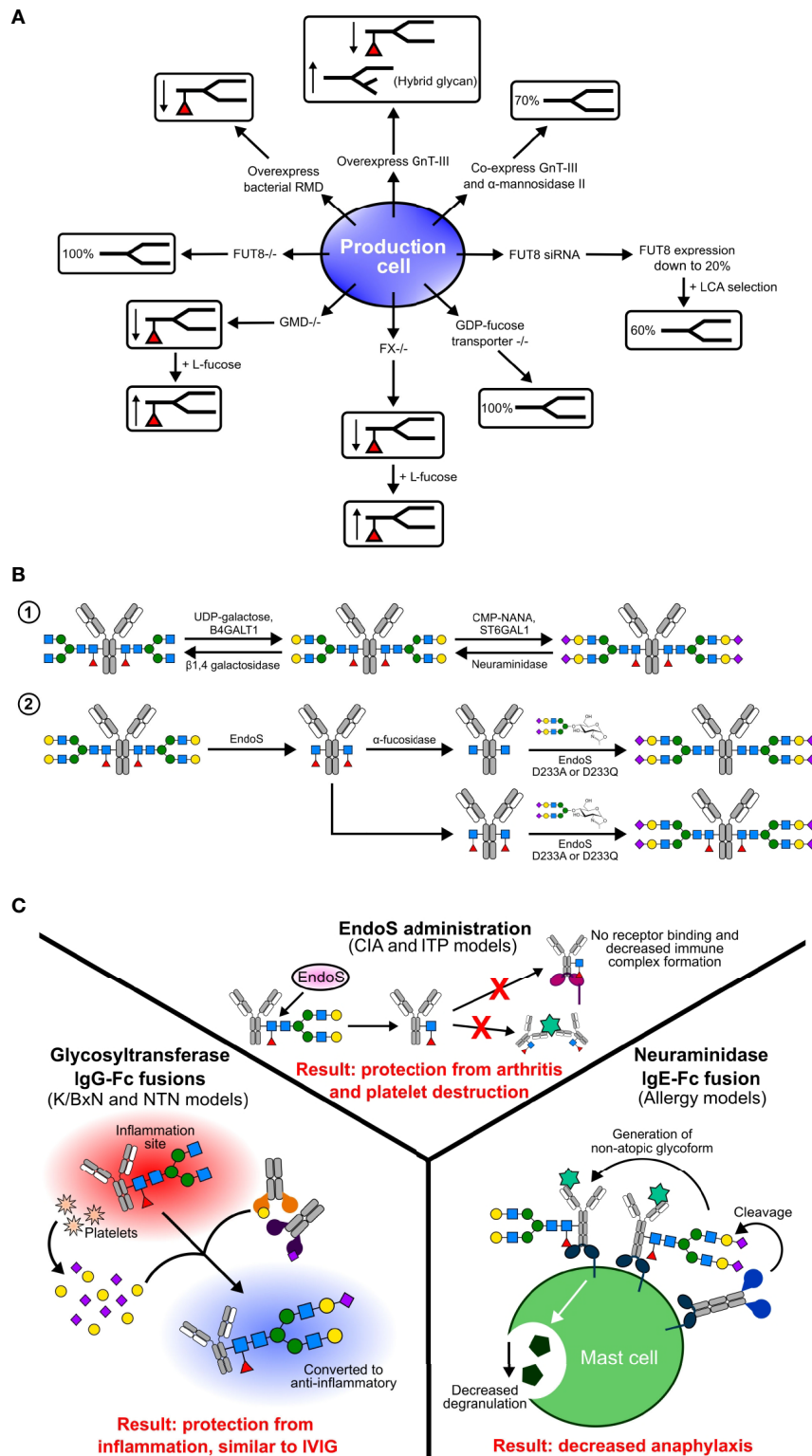
Monoclonal antibody (mAb) based therapeutics are the fastest-growing group of therapeutics for several clinical indications including oncology, autoimmune diseases, inflammatory disease, and bacterial and viral infections. This field is dominated by IgG-based therapeutics. However, IgE has been developed as an immunotherapeutic agent for cancer, and IgA-based therapeutics have been proposed for treatment of bacterial and viral infections, and as anti-inflammatory and anti-tumor agents (10, 11, 150, 157). More testing is needed to determine the best suited glycoforms for these antibody classes. Much of the

glycoengineering focus thus far has revolved around generation of afucosylated IgG, which is reviewed extensively elsewhere (82, 92, 158, 159).

Mammalian host expression systems are used for the production of antibodies to maintain mammalian antibody glycosylation patterns and minimize immunogenicity. However, there are differences in glycosylation patterns between endogenous antibodies produced in humans and mammalian cell lines. Antibody glycosylation is influenced by the host cell, glycosyltransferase expression, and cell culture conditions, such as low dissolved oxygen concentration and a reduced culture reduction potential (160, 161). Glycoforms of therapeutic mAbs produced in CHO, HEK293, mouse myeloma NS0, and Sp2/0 cell lines are heterogeneous with a predominance of the G0F glycoform produced, along with limited galactosylated and sialylated glycoforms. Therapeutic mAbs produced in CHO cells are less galactosylated compared to mAbs produced in mouse myeloma cell lines (162). The rat hybridoma cell line YB2/0 has low α -1,6 fucosyltransferase activity; therefore, this cell line is used for the production of mAbs with lower fucosylation levels. Specific glycosylation patterns, such as the absence of fucose, bisecting GlcNAc, and the presence of high mannose glycans increase ADCC, while galactose increases CDCC and sialic acid increases anti-inflammatory activity (163–167). Since different antibody glycoforms have distinct effects on biological activity, the production of homogenous glycoforms is necessary to improve therapeutic outcomes and maintain treatment quality. Enrichment of specific glycoforms and separation of said glycoforms using chromatography is challenging. Alternatively, two strategies have been employed to generate homogenous glycoforms with tailor-made sugar residues to modify antibody function. Host cell glycosylation pathway manipulation, called mammalian cell line glycoengineering, and *in vitro* glycoengineering are widely used to produce homogeneously glycosylated antibodies (91, 92, 158).

Mammalian Cell Line Engineering

Biosynthetic pathways in mammalian cell lines can be manipulated to produce afucosylated antibodies (**Figure 3A**). This strategy has focused on non-sialylated glycoforms by overexpression of different enzymes, generating gene knockout lines, and using monosaccharides as inhibitors (82, 92, 158). Recombinant glycoproteins and antibodies produced in CHO cells only produce α -2,3 sialylated glycans due to lack of ST6GAL1 gene expression. To increase sialylation, different strategies have been developed, including overexpression of the CMP-sialic acid transporter, overexpression of sialyltransferases, and knock out of genes (168–171). Production cell lines engineered to overexpress trans-Golgi enzymes B4GALT1 and ST6GAL1 have been described to generate IgG with enriched ~70% biantennary sialylated glycoforms (169). Co-expression of B4GALT1 and ST6GAL1 with IgG increased the amount of sialylation to 32% (170). Using gene editing technology, a CHO^{-Mgat2/-Stgal4/-Stgal6/+B4GALT1/+ST6GAL1} clone was generated by knocking out the ST3GAL4, ST3GAL6, and Mgat2 genes to



inhibit α -2,3 sialylation and knocked in the B4GALT1 and ST6GAL1 genes to increase α -2,6 sialylation (171).

Antibody fucosylation is decreased by overexpression of GnT-III. GnT-III is expressed in the Golgi and catalyzes the addition of biGlcNAc on to a β -linked mannose residue of an N-linked glycan. The addition of biGlcNAc increases steric hindrance, inhibits the addition of fucose, and produces hybrid type N-glycans. Although CHO cells do not express GnT-III, overexpression of it in CHO cells resulted in reduced antibody Fc fucosylation due to the addition of biGlcNAc (103, 172). This method is further improved by co-expression of GnT-III and Golgi α -mannosidase II, which results in a 70% decrease in core fucosylation (103, 173).

Gene knock out cell lines were developed by targeting specific genes involved in core fucosylation. The FUT8 gene encoding α -1,6 fucosyltransferase catalyzes the addition of α -1,6 fucose to the innermost GlcNAc. In the CHO-DG44 cell line, small interfering RNAs (siRNAs) targeting FUT8 reduced mRNA expression levels to 20%. Coupling this method with *Lens culinaris agglutinin* (LCA) selection produced 60% afucosylated antibodies with a resulting 100-fold increase in ADCC (174).

Afucosylated antibodies can also be generated by manipulation of GDP-fucose biosynthetic pathways (175). GDP-mannose 4,6-dehydratase (GMD) and GDP-4-keto-6-deoxymannose-3,5-epimerase-4-reductase (FX) catalyze the conversion of GDP-mannose into GDP-fucose. In knockout lines for each of these enzymes, core fucosylation is absent due to a lack of GDP-fucose but can be rescued by addition of L-fucose to the media (176, 177). Alternatively, overexpression of the bacterial GDP-6-deoxy-D-lyxo-4-hexulose reductase (RMD) enzyme reduces core fucosylation by depleting the intermediate GDP-4-keto-6-deoxy-D-mannose used in the synthesis GDP-fucose (175, 178, 179). An additional strategy to generate afucosylated IgG involves the addition of fucose analogs 2-fluorofucose and 5-alkynylfucose to inhibit the biosynthetic pathway of fucosylation (180).

In Vitro Glycoengineering

There is a tremendous improvement in the generation of glycoengineered antibodies through biosynthetic pathways and genetic manipulations in mammalian and non-mammalian cells. However, these methods require complex protocols and special cell line development for each type of glycan addition or deletion. These problems can be overcome by using *in vitro* glycoengineering, where trimming or extending of antibody glycans is performed using substrates, glycosyltransferases, and glycosidases (**Figure 3B**). These approaches have been successfully applied to antibodies generated in both mammalian and non-mammalian cells. There are two types of *in vitro* glycoengineering methods: enzymatic and chemoenzymatic.

In the enzymatic method, the antibody of interest is treated with uridine diphosphate galactose (UDP-Gal) and β -1,4 galactosyltransferase-1 (B4GalT1) to generate the G2F glycoform, which is further modified by treating the product with cytidine 5' mono-phospho-N-acetyl neuraminic acid (CMP-NANA) and α 2,6 sialyltransferase (ST6Gal1) to produce the G2S2F glycoform (55). This method can also be

applied to remove sialic acid and galactose by treatment with neuraminidase and β -1,4 galactosidase. In early studies, lectin enrichment was used to prepare sialylated Fc, but later studies used enzymatic glycoengineering methods to add galactose followed by sialic acid (36, 37). Several studies have shown sialylated IgG1 Fc and sialylated IVIG protect mice from induced arthritis at lower doses compared to IVIG (37, 55). This data is further supported by the use of sialylated IgG Fc clinical trials for the successful treatment of ITP (67). This method is limited by the stepwise addition of sugars.

Chemoenzymatic glycoengineering of IgG antibodies is a two-step process, consisting first of deglycosylation of N-linked glycans using native endoglycosidases followed by the addition of homogenous N-linked glycans using mutant endoglycosidases. This strategy was improved by the discovery of the novel endoglycosidase endo- β -N-acetylglucosaminidase (EndoS) mutants D233A and EndoS D233Q, which allowed the addition of N-linked glycans to GlcNAc or core-fucosylated GlcNAc (181). This is a very robust method that allows for the addition of the entire glycan complex at one time. Using the chemoenzymatic method, Rituximab has been glycoengineered to prepare homogenous G2, S2G2, G2F, and S2G2F glycoforms. Results from *in vivo* and *in vitro* studies have shown that only afucosylated glycoforms increased Fc γ RIIIA binding and elevated ADCC compared to the G2F and G2S2F glycoforms (77). Enzymatic glycoengineering and biosynthetic pathway manipulation are limited to the addition of complex biantennary type glycans, but the chemoenzymatic method allows selective addition of branched glycans. The D165A and D165Q mutants of the bacterial endoglycosidase Endo-F3 allow selective addition of bi- and triantennary N-glycans to the fucose core (182). The Endo-F3 D165A and Endo-S D233A allow site-specific glycoengineering of the Fab and Fc domains, respectively (183).

Currently, antibody glycoengineering efforts are exclusively focused on the Fc-core due to its role in mediating effector functions (63, 77, 82), but it should be noted that the antibody Fab domain also undergoes glycosylation for antigen recognition and other functions (184–186). The therapeutic antibody Cetuximab undergoes glycosylation in the Fab domain at N88 and in the Fc at N297. Glycoengineered Cetuximab without fucose at the Fc core and with sialic acid at Fab region showed increased binding affinity to Fc γ RIIIA and increased ADCC (183). Other applications of chemoenzymatic methods include bioconjugation, site specific labelling, and the synthesis of antibody-drug conjugates.

In Vivo Glycoengineering

Biosynthetic pathway manipulation of cell lines requires more time to establish knock out cell lines but is faster once the cell line is established, whereas *in vitro* glycoengineering methods require more time and effort in the purification steps. Another emerging strategy is glycoengineering circulating IgG antibodies *in vivo* using glycosidases and glycosyltransferases (**Figure 3C**). The first time deglycosylation of circulating IgG antibodies was shown was by *in vivo* administration of EndoS from the human pathogen *Streptococcus pyogenes* (187). EndoS selectively

catalyzes the hydrolysis of the glycosidic bond between the first two N-acetylglucosamine residues of the of the N-linked glycan on the Fc of each IgG subclass (IgG1-4). In the collagen-induced arthritis mouse model, pretreatment of antibodies with EndoS enzyme inhibited the advancement of arthritis, abolished IgG binding to Fc receptors, and disturbed immune complex formation (188). Furthermore, the administration of EndoS has shown a protective effect in a mouse model of IgG-driven ITP (189). However, repeated administration of EndoS triggers an immune response, and using bacterial enzymes in a therapeutic setting raises a safety concern. Alternatively, the bacterial protease IdeS was successful in a trial targeting IgG mediated autoimmune conditions (190–192)

In another strategy of *in vivo* sialylation, human glycosyltransferases B4GalT1 and ST6Gal1 have been fused to IgG Fc to glycoengineer pathogenic antibodies (193). This approach recapitulates sialylated IVIG or IgG anti-inflammatory activity by converting pathogenic antibodies into sialylated, non-pathogenic antibodies. Interestingly, Fc-fused enzymes specifically sialylated pathogenic antibodies only at sites of inflammation, but not the antibodies or other glycoproteins in circulation (193). This specificity of *in vivo* glycoengineering is due to platelets releasing sugar donors, sialic acid and galactose, at sites of inflammation. This strategy has been successfully demonstrated in murine autoimmune disease models, in which Fc-fused enzymes attenuated auto-antibody inflammation by converting autoantibodies into anti-inflammatory mediators (193). By fusing glycoenzymes to IgG Fc, the enzymes' stability and half-life is increased. *In vivo* sialylation has the potential to be applied to those diseases currently treated using IVIG and offers a potential therapeutic strategy for autoimmune and inflammatory conditions.

Removing sialic acid from IgE is an appealing therapeutic strategy for allergic disease. With that in mind, a bacterial neuraminidase enzyme was fused to the IgE Fc Cε2–4 domains (NEUFce), thereby targeting neuraminidase to IgE-bearing cells (111). Administration of this enzyme fusion during murine models of allergic inflammation resulted in attenuation of anaphylaxis (111). However, further testing of modulating antibody sialic acid content *in vivo* is needed.

CONCLUSIONS

Endogenous antibody glycosylation is heterogeneous and varies with age and pathophysiological conditions. Harnessing antibody glycosylation is in its infancy, but applications that

are engaged in this endeavor include the development of biologic therapeutics and using certain glycosylation patterns as biomarkers. Therapeutic antibodies are a rapidly growing class for the treatment of cancer, autoimmune diseases, infectious diseases, and other conditions. Glycosylation of therapeutic antibodies is very sensitive to cell culture and other production conditions and variations in glycosylation impacts the quality of the product. Therapeutic antibody glycosylation is a critical quality attribute because of its impact on effector functions and half-life. In depth understanding of IgG glycosylation has revealed the role of each glycan in modulating IgG function and resulted in the development of therapeutic afucosylated and sialylated antibodies.

Glycosylation across antibody classes regulates the structure and function of antibodies. Several studies have shown that sialic acid has divergent functions in antibody classes. For instance, sialylated IgG1 mediates anti-inflammatory activity, sialylated IgE is associated with allergic pathogenicity, sialylated IgA shows anti-viral activity, and sialylated IgM shows inhibitory effects on T-cell proliferation. For most antibody classes, sialylation exerts profound influence over the effector functions. There are multiple, non-mutually exclusive reasons for this, including influencing receptor binding and introducing addition receptors and co-factors. Further studies are required to characterize specific mechanisms of antibody activity and the involvement of additional receptors. Also, the role of sialylation across all antibody subclasses is in need of more examination. *In vitro* sialylation of IgG markedly enriches sialylated glycoform for desired effector functions. This method has been successfully applied to generate sialylated antibodies to mediate anti-inflammatory activity. Indeed, glycoengineering has applicability across antibody classes is a major advantage. More understanding of the role and regulation of antibody sialylation and glycosylation will likely uncover additional applications for glycoengineering.

AUTHOR CONTRIBUTIONS

RV, SS, and RA wrote the article. All authors contributed to the article and approved the submitted version.

FUNDING

This work was supported by NIH grants (R01 AI155662, R01 AI153441, and R01 AI139669) to RA.

REFERENCES

1. Imbach P. Treatment of Immune Thrombocytopenia With Intravenous Immunoglobulin and Insights for Other Diseases. A Historical Review. *Swiss Med Wkly* (2012) 142:w13593. doi: 10.4414/smw.2012.13593
2. Bayry J, Negi VS, Kaveri SV. Intravenous Immunoglobulin Therapy in Rheumatic Diseases. *Nat Rev Rheumatol* (2011) 7(6):349–59. doi: 10.1038/nrrheum.2011.61
3. Schwab I, Nimmerjahn F. Intravenous Immunoglobulin Therapy: How Does IgG Modulate the Immune System? *Nat Rev Immunol* (2013) 13(3):176–89. doi: 10.1038/nri3401
4. Mullard A. FDA Approves 100th Monoclonal Antibody Product. *Nat Rev Drug Discovery* (2021) 20(7):491–5. doi: 10.1038/d41573-021-00079-7
5. Harris LJ, Larson SB, Hasel KW, Day J, Greenwood A, McPherson A. The Three-Dimensional Structure of an Intact Monoclonal Antibody for Canine Lymphoma. *Nature* (1992) 360(6402):369–72. doi: 10.1038/360369a0

6. Schroeder HW Jr, Cavacini L. Structure and Function of Immunoglobulins. *J Allergy Clin Immunol* (2010) 125(2 Suppl 2):S41–52. doi: 10.1016/j.jaci.2009.09.046
7. Anzel LM, Poljak RJ. Three-Dimensional Structure of Immunoglobulins. *Annu Rev Biochem* (1979) 48:961–97. doi: 10.1146/annurev.bi.48.070179.004525
8. Kerr MA. The Structure and Function of Human IgA. *Biochem J* (1990) 271(2):285–96. doi: 10.1042/bj2710285
9. Keyt BA, Baliga R, Sinclair AM, Carroll SF, Peterson MS. Structure, Function, and Therapeutic Use of IgM Antibodies. *Antib (Basel)* (2020) 9(4):53. doi: 10.3390/antib9040053
10. Sutton BJ, Davies AM, Bax HJ, Karagiannis SN. IgE Antibodies: From Structure to Function and Clinical Translation. *Antib (Basel)* (2019) 8(1):19. doi: 10.3390/antib8010019
11. de Sousa-Pereira P, Woof JM. IgA: Structure, Function, and Developability. *Antib (Basel)* (2019) 8(4):57. doi: 10.3390/antib8040057
12. Rouwendal GJ, van der Lee MM, Meyer S, Reiding KR, Schouten J, de Roo G, et al. A Comparison of Anti-HER2 IgA and IgG1 *In Vivo* Efficacy is Facilitated by High N-Glycan Sialylation of the IgA. *MABs* (2016) 8(1):74–86. doi: 10.1080/19420862.2015.1102812
13. Tchoudakova A, Hensel F, Muriillo A, Eng B, Foley M, Smith L, et al. High Level Expression of Functional Human IgMs in Human PER. *C6 Cells MABs* (2009) 1(2):163–71. doi: 10.4161/mabs.1.2.7945
14. Krapp S, Mimura Y, Jefferis R, Huber R, Sonderrmann P. Structural Analysis of Human IgG-Fc Glycoforms Reveals a Correlation Between Glycosylation and Structural Integrity. *J Mol Biol* (2003) 325(5):979–89. doi: 10.1016/S0022-2836(02)01250-0
15. Yamaguchi Y, Nishimura M, Nagano M, Yagi H, Sasakawa H, Uchida K, et al. Glycoform-Dependent Conformational Alteration of the Fc Region of Human Immunoglobulin G1 as Revealed by NMR Spectroscopy. *Biochim Biophys Acta* (2006) 1760(4):693–700. doi: 10.1016/j.bbagen.2005.10.002
16. A Varki, RD Cummings, JD Esko, P Stanley, GW Hart, et al. eds. *Essentials of Glycobiology*. Cold Spring Harbor (NY) (2015).
17. Stanley P, Schachter H, Taniguchi N, Varki A, Cummings RD, Esko JD, et al. N-Glycans. In: A Varki, RD Cummings, JD Esko, HH Freeze, P Stanley, et al, editors. *Essentials of Glycobiology*. Cold Spring Harbor (NY) (2009).
18. Schwarz F, Aebi M. Mechanisms and Principles of N-Linked Protein Glycosylation. *Curr Opin Struct Biol* (2011) 21(5):576–82. doi: 10.1016/j.sbi.2011.08.005
19. Kornfeld R, Kornfeld S. Assembly of Asparagine-Linked Oligosaccharides. *Annu Rev Biochem* (1985) 54:631–64. doi: 10.1146/annurev.bi.54.070185.003215
20. Varki A, Cummings RD, Esko JD, Freeze HH, Stanley P, Bertozzi CR, et al. *Essentials of Glycobiology*. Cold Spring Harbor (NY) (2009).
21. Butters TD. Control in the N-Linked Glycoprotein Biosynthesis Pathway. *Chem Biol* (2002) 9(12):1266–8. doi: 10.1016/S1074-5521(02)00290-9
22. Nishima W, Miyashita N, Yamaguchi Y, Sugita Y, Re S. Effect of Bisecting GlcNAc and Core Fucosylation on Conformational Properties of Biantennary Complex-Type N-Glycans in Solution. *J Phys Chem B* (2012) 116(29):8504–12. doi: 10.1021/jp212550z
23. Mattu TS, Pleass RJ, Willis AC, Kilian M, Wormald MR, Lellouch AC, et al. The Glycosylation and Structure of Human Serum IgA1, Fab, and Fc Regions and the Role of N-Glycosylation on Fcα Receptor Interactions. *J Biol Chem* (1998) 273(4):2260–72. doi: 10.1074/jbc.273.4.2260
24. Takayasu T, Suzuki S, Kametani F, Takahashi N, Shinoda T, Okuyama T, et al. Amino Acid Sequence of Galactosamine-Containing Glycopeptides in the Hinge Region of a Human Immunoglobulin D. *Biochem Biophys Res Commun* (1982) 105(3):1066–71. doi: 10.1016/0006-291X(82)91078-6
25. Plomp R, Dekkers G, Rombouts Y, Visser R, Koeleman CA, Kammeijer GS, et al. Hinge-Region O-Glycosylation of Human Immunoglobulin G3 (IgG3). *Mol Cell Proteomics* (2015) 14(5):1373–84. doi: 10.1074/mcp.M114.047381
26. Novak J, Julian BA, Tomana M, Mestecky J. IgA Glycosylation and IgA Immune Complexes in the Pathogenesis of IgA Nephropathy. *Semin Nephrol* (2008) 28(1):78–87. doi: 10.1016/j.semnephrol.2007.10.009
27. Iwasaki H, Zhang Y, Tachibana K, Gotoh M, Kikuchi N, Kwon YD, et al. Initiation of O-Glycan Synthesis in IgA1 Hinge Region is Determined by a Single Enzyme, UDP-N-Acetyl-Alpha-D-Galactosamine:Polypeptide N-Acetylgalactosaminyltransferase 2. *J Biol Chem* (2003) 278(8):5613–21. doi: 10.1074/jbc.M211097200
28. Stewart TJ, Takahashi K, Xu N, Prakash A, Brown R, Raska M, et al. Quantitative Assessment of Successive Carbohydrate Additions to the Clustered O-Glycosylation Sites of IgA1 by Glycosyltransferases. *Glycobiology* (2021) 31(5):540–56. doi: 10.1093/glycob/cwaa111
29. Ohyama Y, Renfrow MB, Novak J, Takahashi K. Aberrantly Glycosylated IgA1 in IgA Nephropathy: What We Know and What We Don't Know. *J Clin Med* (2021) 10(16):3467. doi: 10.3390/jcm10163467
30. Nimmerjahn F, Ravetch JV. Divergent Immunoglobulin G Subclass Activity Through Selective Fc Receptor Binding. *Science* (2005) 310(5753):1510–2. doi: 10.1126/science.1118948
31. Franklin EC. Structure and Function of Immunoglobulins. *Acta Endocrinol Suppl (Copenh)* (1975) 194:77–95. doi: 10.1530/acta.0.080S077
32. Spiegelberg HL. Biological Role of Different Antibody Classes. *Int Arch Allergy Appl Immunol* (1989) 90(Suppl 1):22–7. doi: 10.1159/000235071
33. Bruhns P, Iannascoli B, England P, Mancardi DA, Fernandez N, Jorieux S, et al. Specificity and Affinity of Human Fcγ Receptors and Their Polymorphic Variants for Human IgG Subclasses. *Blood* (2009) 113(16):3716–25. doi: 10.1182/blood-2008-09-179754
34. Vidarsson G, Dekkers G, Rispens T. IgG Subclasses and Allotypes: From Structure to Effector Functions. *Front Immunol* (2014) 5:520. doi: 10.3389/fimmu.2014.00520
35. Bournazos S, Wang TT, Dahan R, Maamary J, Ravetch JV. Signaling by Antibodies: Recent Progress. *Annu Rev Immunol* (2017) 35:285–311. doi: 10.1146/annurev-immunol-051116-052433
36. Kaneko Y, Nimmerjahn F, Ravetch JV. Anti-Inflammatory Activity of Immunoglobulin G Resulting From Fc Sialylation. *Science* (2006) 313(5787):670–3. doi: 10.1126/science.1129594
37. Anthony RM, Nimmerjahn F, Ashline DJ, Reinhold VN, Paulson JC, Ravetch JV. Recapitulation of IVIG Anti-Inflammatory Activity With a Recombinant IgG Fc. *Science* (2008) 320(5874):373–6. doi: 10.1126/science.1154315
38. Wang X, Mathieu M, Brezski RJ. IgG Fc Engineering to Modulate Antibody Effector Functions. *Protein Cell* (2018) 9(1):63–73. doi: 10.1007/s13238-017-0473-8
39. Sonderrmann P, Pincetic A, Maamary J, Lammens K, Ravetch JV. General Mechanism for Modulating Immunoglobulin Effector Function. *Proc Natl Acad Sci USA* (2013) 110(24):9868–72. doi: 10.1073/pnas.1307864110
40. Subedi GP, Barb AW. The Structural Role of Antibody N-Glycosylation in Receptor Interactions. *Structure* (2015) 23(9):1573–83. doi: 10.1016/j.str.2015.06.015
41. Nose M, Wiggall H. Biological Significance of Carbohydrate Chains on Monoclonal Antibodies. *Proc Natl Acad Sci USA* (1983) 80(21):6632–6. doi: 10.1073/pnas.80.21.6632
42. Pound JD, Lund J, Jefferis R. Aglycosylated Chimeric Human IgG3 can Trigger the Human Phagocyte Respiratory Burst. *Mol Immunol* (1993) 30(3):233–41. doi: 10.1016/0161-5890(93)90052-D
43. Tao MH, Morrison SL. Studies of Aglycosylated Chimeric Mouse-Human IgG. Role of Carbohydrate in the Structure and Effector Functions Mediated by the Human IgG Constant Region. *J Immunol* (1989) 143(8):2595–601.
44. Pucic M, Knezevic A, Vidic J, Adamczyk B, Novokmet M, Polasek O, et al. High Throughput Isolation and Glycosylation Analysis of IgG-Variability and Heritability of the IgG Glycome in Three Isolated Human Populations. *Mol Cell Proteomics* (2011) 10(10):M111 010090. doi: 10.1074/mcp.M111.010090
45. Jefferis R. Glycosylation of Recombinant Antibody Therapeutics. *Biotechnol Prog* (2005) 21(1):11–6. doi: 10.1021/bp040016j
46. Liu L. Pharmacokinetics of Monoclonal Antibodies and Fc-Fusion Proteins. *Protein Cell* (2018) 9(1):15–32. doi: 10.1007/s13238-017-0408-4
47. Liu H, Nowak C, Andrien B, Shao M, Ponniah G, Neill A. Impact of IgG Fc-Oligosaccharides on Recombinant Monoclonal Antibody Structure, Stability, Safety, and Efficacy. *Biotechnol Prog* (2017) 33(5):1173–81. doi: 10.1002/btpr.2498
48. Higel F, Seidl A, Sorgel F, Friess W. N-Glycosylation Heterogeneity and the Influence on Structure, Function and Pharmacokinetics of Monoclonal Antibodies and Fc Fusion Proteins. *Eur J Pharm Biopharm* (2016) 100:94–100. doi: 10.1016/j.ejpb.2016.01.005

49. Gudelj I, Lauc G, Pezer M. Immunoglobulin G Glycosylation in Aging and Diseases. *Cell Immunol* (2018) 333:65–79. doi: 10.1016/j.cellimm.2018.07.009
50. Li D, Lou Y, Zhang Y, Liu S, Li J, Tao J. Sialylated Immunoglobulin G: A Promising Diagnostic and Therapeutic Strategy for Autoimmune Diseases. *Theranostics* (2021) 11(11):5430–46. doi: 10.1016/j.thno.2021.05.036
51. Imbach P, Wagner HP, Berchtold W, Gaedicke G, Hirt A, Joller P, et al. Intravenous Immunoglobulin Versus Oral Corticosteroids in Acute Immune Thrombocytopenic Purpura in Childhood. *Lancet* (1985) 2(8453):464–8. doi: 10.1016/s0140-6736(85)90400-3
52. Levy Y, Sherer Y, Ahmed A, Langevitz P, George J, Fabrizzi F, et al. A Study of 20 SLE Patients With Intravenous Immunoglobulin—Clinical and Serologic Response. *Lupus* (1999) 8(9):705–12. doi: 10.1191/096120399678841007
53. Hughes RA, Donofrio P, Bril V, Dalakas MC, Deng C, Hanna K, et al. Intravenous Immune Globulin (10% Caprylate-Chromatography Purified) for the Treatment of Chronic Inflammatory Demyelinating Polyradiculoneuropathy (ICE Study): A Randomised Placebo-Controlled Trial. *Lancet Neurol* (2008) 7(2):136–44. doi: 10.1016/S1474-4422(07)70329-0
54. Anthony RM, Wermeling F, Karlsson MC, Ravetch JV. Identification of a Receptor Required for the Anti-Inflammatory Activity of IVIG. *Proc Natl Acad Sci USA* (2008) 105(50):19571–8. doi: 10.1073/pnas.0810163105
55. Washburn N, Schwab L, Ortiz D, Bhatnagar N, Lansing JC, Medeiros A, et al. Controlled Tetra-Fc Sialylation of IVIg Results in a Drug Candidate With Consistent Enhanced Anti-Inflammatory Activity. *Proc Natl Acad Sci USA* (2015) 112(11):E1297–306. doi: 10.1073/pnas.1422481112
56. Samuelsson A, Towers TL, Ravetch JV. Anti-Inflammatory Activity of IVIG Mediated Through the Inhibitory Fc Receptor. *Science* (2001) 291(5503):484–6. doi: 10.1126/science.291.5503.484
57. Nimmerjahn F, Ravetch JV. The Antiinflammatory Activity of IgG: The Intravenous IgG Paradox. *J Exp Med* (2007) 204(1):11–5. doi: 10.1084/jem.20061788
58. Crow AR, Song S, Freedman J, Helgason CD, Humphries RK, Siminovich KA, et al. IVIg-Mediated Amelioration of Murine ITP via FcγRIIb is Independent of SHP1, SHP-1, and Btk Activity. *Blood* (2003) 102(2):558–60. doi: 10.1182/blood-2003-01-0023
59. Fiebiger BM, Maamary J, Pincetic A, Ravetch JV. Protection in Antibody- and T Cell-Mediated Autoimmune Diseases by Antiinflammatory IgG Fcs Requires Type II FcRs. *Proc Natl Acad Sci USA* (2015) 112(18):E2385–94. doi: 10.1073/pnas.1505292112
60. Anthony RM, Kobayashi T, Wermeling F, Ravetch JV. Intravenous Gammaglobulin Suppresses Inflammation Through a Novel T(H)2 Pathway. *Nature* (2011) 475(7354):110–3. doi: 10.1038/nature10134
61. Temming AR, Dekkers G, van de Bovenkamp FS, Plomp HR, Bentlage AEH, Szittner Z, et al. Human DC-SIGN and CD23 do Not Interact With Human IgG. *Sci Rep* (2019) 9(1):9995. doi: 10.1038/s41598-019-46484-2
62. Yu X, Vasiljevic S, Mitchell DA, Crispin M, Scanlan CN. Dissecting the Molecular Mechanism of IVIg Therapy: The Interaction Between Serum IgG and DC-SIGN is Independent of Antibody Glycoform or Fc Domain. *J Mol Biol* (2013) 425(8):1253–8. doi: 10.1016/j.jmb.2013.02.006
63. Blundell PA, Le NPL, Allen J, Watanabe Y, Pleass RJ. Engineering the Fragment Crystallizable (Fc) Region of Human IgG1 Multimers and Monomers to Fine-Tune Interactions With Sialic Acid-Dependent Receptors. *J Biol Chem* (2017) 292(31):12994–3007. doi: 10.1074/jbc.M117.795047
64. Pleass RJ. The Therapeutic Potential of Sialylated Fc Domains of Human IgG. *MAbs* (2021) 13(1):1953220. doi: 10.1080/19420862.2021.1953220
65. Baksmeier C, Blundell P, Steckel J, Schultz V, Gu Q, Da Silva Filipe A, et al. Modified Recombinant Human IgG1-Fc is Superior to Natural Intravenous Immunoglobulin at Inhibiting Immune-Mediated Demyelination. *Immunology* (2021) 164(1):90–105. doi: 10.1111/imm.13341
66. Massoud AH, Yona M, Xue D, Chouiali F, Alturaihi H, Ablona A, et al. Dendritic Cell Immunoreceptor: A Novel Receptor for Intravenous Immunoglobulin Mediates Induction of Regulatory T Cells. *J Allergy Clin Immunol* (2014) 133(3):853–63.e5. doi: 10.1016/j.jaci.2013.09.029
67. Arroyo S, Tiessen RG, Denney WS, Jin J, van Iersel MP, Zeitz H, et al. Hyper-Sialylated IgG M254, an Innovative Therapeutic Candidate, Evaluated in Healthy Volunteers and in Patients With Immune Thrombocytopenia Purpura: Safety, Tolerability, Pharmacokinetics, and Pharmacodynamics. *Blood* (2019) 134(Supplement_1):1090–. doi: 10.1182/blood-2019-125993
68. Nimmerjahn F, Lunemann JD. Expression and Function of the Inhibitory Fcγ-Receptor in CIDP. *J Peripher Nerv Syst* (2011) 16(Suppl 1):41–4. doi: 10.1111/j.1529-8027.2011.00305.x
69. Tackenberg B, Jelcic I, Baerenwaldt A, Oertel WH, Sommer N, Nimmerjahn F, et al. Impaired Inhibitory Fcγ-Receptor IIB Expression on B Cells in Chronic Inflammatory Demyelinating Polyneuropathy. *Proc Natl Acad Sci USA* (2009) 106(12):4788–92. doi: 10.1073/pnas.0807319106
70. Tjon AS, van Gent R, Jaadar H, Martin van Hagen P, Mancham S, van der Laan LJ, et al. Intravenous Immunoglobulin Treatment in Humans Suppresses Dendritic Cell Function via Stimulation of IL-4 and IL-13 Production. *J Immunol* (2014) 192(12):5625–34. doi: 10.4049/jimmunol.1301260
71. Bartsch YC, Eschweiler S, Leliavski A, Lunding HB, Wagt S, Petry J, et al. IgG Fc Sialylation is Regulated During the Germinal Center Reaction Following Immunization With Different Adjuvants. *J Allergy Clin Immunol* (2020) 146(3):652–66.e11. doi: 10.1016/j.jaci.2020.04.059
72. Petry J, Rahmoller J, Duhring L, Lilienthal GM, Lehrian S, Buhre JS, et al. Enriched Blood IgG Sialylation Attenuates IgG-Mediated and IgG-Controlled-IgE-Mediated Allergic Reactions. *J Allergy Clin Immunol* (2021) 147(2):763–7. doi: 10.1016/j.jaci.2020.05.056
73. Wang TT, Maamary J, Tan GS, Bournazos S, Davis CW, Krammer F, et al. Anti-HA Glycoforms Drive B Cell Affinity Selection and Determine Influenza Vaccine Efficacy. *Cell* (2015) 162(1):160–9. doi: 10.1016/j.cell.2015.06.026
74. Chakraborty S, Gonzalez JC, Sievers BL, Mallajosyula V, Chakraborty S, Dubey M, et al. Early Non-Neutralizing, Afucosylated Antibody Responses Are Associated With COVID-19 Severity. *Sci Transl Med* (2022) 14(635):eabm7853. doi: 10.1126/scitranslmed.abm7853
75. Wang TT, Ravetch JV. Functional Diversification of IgGs Through Fc Glycosylation. *J Clin Invest* (2019) 129(9):3492–8. doi: 10.1172/JCI130029
76. Thomann M, Schlothauer T, Dashivets T, Malik S, Avenal C, Bulau P, et al. In Vitro Glycoengineering of IgG1 and its Effect on Fc Receptor Binding and ADCC Activity. *PLoS One* (2015) 10(8):e0134949. doi: 10.1371/journal.pone.0134949
77. Li T, DiLillo DJ, Bournazos S, Giddens JP, Ravetch JV, Wang LX. Modulating IgG Effector Function by Fc Glycan Engineering. *Proc Natl Acad Sci USA* (2017) 114(13):3485–90. doi: 10.1073/pnas.1702173114
78. Scallon BJ, Tam SH, McCarthy SG, Cai AN, Raju TS. Higher Levels of Sialylated Fc Glycans in Immunoglobulin G Molecules can Adversely Impact Functionality. *Mol Immunol* (2007) 44(7):1524–34. doi: 10.1016/j.molimm.2006.09.005
79. Wada R, Matsui M, Kawasaki N. Influence of N-Glycosylation on Effector Functions and Thermal Stability of Glycoengineered IgG1 Monoclonal Antibody With Homogeneous Glycoforms. *MAbs* (2019) 11(2):350–72. doi: 10.1080/19420862.2018.1551044
80. Quast I, Keller CW, Maurer MA, Giddens JP, Tackenberg B, Wang LX, et al. Sialylation of IgG Fc Domain Impairs Complement-Dependent Cytotoxicity. *J Clin Invest* (2015) 125(11):4160–70. doi: 10.1172/JCI82695
81. Dekkers G, Treffers L, Plomp R, Bentlage AEH, de Boer M, Koeleman CAM, et al. Decoding the Human Immunoglobulin G-Glycan Repertoire Reveals a Spectrum of Fc-Receptor- and Complement-Mediated-Effector Activities. *Front Immunol* (2017) 8:877. doi: 10.3389/fimmu.2017.00877
82. Pereira NA, Chan KF, Lin PC, Song Z. The "Less-is-More" in Therapeutic Antibodies: Afucosylated Anti-Cancer Antibodies With Enhanced Antibody-Dependent Cellular Cytotoxicity. *MAbs* (2018) 10(5):693–711. doi: 10.1080/19420862.2018.1466767
83. Shinkawa T, Nakamura K, Yamane N, Shoji-Hosaka E, Kanda Y, Sakurada M, et al. The Absence of Fucose But Not the Presence of Galactose or Bisecting N-Acetylglucosamine of Human IgG1 Complex-Type Oligosaccharides Shows the Critical Role of Enhancing Antibody-Dependent Cellular Cytotoxicity. *J Biol Chem* (2003) 278(5):3466–73. doi: 10.1074/jbc.M210665200
84. Mimura Y, Katoh T, Saldova R, O'Flaherty R, Izumi T, Mimura-Kimura Y, et al. Glycosylation Engineering of Therapeutic IgG Antibodies: Challenges

- for the Safety, Functionality and Efficacy. *Protein Cell* (2018) 9(1):47–62. doi: 10.1007/s13238-017-0433-3
85. Satoh M, Iida S, Shitara K. Non-Fucosylated Therapeutic Antibodies as Next-Generation Therapeutic Antibodies. *Expert Opin Biol Ther* (2006) 6(11):1161–73. doi: 10.1517/14712598.6.11.1161
 86. Kobata A. The N-Linked Sugar Chains of Human Immunoglobulin G: Their Unique Pattern, and Their Functional Roles. *Biochim Biophys Acta* (2008) 1780(3):472–8. doi: 10.1016/j.bbagen.2007.06.012
 87. Sonderrmann P, Huber R, Oosthuizen V, Jacob U. The 3.2-A Crystal Structure of the Human IgG1 Fc Fragment-Fc gammaRIII Complex. *Nature* (2000) 406(6793):267–73. doi: 10.1038/35018508
 88. Ferrara C, Stuart F, Sonderrmann P, Brunner P, Umana P. The Carbohydrate at Fc gammaRIIIa Asn-162. An Element Required for High Affinity Binding to Non-Fucosylated IgG Glycoforms. *J Biol Chem* (2006) 281(8):5032–6. doi: 10.1074/jbc.M510171200
 89. Shields RL, Lai J, Keck R, O'Connell LY, Hong K, Meng YG, et al. Lack of Fucose on Human IgG1 N-Linked Oligosaccharide Improves Binding to Human Fc gammaRIII and Antibody-Dependent Cellular Toxicity. *J Biol Chem* (2002) 277(30):26733–40. doi: 10.1074/jbc.M202069200
 90. Mastrangeli R, Palinsky W, Bierau H. Glycoengineered Antibodies: Towards the Next-Generation of Immunotherapeutics. *Glycobiology* (2019) 29(3):199–210. doi: 10.1093/glycob/cwy092
 91. Li W, Zhu Z, Chen W, Feng Y, Dimitrov DS. Crystallizable Fragment Glycoengineering for Therapeutic Antibodies Development. *Front Immunol* (2017) 8:1554. doi: 10.3389/fimmu.2017.01554
 92. Wang LX, Tong X, Li C, Giddens JP, Li T. Glycoengineering of Antibodies for Modulating Functions. *Annu Rev Biochem* (2019) 88:433–59. doi: 10.1146/annurev-biochem-062917-012911
 93. Chakraborty S, Gonzalez J, Edwards K, Mallajosyula V, Buzzanco AS, Sherwood R, et al. Proinflammatory IgG Fc Structures in Patients With Severe COVID-19. *Nat Immunol* (2021) 22(1):67–73. doi: 10.1038/s41590-020-00828-7
 94. Larsen MD, de Graaf EL, Sonneveld ME, Plomp HR, Nouta J, Hoepel W, et al. Afucosylated IgG Characterizes Enveloped Viral Responses and Correlates With COVID-19 Severity. *Science* (2021) 371(6532):eabc8378. doi: 10.1126/science.abc8378
 95. Arnold JN, Wormald MR, Sim RB, Rudd PM, Dwek RA. The Impact of Glycosylation on the Biological Function and Structure of Human Immunoglobulins. *Annu Rev Immunol* (2007) 25:21–50. doi: 10.1146/annurev.immunol.25.022106.141702
 96. Parekh RB, Dwek RA, Sutton BJ, Fernandes DL, Leung A, Stanworth D, et al. Association of Rheumatoid Arthritis and Primary Osteoarthritis With Changes in the Glycosylation Pattern of Total Serum IgG. *Nature* (1985) 316(6027):452–7. doi: 10.1038/316452a0
 97. Tomana M, Schrohenloher RE, Koopman WJ, Alarcon GS, Paul WA. Abnormal Glycosylation of Serum IgG From Patients With Chronic Inflammatory Diseases. *Arthritis Rheumatol* (1988) 31(3):333–8. doi: 10.1002/art.1780310304
 98. Leirisalo-Repo M, Hernandez-Munoz HE, Rook GA. Agalactosyl IgG is Elevated in Patients With Active Spondyloarthritis. *Rheumatol Int* (1999) 18(5-6):171–6. doi: 10.1007/s002960050080
 99. Dube R, Rook GA, Steele J, Brealey R, Dwek R, Rademacher T, et al. Agalactosyl IgG in Inflammatory Bowel Disease: Correlation With C-Reactive Protein. *Gut* (1990) 31(4):431–4. doi: 10.1136/gut.31.4.431
 100. Ercan A, Cui J, Chatterton DE, Deane KD, Hazen MM, Brintnell W, et al. Aberrant IgG Galactosylation Precedes Disease Onset, Correlates With Disease Activity, and is Prevalent in Autoantibodies in Rheumatoid Arthritis. *Arthritis Rheumatol* (2010) 62(8):2239–48. doi: 10.1002/art.27533
 101. Karsten CM, Pandey MK, Figge J, Kilchenstein R, Taylor PR, Rosas M, et al. Anti-Inflammatory Activity of IgG1 Mediated by Fc Galactosylation and Association of Fc gammaRIIB and Dectin-1. *Nat Med* (2012) 18(9):1401–6. doi: 10.1038/nm.2862
 102. van Osch TLJ, Nouta J, Derksen NIL, van Mierlo G, van der Schoot CE, Wührer M, et al. Fc Galactosylation Promotes Hexamerization of Human IgG1, Leading to Enhanced Classical Complement Activation. *J Immunol* (2021) 207(6):1545–54. doi: 10.4049/jimmunol.2100399
 103. Umana P, Jean-Mairet J, Moudry R, Amstutz H, Bailey JE. Engineered Glycoforms of an Antineuroblastoma IgG1 With Optimized Antibody-Dependent Cellular Cytotoxic Activity. *Nat Biotechnol* (1999) 17(2):176–80. doi: 10.1038/6179
 104. Vieira P, Rajewsky K. The Half-Lives of Serum Immunoglobulins in Adult Mice. *Eur J Immunol* (1988) 18(2):313–6. doi: 10.1002/eji.1830180221
 105. Dombrowicz D, Brini AT, Flamand V, Hicks E, Snouwaert JN, Kinet JP, et al. Anaphylaxis Mediated Through a Humanized High Affinity IgE Receptor. *J Immunol* (1996) 157(4):1645–51.
 106. Gould HJ, Sutton BJ, Beavil AJ, Beavil RL, McCloskey N, Coker HA, et al. The Biology of IGE and the Basis of Allergic Disease. *Annu Rev Immunol* (2003) 21:579–628. doi: 10.1146/annurev.immunol.21.120601.141103
 107. Matsumoto M, Sasaki Y, Yasuda K, Takai T, Muramatsu M, Yoshimoto T, et al. IgG and IgE Collaboratively Accelerate Expulsion of Strongyloides Venezuelensis in a Primary Infection. *Infect Immun* (2013) 81(7):2518–27. doi: 10.1128/IAI.00285-13
 108. Arnold JN, Radcliffe CM, Wormald MR, Royle L, Harvey DJ, Crispin M, et al. The Glycosylation of Human Serum IgD and IgE and the Accessibility of Identified Oligomannose Structures for Interaction With Mannan-Binding Lectin. *J Immunol* (2004) 173(11):6831–40. doi: 10.4049/jimmunol.173.11.6831
 109. Plomp R, Hensbergen PJ, Rombouts Y, Zauner G, Dragan I, Koeleman CA, et al. Site-Specific N-Glycosylation Analysis of Human Immunoglobulin E. *J Proteome Res* (2014) 13(2):536–46. doi: 10.1021/pr400714w
 110. Wu G, Hitchen PG, Panico M, North SJ, Barbouche MR, Binet D, et al. Glycoproteomic Studies of IgE From a Novel Hyper IgE Syndrome Linked to PGM3 Mutation. *Glycoconj J* (2016) 33(3):447–56. doi: 10.1007/s10719-015-9638-y
 111. Shade KC, Conroy ME, Washburn N, Kitaoka M, Huynh DJ, Laprise E, et al. Sialylation of Immunoglobulin E is a Determinant of Allergic Pathogenicity. *Nature* (2020) 582(7811):265–70. doi: 10.1038/s41586-020-2311-z
 112. Chang TW. The Pharmacological Basis of Anti-IgE Therapy. *Nat Biotechnol* (2000) 18(2):157–62. doi: 10.1038/72601
 113. Anvari S, Miller J, Yeh CY, Davis CM. IgE-Mediated Food Allergy. *Clin Rev Allergy Immunol* (2019) 57(2):244–60. doi: 10.1007/s12016-018-8710-3
 114. Garman SC, Wurzburg BA, Tarchevskaya SS, Kinet JP, Jardetzky TS. Structure of the Fc Fragment of Human IgE Bound to its High-Affinity Receptor Fc epsilonRI Alpha. *Nature* (2000) 406(6793):259–66. doi: 10.1038/35018500
 115. Holdom MD, Davies AM, Nettleship JE, Bagby SC, Dhaliwal B, Girardi E, et al. Conformational Changes in IgE Contribute to its Uniquely Slow Dissociation Rate From Receptor Fc epsilonRI. *Nat Struct Mol Biol* (2011) 18(5):571–6. doi: 10.1038/nsmb.2044
 116. Borthakur S, Hibbert RG, Pang MO, Yahya N, Bax HJ, Kao MW, et al. Mapping of the CD23 Binding Site on Immunoglobulin E (IgE) and Allosteric Control of the IgE-Fc epsilonRI Interaction. *J Biol Chem* (2012) 287(37):31457–61. doi: 10.1074/jbc.C112.397059
 117. Nettleton MY, Kochan JP. Role of Glycosylation Sites in the IgE Fc Molecule. *Int Arch Allergy Immunol* (1995) 107(1-3):328–9. doi: 10.1159/000237017
 118. Sayers I, Cain SA, Swan JR, Pickett MA, Watt PJ, Holgate ST, et al. Amino Acid Residues That Influence Fc epsilonRI-Mediated Effector Functions of Human Immunoglobulin E. *Biochemistry* (1998) 37(46):16152–64. doi: 10.1021/bi981456k
 119. Hunt J, Beavil RL, Calvert RA, Gould HJ, Sutton BJ, Beavil AJ. Disulfide Linkage Controls the Affinity and Stoichiometry of IgE Fc epsilon3-4 Binding to Fc epsilonRI. *J Biol Chem* (2005) 280(17):16808–14. doi: 10.1074/jbc.M500965200
 120. Helm B, Marsh P, Vercelli D, Padlan E, Gould H, Geha R. The Mast Cell Binding Site on Human Immunoglobulin E. *Nature* (1988) 331(6152):180–3. doi: 10.1038/331180a0
 121. Helm BA, Sayers I, Padlan EA, McKendrick JE, Spivey AC. Structure/function Studies on IgE as a Basis for the Development of Rational IgE Antagonists. *Allergy* (1998) 53(45 Suppl):77–82. doi: 10.1111/j.1398-9995.1998.tb04945.x
 122. Henry AJ, McDonnell JM, Ghirlando R, Sutton BJ, Gould HJ. Conformation of the Isolated Cepsilon3 Domain of IgE and its Complex With the High-Affinity Receptor, Fc epsilonRI. *Biochemistry* (2000) 39(25):7406–13. doi: 10.1021/bi9928391
 123. Shade KT, Platzter B, Washburn N, Mani V, Bartsch YC, Conroy M, et al. A Single Glycan on IgE is Indispensable for Initiation of Anaphylaxis. *J Exp Med* (2015) 212(4):457–67. doi: 10.1084/jem.20142182

124. Haury M, Sundblad A, Grandien A, Barreau C, Coutinho A, Nobrega A. The Repertoire of Serum IgM in Normal Mice is Largely Independent of External Antigenic Contact. *Eur J Immunol* (1997) 27(6):1557–63. doi: 10.1002/eji.1830270635
125. Jayasekera JP, Moseman EA, Carroll MC. Natural Antibody and Complement Mediate Neutralization of Influenza Virus in the Absence of Prior Immunity. *J Virol* (2007) 81(7):3487–94. doi: 10.1128/JVI.02128-06
126. Griffin DO, Holodick NE, Rothstein TL. Human B1 Cells in Umbilical Cord and Adult Peripheral Blood Express the Novel Phenotype CD20+ CD27+ CD43+ Cd70. *J Exp Med* (2011) 208(1):67–80. doi: 10.1084/jem.20101499
127. Casali P, Schettino EW. Structure and Function of Natural Antibodies. *Curr Top Microbiol Immunol* (1996) 210:167–79. doi: 10.1007/978-3-642-85226-8_17
128. Gronwall C, Vas J, Silverman GJ. Protective Roles of Natural IgM Antibodies. *Front Immunol* (2012) 3:66. doi: 10.3389/fimmu.2012.00066
129. Chou MY, Fogelstrand L, Hartvigsen K, Hansen LF, Woelkers D, Shaw PX, et al. Oxidation-Specific Epitopes Are Dominant Targets of Innate Natural Antibodies in Mice and Humans. *J Clin Invest* (2009) 119(5):1335–49. doi: 10.1172/JCI36800
130. Baumgarth N. The Double Life of a B-1 Cell: Self-Reactivity Selects for Protective Effector Functions. *Nat Rev Immunol* (2011) 11(1):34–46. doi: 10.1038/nri2901
131. Ehrenstein MR, Notley CA. The Importance of Natural IgM: Scavenger, Protector and Regulator. *Nat Rev Immunol* (2010) 10(11):778–86. doi: 10.1038/nri2849
132. Racine R, Winslow GM. IgM in Microbial Infections: Taken for Granted? *Immunol Lett* (2009) 125(2):79–85. doi: 10.1016/j.imlet.2009.06.003
133. Davis AC, Roux KH, Shulman MJ. On the Structure of Polymeric IgM. *Eur J Immunol* (1988) 18(7):1001–8. doi: 10.1002/eji.1830180705
134. Sorensen V, Sundvold V, Michaelsen TE, Sandlie I. Polymerization of IgA and IgM: Roles of Cys309/Cys414 and the Secretory Tailpiece. *J Immunol* (1999) 162(6):3448–55.
135. Pasalic D, Weber B, Giannone C, Anelli T, Muller R, Fagioli C, et al. A Peptide Extension Dictates IgM Assembly. *Proc Natl Acad Sci USA* (2017) 114(41):E8575–E84. doi: 10.1073/pnas.1701797114
136. Sopp JM, Peters SJ, Rowley TF, Oldham RJ, James S, Mockridge I, et al. On-Target IgG Hexamerisation Driven by a C-Terminal IgM Tail-Piece Fusion Variant Confers Augmented Complement Activation. *Commun Biol* (2021) 4(1):1031. doi: 10.1038/s42003-021-02513-3
137. Smith RI, Coloma MJ, Morrison SL. Addition of a Mu-Tailpiece to IgG Results in Polymeric Antibodies With Enhanced Effector Functions Including Complement-Mediated Cytolysis by IgG4. *J Immunol* (1995) 154(5):2226–36.
138. Frutiger S, Hughes GJ, Paquet N, Luthy R, Jaton JC. Disulfide Bond Assignment in Human J Chain and its Covalent Pairing With Immunoglobulin M. *Biochemistry* (1992) 31(50):12643–7. doi: 10.1021/bi00165a014
139. Sorensen V, Rasmussen IB, Sundvold V, Michaelsen TE, Sandlie I. Structural Requirements for Incorporation of J Chain Into Human IgM and IgA. *Int Immunol* (2000) 12(1):19–27. doi: 10.1093/intimm/12.1.19
140. Moh ES, Lin CH, Thaysen-Andersen M, Packer NH. Site-Specific N-Glycosylation of Recombinant Pentameric and Hexameric Human IgM. *J Am Soc Mass Spectrom* (2016) 27(7):1143–55. doi: 10.1007/s13361-016-1378-0
141. Muraoka S, Shulman MJ. Structural Requirements for IgM Assembly and Cytolytic Activity. Effects of Mutations in the Oligosaccharide Acceptor Site at Asn402. *J Immunol* (1989) 142(2):695–701.
142. Arnold JN, Wormald MR, Suter DM, Radcliffe CM, Harvey DJ, Dwek RA, et al. Human Serum IgM Glycosylation: Identification of Glycoforms That can Bind to Mannan-Binding Lectin. *J Biol Chem* (2005) 280(32):29080–7. doi: 10.1074/jbc.M504528200
143. Dorsett B, Cronin W, Chuma V, Ioachim HL. Anti-Lymphocyte Antibodies in Patients With the Acquired Immune Deficiency Syndrome. *Am J Med* (1985) 78(4):621–6. doi: 10.1016/0002-9343(85)90405-X
144. Winfield JB, Fernsten PD, Czyzyk JK. Anti-Lymphocyte Autoantibodies in Systemic Lupus Erythematosus. *Trans Am Clin Climatol Assoc* (1997) 108:127–35.
145. Lobo PI, Schlegel KH, Spencer CE, Okusa MD, Chisholm C, McHedlishvili N, et al. Naturally Occurring IgM Anti-Leukocyte Autoantibodies (IgM-ALA) Inhibit T Cell Activation and Chemotaxis. *J Immunol* (2008) 180(3):1780–91. doi: 10.4049/jimmunol.180.3.1780
146. Lobo PI, Brayman KL, Okusa MD. Natural IgM Anti-Leukocyte Autoantibodies (IgM-ALA) Regulate Inflammation Induced by Innate and Adaptive Immune Mechanisms. *J Clin Immunol* (2014) 34(Suppl 1):S22–9. doi: 10.1007/s10875-014-0027-2
147. Colucci M, Stockmann H, Butera A, Masotti A, Baldassarre A, Giorda E, et al. Sialylation of N-Linked Glycans Influences the Immunomodulatory Effects of IgM on T Cells. *J Immunol* (2015) 194(1):151–7. doi: 10.4049/jimmunol.1402025
148. Lloyd KA, Wang J, Urban BC, Czajkowsky DM, Pleass RJ. Glycan-Independent Binding and Internalization of Human IgM to FCMR, its Cognate Cellular Receptor. *Sci Rep* (2017) 7:42989. doi: 10.1038/srep42989
149. Kumar Bharathkar S, Parker BW, Malyutin AG, Haloi N, Huey-Tubman KE, Tajkhorshid E, et al. The Structures of Secretory and Dimeric Immunoglobulin A. *Elife* (2020) 9:e56098. doi: 10.7554/eLife.56098
150. Breedveld A, van Egmond M. IgA and FcαRI: Pathological Roles and Therapeutic Opportunities. *Front Immunol* (2019) 10:553. doi: 10.3389/fimmu.2019.00553
151. Ramsland PA, Willoughby N, Trist HM, Farrugia W, Hogarth PM, Fraser JD, et al. Structural Basis for Evasion of IgA Immunity by Staphylococcus Aureus Revealed in the Complex of SSL7 With Fc of Human IgA1. *Proc Natl Acad Sci USA* (2007) 104(38):15051–6. doi: 10.1073/pnas.0706028104
152. Tomana M, Matousov K, Julian BA, Radl J, Konecny K, Mestecky J. Galactose-Deficient IgA1 in Sera of IgA Nephropathy Patients is Present in Complexes With IgG. *Kidney Int* (1997) 52(2):509–16. doi: 10.1038/ki.1997.361
153. Tomana M, Novak J, Julian BA, Matousov K, Konecny K, Mestecky J. Circulating Immune Complexes in IgA Nephropathy Consist of IgA1 With Galactose-Deficient Hinge Region and Antigliadin Antibodies. *J Clin Invest* (1999) 104(1):73–81. doi: 10.1172/JCI5535
154. Novak J, Vu HL, Novak L, Julian BA, Mestecky J, Tomana M. Interactions of Human Mesangial Cells With IgA and IgA-Containing Immune Complexes. *Kidney Int* (2002) 62(2):465–75. doi: 10.1046/j.1523-1755.2002.00477.x
155. Steffen U, Koeleman CA, Sokolova MV, Bang H, Kleyer A, Rech J, et al. IgA Subclasses Have Different Effector Functions Associated With Distinct Glycosylation Profiles. *Nat Commun* (2020) 11(1):120. doi: 10.1038/s41467-019-13992-8
156. Maurer MA, Meyer L, Bianchi M, Turner HL, Le NPL, Steck M, et al. Glycosylation of Human IgA Directly Inhibits Influenza A and Other Sialic-Acid-Binding Viruses. *Cell Rep* (2018) 23(1):90–9. doi: 10.1016/j.celrep.2018.03.027
157. Sterlin D, Gorochov G. When Therapeutic IgA Antibodies Might Come of Age. *Pharmacology* (2021) 106(1-2):9–19. doi: 10.1159/000510251
158. Wang Q, Chung CY, Chough S, Betenbaugh MJ. Antibody Glycoengineering Strategies in Mammalian Cells. *Biotechnol Bioeng* (2018) 115(6):1378–93. doi: 10.1002/bit.26567
159. Li S, McCraw AJ, Gardner RA, Spencer DIR, Karagiannis SN, Wagner GK. Glycoengineering of Therapeutic Antibodies With Small Molecule Inhibitors. *Antib (Basel)* (2021) 10(4):44. doi: 10.3390/antib10040044
160. Dionne B, Mishra N, Butler M. A Low Redox Potential Affects Monoclonal Antibody Assembly and Glycosylation in Cell Culture. *J Biotechnol* (2017) 246:71–80. doi: 10.1016/j.jbiotec.2017.01.016
161. Blundell PA, Lu D, Dell A, Haslam S, Pleass RJ. Choice of Host Cell Line Is Essential for the Functional Glycosylation of the Fc Region of Human IgG1 Inhibitors of Influenza B Viruses. *J Immunol* (2020) 204(4):1022–34. doi: 10.4049/jimmunol.1901145
162. Raju TS, Jordan RE. Galactosylation Variations in Marketed Therapeutic Antibodies. *Mabs* (2012) 4(3):385–91. doi: 10.4161/mabs.19868
163. Yu M, Brown D, Reed C, Chung S, Lutman J, Stefanich E, et al. Production, Characterization, and Pharmacokinetic Properties of Antibodies With N-Linked Mannose-5 Glycans. *Mabs* (2012) 4(4):475–87. doi: 10.4161/mabs.20737
164. Jefferis R. Glycosylation as a Strategy to Improve Antibody-Based Therapeutics. *Nat Rev Drug Discovery* (2009) 8(3):226–34. doi: 10.1038/nrd2804

165. Zhong X, Cooley C, Seth N, Juo ZS, Presman E, Resendes N, et al. Engineering Novel Lec1 Glycosylation Mutants in CHO-DUKX Cells: Molecular Insights and Effector Modulation of N-Acetylglucosaminyltransferase I. *Biotechnol Bioeng* (2012) 109(7):1723–34. doi: 10.1002/bit.24448
166. Shi HH, Goudar CT. Recent Advances in the Understanding of Biological Implications and Modulation Methodologies of Monoclonal Antibody N-Linked High Mannose Glycans. *Biotechnol Bioeng* (2014) 111(10):1907–19. doi: 10.1002/bit.25318
167. Liu L. Antibody Glycosylation and its Impact on the Pharmacokinetics and Pharmacodynamics of Monoclonal Antibodies and Fc-Fusion Proteins. *J Pharm Sci* (2015) 104(6):1866–84. doi: 10.1002/jps.24444
168. Wong NS, Yap MG, Wang DI. Enhancing Recombinant Glycoprotein Sialylation Through CMP-Sialic Acid Transporter Over Expression in Chinese Hamster Ovary Cells. *Biotechnol Bioeng* (2006) 93(5):1005–16. doi: 10.1002/bit.20815
169. Nguyen NTB, Lin J, Tay SJ, Mariati, Yeo J, Nguyen-Khuong T, et al. Multiplexed Engineering Glycosyltransferase Genes in CHO Cells via Targeted Integration for Producing Antibodies With Diverse Complex-Type N-Glycans. *Sci Rep* (2021) 11(1):12969. doi: 10.1038/s41598-021-92320-x
170. Raymond C, Robotham A, Spearman M, Butler M, Kelly J, Durocher Y. Production of Alpha2,6-Sialylated IgG1 in CHO Cells. *MAbs* (2015) 7(3):571–83. doi: 10.1080/19420862.2015.1029215
171. Schulz MA, Tian W, Mao Y, Van Coillie J, Sun L, Larsen JS, et al. Glycoengineering Design Options for IgG1 in CHO Cells Using Precise Gene Editing. *Glycobiology* (2018) 28(7):542–9. doi: 10.1093/glycob/cwy022
172. Davies J, Jiang L, Pan LZ, LaBarre MJ, Anderson D, Reff M. Expression of GnTIII in a Recombinant Anti-CD20 CHO Production Cell Line: Expression of Antibodies With Altered Glycoforms Leads to an Increase in ADCC Through Higher Affinity for FC Gamma RIII. *Biotechnol Bioeng* (2001) 74(4):288–94. doi: 10.1002/bit.1119
173. Ferrara C, Brunker P, Suter T, Moser S, Püntener U, Umaña P. Modulation of Therapeutic Antibody Effector Functions by Glycosylation Engineering: Influence of Golgi Enzyme Localization Domain and Co-Expression of Heterologous Beta1, 4-N-Acetylglucosaminyltransferase III and Golgi Alpha-Mannosidase II. *Biotechnol Bioeng* (2006) 93(5):851–61. doi: 10.1002/bit.20777
174. Mori K, Kuni-Kamochi R, Yamane-Ohnuki N, Wakitani M, Yamano K, Imai H, et al. Engineering Chinese Hamster Ovary Cells to Maximize Effector Function of Produced Antibodies Using FUT8 siRNA. *Biotechnol Bioeng* (2004) 88(7):901–8. doi: 10.1002/bit.20326
175. Becker DJ, Lowe JB. Fucose: Biosynthesis and Biological Function in Mammals. *Glycobiology* (2003) 13(7):41R–53R. doi: 10.1093/glycob/cwg054
176. Louie S, Haley B, Marshall B, Heidersbach A, Yim M, Brozynski M, et al. FX Knockout CHO Hosts can Express Desired Ratios of Fucosylated or Afucosylated Antibodies With High Titers and Comparable Product Quality. *Biotechnol Bioeng* (2017) 114(3):632–44. doi: 10.1002/bit.26188
177. Kanda Y, Imai-Nishiya H, Kuni-Kamochi R, Mori K, Inoue M, Kitajima-Miyama K, et al. Establishment of a GDP-Mannose 4,6-Dehydratase (GMD) Knockout Host Cell Line: A New Strategy for Generating Completely Non-Fucosylated Recombinant Therapeutics. *J Biotechnol* (2007) 130(3):300–10. doi: 10.1016/j.jbiotec.2007.04.025
178. von Horsten HH, Ogorek C, Blanchard V, Demmler C, Giese C, Winkler K, et al. Production of Non-Fucosylated Antibodies by Co-Expression of Heterologous GDP-6-Deoxy-D-Lyx-4-Hexulose Reductase. *Glycobiology* (2010) 20(12):1607–18. doi: 10.1093/glycob/cwq109
179. Chan KF, Shahreel W, Wan C, Teo G, Hayati N, Tay SJ, et al. Inactivation of GDP-Fucose Transporter Gene (Slc35c1) in CHO Cells by ZFNs, TALENs and CRISPR-Cas9 for Production of Fucose-Free Antibodies. *Biotechnol J* (2016) 11(3):399–414. doi: 10.1002/biot.201500331
180. Okeley NM, Alley SC, Anderson ME, Boursalian TE, Burke PJ, Emmerton KM, et al. Development of Orally Active Inhibitors of Protein and Cellular Fucosylation. *Proc Natl Acad Sci USA* (2013) 110(14):5404–9. doi: 10.1073/pnas.1222631110
181. Huang W, Giddens J, Fan SQ, Toonstra C, Wang LX. Chemoenzymatic Glycoengineering of Intact IgG Antibodies for Gain of Functions. *J Am Chem Soc* (2012) 134(29):12308–18. doi: 10.1021/ja3051266
182. Giddens JP, Lomino JV, Amin MN, Wang LX. Endo-F3 Glycosynthase Mutants Enable Chemoenzymatic Synthesis of Core-Fucosylated Triantennary Complex Type Glycopeptides and Glycoproteins. *J Biol Chem* (2016) 291(17):9356–70. doi: 10.1074/jbc.M116.721597
183. Giddens JP, Lomino JV, DiLillo DJ, Ravetch JV, Wang LX. Site-Selective Chemoenzymatic Glycoengineering of Fab and Fc Glycans of a Therapeutic Antibody. *Proc Natl Acad Sci USA* (2018) 115(47):12023–7. doi: 10.1073/pnas.1812833115
184. van de Bovenkamp FS, Hafkenscheid L, Rispens T, Rombouts Y. The Emerging Importance of IgG Fab Glycosylation in Immunity. *J Immunol* (2016) 196(4):1435–41. doi: 10.4049/jimmunol.1502136
185. van de Bovenkamp FS, Derksen NIL, Ooijevaar-de Heer P, van Schie KA, Kruithof S, Berkowska MA, et al. Adaptive Antibody Diversification Through N-Linked Glycosylation of the Immunoglobulin Variable Region. *Proc Natl Acad Sci USA* (2018) 115(8):1901–6. doi: 10.1073/pnas.1711720115
186. van de Bovenkamp FS, Derksen NIL, van Breemen MJ, de Taeye SW, Ooijevaar-de Heer P, Sanders RW, et al. Variable Domain N-Linked Glycans Acquired During Antigen-Specific Immune Responses Can Contribute to Immunoglobulin G Antibody Stability. *Front Immunol* (2018) 9:740. doi: 10.3389/fimmu.2018.00740
187. Collin M, Svensson MD, Sjöholm AG, Jensenius JC, Sjöbrink U, Olsen A. EndoS and SpeB From Streptococcus Pyogenes Inhibit Immunoglobulin-Mediated Opsonophagocytosis. *Infect Immun* (2002) 70(12):6646–51. doi: 10.1128/IAI.70.12.6646-6651.2002
188. Nandakumar KS, Collin M, Olsen A, Nimmerjahn F, Blom AM, Ravetch JV, et al. Endoglycosidase Treatment Abrogates IgG Arthritogenicity: Importance of IgG Glycosylation in Arthritis. *Eur J Immunol* (2007) 37(10):2973–82. doi: 10.1002/eji.200737581
189. Collin M, Shannon O, Björck L. IgG Glycan Hydrolysis by a Bacterial Enzyme as a Therapy Against Autoimmune Conditions. *Proc Natl Acad Sci USA* (2008) 105(11):4265–70. doi: 10.1073/pnas.0711271105
190. Stubbs MJ, Thomas M, Vendramin C, Sonesson E, Kjellman C, Jarnum S, et al. Administration of Immunoglobulin G-Degrading Enzyme of Streptococcus Pyogenes (IdeS) for Persistent Anti-ADAMTS13 Antibodies in Patients With Thrombotic Thrombocytopenic Purpura in Clinical Remission. *Br J Haematol* (2019) 186(1):137–40. doi: 10.1111/bjh.15706
191. Jordan SC, Lorant T, Choi J, Kjellman C, Winstedt L, Bengtsson M, et al. IgG Endopeptidase in Highly Sensitized Patients Undergoing Transplantation. *N Engl J Med* (2017) 377(5):442–53. doi: 10.1056/NEJMoa1612567
192. Jordan SC, Legendre C, Desai NM, Lorant T, Bengtsson M, Lonze BE, et al. Imlifidase Desensitization in Crossmatch-Positive, Highly Sensitized Kidney Transplant Recipients: Results of an International Phase 2 Trial (Highdes). *Transplantation* (2021) 105(8):1808–17. doi: 10.1097/TP.0000000000003496
193. Pagan JD, Kitaoka M, Anthony RM. Engineered Sialylation of Pathogenic Antibodies In Vivo Attenuates Autoimmune Disease. *Cell* (2018) 172(3):564–77.e13. doi: 10.1016/j.cell.2017.11.041

Conflict of Interest: The authors declare that the research was conducted in the absence of any commercial or financial relationships that could be construed as a potential conflict of interest.

Publisher's Note: All claims expressed in this article are solely those of the authors and do not necessarily represent those of their affiliated organizations, or those of the publisher, the editors and the reviewers. Any product that may be evaluated in this article, or claim that may be made by its manufacturer, is not guaranteed or endorsed by the publisher.

Copyright © 2022 Vattepu, Sneed and Anthony. This is an open-access article distributed under the terms of the Creative Commons Attribution License (CC BY). The use, distribution or reproduction in other forums is permitted, provided the original author(s) and the copyright owner(s) are credited and that the original publication in this journal is cited, in accordance with accepted academic practice. No use, distribution or reproduction is permitted which does not comply with these terms.

Advantages of publishing in Frontiers



OPEN ACCESS

Articles are free to read
for greatest visibility
and readership



FAST PUBLICATION

Around 90 days
from submission
to decision



HIGH QUALITY PEER-REVIEW

Rigorous, collaborative,
and constructive
peer-review



TRANSPARENT PEER-REVIEW

Editors and reviewers
acknowledged by name
on published articles

Frontiers

Avenue du Tribunal-Fédéral 34
1005 Lausanne | Switzerland

Visit us: www.frontiersin.org

Contact us: frontiersin.org/about/contact



REPRODUCIBILITY OF RESEARCH

Support open data
and methods to enhance
research reproducibility



DIGITAL PUBLISHING

Articles designed
for optimal readership
across devices



FOLLOW US

@frontiersin



IMPACT METRICS

Advanced article metrics
track visibility across
digital media



EXTENSIVE PROMOTION

Marketing
and promotion
of impactful research



LOOP RESEARCH NETWORK

Our network
increases your
article's readership